Charles University in Prague

Faculty of Sciences

Program: Molecular and Cell Biology, Genetics and Virology

SOŇA HUBÁČKOVÁ

DNA damage and signalling pathways in cellular senescence

PhD Thesis

Academy of Sciences of the Czech Republic

Institute of Molecular Genetics

Department of Genome Integrity

Supervisor: Zdeněk Hodný, M.D., Ph.D.

Prague, 2012

The author of thesis, Soňa Hubáčková, declares that the entire content of this thesis or its major part was not previously utilized for obtaining of the same or other academic degree.

Prague

Signature

Acknowledgements:

I would like to thank my supervisor Zdeněk Hodný, M.D., Ph.D. for giving me the opportunity to work in his team in excellent scientific environment, for helpful discussions about the projects, experimental settings and writing the papers and Prof. Jiří Bártek, M.D., Ph.D. for scientific support.

I also thank to all my colleagues from Department of Genome Integrity who created a friendly atmosphere and for their helpful assistance and advices. Thanks go to Lenka Kyjacová and Honza Benada for the evening scientific discussions with glass of wine. Special thanks belong to Markéta Vančurová for her ability to always make me laugh.

I am also grateful to people from dance formations „Prague DC“ under the supervision of Jitka Veselá and „Female Afro Dancers“ under the supervision of Simona Prokůpková for taking care about my mental health at the times of absolute hopelessness.

Last but not least, I would like to thank my family for their constant support and love, which make this work possible and Vladimír Čermák not only for his unlimited love and patience with my late night arrivals and weekends spent in the lab, but also for his technical support with my experiments, helpful and critical discussions about my projects and corrections of this thesis.

This work was supported by: Grant Agency of the Czech Republic (Projects 204/08/1418 and 301/08/0353), the European Commission 7th Framework Programme (Project TRIREME), Grant Agency of the Academy of Sciences of the Czech Republic (Project IAA500390501) and Institutional Grant (Project AV0Z5039906).

Contents

Abbreviations

β-gal	beta-galactosidase
AML	acute myeloid leukaemia
ATM	ataxia telangiectasia mutated
ATP	adenosintriphosphate
ATR	ataxia telangiectasia and Rad3 related
BAK	Bcl-2 antagonist/killer
BAX	BH domain proteins Bcl-2-associated protein X
BLM	Bloom syndrome protein
BRCA1	breast cancer type 1 susceptibility protein
BST2	bone marrow stromal antigen 2
C/EBPbeta	CCAAT/enhancer binding protein beta
CBP	CREB binding protein
CDK	cyclin dependent kinase
Chk1	checkpoint kinase 1
Chk2	checkpoint kinase 2
CK2	casein kinase 2
CSF1	colony-stimulating factor 1
CXCL	chemokine (CXC motif) ligand
CXCR2	chemokine (CXC motif) receptor 2
DAPI	4,6-diamidino-2-phenylindole
DAXX	death-associated protein 6
DNA	deoxyribonucleic acid
DNA-PK	deoxyribonucleic acid protein kinase
ds break	double strand break
ERK	extracellular-signal-regulated-kinase
GAS	gamma activated site
GADD45	growth arrest or DNA damage-inducible protein
GRIM-19	gene associated with retinoic-interferon-induced mortality 19
GSK3beta	glycogen synthase kinase 3 beta

HIRA	histone cell cycle regulation defective homolog A
HP1	heterochromatin protein 1
HPV	human papillomavirus
HSV1	after herpes simplex virus type-1
ICP0	infected cell protein 0
IFN	interferon
IFNAR	interferon alpha/beta receptor
IL	interleukin
IRF	interferon regulatory factor
ISG	interferon-stimulated gene
ISGF3	interferon-stimulated gene factor 3
ISRE	interferon-stimulated response element
Jak	Janus kinase
KLHL20	Kelch-like protein 20
KPNA1	nuclear import adaptor karyopherin-α
MAPK	mitogen-ativated protein kinase
MCP1	monocyte chemotactic protein-1
MDM2	mouse double minute 2
MEK	mitogen-activated protein kinase kinase
Mx1	myxovirus resistance protein 1
NADH	nicotinamide adenine dinucleotide
NADPH	nicotinamide adenine dinucleotide phosphate
NBs	nuclear bodies
NBS	Nijmegen breakage syndrome
NDHII	nuclear DNA helicase II
NF1	nuclear factor 1
NFκB	nuclear factor κB
NLS	nuclear localization signal
NUP	nucleoporin
OAS	2'-5'-oligoadenylate synthetase

OGG1	8-Oxoguanine glycosylase
OIS	oncogene-induced senescence
ORF61	open reading frame 61 protein
PA	plasminogen activator
PAI	plasminogen activator inhibitor
PCR	polymerase chain reaction
PI3K	phosphatidylinositol 3-kinases
PIAS	protein inhibitor of activated STAT
PKR	double-stranded RNA activated protein kinase
PML	promyelocytic leukemia protein
POD	PML oncogenic domain
PRD	positive regulatory domain
PTP	protein tyrosine phosphatase
PUMA	p53 upregulated modulator of apoptosis
RANTES	chemokine (C-C motif) ligand 5 (also known like CCL5)
RARalpha	retinoic acid receptor alpha
Rb	retinoblastoma protein
RNA	ribonucleic acid
RNAi	ribonucleic acid interference
RNF	RING finger protein
ROS	reactive oxygene species
SA β-gal	senescence-associated beta-galactosidase
SAHF	senescence-associated heterochromatin foci
SASP	senescence-associated secretory phenotype
SH2	sarc homology 2
SIAH	seven in absentia homolog
SMS	senescence messaging secretome
SOCS	suppressor of cytokine signalling
SOD	super oxide dismutase
SP100	speckled protein of 100 kDa

STAT	signal transducer and activator of transcription
SUMO	small ubiquitin-like modifier
TGFbeta	transforming growth factor beta
TNF	tumour necrosis factor
TopBP1	DNA topoisomerase 2-binding protein 1
TRIM	tripartite motif
tPA	tissue plasminogen activator
uPA	urinary plasminogen activator
UV	ultraviolet
WIP1	wild-type p53 induced phosphatase 1
WRN	Werner RecQ DNA helicase
X-gal	5-bromo-4-chloro-3-indolyl-β-D-galactopyranoside

1. Abstract

Organisms such as mammals need tissue renewal as an important process for maintenance of their viability. Because proliferation is essential also for tumourigenesis, cells need tumour-suppressor mechanisms to protect organism against cancer. Cellular senescence, the permanent state of cell-cycle arrest, features one of these intrinsic barriers against tumourigenesis after DNA damage and understanding of this process may lead to finding of novel therapeutic targets and to optimization of chemotherapy for patients with cancer.

In the first part of the PhD thesis, we investigated activation of JAK/STAT signalling pathway in drug-induced senescence. We used genotoxic drugs like aphidicolin, camptothecine, 5-bromo- 2´-doexyuridin, etoposide or thymidine to induce premature senescence in normal and cancer cells. All this chemicals were able to persistently activate JAK/STAT signalling in monitored cells. Activation of STATs was accompanied with up-regulation of expression of interferon-stimulated genes (ISGs), such as MX1, IRF1, IRF7 and PML. Since IRF1 and IRF7 can be directly involved in stimulation of the IFN genes, we show activated expression as well as secretion of IFNbeta and IFNgamma, but not IFNalpha in drug-induced senescent cells. Furthermore, an inhibition of JAK1 as a major kinase of STAT activation led to suppression of STAT activation and expression of ISGs, supporting a dominant role of JAK1 in activation of interferon response in drug-induced senescent cells. Besides interferons, we found significantly elevated expression and secretion of several other cytokines, like pro-inflammatory IL1, IL6, IL8 and IL10 or TNFalpha. Because JAK/STAT is activated through cytokines (mainly by interferons and IL6), our results suggest a positive feedback loop between JAK/STAT prolonged induction and cytokine secretion.

Promyelocytic leukaemia protein (PML) is one of the well known tumour suppressor upregulated in almost all forms of cellular senescence. It is an essential component of nuclear structures known as PML NB nuclear bodies (NBs) whose accumulation occurs in response to stress. These bodies represent sites where activation of many regulators of cell cycle progression including p53 and Rb proceeds. As we showed, PML NB also colocalize with sites of double strand breaks detected by accumulation of gammaH2AX or 53BP1. In drug-induced senescence, we found that upregulation of PML, a building component of PML NBs belonging to interferon-

stimulated genes, is mediated by JAK/STAT pathway and not by p53, as knockdown of JAK kinase family abolished activation of JAK/STAT pathways as well as PML gene expression and formation of PML NBs in senescent cells in contrast to knockdown of p53, which has no effect on level of PML mRNA and protein. Next we found that transcription of PML is controlled through the Interferon Stimulated Response Element (ISRE) located on its proximal promoter, which is known binding site for STATs, and deletion of this sequence suppressed the transcription efficiency of PML promoter.

The number of PML NBs differs in various cell types cultivated under unperturbed conditions. Therefore we analyzed, whether PML transcription is regulated by JAK/STAT signalling pathway also on its basal level. Interestingly, we found that the number of PML NBs and the levels of PML transcript and protein correlate with activity of STAT3, but not STAT1 or STAT5 in three model cell lines selected for low (U2OS), middle (HeLa) and high PML expression (BJ). Similar correlation was observed between secretion of IL6 - a major activator of STAT3 signalling pathway - and PML NBs levels. Knock-down of STAT3 by specific siRNA as well as a depletion of IL6 from medium by neutralizing antibodies down-regulate PML expression. We found that IL6 alone is able to activate PML transcription in exposed cells. Using chromatin immunoprecipitation, we proved direct binding of STAT3 but not STAT5 to ISRE of PML gene regulatory region.

STAT3 is a main effector activated by IL6, but recent works described IL6-dependent activation of NFkB, a transcription regulator of set of genes involved in immune response, inflammation, proliferation and DNA damage response through IL6/PI3K/Akt signalling pathway. Interestingly, we found that downregulation of NEMO, a molecule important for NFkB activation, also led to downregulation of PML transcription after IL6 treatment.

It is reported that PML NBs play an important role as a docking site for many proteins involved in DNA damage signalling and senescence including those involved in formation of so called „senescence-associated heterochromatin foci“ (SAHF), such as HIRA, HP1 and Rb. While HP1 is well known family of proteins playing role in heterochromatinization, Rb was recently found as the protein involved in formation of SAHF after binding to PML NBs. Elevation of PML NBs was found in all types of senescence, therefore we investigated a presence of SAHF in different types of senescence. We found that all tested cell types formed SAHF under the

condition of oncogene-induces senescence but not after treatment with etoposide, doxorubicin, hydroxyurea or bacterial genotoxins where their formation was cell type specific and correlated with accumulation of p16 in cells. These results indicate that SAHFs are not a common feature of cellular senescence. Since SAHF formation was described to play the role in silencing of genes important for maintenance of cell proliferation, our results show that these structures are not necessary for induction of senescence but if they are present they support development of senescence through activation/stabilization of p16/Rb pathway.

Abstrakt

Pro mnohobuněčné organismy včetně savců představuje regenerace tkání důležitý proces pro zachování jejich životaschopnosti. Vzhledem k tomu, že je proliferace buněk klíčová i pro vznik nádorů, musely si organismy vyvinout mechanismy chránící je proti zhoubnému bujení. Buněčná senescence jako permanentní zástava buněčného cyklu představuje jednu z bariér proti vzniku nádorů po poškození DNA. Pochopení tohoto procesu proto může vést k nalezení nových terapeutických cílů a optimalizaci chemoterapie u pacientů s rakovinou.

V první části disertační práce jsme se zabývali aktivací signální dráhy JAK/STAT u buněčné senescence vyvolané chemoterapeutiky jak v normálních tak nádorových buňkách. Pro tento účel jsme použili genotoxické látky afidikolin, kamptotecin, 5-brom-2'-deoxyuridin, etoposid nebo tymidin. Zjistili jsme, že všechny tyto chemikálie jsou schopny dlouhodobě aktivovat signální dráhy JAK/STAT ve sledovaných buňkách. Aktivace těchto drah byla doprovázena zvýšením exprese genů stimulovaných interferony (ISGs), jako jsou MX1, IRF1, IRF7 a PML. IRF1 a IRF7 se můžou přímo podílet na indukci genů kódujících interferony a u chemicky indukovaných senescentních buněk jsme skutečně zjistili zvýšenou expresi a sekreci IFNbeta a IFNgama, avšak překvapivě ne genů ze skupiny IFNalfa. Inhibice JAK1 jakožto hlavní kinázy umožňující přenos signálu z membránových receptorů stimulovaných interferony vedla jak k potlačení aktivace proteinu STAT1 tak k zástavě exprese ISGs, což podporuje dominantní roli JAK1 v aktivaci interferonové odpovědi u chemicky indukovaných senescentních buněk. Kromě interferonů jsme našli výrazně zvýšenou expresi a sekreci některých dalších cytokinů, jako jsou prozánětlivé cytokiny IL1, IL6, IL8 a IL10 nebo TNFalfa. Vzhledem k tomu, že je signalizace JAK/STAT v buňce aktivována nejen přes interferony, ale obecně přes složitou síť cytokinů, naše výsledky naznačují pozitivní zpětnou vazbu mezi sekrecí cytokinů a dlouhodobou signalizací JAK/STAT pozorovanou u chemicky indukovaných senescentních buněk.

PML je jedním z nádorových supresorů a jeho zvýšená hladina byla detekována u všech forem buněčné senescence. Tento protein je nezbytnou součástí jaderných struktur známých jako

jaderná tělíska PML, jejichž zvýšená akumulace se vyskytuje během reakce na stres. Bylo popsáno, že tato tělíska představují důležité místo pro aktivaci či modifikaci mnoha proteinů spojených s regulací buněčného cyklu, včetně proteinů p53 a Rb. Jak ukazujeme v naší práci, tělíska PML jsou také lokalizována do míst vzniku zlomu DNA dvoušroubovice. Zjistili jsme, že zvýšení hladiny proteinu PML, základní stavební složky PML tělísek, se u chemicky indukovaných senescentních buněk děje nejen na základě stabilizace proteinu, ale také zvýšením exprese genu PML. PML patří do skupiny genů stimulovaných interferony a překvapivým nálezem bylo zjištění, že zvýšení jeho exprese u senescence indukované chemicky je zprostředkováno signální dráhou JAK/STAT a ne skrze aktivaci p53, jehož schopnost indukovat expresi PML byla popsána u onkogenně indukované senescence. Zablokováním všech kináz z rodiny JAK u chemicky indukovaných senescentních buněk jsme docílili jak inaktivace proteinů STAT1 a STAT3, tak i snížení hladiny exprese genu PML a tvorby PML tělísek na rozdíl od blokace p53 proteinu, která neměla na expresi genu PML žádný vliv. Dále jsme zjistili, že exprese PML je řízena prostřednictvím konkrétní sekvence na promotoru PML (ISRE - Interferon Stimulated Response Element), která představuje vazebné místo pro transkripční faktor STAT1. Odstraněním této sekvence byla u chemicky indukovaných senescentních buněk transkripce genu PML potlačena.

Počet jaderných tělísek PML se liší u různých typů buněk. Na základě výsledků zmiňovaných výše jsme analyzovali, zda-li je transkripce PML u buněk regulována pomocí drah JAK/STAT také na bazální úrovni. K tomuto experimentu jsme použili tři modelové buněčné linie s nízkou (U2OS), střední (HeLa) a vysokou (BJ) hladinou PML. Zjistili jsme, že počet tělísek PML stejně jako hladina mRNA a proteinu PML koreluje s aktivací STAT3, ale ne STAT1 nebo STAT5. Podobná korelace byla pozorována mezi hladinou sekretovaného IL6 - hlavního aktivátoru STAT3 signální dráhy - a počtem tělísek PML. Snížení hladiny STAT3 pomocí specifické siRNA stejně jako neutralizace IL6 v médiu pomocí specifické protilátky snížily bazalní hladinu PML v buňkách. Zjistili jsme, že IL6 je sám o sobě schopen aktivovat transkripci PML u exponovaných buněk. Pomocí chromatinové imunoprecipitace jsme prokázali přímou vazbu STAT3, ale ne STAT5 na promotor genu PML.

Aktivace STAT3 představuje hlavní cíl signalizace spouštěné IL6, nicméně několik prací naznačilo aktivaci NFkapaB závislou na IL6. NFkapaB je transkripční faktor regulující geny podílející se na řízení imunitních reakcí, zánětu, proliferace nebo odpovědi na poškození DNA a to prostřednictvím signální dráhy IL6/PI3K/Akt. Zjistili jsme, že snížení exprese proteinu NEMO, který je nezbytný pro aktivaci NFkapaB, vedlo ke snížení transkripce PML. Další experimenty prokázaly, že NFkapaB reguluje transkripci PML regulací exprese IL6 spíše než přímou indukcí PML.

Bylo popsáno, že tělíska PML hrají důležitou roli v regulaci řady proteinů zapojených do odpovědi na poškození DNA a rozvoje senescence, včetně proteinů zapojených do tvorby tzv. "se senescencí-asociovaných heterochromatinových fokusů" (SAHF) jako je Hira, HP1 a Rb. Zatímco role faktorů z rodiny HP1 v tvorbě heterochromatinu je již dlouho známa, utváření SAHF po vyvázání Rb proteinu tělísky PML bylo popsáno teprve nedávno. Zvýšená tvorba tělísek PML byla zjištěna u všech typů senescence, proto jsme testovali, zda-li toto platí i pro SAHF, což by z nich činilo univerzální marker senescence, který doposud není znám. Zjistili jsme, že všechny testované typy buněk tvořily SAHF v případě onkogenně indukované senescence, ale po vyvolání senescence chemikáliemi jako je etoposid, doxorubicin, hydroxyurea nebo bakteriálními genotoxiny, byl vznik SAHF závislý na buněčném typu. I když jsme nedetekovali SAHF ve všech případech senescence a nemůžeme je tudíž použít jako univerzální marker, objevili jsme korelaci mezi tvorbou SAHF a hromaděním inhibitoru cyklin-dependentních kináz p16INK4A v buňkách. Vzhledem k tomu, že byla popsaná role SAHF v umlčování genů regulujících buněčnou proliferaci, naše výsledky naznačují, že tyto tento typ heterochromatinizace není nezbytně nutný pro indukci senescence. Nicméně pokud se tyto struktury v buňce vyskytnou, podporují vznik senescence přes aktivaci/stabilizaci p16/Rb dráhy.

2. Aims of the study

The main aim of the study was to evaluate the role of signalling pathways in mechanism of cellular senescence.

The specific aims of this study were:

- To characterize cytokine expression during cellular senescence
- To investigate the role of cytokine signalling pathways activated during cellular senescence in regulation of expression of tumour suppressors associated with DNA damage and cellular senescence
- To analyze the role of JAK/STAT pathway in regulation of expression of PML in cellular senescence

3. Introduction

3.1. DNA damage response in cellular senescence

Cell division is essential for survival and development of multicellular organisms. One of crucial tasks fulfilled during the cell division is a precise duplication of genome followed by equal dividing of chromosome copies into subsequent cell generations[1]. Cell cycle of all proliferating eukaryotic cells can be divided into four phases: G1, S, G2, and M. Each transition point, G1/S and G2/M, as well as S-phase progression, is tightly controlled by so called cell cycle checkpoints. For example, at the site of G1/S-checkpoint, cell controls its ability to start DNA replication, whereas at G2/M-checkpoint it is checked whether all genome was completely replicated and thus whether the cell is prepared for division. If there is some problem, the checkpoint is activated resulting in stop of cell cycle progression at the particular checkpoint until the problem is solved. This control is provided by concerted action of many factors including so called checkpoint kinases. Correct activity of these kinases have crucial role in protection of cells against cancer development after DNA damage via the control of cell cycle and cell proliferation. Thus, the cell cycle checkpoints are signalling pathways operating both under normal growth conditions and are amplified upon an increase of DNA damage[2].

DNA damage includes especially covalent changes in structure of DNA, where DNA backbone is broken on one or both strands or chemically modified, and non-covalent anomalous structures, including base-pair mismatches, loops, and “bubbles” arising from a string of mismatches[3]. According to type of damage, different repair mechanisms are activated. These repair mechanisms may be simple and direct, for example removing of 8-oxoguanine (an oxidized form of guanine nucleotide) and its replacement by correct nucleotide[4]. In contrast, repair of double strand break is a complex process needing various proteins involved in recognition of damaged site, stabilization of damaged DNA, recruitment of mediator proteins and proteins, which execute the repair itself[5]. Independently of type of lesion, DNA damage activates cellular checkpoints which slow or arrest (reversibly or irreversibly) cell-cycle progression, thereby allowing time for appropriate repair mechanisms to correct genetic lesions before they are passed onto the next generation of daughter cells[6].

DNA double strand breaks (DSBs) are caused by oxidative stress, ionizing radiation, various types of chemotherapeutic drugs and represent one of the most harmful types of DNA

damage. Disruption of chromosomal structure stability leads to risk of malignant transformation and cancer development after chromosomal rearrangement[7]. Cellular response to DNA DSBs include sensor proteins recognizing sites of DNA damage like MRE11, RAD50 and NBS1, which relocalize to the sites of DSBs and form MRN complex observable with specific antibodies by optical microscopy as so called DNA damage foci[8]. Formation of MRN complex on DNA breaks then recruit and activate sensor transducing kinases ATM (ataxia telangiectasia mutated kinase)[9]. Rather than by MRN complex, ATR (ATM and Rad3 related kinase) is recruited to the sites of damage by its binding protein ATRIP, which recognizes RPA (replication protein A) bound on single stranded DNA[10]. Therefore in contrast to ATM, which is activated mostly by double strand breaks, ATR is preferentially activated by events leading to single stranded DNA like DNA replication or UV-irradiation. When activated, ATM and ATR phosphorylate signal transducer checkpoint kinases (also called serine/threonine signal transducing kinases or effector kinases) Chk1 and Chk2[11]. Previous studies showed activation of Chk1 by ATR and Chk2 by ATM, but recent papers indicate involvement of both sensor kinases in phosphorylation of checkpoint kinases, because in cells with downregulation of ATM phosphorylation of Chk2 was observed and vice versa[12]. Chk1/Chk2 phosphorylate several substrates including CDC25, its phosphotylation at multiple serine residues results in its ubiquitination and degradation in proteasome. CDC25 is a dual specific phosphatase removing inhibitory phosphate residue from target Cyclin-Dependent Kinases (Cdks). Thus, degradation of CDC25 prevents entry into S-phase[13]. Beside CDC25, Chk1 and Chk2, ATM phosphorylates another cell cycle regulator p53 on Thr18, Ser15 or Ser20, which then activates expression of p21CIP1, a cyclin-dependent kinase inhibitor preventing binding of cyclin E on CDK2 or cyclin D on CDK4/6 and thus blocks the cell in G1-phase[14].

Next to checkpoint activation, ATM and ATR are able to amplify DNA damage signal by phosphorylation of histone H2AX, a H2A histone variant, on serine 139 (termed gammaH2AX), resulting to binding and ATM-dependent phosphorylation of another adaptor protein, MDC1 on this histone. Phosphorylated MDC1 recruits ubiquitin E3 ligase RNF8, which in co-operation with E2 conjugating enzyme UBC13 ubiquitinates H2AX[15]. This ubiquitination creates a binding site for another E3 ubiquitin ligase RNF168. RNF168, again with co-operation with UBC13, increases ubiquitination of histones[16]. These modifications are essential for binding of

other proteins of DNA damage cascade like BRCA1 and 53BP1. Defective S-phase checkpoint was observed in cells lacking 53BP1 or BRCA1, for example breast cancer is often accompanied with loss of BRCA1 expression[17].

p53 is a transcription factor involved in tumour suppression by modification of mitochondrial metabolism, induction of factors mediating DNA repair, senescence or apoptosis[18]. The activation of proteins important for cell cycle arrest (p21waf1, 14-3-3 or growth arrest or DNA damage-inducible gene, GADD45alpha) as well as for apoptosis (p53 upregulated modulator of apoptosis PUMA; BH domain proteins Bcl-2-associated protein X, BAX; and Bcl-2 antagonist/killer, BAK) was observed[19]. Under unperturbed condition, p53 is present in cell at low level due to negative regulation by E3 ubiquitin ligase MDM2 (mouse double minute 2)[20] and by its dephosphorylation due to WIP1 (wild-type p53 induced phosphatase 1)[21]. This downregulation and deactivation of p53 represents negative feedback, because both proteins are activated by p53. After DNA damage, p53 is stabilized by phosphorylation and acetylation together with degradation of MDM2 and WIP1. p53-driven expression of p21waf1 (p21) then promotes cell cycle arrest[21, 22].

Since p53 plays a key role in inhibition of tumorigenesis, its inactivation was found in approximately 50% of human cancers[23]. p53 was also found to cooperate with immune system. Reactivation of p53 in p53-deficient mice with developed liver carcinoma results in senescence of tumour cells accompanied with upregulation of several pro-inflammatory cytokines including colony-stimulating factor 1 (CSF1), monocyte chemotactic protein 1 (MCP1), chemokine CXC motif ligand 1 (CXCL), and interleukin 15 (IL-15), that attract macrophages, neutrophils and natural killer cells into site of tumour to help to decrease tumour progression[24].

Activated CDKs in G1-phase promotes cell cycle progression by phosphorylation of Rb. In reaction to phosphorylation, Rb loses interaction with transcription factor E2F, which plays crucial role in preparation of cell to enter S-phase. After DNA damage and p53 activation, CDKs are inhibited, which results in hypophosphorylation of Rb, formation of E2F-Rb repressive complex and cell cycle arrest. Since p21 is not the only protein involved in CDK inactivation (p15INK4B, p16INK4A, p27KIP1 and p57KIP2 are also involved), p53-independent hypo-

phosphorylation of Rb was observed after p16INK4A activation in response to DNA damage[25].

Taking together, DNA damage triggers cascade of repairing mechanisms that include recognition of DNA damage site, recruitment of proteins involved in repair and arrest of cell cycle. At conditions the DNA lesion is irreparable, persistent DNA damage signalling followed with inhibition of CDKs via activated checkpoints results in permanent cell cycle arrest or cell death. Thus p53 and Rb present two crucial regulators of senescence and apoptosis[26].

3.1.1. Cellular senescence

More than half a century ago, L. Hayflick described a process that is limiting the proliferation of normal human cells in culture and termed it cellular senescence[27]. Later, cellular senescence was shown to be not only the consequence of "aging in vitro" but also a component of tumour suppressive mechanisms[28] (note, the term cellular aging is used as a general description of all features related to cell aging including terminally differentiated cells, whereas the term cellular senescence is used in strictly specific context linked to cell proliferation as described below).

Genome is continually damaged by environmental insults or in dividing cells by errors during DNA replication and mitosis. Depending on the level and type of damage, cells can repair the damage or has to be eliminated to prevent propagation of cells with damaged genome. In rapidly dividing cells as are epithelial cells, there is a major risk of generating mistakes in repair mechanisms themselves resulting in so called "mutator phenotype"[29]. If mutations hit the growth or survival pathways leading to their hyperactivation, cancer can develop. If the cell is not able to repair the damage, there are two mechanisms the normal cell can undergo to suppress the uncontrolled proliferation: to commit suicide by apoptosis or by other type of programmed cells death or undergo irreversible cell cycle arrest – cellular senescence[30]. The border between apoptosis and senescence in sense of regulatory mechanisms involved is not strict because many activated proteins and pathways are shared by both tumour barriers. The processes how the cell decides between these two essentially distinct tumour suppressive mechanisms are still not well understood. Recent studies provide some insight into the mechanism of decision. Generally, duration of stress stimuli as well as the amount and type of DNA damage was described to be crucial for decision, if cell undergo senescence or apoptosis[31]. p53 is known

tumour suppressor that play the role in controlling decision between life and death and is one of the most important proteins activated by various types of stresses leading to or resulting from DNA damage[32]. Detailed mechanism described recently shows changes in two crucial amino acids in DNA binding core domain of p53 cause conformational changes leading to inability of p53 to activate the expression of proapoptotic genes. Rather, increased expression of cell cycle arrest genes was observed after p53 amino acid changes due to preferential binding of p53 on their promoter[33]. In Li-Fraumeni syndrome, an autosomal hereditary disorder with inability of the cells to undergo apoptosis, mutations in these amino acids were detected[34]. So it seems that DNA binding cooperativity of p53 may be one of the mechanisms which modulate cell decision between cell cycle arrest and apoptosis.

In general, senescence appears to be beneficial, because it protects organisms from tumorigenesis by induction of proliferation arrest in damaged cells. However, senescent cells lost ability of normal regeneration[35]. Therefore from point of homeostasis maintenance, senescence can be deleterious because it contributes to reduction of tissue renewal and function by disruption of tissue structure and changed functional status of cells undergoing senescence. Senescent cells were found in tissues associated with many age-related diseases, as cardiac arrhythmias, vascular disease, impaired wound healing, osteoporosis, lordokyphosis, sarcopenia or cataract[36] and thus it was suggested that they contribute to organismal aging. Removal of senescent cells can therefore prevent or delay tissue dysfunction and extend health. Importantly, senescent cells are able to produce various immunomodulatory factors[37]. It was shown that senescent cells are able to recruit immune cells, especially macrophages after their activation by CD4+ T-lymphocytes, by secreted pro-inflammatory cytokines to execute the clearance of senescent cells. Nonetheless, clearance of big amount of senescent cells from tissue without their compensation results in damage and dysfunction of appropriate organ[38]. Furthermore, as will be discussed in more detail in chapter 3.4, senescent cells are also able to induce senescence in their neighbourhood by specific secretome, thus surrounding tumour cells may also undergo senescence – bystander senescence[39]. Therefore, senescent cells prevent rapid growth of the tumour and absence of these cells increases tumour progression, invasion and deteriorates prognosis because of inability to recruit cells of immune system into tumour to eliminate it[40]. The function of immune system is suppressed with advancing age, which may be the reason why

senescent cells accumulate being not effectively eliminated in aging organism and the incidence of cancer increases[41]. Many works descibe that cellular senescence suppress tumorigenesis in vivo[42] However, some data indicate that senescent human fibroblasts stimulate premalignant, but not normal epithelial cells to proliferate and form tumours in old tissue, which indicates that cellular senescence is a pleiotropic process protecting from carcinogenesis early in live, but helps to promote it in aged organism[43]. It was shown that MMP3 produced by senescent fibroblast reorganize tissue structure in mammary glands and thus creates conditions for progression of premalignant mammary epithelial cells[44]. On the other hand, in a case of fibrosis repression, cleavage of extracellular matrix by proteinases looks to be beneficial as will be discussed later[45].

3.1.1.1 Characteristics of senescent cells

Although cellular senescence and apoptosis represent the barrier against tumorigenesis they differ in manner how they do this. While apoptosis kills and eliminates cancer cells from organism, senescence essentially irreversibly blocks the progress of cell with damaged genome throughout the cell cycle[46, 47]. Phase of the cell cycle, where the growth is arrested, depend on species, cell origin and type of damage. Note however, there is no specific marker common to all types of senescence or type of cells or cell line. Senescent phenotype is therefore characterized as a combination of permanent cell cycle arrest with further changes represented by altered cellular morphology, increased activity of senescence-associated beta-galactosidase (SA B-gal)[48], increased formation of senescence-associated heterochromatin foci and promyelocytic leukaemia protein nuclear bodies (PML NBs), permanent DNA damage foci, and a specific secretome[49]. Some of these markers have been also identified in vivo in cells from age-related pathologies.

3.1.1.1.1 Morphology

Senescent cells display completely different phenotype in comparison to cells they arise from. They increase in size, nucleus becomes enlarged, which is mostly accompanied with increased ploidity of cells, and cytoplasm spreading (Fig. 1)[27, 50]. The cytoskeleton of senescent fibroblast cells shows increased proportion of vimentin in contrast to downregulation of tubulin and actin, where actin builds up a network of long and thin fibers in comparison with

short and thick stress fibers in young fibroblasts. Also the increase of amount and size of focal adhesions was detected in senescent cells[51, 52].

3.1.1.1.2 Senescence-associated beta-galactosidase

In 1995 Dimri et al. found increased level of beta-galactosidase activity under the pH 6.0 of assay condition in lysates of replicative senescent cells and called it senescence-associated beta-galactosidase (SA-B-gal)[53]. Later it was described that this increase of activity is connected with enlargement of lysosomal compartment in senescent cells, where this enzyme is localized. Beta-galactosidase represents an essential enzyme in the human body, which takes part in gain of energy not only from saccharides but also for example from glycoproteins. Its enzymatic activity is usually detected by staining of cells with the chromogenic substrate 5-bromo-4-chloro-3-indolyl-B-galactopyranoside (known as X-gal), which cleaves beta-galactosidase and generates indigo colour (Fig. 1)[54]. Even though it was proved that not all senescent cells contain increased level of B-galactosidase, it still remains the most widely used biomarker of senescent phenotype.

3.1.1.1.3 Senescence-associated heterochromatin foci

Another mechanistically important aspect of cellular senescence is formation of chromatin structures called senescence-associated heterochromatin foci (SAHF). These domains of heterochromatin can be detected cytologically as compacted foci of heterochromatin stained by DAPI. It was found that these DAPI foci contain numerous proteins characteristic of transcriptionally inactive heterochromatin, including hypoacetylated histones, methylated histone H3 on Lys 9 (H3K9me)[55] (Fig. 2), and heterochromatin protein 1-alpha, -beta and -gamma (HP1alpha, beta and gamma). It is interesting that SAHF formation was observed mainly in oncogene-induced senescence (OIS), rarely in stress-induced or replicative senescence, therefore their formation is not prerequisite for development of senescence (for detailed description of types of senescence - see below)[55].

Other specific features of cellular senescence such as multiplication of PML nuclear bodies and specific secretome will be discussed later.

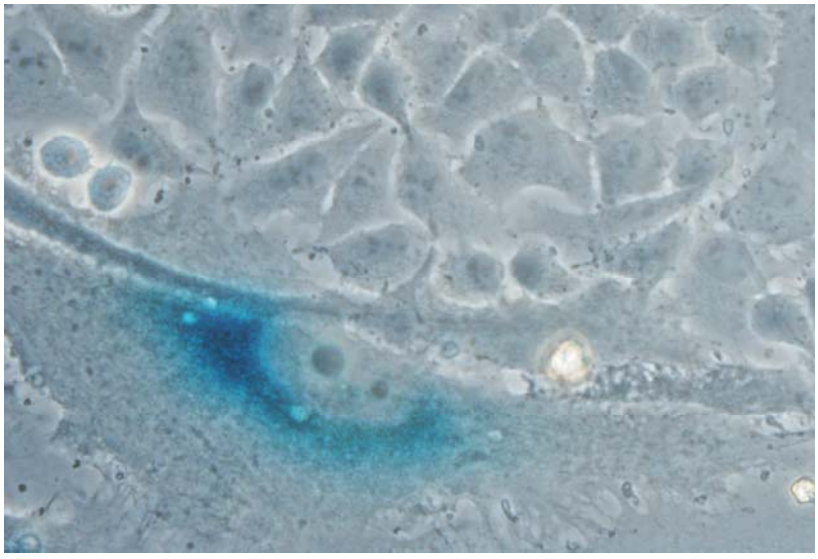

Figure 1. Morphological changes in aphidicolin-induced senescent A549 cell in comparison with non-treated A549 in mixed culture. Blue stain indicates activation of SA-B-galactosidase, which was detected using X-gal substrate (Hubáčková S., unpublished data).

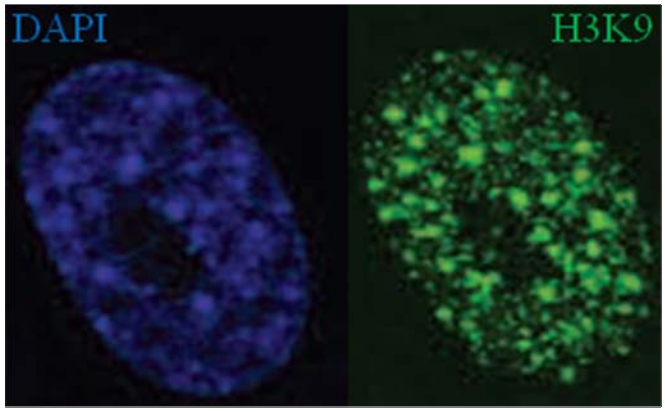

Figure 2. Detection of SAHF by DAPI staining and by using antibody against trimethylated histone H3 on Lys 9 in RAS transformed BJ cells (Kosar M. et al., 2011).

3.1.1.2 Causes of cellular senescence

3.1.1.2.1 Replicative senescence

As already mentioned, in the middle of 20th century Hayflick documented the fact that cells have only a limited capacity for proliferation in culture. This observation generated the idea that replicative senescence, how it is termed, might act to suppress tumorigenesis in vivo.

Hayflick also pronounced a hypothesis that replicative senescence causes premature organismal aging, nowadays known as progeria, a disease, where symptoms resembling aspects of aging are manifested at early age[56].

For a long time stayed unclear what limits the cell proliferation. Studies of telomere length regulation provided the first molecular mechanism capable of counting cell divisions and implementing cell cycle arrest. Telomeres consist of repetitive DNA elements at the end of linear chromosomes that protect the DNA ends from degradation and recombination. Elongation of chromosomal ends is ensured by telomerase, a ribonucleoprotein with DNA polymerase activity, which decreased its activity with ageing[57]. Due to inability of the replication machinery to copy the exact ends of linear molecules (Olovnikov's end replication problem hypothesis), it was proposed that telomeres become shorter with every round of cell division. When telomeres reach a critically short length, they can behave as double-strand DNA breaks, activate the p53 tumour suppressor resulting in cell cycle arrest and telomere-initiated senescence. Loss of telomeres also propagates via losing of ability to protect the ends of chromosome from end-to-end fusions, which generate unstable dicentric chromosomes. Because telomere shortening limits not only the proliferation of normal cells, but also the transformed tumour cells, these cells develop mechanisms how to bypass this[58, 59].

Telomerase is normally expressed at high level in very few primary cells such as embryonic stem cells or adult male germline cells, but it is almost undetectable in most normal somatic cells with the exception of proliferative cells of renewal tissues(ref.). In tumour cells, the activation of this enzyme represents one of the mechanisms how to stabilize telomeres and avoid replicative senescence. It was proved in vitro that ectopic expression of telomerase was able to prevent telomere shortening, which resulted in immortalization of cells indicating that telomere shortening is linked to replicative senescence[60, 61]. However, this year was published an observation, that telomere shortening is not the only one mechanism for senescence induction. A significant fraction of persistent DNA damaged signals caused by exogenous DNA damaging treatments was shown to be at telomeres. It was found that localization of telomeric factor TRF2 next to the site of double strand break resist DNA repair and prolonged DDR signalling which may signal to trigger senescence establishment. These results were supported by investigation on tissue from old primates, where DNA damage markers were accumulated at telomeres, which

were not critically short and trigger persistent DNA damage response and cellular senescence[62].

3.1.1.2.2 Oncogene-induced senescence

Cellular senescence is a process that is triggered not only by telomeric dysfunction, but also by other forms of stress including oncogene activation. Oncogenes are mutant version of normal genes that have the potential to transform cells in conjunction with additional mutations. This phenomenon was first observed when constitutively activated RAS, member of MAPK pathway and transducer of mitogenic signals, was upregulated in primary fibroblasts[63]. Upon its overexpression or constitutive activation, cells underwent cell cycle arrest, which was associated with many of the hallmarks of cells that undergo replicative senescence. Later was described that also other members of the RAS signalling pathway as BRAF, MEK and ERK as well as pro-proliferative nuclear proteins from E2F family are able to cause senescence when overexpressed or constitutively active[64, 65].

In normal cells, the activation of RAS induces an aberrant proliferation response that later results in cell cycle arrest and senescence. Increase of mitochondrial mass, production of reactive oxygen species (ROS) and decrease of ATP level in dependence on mitochondrial dysfunction after RAS activation was described. Increased pool of ROS in cell results in purine oxidation (mainly 8-oxoguanine) and development of DNA damage. Elimination of these oxidized deoxyribonucleotides prevents RAS-induced senescence. Activated RAS strongly induces both p53 and Rb, but their role in process of mitochondria destabilization remains unclear. Data referred by Moiseeva et al. indicate necessity of these proteins for induction of mitochondrial injury and ROS production after RAS activation[66]. As the possible mechanisms, p53 may be localized into mitochondria where it inhibits the respiratory chain or several of its target genes may activate mitochondrial ROS production[67]. Secondly, Rb protein was described to regulate mitochondrial biogenesis in erythropoesis[68]. However, further studies are required to find the mechanism of this regulation.

3.1.1.2.3 Stress-induced senescence

In contrast to replicative or oncogene-induced senescence, DNA damage in stress-induced senescence is caused directly by physico-chemical agents[69]. Among most common

inducers of physical nature belongs ionizing and ultraviolet radiation. While ionizing radiation produces variety of lesions that include DNA single-strand breaks, DNA double-strand breaks, DNA base alterations, and DNA-DNA or DNA-protein cross-links[70], UV-irradiation causes mainly single strand breaks as the result of repair of cross-links formed between adjacent cytosine and thymine bases creating pyrimidine dimmers[71]. In both cases DNA damage leads to activation of DNA damage response including cell cycle checkpoint activation, cell cycle arrest and repair of damaged DNA as mentioned above in detail. Besides short-wavelength radiation, changes in extracellular environment like reduction of pH, increase of oxygen or temperature changes leads to DNA damage[72, 73]. But rather then direct damage, they increase levels of ROS in the cell, which results mainly in formation of 8-oxoguanine, an oxidized form of guanine nucleotide, which is able to pair with adenine and to cause point mutations[74].

3.1.1.2.4 Drug-induced senescence

Drug-induced senescence represents subgroup of stress-induced senescence. As well as in previous case, premature senescence is likely caused by replicative stress after DNA damage. Here, DNA damage represented mainly by single or double strand breaks, is caused by variety of chemicals often used also in chemotherapy. Most used drugs are DNA-binding agents or inhibitors of topoisomerase I and II (such as camptothecine and etoposide), where the inability to release the pressure in DNA replication fork cause DNA breaks, activation of repair mechanisms and cell cycle arrest[75, 76]. Except this mechanism, inhibition of DNA replication by inactivation of DNA polymerases or ribonucleotide reductase (e.g. by aphidicolin and hydroxyurea) was observed[77]. Another group of senescence-inducing chemicals belongs for example to inhibitors of respiratory chain in mitochondria leading to increase of ROS production and DNA point mutation. Distamycin A then belongs to the group of chemicals, which are able to bind into DNA grooves and cause DNA damage during replication due to block of replication fork and making a tension on DNA chain[78]. Nucleotide analogs like 5-bromo-2-deoxyuridine (BrdU) incorporate into DNA and cause DNA damage during replication[79].

3.2 JAK/STAT signalling pathway

Cytokines are small molecules playing a key role in development, hematopoesis, immune response, cell growth, differentiation, apoptosis and many other biological processes. JAK/STAT pathway is one of the important signalling activated by cytokines that execute their biological functions.

Cytokine-receptor binding induces receptor dimerization and tyrosine phosphorylation which is necessary for activation of Janus family tyrosine kinases associated with the receptors. In mammals, four JAKs (JAK1, JAK2, JAK3 and TYK2) were identified. A combination of type of JAK kinases is specific for each receptor, where JAK1 was found to be present on all receptors except signalling to STAT4. Activation of JAK kinases leads to generation of docking site on receptors for STAT proteins through its SH2 domain. After following JAK-kinase-mediated phosphorylation on tyrosine residue, STATs forms homo- or heterodimers and translocate into nucleus due to exposure of nuclear localization signal (NLS) (Fig. 3). In several STAT proteins, second phosphorylation on serine residue was observed which was found to increase STAT transcriptional activity[80].

STAT family includes seven members. All of them contain conserved N-terminal oligomerization domain, central DNA binding domain and C-terminal SH2 domain important for receptor binding. Each STAT was found to be activated by different group of cytokines through different receptors – interferons are the most important activators of STAT1 and 2, IL6 and other members of IL6 family was described to activate STAT3. IL12 activates STAT4, prolactin or IL2 regulates STAT5 and IL4 was observed to phosphorylate STAT6 through its receptor[81].

Constitutive activation of some JAK/STAT pathways may lead to tumourigenesis, therefore there must be a regulation mechanism how to control these pathways. Most components of JAK/STAT pathways are activated by phosphorylation, therefore tyrosine dephosphorylation by phospho-tyrosine phosphatase (PTP) is a major tool of negative regulation. Suppressors of cytokine signalling family (SOCS) bind to cytokine receptor and prevent either STAT phosphorylation by JAK kinase or binding and phosphorylation of JAK kinase on receptor. Activated STAT may be blocked by proteins belonging to afamily of protein inhibitors of activated STAT (PIAS), which inhibit JAK/STAT mediated gene expression by blocking

STATs DNA binding activity. Many of these regulators are activated immediately after STAT activation as a result of induced transcription by STAT itself[82, 83].

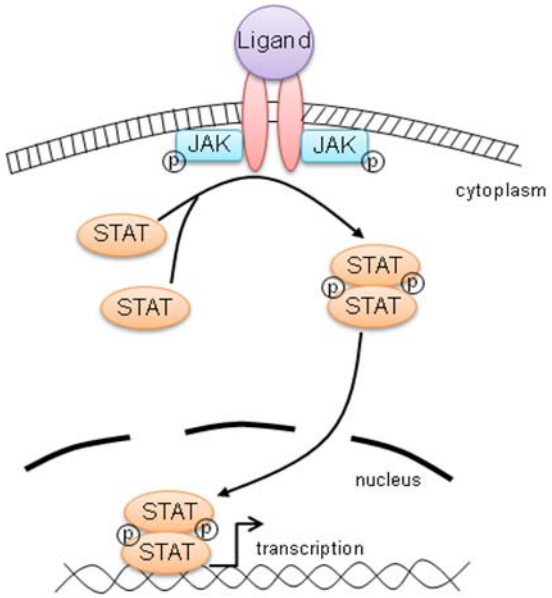

Figure 3. Schematic model of JAK/STAT signalling pathway

3.2.1 The role of JAK/STAT pathway in viral infection

The most important role of JAK/STAT signalling was found during viral infections, where IFNs are involved in numerous immune interactions as inducers, regulators, and effectors of both innate and adaptive antiviral mechanisms. As demonstrated by loss of responsiveness to both types of IFNs and enhanced susceptibility to bacterial and viral pathogens in STAT1 or IFNAR (interferon-alpha receptor) knock-out mice, IFNs play a key role in the outcome of a viral infection[84, 85].

After viral infection, activation of transcription factors essential for expression of IFN genes is induced. In this process, mainly four members of interferon regulated factor (IRF-1, IRF-3, IRF-5 and IRF-7) family have been implicated. IRFs contain potential virus-mediated phosphorylation sites in the C-terminal region. After phosphorylation, they translocate into nucleus and bind to interferon alpha or beta promoter region containing so called positive regulatory domains (PRD I – IV) representing binding sites for IRFs and NFkB. After interferon

autocrine signalling, IRFs are already activated independently on virus through STAT mediated expression and activation[86].

Double-stranded RNA activated protein kinase (PKR) is a dual-specificity kinase, which is known to be activated by autophosphorylation upon binding to viral dsDNA and then phosphorylates the alpha subunit of the eukaryotic initiation factor eIF-2, a modification that results in the inhibition of protein synthesis and protection of cell against viral infection. PKR was also found to be strongly activated after IFN type I signalling through activation of JAK1 kinase where PKR acts as substrate of activated JAK[87]. Besides eIF-2alpha phosphorylation, PKR was found to be important activator of STAT1 on serine 727, which increases its transcription activity and expression of IFN-stimulated genes and IFN secretion[88].

Mx1 protein, a member of dynamin-like large guanosine triphosphatases (GTPases) involved in intracellular vesicle trafficking, represents next important component of antiviral defence induced by interferons. Mx1 protein is known to inhibit virus translocation into nucleus and its replication. Since Mx1 gene contains ISRE binding element, inhibition of JAK kinase signalling leads to downregulation of expression and induction of Mx1 and enhanced risk of viral infection[89].

Altogether, the activation of IFN-JAK/STAT pathway after viral infection results not only in induction and activation of numerous intrinsic antiviral factors, such as RNA-activated protein kinase (PKR), the 2-5A system or Mx1 but also in amplification of IFN positive regulatory loop and in enhanced signalling to immune system.

3.2.2 Involvement of JAK/STAT signalling pathways in development of cellular senescence

Besides viral infections, IFN-JAK/STAT signalling pathway was observed to be activated also in senescent cells[90]. Few years ago, Moiseeva et al. described that prolonged exposure of cells to interferon beta induces cell cycle arrest due to activation of p53. They observed the accumulation of gammaH2AX foci as well as phosphorylated forms of ATM and Chk2 in dependence on increased levels of ROS. Authors also speculate the role of STAT1 in acetylation and thus stabilization of p53 protein. Similarly, induction of senescence after constitutive exposure to interferon gamma was observed[91].

To show a direct role of STATs in senescence development, Malette et al. published that constitutively-activated form of STAT5A (ca-STAT5A) induces the Rb pathway by down-regulating Myc protein. As a consequence, cells expressing ca-STAT5 decrease expression of Myc targets such as CDK4 and increase CDK inhibitor p15INK4b (no effect on activation of p21waf1 or p16INK4a was observed)[92]. The same group also proved the induction of senescence after overexpression of promyelocytic leukemia protein (PML), a known target of STAT signalling, which will be discussed in next chapter[93]. Next to this work, Kuilman et al. described the role of IL6-JAK/STAT3 in promotion and maintenance of oncogene-induced cellular senescence (see Chapter 3.4.3.1).

3.2.3 STAT3 in oncogenesis

Signal transducer and activator of transcription 3 (STAT3) is a member of STAT family that was found to control a key signalling pathway in the development of many malignant diseases. Its role was observed in the regulation of apoptosis, cell differentiation, proliferation, angiogenesis, metastasis and immune responses that candidate this protein for cancer therapy[94].

Most of the major human malignancies like leukaemia, melanoma or breast and prostate carcinomas show elevated levels of constitutively activated STAT3 as well as elevation of STAT3-regulated gene expression. For many cancers, poor prognosis is associated with elevated levels of activated STAT3. STAT3-activated genes block apoptosis, favour cell proliferation and survival, promote angiogenesis and metastasis, and inhibit antitumor immune responses, thus inhibition of STAT3 signalling leads to decrease of tumorigenicity. The mechanism of constitutive activation of STAT3 depends on increased production of cytokines (especially IL6) and cytokine receptors, which affect the cell by autocrine/paracrine manner[95]. Also decreased expression of SOCS and PIAS proteins as well as the loss of PTP was observed in cancer cells. Mutation in JAK2 kinase resulting in its hyperactivation and constitutive STAT3 signalling was observed in some myeloproliferative disorders[96].

3.2.4 Non-canonical JAK/STAT signalling

As mentioned above, STATs are normally localized in cytoplasm in their latent form and they are translocated to the nucleus after phosphorylation and dimerization. However, it was

found previously that STAT1 and STAT3 also play important roles in mediating gene expression without tyrosine phosphorylation. Unphosphorylated STAT1 was found to activate expression of LMP2 as heterodimer with IRF1[97]. Also STAT1-dependent expression of many immune regulatory genes (e.g., IFI27, IFI44, OAS, and BST2) without STAT1 tyrosine phosphorylation and prolonged immune response to IFN treatment long after STAT1 dephosphorylation was observed[98]. In contrast, unphosphorylated STAT3 is able to bind to NFkB in competition with IkB, which results in NFkB activation and relocalization of this complex to nucleus, where it promotes expression of, for example, RANTES gene[99].

Phosphorylation of STAT1 is essential for its homo- or heterodimerization through conformational changes and for its binding on promoter of interferon-regulated genes containing palindromic element for two STATs subunits. It was observed that unphosphorylated STAT1 monomer is able to bind on the half of this palindrome sequence with weaker affinity, which may be increased by interaction of STAT1 with protein, whose binding site is nearby[97]. In a case of unphosphorylated STAT3, except its role as NFkB co-activator, there was found the ability of STAT3 to bind to GAS (gamma-activated sequence) element as well as to AT-rich DNA sequence sites and to recognize specific DNA structures, such as 4-way junctions and DNA nodes, within negatively supercoiled plasmid DNA. C-terminal truncated STAT3 isoform was found to recognize single-stranded spacers within cruciform structures. All these data suggest a role of unphosphorylated STAT3 as a chromatin organizer[100].

Since phosphorylation is necessary also for exposure of nuclear localization signal, there is a question, how are unphosphorylated STATs translocated into nucleus. After discovery of importin-mediated transport into nucleus, importin alpha5 was found to be necessary for translocation of tyrosine-phosphorylated STAT1, but there was no role of this importin as well as import receptor p97 for translocation of latent, unphosphorylated STAT1[101]. Recently, Fielhaber et al. published mechanism where latent STAT1 was translocated into nucleus in complex with mTOR through interaction with nuclear import adaptor karyopherin-α (KPNA1) after rapamycin treatment[102]. In contrast to STAT1, it was found that STAT3 binds to importin alpha3 or alpha6 through its coiled-coil domain independently on its phosphorylation[103].

3.2.5 The role of STAT3 in mitochondrial regulation

STAT3 is a cytoplasmic protein, which after translocation into nucleus acts as a key transcription factor of many genes. Discovery of unphosphorylated STAT3 involved in gene expression started the search for additional roles of STAT3 in controlling the cellular processes. In 2008, Pravin Sehgal for a first time pronounced the idea of STAT3 localization also into cytoplasmic compartments like mitochondria[104]. One year later David Levy and his colleagues brought evidence of STAT3 localized into mitochondria and its role in regulation of mitochondrial metabolic function after RAS transformation. They found that this localization does not require tyrosine phosphorylation. After RAS activation, the presence of mitochondrial STAT3 decreases cellular requirement of glucose. This metabolic shift represents an important attribute of tumour cells to growth in nutrition poor environment and provide an attractive target for therapeutic approaches to cancer[105].

During search for its localization in mitochondria, STAT3 was found to bind to complex I of respiratory chain. Since mitochondrial respiration produces reactive oxygen species, recent studies indicate that the inhibition of STAT3 increases mitochondrial membrane potential, production of ROS and causes DNA damage (Fig. 4). Upregulation of mitochondrial electron transport connected with downregulation of STAT3 mitochondrial pool was observed in several pathologic settings such as myocardial ischemia. The regulation of mitochondrial respiration here represents a cardioprotective mechanism to decrease cellular injury during ischemia, since experiments with reconstruction of mitochondrial STAT3 level showed decreased incidence of this disease in mice[106].

Mechanism of STAT3 translocation into mitochondria remains unclear. One possible alternative includes phosphorylation of STAT3 on serine 727, which induces its interaction with GRIM-19, a subunit of mitochondrial complex I, and their co-translocation to the mitochondria[107]. Phosphorylation of STAT3 on serine 727 was shown to be dependent on activation by ERK kinase, a member of mitogen-activated protein (MAP) kinases. There is a speculation that ERK-meidated serine 727 phosphorylation negatively modulates STAT3 tyrosine phosphorylation, its dimer formation, nuclear translocation, and the DNA binding activity, but more evidence to support this mechanism is required[108].

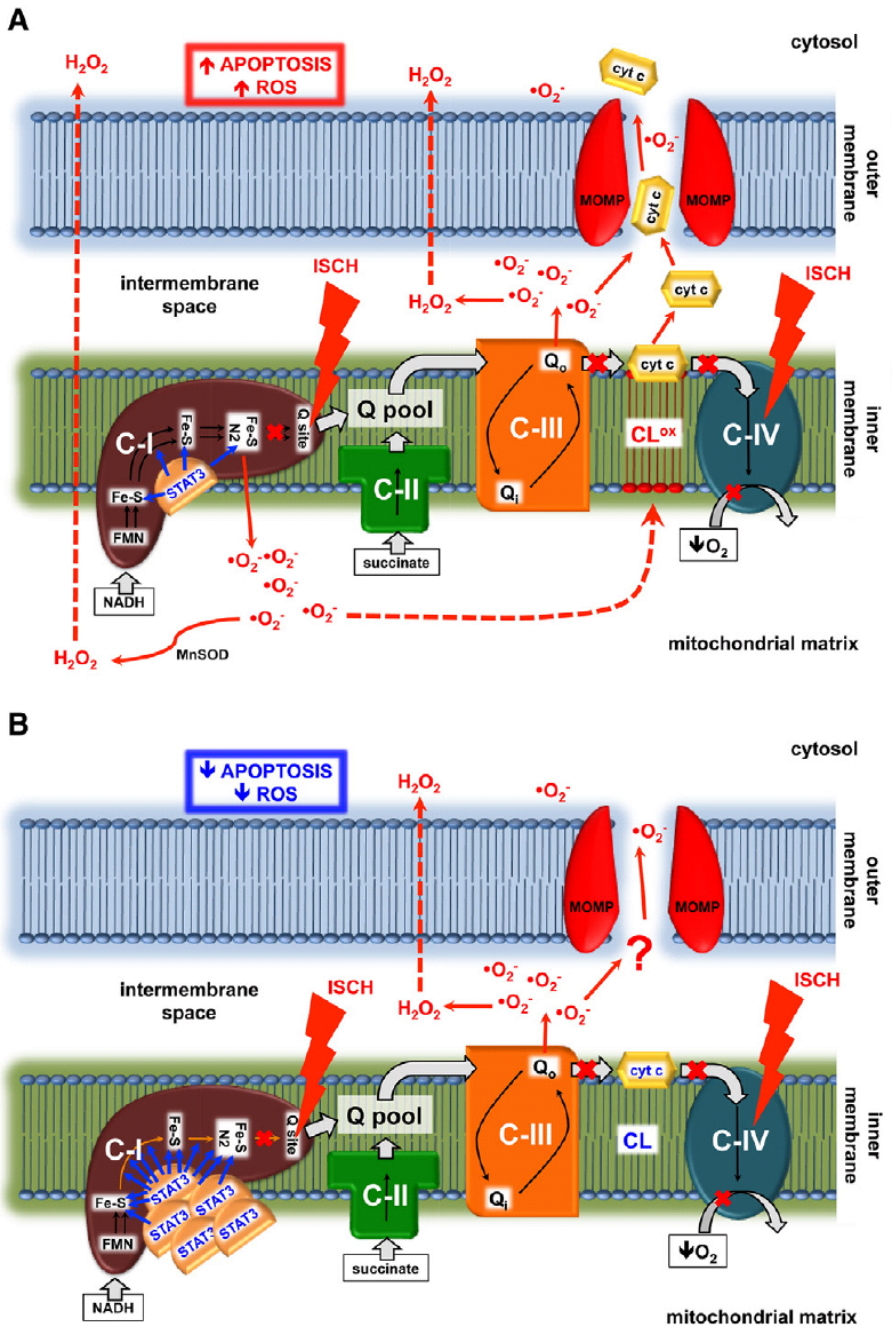

Figure 4. Mechanism of role of STAT3 as A) ROS inducer in low level or B) ROS inhibitor in high concentration in heart mitochondria during ischemia (Szczepanek K. et al., 2011).

3.3 Promyelocytic leukaemia protein

PML protein was originally discovered in patients with acute promyelocytic leukaemia (APL), which represents a highly malignant subtype of acute myeloid leukaemia (AML) comprising about 10% of all AML cases. Translocation of PML and retinoic acid receptor alpha (RARalpha) gene was found in almost 95% of APL patients, which results in inability of PML to assemble into microspeckles known as PML NBs and inhibits its function. PML-RARalpha fusion was then described to induce maturation block at the promyelocytic level[109].

3.3.1 Structure of PML

PML belongs to a tripartite motif family (TRIM), which contains zinc-finger RING domain, one or two cysteine/histidine-rich domains (B-box) and alpha-helical coiled-coil domain that allows PML to interact with other proteins and to form PML NBs[110]. As a result of alternative splicing of PML gene, we can recognize seven PML isoforms (I – VII) utilizing nine exons. All isoforms share N-terminus but differ in C-terminus (Fig. 5). Six isoforms (isoform I-VI) are localized in nucleus whereas isoform VII is in cytoplasm due to lack of exon 6 containing nuclear localization signal[111]. Molecular weight of unmodified PML isoforms ranges from 70 to 95 kDa. The function of individual isoforms differs – for example only PML IV was observed to promote senescence[112], whereas PML III interacts with centrosomes. PML II is able to make structures called PML fibers (Fig. 5). Also the level of individual isoforms varies in different type of cells – PML I was found to be a major isoform in nontransformed cells, but its level dramatically decreases in tumour cells in comparison with other isoforms suggesting its role in tumorigenesis[113].

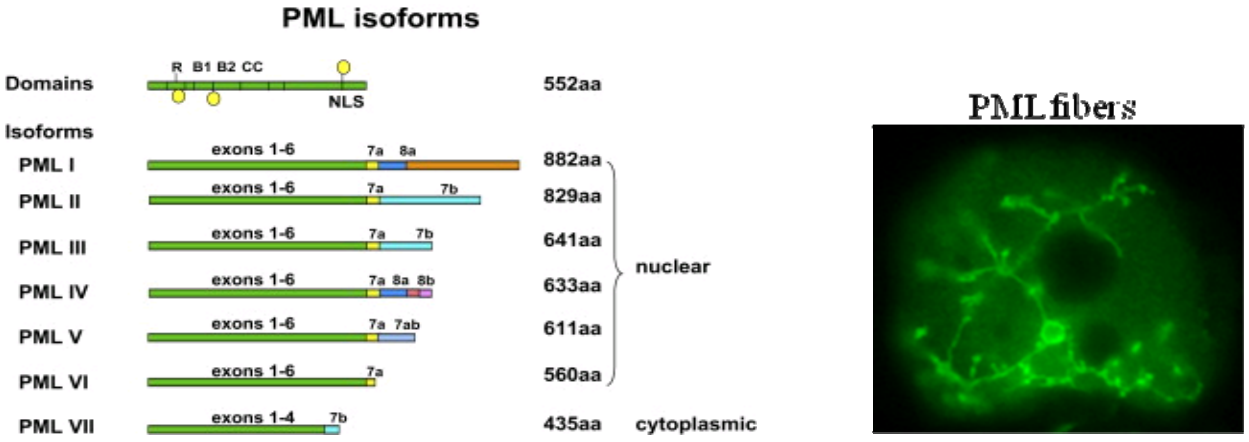

Figure 5. PML isoforms (left panel); PML fiber structure in HeLa cell after treatment with 0.5 μM camptothecin for 4 days (right panel); (left panel: Everett R.D. et al., 2007; right panel: Hubáčková S., unpublished data).

3.3.2 Transcriptional regulation of PML gene

PML was shown to be strongly induced during viral infection[114]. Since infections are accompanied with interferon signalling and JAK/STAT pathway activation, initiation of PML expression by this pathway was studied. In vitro experiments showed increased expression of PML as well as elevation of PML NBs number after IFN alpha, beta or gamma treatment[115]. Two important STAT binding sites were identified in PML gene regulatory region: IFN-stimulated response element (ISRE, at position of 595-628 bp from transcription start) and IFNgamma-activated site (GAS, at position 342-390 from transcription start). Binding of heterotrimer of STAT1, STAT2 and IRF9 (also known as p48 protein) forming ISGF3 complex on ISRE element after IFN type I (IFNalpha and beta) signalling or binding of STAT1 homodimer after IFNgamma on GAS was showed[116].

PML promoter also contains p53 responsive element. p53 was found to be required for induction of PML expression in response to oncogenic RAS that indicates PML participation in p53-mediated processes including cell cycle arrest or apoptosis[117].

Surprisingly, the activation of PML expression by beta-catenin was observed. Beta-catenin is a key component of Wnt signalling pathway playing a role in development and also cell cycle regulation. There is not known binding site for beta-catenin on PML promoter, but

experiments with PML promoter deletion mutants showed that beta-catenin acts through -78/+121 part of promoter[118].

IRF3 and IRF8 were found to regulate PML expression in astrocytes and macrophages, respectively, however their binding sites on PML promoter region have been not identified yet[119, 120].

Putative binding sites for NFkB, C/EBPbeta or nuclear factor 1 (NF1) was found on PML promoter in silico, but their involvement in PML regulation was not proved yet (data from Gene Cards).

3.3.3 Posttranslational modifications of PML

PML is subject of several posttranslational modifications, such as phosphorylation, ubiquitylation and sumoylation.

3.3.3.1 Sumoylation

SUMOylation (conjugation of small ubiquitin-homologous protein) represents the most important modification of PML prerequisite for PML NBs formation. Three SUMO modification sites of PML at lysine 65 (in the zinc finger domain), 160 (in the cysteine/histidine-rich domain) and 490 was found[121]. SUMOylation on lysine 65 plays a key role, because PML modified at this site is able to bind to SUMO binding motif situated on the exon 7 on the next PML molecule and to form PML NB[122].

3.3.3.2 Phosphorylation

Phosphorylation represents an important regulation of PML function. Similarly to other proteins, phosphorylation of some PML serine and tyrosine residues was found[123]. At normal cultivation conditions in vitro, phosphorylation of PML is observed mainly in mitotic cells and is connected with SUMO de-conjugation and PML NBs‘ destabilization. After the cell passes mitosis, PML becomes dephosphorylated and re-sumoylated and is able to restore nuclear bodies[124]. Following DNA damage, phosphorylation of PML by Chk2 in interphase cells was observed[125]. Casein kinase 2 (CK2), oncogenic kinase frequently up-regulated in tumour cells, was described to phosphorylate PML on serine 517, which provides a signal for PML ubiquitin-mediated degradation. Inhibition of this kinase correlates with decrease of tumorigenicity due to PML stabilization[126].

3.3.3.3 Ubiquitination

Polyubiquitination plays a key role in protein targeting for degradation in proteasome. Except CK2 described previously, several other proteins target PML for proteasomal degradation results in its ubiquitination by ubiquitin ligase RNF4[127]. The E2 ubiquitin conjugase UBC8 cooperates with the E3 ubiquitin ligase SIAH (seven in absentia homolog) to degrade PML in leukemic cells[128]. Under hypoxia, PML was found to be degraded by KLHL20 (Kelch-like protein 20), a Cullin 3-based ubiquitin ligase resulting in promote tumour growth promotion[129].

3.3.4 PML nuclear bodies

3.3.4.1 Structure of PML nuclear bodies

PML nuclear bodies also called nuclear domain 10 (ND10) or PML oncogenic domains (PODs) are dynamic, spherical and macromolecular structures resulting from assembly of multiple cellular proteins into distinct bodies. Their size varies between 0.1 to 1 μm. Number of PML NBs depends on cell type, cells with two or more than thirty bodies were observed[130]. More than hundred proteins, which belong to various groups like transcription factors (SP100, DAXX), DNA damage repair proteins (MRN11, Rad50, BLM), proteins involved in cell cycle regulation (Rb, p53) or chromatin remodelling proteins (HP1, HIRA) were identified in association with PML NBs. These proteins we may be divided into two groups: proteins present in bodies persistently or transiently[131-133].

There are probably several subtypes of PML NBs depending on their composition (and function). As the example of persistently present proteins are speckled protein of 100 kDa (SP100), DAXX, SUMO and Bloom syndrome helicase (BLM) and of course PML, which was found essential for PML NB formation[134].

Except ‚classical' bodies, PML association with specific nucleolar structures or containing nucleolar proteins were observed. This localization is prominent after disturbance of nucleolar functions – e.g. inhibition of rRNA processing, or activity of Pol I and II leading to nucleolar segregation. In these so called donut-like structures, presence of SP100 or SUMO proteins remains preserved. Nucleophosmin (B23), the protein known to accumulate in granular component of nucleolus, as well as nuclear DNA helicase II (NDHII) or transcription factor UBF

were found to be enriched in these PML nucleolar structures[135] (Fig. 6). Although the role of PML in nucleolar function is not clear, the absence of these nucleolar PML structures in rapid growing cells indicates their participation in cell cycle regulation[132].

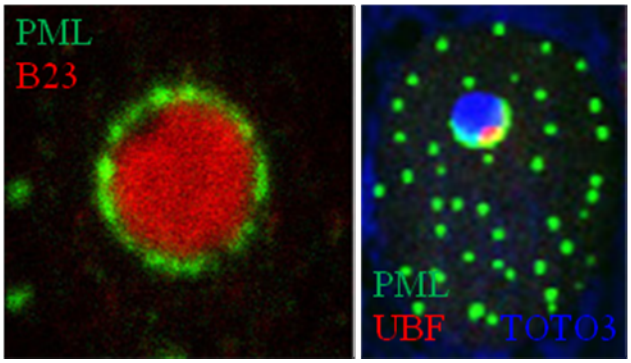

Figure 6. Accumulation of B23 in nucleolar PML "donut" in hMSC cells (left); colocalization of nucleolar PML with UBF in hMSC cells, RNA stained by TOTO3 was used as a marker of nucleoli (right). Comparison with classic PML NBs is shown (Janderova-Rossmeislova et al., 2007).

3.3.4.2 Presence of PML NBs during cell cycle

Similar to many other nuclear proteins, PML changes its intracellular distribution during progression of cell cycle. Increased number of PML NBs in S-phase was found to depend on chromatin doubling during replication, where at the end of S-phase two-fold elevation of PML NBs was observed as well as their binding on chromatin was proved by electron microscopy. Rather than de novo synthesis of PML protein during S-phase, fission of existing PML NBs was observed. Mechanism of this fission is still unknown[136].

During mitosis, PML NBs lose their components such as SUMO-1, DAXX and Sp100 in dependence on PML protein phosphorylation[137]. Part of the PML NBs remains associated with mitotic chromosomes, providing a possible nucleation site for PML nuclear body formation in subsequent G1. After nuclear envelope degradation in prometaphase, PML was identified in a cytoplasmic compartments that contain high concentrations of nucleoporins, especially NUP98, NUP153, NUP214 and Mab414. After finishing mitosis, these structures were able to move on microtubule filament and dock at nuclear membrane. Although PML NBs are dissolved, PML

itself is not degraded during mitosis, but provides a building material for restoration of PML NBs in daughter cells[138].

3.3.5 Function of PML

PML protein is involved in many cellular processes like gene transcription, proteasomal degradation, viral pathogenicity, DNA damage repair, cellular senescence, tumour suppression or apoptosis, although depletion of this protein is not lethal and PML knockout mice are viable but with increase incidence of tumours and sensitivity to infections. PML NBs were found to provide a storage site allowing the cell to maintain proper levels of various nuclear factors. Secondly, post-translational modifications of several proteins take place here[139].

3.3.5.1 Role of PML in DDR

Since colocalization of PML NBs with 53BP1 and γH2AX in the later phase, but not early after DNA damage, was observed, a proposition about the necessity of PML for formation of persistent DNA lesions was expressed (Fig. 7). However, knockdown of PML as well as using inactive PML-RARalpha fusion protein or inhibition of PML NB assembly using viral E1 protein do not indicate direct involvement of PML in DNA damage repair[140].

However, PML was found in tight contact with checkpoint kinase Chk2, ATM or BLM (a member of the RecQ DNA helicase family). It was speculated that PML may play a role as a marker of double strand breaks due to increased number of so called microbodies resulting from fission of classic PML nuclear bodies after DNA damage. There is a hypothesis that ATM is able to phosphorylate PML and than to cause its de-SUMOylation and the release from nuclear body. An inactivation or loss of factors like Nbs1, ATM, ATR or Chk2 inhibits PML microbody formation[132, 133].

NBS1 (Nijmegen breakage syndrome protein) was found to interact with PML NBs through binding with SP100 rather than PML itself. As already mentioned, NBS1 interacts with RAD50 and MRE11 to form MRN complex involved in DNA repair. Following DNA damage, MRN complex appears to leave PML NBs and goes to the sites of DNA breaks to activate DNA damage response. After damage repair, MRN complex was shown to re-localize back into PML NBs[141]. In contrast, TopBP1 (DNA topoisomerase 2-binding protein 1) forms nuclear foci that do not interact with PML NBs at normal condition, but there is a strong colocalization after DNA

damage, which blocks TopBP1 function and thus represents another mechanism, how cell inhibits cell cycle[142].

WRN, RecQ DNA helicase responsible for the autosomal disorder Werner syndrome (WS), is also linked to PML NBs. WRN is able to interact with p53 to enhance activation of p53-dependent genes. In normally proliferating cells, WRN is localized in nucleolus, but after DNA damage it relocalizes to nucleplasmic foci (containing also RAD51 and RPA), which co-associate with PML NBs. This relocalization leads to increase of p53 activation and growth arrest[143].

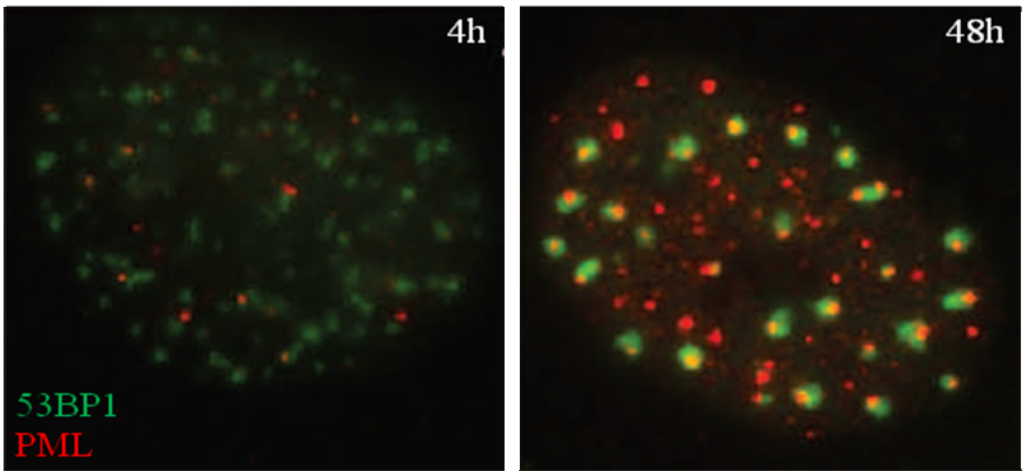

Figure 7. Colocalization of 53BP1 with PML NBs 4 hour and 48 hours after 0.5 μM camptothecin treatment in BJ cells (Hubackova et al., 2010).

3.3.5.2 Role of PML in cellular senescence

As mentioned, PML is increased in all types of senescence. In search whether PML alone is able to induce senescence, only PML isoform IV was found to arrest cell cycle. PML IV was found to bind CBP acetyltransferase and p53 to form a trimeric complex, where CBP acetylates p53 on lysine 382 and thus stabilize it[112]. This p53 stabilization was lost in PML-/- mouse fibroblasts[144].

Since PML promoter contains p53 binding site, activation of PML expression by RAS-induced p53 was shown. PML in turn helps to increase p53 phosphorylation and

stabilization[117]. Moreover, PML increases levels of p16ink4a and pool of hypophosphorylated Rb, which is sufficient to promote premature senescence.

Ferbeyre et al. later showed another mechanism, how PML IV over-expression induces cell cycle arrest and senescence. Phosphorylation of Rb protein is necessary for E2F release and activation of its transcription targets necessary for S-phase progression. These authors showed that PML IV is able to bind Rb and protect its phosphorylation and subsequent E2F activation. Return of E2F back into PML expressing cells rescued proliferation arrest and senescence[145].

HP1 and HIRA proteins, involved in formation of senescence-associated heterochromatin foci, a place where gene transcription is silenced, were found to cooperate with PML NBs after RAS transformation, thus facilitating promotion of oncogene-induced senescence[146, 147].

3.3.5.3 Role of PML in tumour development

PML is a strong tumour suppressor, thus it is not surprising that its levels in many types of human tumours are downregulated. Rather than inhibition of its expression, degradation in proteasome was observed. PML overexpression in cancer cells induces cell cycle arrest and decreases tumorigenicity of these cells[148]. Mice injected with prostate cancer cells with restored PML had decreased incidence of tumours than control mice injected with empty vector. Downregulation of PML in tumour cells also helps them to proliferate faster, because PML was describe to decrease the level of cyclin D1. As, mentioned, the well known example of PML inhibition during development of malignancy is fusion of PML gene with receptor of retinoic acid gene (RARalpha), which results in acute myeloid leukaemia. The overexpression of normal PML bypasses tumorigenicity of these cells[149].

3.3.5.4 Role of PML in viral defence

Any stage in virus replication may be a target for inhibition by IFNs, including entry, transcription, RNA stability, initiation of translation, maturation assembly and release. Since PML was shown to be induced by IFNs, its role in cell protection against virus has been studied[130]. PML is involved in some steps of antiviral defence. A decrease of Human Foamy Virus (HFV) gene expression was observed after PML induction or after IFN treatment. N-terminal region of PML interacts with viral transactivator protein Tas and inhibits its ability to activate expression of viral genes necessary for its replication[150]. DNA viruses have the ability

to incorporate their DNA into the host genome. Interestingly, PML was found to accumulate de novo in PML NBs close to places of incorporated viral genomes. This results in block of viral replication by inhibition of DNA polymerase complex binding to viral DNA. PML was also observed to target viral proteins for degradation by nuclear structure called clastosome with proteosomal activity[151].

Some viruses developed strategies how to overcome this defence. For example, after herpes simplex virus type-1 (HSV-1) infection, infected cell protein 0 (ICP0) is one of the first viral proteins expressed. ICP0 is an E3 ubiquitin ligase of the RING finger class proteins which localizes into PML NBs and induces the proteasome-dependent degradation of PML, SUMO and SP100[152]. Varicella-zoster virus (VZV) uses similar mechanism, but rather then PML degradation, it disrupts PML NBs by binding of its open reading frame 61 (ORF61) protein containing SUMO interacting motif on SUMOylated PML, which results in inability of PML to assembly into bodies[153]. Rabdhoviridae replicate in cytoplasm and Rabies virus phosphoprotein P is able to cluster cytoplasmic PML isoform thus inhibiting its anti-viral function[154].

3.4 Cytokine signalling

3.4.1 The role of cytokines in inflammation and cancer

Recent data have expanded the concept that inflammation is a critical component of tumour progression. Many cancers arise from site of infection, inflammation and chronic cytokine signalling. Organism produces a wide range of signals in response to tissue injury aiming to heal it. Chemotactic cytokines produced by infected cells recruit cells of immune system (mainly neutrophils and monocytes) into site of damage. Persisting signalling of these cytokines, especially pro-inflammatory TNFalpha, IL6, IL8 and IL1beta was found to be responsible for chronic diseases and cancer development[155].

During phagocytosis, leukocytes produce high level of relative oxygen and nitrogen species, which results in DNA damage in surrounding proliferating cells. A bypass of p53 function was also observed in cells surrounding infiltrated tissue. This together with production of DNA damage agents by either immune cells or infected cells and with ability of some cytokines to induce oncogenes (e.g. IL6 activates STAT3 signalling, which is connected with several malignancies), creates an environment for accumulation of potential oncogenic mutation and cancer development[156].

3.4.2 Cytokine signalling in DNA damage and senescence

The cessation of cell proliferation and senescence-associated changes in gene expression are accompanied with a robust increase in the mRNA levels and secretion of numerous cytokines, chemokines, growth factors and proteases. This phenomenon was termed senescence-associated secretory phenotype (SASP) or senescence messaging secretome (SMS). The SASP, or at least selected components of the SASP, play important roles in autocrine and paracrine signalling[157].

As the SASP results primarily from genomic damage response, one of its beneficial functions may be to communicate with cells of the immune system through secretion of pro-inflammatory cytokines to signal that there is a damaged cell and potential risk of tumour development. Senescent cells express ligands for cytotoxic immune cells and are eliminated mainly by natural killer cells[158]. SASP is not an acute inflammatory response, but develops progressively after DNA damage and persists for a long time. One of the possible mechanisms

involves the activation of p38 stress MAPK kinase in response to DNA damage, but independently on p53 activation or Rb dephosphorylation. In turn, the p38 pathway induces the expression of IL1beta, a cytokine which triggers autocrine/paracrine signalling and activates NFkB, a well known transcription activator of many cytokines including IL6 or IL8 involved in SASP. Inhibition of p38 activation after DNA damage results in downregulation of cytokine expression and secretion[159].

SASP may also function in regeneration of a tissue after damage, as induction of senescence has been observed in sites of skin wounding or liver damage. Senescence in skin fibroblasts appeared to be important for limiting fibrosis during damage repair by elimination of collagen and fibronectin, two proteins participating in fibrosis expansion, due to secretion of matrix metalloproteinases, which cleave these molecules[160].

Finally, the SASP includes factors that help maintain the tumour suppressive growth arrest, as will be discussed below.

Cellular senescence arrests tumour growth and eliminates damaged cells from proliferating pool (and likely from organism, see below), so it looks counterintuitive that this mechanism may have also adverse effects. Accumulating evidence shows that senescent cells can have deleterious effects on the tissue microenvironment. As noted earlier, senescent cells represent targets for immune cells. It was observed that in an old organism the activity of the immune system declines and may become insufficient to clear senescent cells, which can result in overproduction of these cells and accumulation of tissue damage, for example because of the increase in oxidative stress due to aberrant mitochondria[161].

In addition, increased numbers of senescent cells lead to decline or inhibition of body organ functions in an age-dependent manner. A relation has been found between the accumulation of senescent cells and age-related diseases. For example, cytokine secretion from senescent endothelial cells has been implicated in vascular calcification or formation of atherosclerotic lesions, two major risk factors for cardiovascular disease development in old people. Furthermore, senescent osteoblasts have been shown to participate in age-related osteoporosis and cell senescence also promotes many neurodegenerative diseases[162].

It has been found than not only the local microenvironment pathology, but also a variety of chronic degenerative diseases as well as cancer can be induced by circulating pro-inflammatory cytokines like IL6[163].

Thus, at present, senescent cells and their secretory phenotype seem to be both beneficial (tumour suppression) and deleterious (age-related diseases) depending on the circumstances and their ability to communicate with surrounding cells including cells of the immune system.

3.4.3 Maintenance of senescence by SASP

Cytokine signalling is involved in the activation of distinct pathways and regulates many cellular processes. It has also been implicated in the decision mechanisms controlling cellular senescence. Cytokines were found to activate the tumour suppressor pathways that establish the senescence related growth arrest. Following section describes several most common cytokines that has been found to be produced by senescent cells and their role in the maintenance of this phenotype.

3.4.3.1 Role of IL6 in senescence

IL6 was determined to have pleiotropic functions in a wide range of cells expressing gp130 and membrane bound IL6 receptor. This cytokine was found to have important role in human malignancies as an activator of STAT3 oncogene. Pre-clinically tested IL6 or IL6-R antibody showed tumour growth inhibition either alone or in combination with chemotherapy[164].

Oncogene-induced senescence, as all other types of senescence, is also accompanied with activation of pro-inflammatory cytokines. Unexpectedly, IL6 has been found to be necessary for execution of OIS since its depletion abolished both senescence entry and maintenance. IL6 has also been found to cooperate with C/EBPbeta transcription factor to amplify the inflammatory network, including IL8. In addition to the cytokine profile changes, downregulation of SAHF formation and p15 expression were observed after IL6 depletion in a model of OIS[165].

This observation is in contrast with the cytostatic role of IL6. Comparison of conditions where IL6 plays a role as an oncogene or as a senescence inducer revealed functionally different pools of this cytokine. Also the genetic background of the IL6 target cells, whether normal or transformed, contributes to specifying the biological response to IL6[166].

3.4.3.2 IL8 signalling

IL8 is together with IL6 one of the most abundant cytokines expressed in senescent cells. Overexpression of the chemokine binding receptor CXCR2 (also known as IL8RB), which is regulated by the NFkB and C/EBPbeta transcription factors, was found in OIS. Knockdown of this receptor moderates both replicative and oncogene-induced senescence in p53-dependent manner, as p53-/- MEF are resistant to CXCR2 overexpression or IL8 treatment and continue with proliferation. These results together with IL6 experiments suggest that senescent cells activate a self-amplifying secretory program, in which cytokines reinforce growth arrest[167].

3.4.3.3 TGFbeta1 in senescence

TGFbeta1 is another cytokine described to induce senescence[168]. TGFbeta signalling leads to SMAD2 and SMAD3 phosphorylation and heterotrimerization with SMAD4 coactivator. Relocalization of SMAD2/3/4 complex into nucleus triggers expression of genes linked also to cell cycle arrest. TGFbeta1 dependent growth arrest in G1 was accompanied by increased level of p15, p16 and activation of p53 [169]. Depletion of TGFbeta from cultivation medium results in constitutive Rb phosphorylation and induction of CDK2 and 4 kinase activity in mouse keratinocytes[170].

3.4.3.4 Plasminogen activator inhibitor (PAI)

Plasminogen activator inhibitor (PAI) is a serine protease inhibitor that functions as the principal inhibitor of tissue specific tissue (tPA) and urokinase (uPA) plasminogen activators, which catalyze the conversion of plasminogen to plasmin. Activated plasmin was found necessary for cellular movement and formation of metastasis[171]. Plasmin activates Rho kinase, which is important for actin polymerization and reorganization in leading edge during cell movement. Thus the activation of PAI and its inhibition of both plasminogen activators observed in senescent cells help to induce senescent phenotype also in absence of p53. Depletion of PAI from medium or induction of PA delays the onset of senescence. PAI was also suggested to inhibit PI3K-AKT pathway, thereby activating GSK3beta, which in turn decreases expression of cyclin D1[172].

3.4.4. Propagation of DNA damage and senescence by cytokine signalling in so called bystander effect

Cellular senescence is accompanied with increase of levels of more than fifty secreted cytokines involved in intercellular signalling. As was described previously, SASP serves as signalling for immune system but may also amplify senescent phenotype by autocrine manner. Since many pro-inflammatory cytokines were found to induce growth arrest themselves without prior damage, there was a question, if SASP is also able to influence normal surrounding cells.

It was shown using a model of irradiated cells that their medium enriched with cytokines is able to cause DNA damage in non-treated cells in mechanism so called „bystander effect“[173]. In vivo experiments on mouse model showed presence of DNA damage in tissue, which was not directly irradiated and was localized 0.7 centimeter apart of irradiated field. Using several methods, it was proved that the energy resulting from nuclear DNA radiation is not required to trigger this effect[174].

Cells are able to communicate not only by cytokine signalling, but also through mutual contacts by various connections, like GAP junction, where small signalling molecules may go through the cells. In experiment with mixed culture of irradiated and non-irradiated (bystander) cells there were no differences in γH2AX induction in bystander cells directly touching irradiated cell and that one which was not in direct contact. This indicates a role of cytokine/receptor signalling in development of bystander effect[175].

Rather than DNA double strand breaks observed in direct irradiated cells, point mutations were found to induce DNA damage signalling in bystander cells. By using 2,7-difluorofluorescein, free radicals were detected in cells treated with conditioned medium from irradiated cells. Free radical scavengers like N-acetylcysteine, filipin or 2-(4-carboxyphenyl)-4,4,5,5-tetramethylimidazoline-1-oxyl-3-oxide (c-PTIO) decrease formation of γH2AX foci in bystander cells. Superoxide dismutase (SOD) and NADPH oxidase are able to reduce ROS normally produced in cells as a product of mitochondria respiration. The overexpression of these enzymes decreases activation of γH2AX in bystander cells so there is a question, why they are not activated after treatment with medium from irradiated cells[176, 177]. Since induction of DNA damage in bystander cells is a long-term process, one possible mechanism may include inhibition of gene expression. In a genome-wide microarray comparing the changes in transcript

profiles in Me45 (human melanoma) cells grown in culture medium from normal or irradiated cells, the decrease in transcripts coding proteins involved in oxidative phosphorylation pathway like mitochondrial ATP synthase subunits, lysosomal proton-transporting ATPase subunits, subunits and proteins complexing cytochrome c oxidase and NADH dehydrogenase, succinate dehydrogenase, and ubiquinol-cytochrome c reductase was found, which again indicates changes in mitochondrial potential and ROS production in bystander cells[178].

γH2AX is activated by effector kinases as ATM, DNA-protein kinase (DNA-PK) or ATR after their activation and recruitment to the site of damage. Inhibition of ATM and DNA-PK could not suppress the induction of bystander γH2AX foci in glioma cells whereas the mutation of ATR abrogated bystander foci induction. Moreover, Seckel cells lacking ATR were not able to induce gammaH2AX in bystander cells. ATM was found to act downstream from ATR and its phosphorylation is dependent on ATR activation in bystander cells, which was also proved for UV-treatment, where base mutations and single strand DNA damage are induced. ATM then phosphorylates Chk2 or p53 and activates p21 which results in cell cycle arrest[179, 180].

It is interesting that some cell lines do not show bystander effect at conditions the other cell lines do. Human dermal fibroblasts (HDF) treated with medium from cells irradiated with 2 Gy rapidly induce DNA damage in bystander cells in comparison with HeLa cells which underwent the same process. Different level of cytokines after irradiation was found between these two cell lines. It was observed that some cytokines like MCP1 may prevent DNA damage induction, so bystander effect depends on their ratio with pro-inflammatory damaging cytokines produced by different type of cells[181].

Not only DNA damage but also induction of senescence in bystander cells was observed. Growth arrest, enhanced activity of beta-galactosidase, enlarged cell size and induction of p21 was found in MCF7 breast cancer cells after treatment with conditioned medium from senescent cells treated with doxorubicin, which was not caused by residual chemical in conditioned medium[182].

All this observations indicate that not only direct damage but also long-term exposition to stress-induced cytokines trigger activation of DNA damage response and may induce growth arrest and senescence on basis of ROS-dependent induction of DNA breaks formation, which means potential risk for normal cells to become a part of carcinogenic spreading and clarify

mechanism, how senescent cells are able to amplify their number resulting in organ dysfunction and development of age-related diseases.

4. List of used methods

Cell culture

Immunoblotting

Immunofluorescence

shRNA and siRNA transfection

β-galactosidase assay

Quantitative real time RT-PCR

Nuclear extraction

Plasmid cloning and transfection

Determination of cytokine secretion by FACS beads

Chromatin Immunoprecipitation (ChIP)

B9 proliferation assay

Luciferase assay

5. List of publications

#1 **Cytokine expression and signaling in drug-induced cellular senescence.**

Novakova Z, **Hubackova S**, Kosar M, Janderova-Rossmeislova L, Dobrovolna J, Vasicova P, Vancurova M, Horejsi Z, Hozak P, Bartek J, Hodny Z.

Oncogene. 2010 Jan 14;29(2):273-84.

#2 **Regulation of the PML tumor suppressor in drug-induced senescence of human normal and cancer cells by JAK/STAT-mediated signaling.**

Hubackova S, Novakova Z, Krejcikova K, Kosar M, Dobrovolna J, Duskova P, Hanzlikova H, Vancurova M, Barath P, Bartek J, Hodny Z.

Cell Cycle. 2010 Aug 1;9(15):3085-99

#3 **Interleukin 6 signaling regulates PML gene expression in human normal and cancer cells.**

Hubackova S, Krejcikova K, Bartek J and Hodny Z.

J Biol Chem. 2012 Aug 3;287(32):26702-14

#4 **Senescence-associated heterochromatin foci are dispensable for cellular senescence, occur in a cell type- and insult-dependent manner and follow expression of p16(ink4a).**

Kosar M, Bartkova J, **Hubackova S**, Hodny Z, Lukas J, Bartek J.

Cell Cycle. 2011 Feb 1;10(3):457-68

#5 Cytokines shape chemotherapy-induced and 'bystander' senescence.

Hodny Z, **Hubackova S**, Bartek J.

Aging (Albany NY). 2010 Jul;2(7):375-6 review

6. Participation of Sona Hubackova on presented publications

Research paper #1 – Sona Hubackova as co-author participated on measurement of IL6 and IL8 cytokine expression and secretion, elaborated experiments with JAK/JAK1 and IL6 inhibition

Research paper #2 – Sona Hubackova as a first author elaborated major part of experimental results, participated on manuscript preparation and submission

Research paper #3 - Sona Hubackova as a first author elaborated all experimental results except some qRT PCR measurements, participated on manuscript preparation and submission

Research paper #4 - Sona Hubackova as co-author participated on pilot experiments concerning induction of SAHF in drug-induced senescence

7. Linking of publications

Publication #1 characterizes cytokine expression and provides the insight into role of JAK/STAT signalling pathways in expression of tumour suppressors in chemically-induced senescence. We show the activation of IFN-JAK/STAT signalling pathway is involved in expression of many ISGs including potent tumour suppressors such as IRF1 and PML. More than two dozens of cytokine genes including interferon beta and gamma, IL6 and IL8 were induced by this form of senescence.

Since tumour suppressor PML belongs to family of genes induced by IFN-JAK/STAT pathway, in **publication #2** we focused on activation of PML transcription by JAK/STAT signalling in chemically-induced senescence. We show the importance of ISRE (STAT binding element) on PML promoter for PML transcription after DNA damage and senescence induction. The role of p53, another described transcription factor inducing PML transcription was also studied.

Publication #3 documents that PML transcription is activated by JAK/STAT3 pathway under unperturbed cell culture conditions. Furthermore, the role of transcription factor NFkB and IL6 cytokine as its target was examined.

PML and PML NBs are functionally linked to formation of senescence-associated heterochromatin foci (SAHF). To investigate the prerequisite of heterochromatinization for senescence induction and maintenance, in **publication #4** we monitored the formation of SAHF in three main forms of cellular senescence (i.e. replicative, oncogene-induced and drug-induced) in different cell types. Furthermore, correlation of SAHF formation with p16 was studied.

8. Discussion

1. Cytokine expression and signalling in drug-induced cellular senescence.

Cellular senescence, a barrier against tumorigenesis, is accompanied with many processes like irreversible cell cycle arrest and activation of tumour suppressor genes. In this study we provide an insight into the activation of JAK/STAT signalling pathway in premature senescence induced in tumour cells by various types of drugs used in chemotherapy, which may help to understand this phenotype and its clinical relevance.

IFN-JAK/STAT signalling pathway is known to be an important part of defence mechanisms against viral infection, where the activation of this pathway protects against viral replication in the cell and activates cells of the immune system. In contrast to viral infection, where JAK/STAT1 pathway is activated only transiently, we found a prolonged activation of JAK/STAT1 signalling (for several days) in cells induced to premature senescence by different drugs. The key phosphorylation of STAT1 on tyrosine 701 and serine 727, which are necessary for STAT1 translocation to nucleus and its transcription activity, were detected. After STAT1 activation, the induction of its downstream targets including tumour suppressors like IRF1, IRF7 (interferon regulated factor 1 and 7), STAT1 and MX1 (myxovirus 1 protein) was observed. IRFs were described to induce expression of interferons and consistent with this we showed for the first time the activation of expression and secretion of IFNβ and IFNγ in senescent cells. Surprisingly, there were no changes in eight IFNα isoforms measured, which indicates different regulation of IFNα and IFNβ genes in drug-induced senescence. Recent studies implicate the interferon regulatory factors IRF-3 and IRF-7 as key common activators of the IFNα and IFNβ genes. The discrepancies in expression of INFα and IFNβ observed in drug-induced senescent cells may be explained by different binding preference of IRF-3 and IRF-7 to promoters of individual interferon genes [183]. Long term persistence of IFN-JAK/STAT signalling indicates an engagement of a positive autocrine/paracrine regulatory loop involving IRFs, which is reminiscent of that operating in virus-infected cells[86]. In addition to interferons, elevated levels of more than two dozens of cytokines including IL6, IL8, IL24, TNF family, IL1β and IL20 were

found in drug-induced senescent cells. Note, the spectrum of cytokines detected is significantly broader than those reported for other types of senescence.

JAK family kinases play a crucial role in signal transmission from activated receptors. Downregulation of JAK1, a kinase capable to activate all STAT family members, as well as chemical inhibition of all JAK kinases with a specific inhibitor, blocked STAT1 phosphorylation and abolished subsequent downstream events such as induction of IRF1, MX1 and STAT1 itself both on mRNA and protein levels, but had no effect on activation of p53/p21 and p16/Rb pathways, two critical mechanisms in establishment of senescence, SA-beta-gal induction and development of senescent phenotype in general after drug treatment. These results were underscored by experiments where cellular senescence was induced in cell lines without JAK/STAT activation and thus indicate that JAK/STAT pathways are not prerequisite for drug-induced senescence in tumour cells.

At the time we have had been finishing this study, two studies reported quite unexpected findings that IL6 and IL8 are directly implicated in the induction and maintenance of oncogene-induced senescence[165, 167]. Although we confirmed the production of these cytokines also in drug-induced senescent cells, in contrast to study of Kuilman et al., knockdown of IL6 (> 90% efficient) was not able to prevent chemically-induced senescence, as well as activation of p53 and hypophosphorylation of Rb. Despite of IL6 knockdown, activation of STAT3 remained unchanged in drug-induced senescent cells, which indicates more complex mechanism of JAK/STAT3 activation in drug-induced senescence - likely due to a redundant role of multiple ligands capable of activation of this signalling pathway (such as interferons [184]).

In this work we show that activation of DNA damage signalling and induction of senescence in response to various drugs activates but is not dependent on JAK/STAT signalling. This indicates that this form of senescence differs from oncogene-induced senescence which induction and maintenance appears to be dependent solely on IL6 production. Nevertheless, the activation of JAK/STAT1 and STAT3 pathways in senescent cells plays an important role in induction of senescence-associated secretory phenotype (SASP), especially in induction of expression and secretion of interferons, which play an important role in immune cell activation and recruitment to the place of inflammation, and expression of important tumour suppressors IRF1, IRF7 and PML. We speculate that the production of cytokines and chemokines by

senescent cells contributes to their clearance by innate immunity, as is indicated in recent studies. Notably, the capability of SaOS cells, which lack functional p53 and Rb, to undergo drug-induced senescence, suggests involvement of other (i.e. p53/pRb-independent) senescence-inducing mechanism. One such candidate may be based on IRF1/p21Waf1/cip1 axis, which is activated by interferons in drug-induced senescence. If confirmed experimentally, this will support the importance of cytokine signalling in development of this form of senescence.

2. Regulation of the PML tumour suppressor in drug-induced senescence of human normal and cancer cells by JAK/STAT-mediated signalling.

The induction of PML and its accumulation in nuclear compartment known as PML nuclear bodies are among the well known markers found in all type of senescence and decreased levels of this tumour suppressor were found in more than two thirds of human cancer types [185]. In the previous work discussed we described the activation of JAK/STAT1 and JAK/STAT3 signalling pathways in drug-induced senescent cells. Since PML belongs to the group of interferon stimulated genes[116], we tested whether PML is directly induced by activated JAK/STAT pathway in senescent cells. We found the elevated levels of PML protein, PML NBs and also PML mRNA in tumour cell lines and human primary fibroblasts after treatment with various types of drugs. Experiments with cycloheximide, which blocks de novo protein synthesis, showed that elevation of PML NB and PML protein in senescent cells is accompanied by the increase of PML transcript rather than PML stabilization at protein level. During these experiments, significantly longer PML half-life was observed in comparison with data published by Scaglioni et al. (>24 vs. 3 hrs.). Since they measured PML stability only in virally transformed HEK293 and mouse 3T3 cells and analyzed only one PML isoform, we suggest that PML protein turnover may vary among cell types, the nature of stress and PML isoforms[126].

PML NBs were described to be a docking site for many proteins involved in regulation of the cell cycle and DNA damage response signalling. Colocalization of PML NBs with DNA damage foci not immediately, but in later phases after DNA damage induction [133] suggests their role in formation of persistent DNA damage foci, which may block cell cycle recovery

possibly due to irreparability of specific type of DNA lesions. In agreement with these studies, we also found colocalization of PML NBs with sites of long-term persisting DNA damage foci (positive for modified histone H2AX and other markers of DNA double strand breaks such as 53BP1), but not with acute DNA damage foci formed within first 12 hours after treatment by different DNA damaging drugs. Therefore, formation of PML NBs close to the sites of DNA damage might remark problematic lesions without chance to be repaired, which results in persistent activation of DNA damage response taking place partially in PML NBs. Although Campisi et al. shows that inhibition of PML NBs formation has no effect on persistent DNA damage foci induction[140], different role of PML NBs in DNA damage response is still not excluded.

Stadler et al. described binding of STAT1 and STAT2 on PML promoter after interferon stimulation[116]. In our work, we observed that downregulation of JAK1 kinase abrogates STAT1 activation and induction of its downstream targets. Here we used a specific inhibitor to block all four JAK kinases and demonstrated decreased PML expression in drug-induced senescent cells. Moreover, a decrease in the level of JAK1 kinase induced with a specific siRNA results again in downregulation of PML expression indicating an important role of this specific kinase in regulation of PML transcription. Since inhibition of JAK signalling abrogates PML expression only partially (50%), additional mechanisms such as the regulation by NFkB pathway, which is known to be induced in senescent cells and the putative NFkB or Sp1 binding motifs were found on PML promoter, may be involved in PML gene regulation. Beside interferons, JAK1 kinase may be activated by many other cytokines which we found expressed after genotoxic stress, for example IL6, IL8 and IL10. Therefore, there might be some redundancy in activation of JAK/STAT signalling, which can explain the differences between various forms of senescence, as mentioned above. Which cytokine(s) produced by senescent cells is involved in activation of JAK/STAT signalling and expression of PML is a task for future studies.

PML promoter contains several STAT binding sites. Stadler et al. identified two specific DNA binding elements, ISRE at position 628-595 and GAS at position 390-342 relative to transcription start site, which mediate induction of PML expression after interferon treatment[116]. Our results using gel retardation assay demonstrated the involvement of ISRE,

but not GAS element, in regulation of PML transcription in drug-induced senescent cells. Reporter assay with wild type proximal PML promoter (1.44 kb) and PML promoter lacking the ISRE element verified these results, which strongly indicate the necessity of ISRE element in chemically induced PML transcription. It was described recently that STAT-IRF1 heterodimer binds on ISRE element of LMP2 promoter[97]. Since the overexpression of IRF1 leads to elevation of PML transcript[119] and since we detected elevated level of IRF1 dependent on JAK/STAT activation after genotoxic stress (discussed above), there is a possibility that PML is regulated also by this transcription factor. However, this hypothesis needs further experimental clarification.

The activation of DNA damage response in cellular senescence includes stabilization of p53. Since p53 was described to regulate PML expression in mouse embryonal fibroblasts after RAS activation[117], we tested whether p53 may regulate PML also in our model of drug-induced senescence. For this experiment, we used p53 wild type and p53 knock-out HCT116 cell lines. Both cell lines were able to respond with induction of both PML mRNA and protein and development of senescent phenotype after drug treatment indicating that p53 is not necessary for increased PML expression (and senescence per se) under these conditions. When we inhibited the activity of kinases JAK with the specific inhibitor after drug treatment, we clearly showed a decrease of PML protein level as well as transcript in both cell lines providing the evidence the JAK/STAT pathway is involved in PML regulation in senescent cells. These results were verified using U2OS cells with tetracycline-regulated expression of dominant negative form p53 (U2OS DN-p53 tet-off system[186]) where we also observed no differences in PML expression after DNA damaging drug treatment between wild type and dominant negative p53-expressing cells. There is a question, whether and how the activation of DDR after genotoxic stress may contributes to JAK/STAT activation and PML transcription. Beside the activation of cytokine expression through activation of p38MAPK/NFkB/IL1, IL6, IL8 pathway[159], an activation of c-ABL kinase via ATM[187] and subsequent STAT1 phosphorylation can be also involved.

Our results provide novel mechanistic insight into the regulation of PML mRNA expression during drug-induced genotoxic stress and point to the significance of autocrine/paracrine stimulation in development of senescent phenotype, as was described in our previous study.

3. Interleukin 6 signalling regulates PML gene expression in human normal and cancer cells.

In our previous studies we found the activation of JAK/STAT signalling pathways in drug-induced prematurely senescent cells and its role in induction of PML gene expression in these cells. As already mentioned, PML protein is the well described tumour suppressor, but regulation of its expression is poorly understood. Two signalling pathways, JAK/STAT and p53 were reported to participate in regulation of PML gene transcription after interferon stimulation and oncogenic RAS activation[116, 117]. Both of these studies described transient elevation of PML mRNA and protein under the stress conditions, but none has addressed the mechanism of constitutive expression of this antiviral and tumour suppressor under unperturbed conditions.

As described previously, various cell lines and primary cells express different levels of PML protein under unperturbed conditions in vitro[188]. We selected three human cell types that feature low (U2OS), medium (HeLa) and high (BJ, at population doublings <35) numbers of PML nuclear bodies. By qRT-PCR, we confirmed a correlation between PML protein level and PML mRNA in these three types of cells. Intriguingly, similar to drug-induced senescent cells, we found the direct involvement of cytokine autocrine/paracrine signalling in regulation of basal levels of PML. We observed increased PML transcription and protein induction in U2OS cells treated with conditioned medium from BJ cells (i. e. cells with high level of basal PML). As we observed no changes in the level of DNA damage response (measured by activation of p53 and phosphorylation of histone H2AX as a marker of double strand breaks) and activity of stress signalling (determined as the activation of p38MAPK), we ruled out any effect of activated p53 on PML transcription. When we analyzed the activity of the STAT pathways (STAT1/2, STAT3, STAT5) in our three selected cell types, we found direct correlation of activated STAT3, but not STAT1 and STAT5 with PML NBs, PML mRNA and protein levels. Using specific cytokine FACS beads assay, we determined conformity in the amount of STAT3 activating ligand IL6 secreted into culture media. IL6 added into culture medium of U2OS or HeLa cells induced PML transcription and the increase of number of PML NBs. Depletion of IL6 from medium using a specific neutralizing antibody or knock-down of STAT3 by siRNA decreased STAT3 active form, PML NBs, PML mRNA and protein level in BJ cells. Kinetic study of STAT3 activation and PML expression after IL6 treatment showed delayed responsiveness of U2OS cells, where phosphorylation of STAT3 on tyrosine 705 was observed not before 48 hours after treatment and

correlated with delayed increase of total STAT3, which indicates the correlation between constitutive level of STAT3 and the dynamics of response to IL6. In comparison with U2OS cells, the response of HeLa cells, which possess higher basal level of STAT3 protein, was fast approaching the rate characteristic for JAK/STAT signalling. Since STAT3 protein is regulated by itself in positive feedback, we suggest that U2OS cells with low level of STAT3 need more time to express it, which likely generates a delay observed in response of PML gene expression to IL6 treatment.

Deletion of PML ISRE element at position (-595/-628) led to a decrease of luciferase reporter gene activity in cells exposed to interferon alpha or beta as well as in cells exposed to various DNA damaging drugs inducing premature senescence. We confirmed the importance of this element also for the regulation of basal PML transcription. We proved the direct binding of STAT3 on PML promoter using chromatin immunoprecipitation. This is not so unexpected, as all members of the STAT family recognize similar consensus binding site. In fact, the PML ISRE element resembles STAT3 consensus better than that of STAT1[189]. Taking together, our data indicate that IL6 controls PML gene expression under unperturbed conditions via JAK/STAT3 signalling and activated STAT3 binds directly to PML gene promoter.

In addition to JAK/STAT3 activation, binding of IL6 on its receptor triggers also the PI3K/Akt pathway[190] which controls NFkB activation. Indeed, the active form of Akt kinase correlated with secreted IL6 in all three cell lines tested. Knock-down of NEMO, the gamma subunit of IKK kinase and a key component of NFkB activation, resulted in suppression of PML gene transcription and protein induction, but simultaneously led to decrease in IL6 expression and secretion and STAT3 activation. Consistent with the known ability of NFkB to control the expression of IL6 gene, the effect of NEMO knock-down on PML expression and down-regulation of NFkB activity was abolished by recombinant IL6, which suggests indirect role of NFkB in PML regulation via modulation of IL6 production. Combined knock-down of NEMO and STAT3 did not result in additive or synergistic effect on PML expression which support our conclusion that NFkB acts in series with STAT3 signalling rather than in parallel (Fig. 5I). Despite these results we still cannot exclude the possibility that PML may be partially regulated by NFkB, as several putative NFkB binding site are present on PML promoter. As was discussed in previous work[97], the involvement of IRF1 in regulation of PML basal level is another

alternative . Since IRF1 gene is known target of NFkB, the decreased level of PML transcription after IL6 or NEMO depletion may be partially influenced by inhibition of IRF1 expression, as is shown on figure 5H.

In summary, the novel finding of this study is that in addition to IFN-JAK/STAT1 pathway, IL6-JAK/STAT3 signalling controls also PML gene expression. Since IL6 is a well known signalling molecule that mobilizes organism-protective systems including innate and acquired immunity, our results indicate, that IL6 also can help to protect the organism by activation of PML tumour suppressor gene.

4. Senescence-associated heterochromatin foci are dispensable for cellular senescence, occur in a cell type- and insult-dependent manner and follow expression of p16 ink4a.

As shown in Chapter 3.1.1.1, senescent cells have many specific characteristics, but there is no universal marker characterizing all forms of senescence, which complicates detection of senescent cells especially in vivo, where senescence characteristic morphological changes or expression of B-galactosidase are hardly applicable. As discussed above, the increase in PML protein level was found in all type of senescent cells, but induction of PML transcription may also reflect not only senescence but other cellular responses to stress such as viral infection. Formation of senescence-associated heterochromatin foci (SAHF) is accompanied with reduction of transcription in the cell including transcription of the genes necessary for cell cycle progression[191]. SAHF were observed in several forms of cellular senescence, which makes them the candidate for the universal senescence marker. However, previous studies focused mostly on the mechanism of SAHF formation, such as involvement of pRb pathway in SAHF formation or mechanisms of chromatin modifications, the role of SAHF in transcriptional control of the cell cycle promoting genes, all mainly in the context of oncogene-induced senescence. Since SAHF have been studied mostly using fibroblasts, which are in fact not the best model for studying cancer pathologies that most frequently affect epithelial cells, we wanted to examine the relevance of SAHF in a broader spectrum of cell types, including neonatal human epidermal keratinocytes (HEKn), furthermore the occurrence of SAHF in various types of senescence and whether these structures are applicable for detection of cellular senescence in vivo.

First, our experiments showed that SAHF formation differs not only between the types of cellular senescence, but also varies among cell types exposed to the same senescence-inducing stimulus. We showed that some cells (MRC5) are more sensitive to formation of these structures during oncogene-induced as well as replicative or drug-induced senescence in comparison with others (BJ and HEKn). Importantly, we showed the formation of SAHF after treatment with several chemotherapeutic drugs or bacterial toxin produced by facultative pathogenic strains of Gram-negative bacteria Haemophilus ducreyi (i.e. cytolethal distending toxin, CDT;[192]) in MRC5 fibroblasts, but not in BJ fibroblasts or normal keratinocytes.

Secondly, Bartkova et al. observed the presence of heterochromatinization markers H3K9Me3 and HP1gamma in clinical specimens of premalignant human lesions[193]. Therefore we investigated whether typical DNA-DAPI defined SAHF could be detected in human tissues and tumours. Experiments with paraffin sections prepared from fibroblasts undergoing oncogene-induced senescence and stained by DAPI showed that routine tissue processing might reduce, but not completely prevent the ability to detect SAHF. Using exactly the same procedure of immunofluorescent staining on series of sections from tissues of human urinary bladder tumours (n=19), normal human bladder (n=5), colon (n=16), colorectal adenomas (grade III, n=38) and colon carcinomas (n=44), no clear evidence of DNA-DAPI-defined formation of SAHF was observed despite the positive expression pattern of H3K9Me3, HP1gamma and senescence-associated beta-galactosidase activity. Thus our results suggest that identification of senescent cells through detection of DAPI-defined SAHF may not be feasible.

Finally, correlation between the ability to form SAHF and the increased level of p16INK4a in various types of senescence was studied. p16 is an important CDK inhibitor whose involvement in cellular senescence was described and explained by its ability to induce hypophosphorylation of the Rb protein. High expression of p16 was identified as a marker of senescent cells in the skin of old people[194]. However, the induction of senescence was also observed in cells with low level of p16 due to activation of p53/p21 axis and possibly other mechanisms activating cell cycle checkpoints. We found the activation of p16 strongly correlated with the ability of cells to form SAHF at particular conditions, especially after RAS induction, in contrast for example to BJ cells, where virtually undetectable levels of p16 after treatment with various drugs or CDT correspond with their inability to form SAHF. These findings support

previous observation that p16 is not essential for every mode of cellular senescence, but is critical for heterochromatinization, engagement of Rb and irreversible cell cycle arrest.

9. Conclusions

In this work we wanted to contribute to understanding molecular mechanisms of cellular senescence, important tumorigenesis barrier, with the aim to identify the role of cytokines and cytokine controlled signalling pathways in functional status of senescent cells.

This work brings new findings, which can be summarized as follows:

- commonly used chemotherapeutic drugs are able to induce premature cellular senescence in normal and cancer cells accompanied with the activation of complex cytokine network including many pro-inflammatory cytokines
- autocrine/paracrine signalling mediated by these cytokines helps to induce and maintain senescence phenotype including the expression of tumour suppressor genes in senescent cells
- activation of JAK/STAT signalling pathways in senescent cells contributes to maintenance of cytokine environment by regulation of expression of various cytokines, nonetheless does not play the crucial role in induction of drug-induced senescence
- secretion of cytokines by senescent cells and their autocrine/paracrine effects through JAK/STAT pathways play the essential role in activation of PML gene transcription rather than by induction via DNA damage response-activated p53
- IL6 is not essential for maintenance of drug-induced senescence, in contrary to oncogene-induced senescence
- apart from genotoxic stress-induced senescence phenotype, cytokine driven JAK/STAT3 activation plays the important role in induction of PML gene expression also under the unperturbed condition
- formation of senescence-associated heterochromatinization is not universal for all types of senescence and is not necessary for induction of senescence, namely for drug-induced and replicative senescence
- formation of SAHF correlates with induction of p16, which underscores their causal role in maintenance of senescence mediated through p16/Rb pathway

10. Significance of results and future prospects

Since various drugs used in this study are routinely applied for diagnostic and therapeutic purposes in clinical settings, all findings summarized in this work are relevant for clinical aspects of cancer biology. Knowledge of consequence of autocrine/paracrine activation of JAK/STAT/PML pathways may show their clinical relevance with regard to the development of so-called “bystander effects” observed after radiotherapy and chemotherapy. In our future plans, we will study the effects of genotoxic stress-induced cytokine signalling on cancer microenvironment in more detail with the aim to better understand its benefits/disadvantages for organism during therapy of cancer.

11. References

1. Halazonetis, T.D., V.G. Gorgoulis, and J. Bartek, *An oncogene-induced DNA damage model for cancer development.* Science, 2008. 319(5868): p. 1352-5.

2. Perry, J.A. and S. Kornbluth, *Cdc25 and Wee1: analogous opposites?* Cell Div, 2007. 2: p. 12.

3. Germann, M.W., C.N. Johnson, and A.M. Spring, *Recognition of damaged DNA: structure and dynamic markers.* Med Res Rev, 2010.

4. Faucher, F., S. Doublie, and Z. Jia, *8-oxoguanine DNA glycosylases: one lesion, three subfamilies.* Int J Mol Sci, 2012. 13(6): p. 6711-29.

5. Yang, J., et al., *ATM, ATR and DNA-PK: initiators of the cellular genotoxic stress responses.* Carcinogenesis, 2003. 24(10): p. 1571-80.

6. Bartek, J. and J. Lukas, *DNA damage checkpoints: from initiation to recovery or adaptation.* Curr Opin Cell Biol, 2007. 19(2): p. 238-45.

7. Jackson, S.P. and J. Bartek, *The DNA-damage response in human biology and disease.* Nature, 2009. 461(7267): p. 1071-8.

8. Grenon, M., C. Gilbert, and N.F. Lowndes, *Checkpoint activation in response to double-strand breaks requires the Mre11/Rad50/Xrs2 complex.* Nat Cell Biol, 2001. 3(9): p. 844-7.

9. Lee, J.H. and T.T. Paull, *Direct activation of the ATM protein kinase by the Mre11/Rad50/Nbs1 complex.* Science, 2004. 304(5667): p. 93-6.

10. Zou, L. and S.J. Elledge, *Sensing DNA damage through ATRIP recognition of RPA-ssDNA complexes.* Science, 2003. 300(5625): p. 1542-8.

11. Ahn, J.Y., et al., *Threonine 68 phosphorylation by ataxia telangiectasia mutated is required for efficient activation of Chk2 in response to ionizing radiation.* Cancer Res, 2000. 60(21): p. 5934-6.

12. Wang, X.Q., et al., *ATR dependent activation of Chk2.* J Cell Physiol, 2006. 208(3): p. 613-9.

13. Bartek, J. and J. Lukas, *Chk1 and Chk2 kinases in checkpoint control and cancer.* Cancer Cell, 2003. 3(5): p. 421-9.

14. Harper, J.W., et al., *The p21 Cdk-interacting protein Cip1 is a potent inhibitor of G1 cyclin-dependent kinases.* Cell, 1993. 75(4): p. 805-16.

15. Mailand, N., et al., *RNF8 ubiquitylates histones at DNA double-strand breaks and promotes assembly of repair proteins.* Cell, 2007. 131(5): p. 887-900.

16. Doil, C., et al., *RNF168 binds and amplifies ubiquitin conjugates on damaged chromosomes to allow accumulation of repair proteins.* Cell, 2009. 136(3): p. 435-46.

17. Konishi, H., et al., *Mutation of a single allele of the cancer susceptibility gene BRCA1 leads to genomic instability in human breast epithelial cells.* Proc Natl Acad Sci U S A, 2011. 108(43): p. 17773-8.

18. Molchadsky, A., et al., *p53 is balancing development, differentiation and de-differentiation to assure cancer prevention.* Carcinogenesis, 2010. 31(9): p. 1501-8.

19. Vousden, K.H. and X. Lu, *Live or let die: the cell's response to p53.* Nat Rev Cancer, 2002. 2(8): p. 594-604.

20. Pei, D., Y. Zhang, and J. Zheng, *Regulation of p53: a collaboration between Mdm2 and Mdmx.* Oncotarget, 2012. 3(3): p. 228-35.

21. Lu, X., et al., *The Wip1 phosphatase and Mdm2: cracking the "Wip" on p53 stability.* Cell Cycle, 2008. 7(2): p. 164-8.

22. Fang, S., et al., *Mdm2 is a RING finger-dependent ubiquitin protein ligase for itself and p53.* J Biol Chem, 2000. 275(12): p. 8945-51.

23. Goh, A.M., C.R. Coffill, and D.P. Lane, *The role of mutant p53 in human cancer.* J Pathol, 2011. 223(2): p. 116-26.

24. Komarova, E.A., et al., *p53 is a suppressor of inflammatory response in mice.* FASEB J, 2005. 19(8): p. 1030-2.

25. Rayess, H., M.B. Wang, and E.S. Srivatsan, *Cellular senescence and tumor suppressor gene p16.* Int J Cancer, 2012. 130(8): p. 1715-25.

26. Lieber, M.R. and Z.E. Karanjawala, *Ageing, repetitive genomes and DNA damage.* Nat Rev Mol Cell Biol, 2004. 5(1): p. 69-75.

27. Hayflick, L., *The Limited in Vitro Lifetime of Human Diploid Cell Strains.* Exp Cell Res, 1965. 37: p. 614-36.

28. Reddel, R.R., *Senescence: an antiviral defense that is tumor suppressive?* Carcinogenesis, 2010. 31(1): p. 19-26.

29. Bartek, J., J. Lukas, and J. Bartkova, *DNA damage response as an anti-cancer barrier: damage threshold and the concept of 'conditional haploinsufficiency'.* Cell Cycle, 2007. 6(19): p. 2344-7.

30. Hanahan, D. and R.A. Weinberg, *The hallmarks of cancer.* Cell, 2000. 100(1): p. 57-70.

31. Rodier, F. and J. Campisi, *Four faces of cellular senescence.* J Cell Biol, 2011. 192(4): p. 547-56.

32. Rodier, F., J. Campisi, and D. Bhaumik, *Two faces of p53: aging and tumor suppression.* Nucleic Acids Res, 2007. 35(22): p. 7475-84.

33. Schlereth, K., et al., *DNA binding cooperativity of p53 modulates the decision between cell-cycle arrest and apoptosis.* Mol Cell, 2010. 38(3): p. 356-68.

34. Gu, J., et al., *Mechanism of functional inactivation of a Li-Fraumeni syndrome p53 that has a mutation outside of the DNA-binding domain.* Cancer Res, 2001. 61(4): p. 1741-6.

35. Blagosklonny, M.V., *Cell cycle arrest is not yet senescence, which is not just cell cycle arrest: terminology for TOR-driven aging.* Aging (Albany NY), 2012. 4(3): p. 159-65.

36. Baker, D.J., et al., *Clearance of p16Ink4a-positive senescent cells delays ageing-associated disorders.* Nature, 2011. 479(7372): p. 232-6.

37. Laberge, R.M., et al., *Glucocorticoids suppress selected components of the senescence-associated secretory phenotype.* Aging Cell, 2012. 11(4): p. 569-578.

38. Krizhanovsky, V., et al., *Implications of cellular senescence in tissue damage response, tumor suppression, and stem cell biology.* Cold Spring Harb Symp Quant Biol, 2008. 73: p. 513-22.

39. Nelson, G., et al., *A senescent cell bystander effect: senescence-induced senescence.* Aging Cell, 2012. 11(2): p. 345-9.

40. Kang, T.W., et al., *Senescence surveillance of pre-malignant hepatocytes limits liver cancer development.* Nature, 2011. 479(7374): p. 547-51.

41. Campisi, J., *Cellular senescence: putting the paradoxes in perspective.* Curr Opin Genet Dev, 2011. 21(1): p. 107-12.

42. Yeager, T.R., et al., *Overcoming cellular senescence in human cancer pathogenesis.* Genes Dev, 1998. 12(2): p. 163-74.

43. Krtolica, A., et al., *Senescent fibroblasts promote epithelial cell growth and tumorigenesis: a link between cancer and aging.* Proc Natl Acad Sci U S A, 2001. 98(21): p. 12072-7.

44. Parrinello, S., et al., *Stromal-epithelial interactions in aging and cancer: senescent fibroblasts alter epithelial cell differentiation.* J Cell Sci, 2005. 118(Pt 3): p. 485-96.

45. Krizhanovsky, V., et al., *Senescence of activated stellate cells limits liver fibrosis.* Cell, 2008. 134(4): p. 657-67.

46. Ellis, R.E., J.Y. Yuan, and H.R. Horvitz, *Mechanisms and functions of cell death.* Annu Rev Cell Biol, 1991. 7: p. 663-98.

47. Hampel, B., et al., *Differential regulation of apoptotic cell death in senescent human cells.* Exp Gerontol, 2004. 39(11-12): p. 1713-21.

48. Campisi, J. and F. d'Adda di Fagagna, *Cellular senescence: when bad things happen to good cells.* Nat Rev Mol Cell Biol, 2007. 8(9): p. 729-40.

49. Lawless, C., et al., *Quantitative assessment of markers for cell senescence.* Exp Gerontol, 2010. 45(10): p. 772-8.

50. Freund, A., et al., *Lamin B1 loss is a senescence-associated biomarker.* Mol Biol Cell, 2012. 23(11): p. 2066-75.

51. Nishio, K., et al., *Senescence and cytoskeleton: overproduction of vimentin induces senescent-like morphology in human fibroblasts.* Histochem Cell Biol, 2001. 116(4): p. 321-7.

52. Wang, E. and D. Gundersen, *Increased organization of cytoskeleton accompanying the aging of human fibroblasts in vitro.* Exp Cell Res, 1984. 154(1): p. 191-202.

53. Dimri, G.P., et al., *A biomarker that identifies senescent human cells in culture and in aging skin in vivo.* Proc Natl Acad Sci U S A, 1995. 92(20): p. 9363-7.

54. Lee, B.Y., et al., *Senescence-associated beta-galactosidase is lysosomal beta-galactosidase.* Aging Cell, 2006. 5(2): p. 187-95.

55. Narita, M., et al., *Rb-mediated heterochromatin formation and silencing of E2F target genes during cellular senescence.* Cell, 2003. 113(6): p. 703-16.

56. Hayflick, L., *Human cells and aging.* Sci Am, 1968. 218(3): p. 32-7.

57. Hemann, M.T., et al., *The shortest telomere, not average telomere length, is critical for cell viability and chromosome stability.* Cell, 2001. 107(1): p. 67-77.

58. d'Adda di Fagagna, F., et al., *A DNA damage checkpoint response in telomere-initiated senescence.* Nature, 2003. 426(6963): p. 194-8.

59. Takai, H., A. Smogorzewska, and T. de Lange, *DNA damage foci at dysfunctional telomeres.* Curr Biol, 2003. 13(17): p. 1549-56.

60. Bodnar, A.G., et al., *Extension of life-span by introduction of telomerase into normal human cells.* Science, 1998. 279(5349): p. 349-52.

61. Masutomi, K., et al., *Telomerase maintains telomere structure in normal human cells.* Cell, 2003. 114(2): p. 241-53.

62. Fumagalli, M., et al., *Telomeric DNA damage is irreparable and causes persistent DNA-damage-response activation.* Nat Cell Biol, 2012. 14(4): p. 355-65.

63. Serrano, M., et al., *Oncogenic ras provokes premature cell senescence associated with accumulation of p53 and p16INK4a.* Cell, 1997. 88(5): p. 593-602.

64. Lin, A.W., et al., *Premature senescence involving p53 and p16 is activated in response to constitutive MEK/MAPK mitogenic signaling.* Genes Dev, 1998. 12(19): p. 3008-19.

65. Michaloglou, C., et al., *BRAFE600-associated senescence-like cell cycle arrest of human naevi.* Nature, 2005. 436(7051): p. 720-4.

66. Moiseeva, O., et al., *Mitochondrial dysfunction contributes to oncogene-induced senescence.* Mol Cell Biol, 2009. 29(16): p. 4495-507.

67. Vaseva, A.V., et al., *p53 opens the mitochondrial permeability transition pore to trigger necrosis.* Cell, 2012. 149(7): p. 1536-48.

68. Sankaran, V.G., S.H. Orkin, and C.R. Walkley, *Rb intrinsically promotes erythropoiesis by coupling cell cycle exit with mitochondrial biogenesis.* Genes Dev, 2008. 22(4): p. 463-75.

69. Dierick, J.F., et al., *Stress-induced premature senescence and replicative senescence are different phenotypes, proteomic evidence.* Biochem Pharmacol, 2002. 64(5-6): p. 1011-7.

70. Sachs, R.K., et al., *DNA damage caused by ionizing radiation.* Math Biosci, 1992. 112(2): p. 271-303.

71. Tavana, O., et al., *Absence of p53-dependent apoptosis leads to UV radiation hypersensitivity, enhanced immunosuppression and cellular senescence.* Cell Cycle, 2010. 9(16): p. 3328-36.

72. Xiao, H., et al., *Acidic pH induces topoisomerase II-mediated DNA damage.* Proc Natl Acad Sci U S A, 2003. 100(9): p. 5205-10.

73. Paul, C., et al., *A single, mild, transient scrotal heat stress causes DNA damage, subfertility and impairs formation of blastocysts in mice.* Reproduction, 2008. 136(1): p. 73-84.

74. Fortini, P., et al., *8-Oxoguanine DNA damage: at the crossroad of alternative repair pathways.* Mutat Res, 2003. 531(1-2): p. 127-39.

75. Rudolf, E., S. John, and M. Cervinka, *Irinotecan induces senescence and apoptosis in colonic cells in vitro.* Toxicol Lett, 2012.

76. Patro, B.S., et al., *WRN helicase regulates the ATR-CHK1-induced S-phase checkpoint pathway in response to topoisomerase-I-DNA covalent complexes.* J Cell Sci, 2011. 124(Pt 23): p. 3967-79.

77. Kim, H.S., et al., *p21WAF/CIP1/SDI1 is upregulated due to increased mRNA stability during hydroxyurea-induced senescence of human fibroblasts.* Mech Ageing Dev, 2005. 126(12): p. 1255-61.

78. Chen, X., et al., *Binding of two distamycin A molecules in the minor groove of an alternating B-DNA duplex.* Nat Struct Biol, 1994. 1(3): p. 169-75.

79. Michishita, E., et al., *5-Bromodeoxyuridine induces senescence-like phenomena in mammalian cells regardless of cell type or species.* J Biochem, 1999. 126(6): p. 1052-9.

80. Rawlings, J.S., K.M. Rosler, and D.A. Harrison, *The JAK/STAT signaling pathway.* J Cell Sci, 2004. 117(Pt 8): p. 1281-3.

81. Hoey, T. and U. Schindler, *STAT structure and function in signaling.* Curr Opin Genet Dev, 1998. 8(5): p. 582-7.

82. You, M., D.H. Yu, and G.S. Feng, *Shp-2 tyrosine phosphatase functions as a negative regulator of the interferon-stimulated Jak/STAT pathway.* Mol Cell Biol, 1999. 19(3): p. 2416-24.

83. Greenhalgh, C.J. and D.J. Hilton, *Negative regulation of cytokine signaling.* J Leukoc Biol, 2001. 70(3): p. 348-56.

84. Goody, R.J., et al., *JAK-STAT signaling pathways are activated in the brain following reovirus infection.* J Neurovirol, 2007. 13(4): p. 373-83.

85. Malmgaard, L., *Induction and regulation of IFNs during viral infections.* J Interferon Cytokine Res, 2004. 24(8): p. 439-54.

86. Honda, K., et al., *IRF-7 is the master regulator of type-I interferon-dependent immune responses.* Nature, 2005. 434(7034): p. 772-7.

87. Nakayama, Y., et al., *Role of PKR and Type I IFNs in viral control during primary and secondary infection.* PLoS Pathog, 2010. 6(6): p. e1000966.

88. Karehed, K., et al., *IFN-gamma-induced upregulation of Fcgamma-receptor-I during activation of monocytic cells requires the PKR and NFkappaB pathways.* Mol Immunol, 2007. 44(4): p. 615-24.

89. Haller, O., P. Staeheli, and G. Kochs, *Interferon-induced Mx proteins in antiviral host defense.* Biochimie, 2007. 89(6-7): p. 812-8.

90. Fulop, T., et al., *Cytokine receptor signalling and aging.* Mech Ageing Dev, 2006. 127(6): p. 526-37.

91. Moiseeva, O., et al., *DNA damage signaling and p53-dependent senescence after prolonged beta-interferon stimulation.* Mol Biol Cell, 2006. 17(4): p. 1583-92.

92. Mallette, F.A., et al., *Myc down-regulation as a mechanism to activate the Rb pathway in STAT5A-induced senescence.* J Biol Chem, 2007. 282(48): p. 34938-44.

93. Mallette, F.A., et al., *Human fibroblasts require the Rb family of tumor suppressors, but not p53, for PML-induced senescence.* Oncogene, 2004. 23(1): p. 91-9.

94. Kortylewski, M. and H. Yu, *Stat3 as a potential target for cancer immunotherapy.* J Immunother, 2007. 30(2): p. 131-9.

95. Frank, D.A., *STAT3 as a central mediator of neoplastic cellular transformation.* Cancer Lett, 2007. 251(2): p. 199-210.

96. McLornan, D., M. Percy, and M.F. McMullin, *JAK2 V617F: a single mutation in the myeloproliferative group of disorders.* Ulster Med J, 2006. 75(2): p. 112-9.

97. Chatterjee-Kishore, M., et al., *How Stat1 mediates constitutive gene expression: a complex of unphosphorylated Stat1 and IRF1 supports transcription of the LMP2 gene.* EMBO J, 2000. 19(15): p. 4111-22.

98. Cheon, H. and G.R. Stark, *Unphosphorylated STAT1 prolongs the expression of interferon-induced immune regulatory genes.* Proc Natl Acad Sci U S A, 2009. 106(23): p. 9373-8.

99. Yang, J., et al., *Unphosphorylated STAT3 accumulates in response to IL-6 and activates transcription by binding to NFkappaB.* Genes Dev, 2007. 21(11): p. 1396-408.

100. Timofeeva, O.A., et al., *Mechanisms of unphosphorylated STAT3 transcription factor binding to DNA.* J Biol Chem, 2012. 287(17): p. 14192-200.

101. Meyer, T., et al., *Constitutive and IFN-gamma-induced nuclear import of STAT1 proceed through independent pathways.* EMBO J, 2002. 21(3): p. 344-54.

102. Fielhaber, J.A., et al., *Regulation of karyopherin alpha1 and nuclear import by mammalian target of rapamycin.* J Biol Chem, 2012. 287(18): p. 14325-35.

103. Liu, L., K.M. McBride, and N.C. Reich, *STAT3 nuclear import is independent of tyrosine phosphorylation and mediated by importin-alpha3.* Proc Natl Acad Sci U S A, 2005. 102(23): p. 8150-5.

104. Sehgal, P.B., *Paradigm shifts in the cell biology of STAT signaling.* Semin Cell Dev Biol, 2008. 19(4): p. 329-40.

105. Gough, D.J., et al., *Mitochondrial STAT3 supports Ras-dependent oncogenic transformation.* Science, 2009. 324(5935): p. 1713-6.

106. Szczepanek, K., et al., *Mitochondrial-targeted Signal transducer and activator of transcription 3 (STAT3) protects against ischemia-induced changes in the electron transport chain and the generation of reactive oxygen species.* J Biol Chem, 2011. 286(34): p. 29610-20.

107. Lufei, C., et al., *GRIM-19, a death-regulatory gene product, suppresses Stat3 activity via functional interaction.* EMBO J, 2003. 22(6): p. 1325-35.

108. Chung, J., et al., *STAT3 serine phosphorylation by ERK-dependent and -independent pathways negatively modulates its tyrosine phosphorylation.* Mol Cell Biol, 1997. 17(11): p. 6508-16.

109. de The, H., et al., *The PML-RAR alpha fusion mRNA generated by the t(15;17) translocation in acute promyelocytic leukemia encodes a functionally altered RAR.* Cell, 1991. 66(4): p. 675-84.

110. Jensen, K., C. Shiels, and P.S. Freemont, *PML protein isoforms and the RBCC/TRIM motif.* Oncogene, 2001. 20(49): p. 7223-33.

111. Fagioli, M., et al., *Alternative splicing of PML transcripts predicts coexpression of several carboxy-terminally different protein isoforms.* Oncogene, 1992. 7(6): p. 1083-91.

112. Bischof, O., et al., *Deconstructing PML-induced premature senescence.* EMBO J, 2002. 21(13): p. 3358-69.

113. Condemine, W., et al., *Characterization of endogenous human promyelocytic leukemia isoforms.* Cancer Res, 2006. 66(12): p. 6192-8.

114. Chelbi-Alix, M.K., et al., *Resistance to virus infection conferred by the interferon-induced promyelocytic leukemia protein.* J Virol, 1998. 72(2): p. 1043-51.

115. Chelbi-Alix, M.K., et al., *Induction of the PML protein by interferons in normal and APL cells.* Leukemia, 1995. 9(12): p. 2027-33.

116. Stadler, M., et al., *Transcriptional induction of the PML growth suppressor gene by interferons is mediated through an ISRE and a GAS element.* Oncogene, 1995. 11(12): p. 2565-73.

117. de Stanchina, E., et al., *PML is a direct p53 target that modulates p53 effector functions.* Mol Cell, 2004. 13(4): p. 523-35.

118. Shtutman, M., et al., *PML is a target gene of beta-catenin and plakoglobin, and coactivates beta-catenin-mediated transcription.* Cancer Res, 2002. 62(20): p. 5947-54.

119. Dror, N., et al., *Interferon regulatory factor-8 is indispensable for the expression of promyelocytic leukemia and the formation of nuclear bodies in myeloid cells.* J Biol Chem, 2007. 282(8): p. 5633-40.

120. Kim, T.K., et al., *Direct transcriptional activation of promyelocytic leukemia protein by IFN regulatory factor 3 induces the p53-dependent growth inhibition of cancer cells.* Cancer Res, 2007. 67(23): p. 11133-40.

121. Duprez, E., et al., *SUMO-1 modification of the acute promyelocytic leukaemia protein PML: implications for nuclear localisation.* J Cell Sci, 1999. 112 (Pt 3): p. 381-93.

122. Zhong, S., et al., *Role of SUMO-1-modified PML in nuclear body formation.* Blood, 2000. 95(9): p. 2748-52.

123. Chang, K.S., et al., *The PML gene encodes a phosphoprotein associated with the nuclear matrix.* Blood, 1995. 85(12): p. 3646-53.

124. Chen, Y.C., et al., *Live cell dynamics of promyelocytic leukemia nuclear bodies upon entry into and exit from mitosis.* Mol Biol Cell, 2008. 19(7): p. 3147-62.

125. Yang, S., et al., *PML-dependent apoptosis after DNA damage is regulated by the checkpoint kinase hCds1/Chk2.* Nat Cell Biol, 2002. 4(11): p. 865-70.

126. Scaglioni, P.P., et al., *A CK2-dependent mechanism for degradation of the PML tumor suppressor.* Cell, 2006. 126(2): p. 269-83.

127. Percherancier, Y., et al., *Role of SUMO in RNF4-mediated promyelocytic leukemia protein (PML) degradation: sumoylation of PML and phospho-switch control of its SUMO binding domain dissected in living cells.* J Biol Chem, 2009. 284(24): p. 16595-608.

128. Pietschmann, K., et al., *Differential regulation of PML-RARalpha stability by the ubiquitin ligases SIAH1/SIAH2 and TRIAD1.* Int J Biochem Cell Biol, 2012. 44(1): p. 132-8.

129. Yuan, W.C., et al., *A Cullin3-KLHL20 Ubiquitin ligase-dependent pathway targets PML to potentiate HIF-1 signaling and prostate cancer progression.* Cancer Cell, 2011. 20(2): p. 214-28.

130. Everett, R.D. and M.K. Chelbi-Alix, *PML and PML nuclear bodies: implications in antiviral defence.* Biochimie, 2007. 89(6-7): p. 819-30.

131. Dellaire, G., R. Farrall, and W.A. Bickmore, *The Nuclear Protein Database (NPD): sub-nuclear localisation and functional annotation of the nuclear proteome.* Nucleic Acids Res, 2003. 31(1): p. 328-30.

132. Dellaire, G. and D.P. Bazett-Jones, *PML nuclear bodies: dynamic sensors of DNA damage and cellular stress.* Bioessays, 2004. 26(9): p. 963-77.

133. Carbone, R., et al., *PML NBs associate with the hMre11 complex and p53 at sites of irradiation induced DNA damage.* Oncogene, 2002. 21(11): p. 1633-40.

134. Ishov, A.M., et al., *PML is critical for ND10 formation and recruits the PML-interacting protein daxx to this nuclear structure when modified by SUMO-1.* J Cell Biol, 1999. 147(2): p. 221-34.

135. Janderova-Rossmeislova, L., et al., *PML protein association with specific nucleolar structures differs in normal, tumor and senescent human cells.* J Struct Biol, 2007. 159(1): p. 56-70.

136. Dellaire, G., et al., *The number of PML nuclear bodies increases in early S phase by a fission mechanism.* J Cell Sci, 2006. 119(Pt 6): p. 1026-33.

137. Sternsdorf, T., K. Jensen, and H. Will, *Evidence for covalent modification of the nuclear dot-associated proteins PML and Sp100 by PIC1/SUMO-1.* J Cell Biol, 1997. 139(7): p. 1621-34.

138. Jul-Larsen, A., et al., *Cell-cycle regulation and dynamics of cytoplasmic compartments containing the promyelocytic leukemia protein and nucleoporins.* J Cell Sci, 2009. 122(Pt 8): p. 1201-10.

139. Zimber, A., Q.D. Nguyen, and C. Gespach, *Nuclear bodies and compartments: functional roles and cellular signalling in health and disease.* Cell Signal, 2004. 16(10): p. 1085-104.

140. Rodier, F., et al., *DNA-SCARS: distinct nuclear structures that sustain damage-induced senescence growth arrest and inflammatory cytokine secretion.* J Cell Sci, 2011. 124(Pt 1): p. 68-81.

141. Lombard, D.B. and L. Guarente, *Nijmegen breakage syndrome disease protein and MRE11 at PML nuclear bodies and meiotic telomeres.* Cancer Res, 2000. 60(9): p. 2331-4.

142. Xu, Z.X., et al., *PML colocalizes with and stabilizes the DNA damage response protein TopBP1.* Mol Cell Biol, 2003. 23(12): p. 4247-56.

143. Liu, J., et al., *Promyelocytic leukemia protein interacts with werner syndrome helicase and regulates double-strand break repair in gamma-irradiation-induced DNA damage responses.* Biochemistry (Mosc), 2011. 76(5): p. 550-4.

144. Pearson, M., et al., *PML regulates p53 acetylation and premature senescence induced by oncogenic Ras.* Nature, 2000. 406(6792): p. 207-10.

145. Vernier, M., et al., *Regulation of E2Fs and senescence by PML nuclear bodies.* Genes Dev, 2011. 25(1): p. 41-50.

146. Zhang, R., et al., *Formation of MacroH2A-containing senescence-associated heterochromatin foci and senescence driven by ASF1a and HIRA.* Dev Cell, 2005. 8(1): p. 19-30.

147. Jiang, W.Q., et al., *HP1-mediated formation of alternative lengthening of telomeres-associated PML bodies requires HIRA but not ASF1a.* PLoS One, 2011. 6(2): p. e17036.

148. Pandolfi, P.P., *Oncogenes and tumor suppressors in the molecular pathogenesis of acute promyelocytic leukemia.* Hum Mol Genet, 2001. 10(7): p. 769-75.

149. Lai, H.K. and K.L. Borden, *The promyelocytic leukemia (PML) protein suppresses cyclin D1 protein production by altering the nuclear cytoplasmic distribution of cyclin D1 mRNA.* Oncogene, 2000. 19(13): p. 1623-34.

150. Regad, T., et al., *PML mediates the interferon-induced antiviral state against a complex retrovirus via its association with the viral transactivator.* EMBO J, 2001. 20(13): p. 3495-505.

151. Ishov, A.M. and G.G. Maul, *The periphery of nuclear domain 10 (ND10) as site of DNA virus deposition.* J Cell Biol, 1996. 134(4): p. 815-26.

152. Tavalai, N. and T. Stamminger, *Interplay between Herpesvirus Infection and Host Defense by PML Nuclear Bodies.* Viruses, 2009. 1(3): p. 1240-64.

153. Wang, L., et al., *Disruption of PML nuclear bodies is mediated by ORF61 SUMO-interacting motifs and required for varicella-zoster virus pathogenesis in skin.* PLoS Pathog, 2011. 7(8): p. e1002157.

154. Chelbi-Alix, M.K., et al., *Rabies viral mechanisms to escape the IFN system: the viral protein P interferes with IRF-3, Stat1, and PML nuclear bodies.* J Interferon Cytokine Res, 2006. 26(5): p. 271-80.

155. Lu, H., W. Ouyang, and C. Huang, *Inflammation, a key event in cancer development.* Mol Cancer Res, 2006. 4(4): p. 221-33.

156. Freund, A., et al., *Inflammatory networks during cellular senescence: causes and consequences.* Trends Mol Med, 2010. 16(5): p. 238-46.

157. Davalos, A.R., et al., *Senescent cells as a source of inflammatory factors for tumor progression.* Cancer Metastasis Rev, 2010. 29(2): p. 273-83.

158. Soriani, A., et al., *ATM-ATR-dependent up-regulation of DNAM-1 and NKG2D ligands on multiple myeloma cells by therapeutic agents results in enhanced NK-cell susceptibility and is associated with a senescent phenotype.* Blood, 2009. 113(15): p. 3503-11.

159. Freund, A., C.K. Patil, and J. Campisi, *p38MAPK is a novel DNA damage response-independent regulator of the senescence-associated secretory phenotype.* EMBO J, 2011. 30(8): p. 1536-48.

160. Shivshankar, P., et al., *Caveolin-1 deficiency protects from pulmonary fibrosis by modulating epithelial cell senescence in mice.* Am J Respir Cell Mol Biol, 2012. 47(1): p. 28-36.

161. Campisi, J., *Senescent cells, tumor suppression, and organismal aging: good citizens, bad neighbors.* Cell, 2005. 120(4): p. 513-22.

162. Vasto, S., et al., *Inflammatory networks in ageing, age-related diseases and longevity.* Mech Ageing Dev, 2007. 128(1): p. 83-91.

163. Takahashi, S., et al., *Elevation of circulating plasma cytokines in cancer patients with high plasma parathyroid hormone-related protein levels.* Endocr Relat Cancer, 2003. 10(3): p. 403-7.

164. Heinrich, P.C., et al., *Principles of interleukin (IL)-6-type cytokine signalling and its regulation.* Biochem J, 2003. 374(Pt 1): p. 1-20.

165. Kuilman, T., et al., *Oncogene-induced senescence relayed by an interleukin-dependent inflammatory network.* Cell, 2008. 133(6): p. 1019-31.

166. Ancrile, B., K.H. Lim, and C.M. Counter, *Oncogenic Ras-induced secretion of IL6 is required for tumorigenesis.* Genes Dev, 2007. 21(14): p. 1714-9.

167. Acosta, J.C., et al., *Chemokine signaling via the CXCR2 receptor reinforces senescence.* Cell, 2008. 133(6): p. 1006-18.

168. Tremain, R., et al., *Defects in TGF-beta signaling overcome senescence of mouse keratinocytes expressing v-Ha-ras.* Oncogene, 2000. 19(13): p. 1698-709.

169. Glick, A.B., et al., *Targeted deletion of the TGF-beta 1 gene causes rapid progression to squamous cell carcinoma.* Genes Dev, 1994. 8(20): p. 2429-40.

170. Vijayachandra, K., J. Lee, and A.B. Glick, *Smad3 regulates senescence and malignant conversion in a mouse multistage skin carcinogenesis model.* Cancer Res, 2003. 63(13): p. 3447-52.

171. Brown, N.J., *Therapeutic potential of plasminogen activator inhibitor-1 inhibitors.* Ther Adv Cardiovasc Dis, 2010. 4(5): p. 315-24.

172. Kortlever, R.M., P.J. Higgins, and R. Bernards, *Plasminogen activator inhibitor-1 is a critical downstream target of p53 in the induction of replicative senescence.* Nat Cell Biol, 2006. 8(8): p. 877-84.

173. Zhou, H., et al., *Induction of a bystander mutagenic effect of alpha particles in mammalian cells.* Proc Natl Acad Sci U S A, 2000. 97(5): p. 2099-104.

174. Koturbash, I., et al., *Irradiation induces DNA damage and modulates epigenetic effectors in distant bystander tissue in vivo.* Oncogene, 2006. 25(31): p. 4267-75.

175. Ko, M., et al., *Neoplastic transformation in vitro by low doses of ionizing radiation: role of adaptive response and bystander effects.* Mutat Res, 2006. 597(1-2): p. 11-7.

176. Shao, C., et al., *Nitric oxide-mediated signaling in the bystander response of individually targeted glioma cells.* Cancer Res, 2003. 63(23): p. 8437-42.

177. Yang, H., N. Asaad, and K.D. Held, *Medium-mediated intercellular communication is involved in bystander responses of X-ray-irradiated normal human fibroblasts.* Oncogene, 2005. 24(12): p. 2096-103.

178. Rzeszowska-Wolny, J., et al., *X-irradiation and bystander effects induce similar changes of transcript profiles in most functional pathways in human melanoma cells.* DNA Repair (Amst), 2009. 8(6): p. 732-8.

179. Burdak-Rothkamm, S., et al., *ATR-dependent radiation-induced gamma H2AX foci in bystander primary human astrocytes and glioma cells.* Oncogene, 2007. 26(7): p. 993-1002.

180. Burdak-Rothkamm, S., K. Rothkamm, and K.M. Prise, *ATM acts downstream of ATR in the DNA damage response signaling of bystander cells.* Cancer Res, 2008. 68(17): p. 7059-65.

181. Dieriks, B., et al., *Medium-mediated DNA repair response after ionizing radiation is correlated with the increase of specific cytokines in human fibroblasts.* Mutat Res, 2010. 687(1-2): p. 40-8.

182. Di, X., et al., *A chemotherapy-associated senescence bystander effect in breast cancer cells.* Cancer Biol Ther, 2008. 7(6): p. 864-72.

183. Lin, R., et al., *Selective DNA binding and association with the CREB binding protein coactivator contribute to differential activation of alpha/beta interferon genes by interferon regulatory factors 3 and 7.* Mol Cell Biol, 2000. 20(17): p. 6342-53.

184. Ho, H.H. and L.B. Ivashkiv, *Role of STAT3 in type I interferon responses. Negative regulation of STAT1-dependent inflammatory gene activation.* J Biol Chem, 2006. 281(20): p. 14111-8.

185. Gurrieri, C., et al., *Loss of the tumor suppressor PML in human cancers of multiple histologic origins.* J Natl Cancer Inst, 2004. 96(4): p. 269-79.

186. Thullberg, M., et al., *Monoclonal antibody probes for p21WAF1/CIP1 and the INK4 family of cyclin-dependent kinase inhibitors.* Hybridoma, 2000. 19(1): p. 63-72.

187. Baskaran, R., et al., *Ataxia telangiectasia mutant protein activates c-Abl tyrosine kinase in response to ionizing radiation.* Nature, 1997. 387(6632): p. 516-9.

188. Stuurman, N., et al., *A monoclonal antibody recognizing nuclear matrix-associated nuclear bodies.* J Cell Sci, 1992. 101 (Pt 4): p. 773-84.

189. Ehret, G.B., et al., *DNA binding specificity of different STAT proteins. Comparison of in vitro specificity with natural target sites.* J Biol Chem, 2001. 276(9): p. 6675-88.

190. Wegiel, B., et al., *Interleukin-6 activates PI3K/Akt pathway and regulates cyclin A1 to promote prostate cancer cell survival.* Int J Cancer, 2008. 122(7): p. 1521-9.

191. Dimauro, T. and G. David, *Chromatin modifications: the driving force of senescence and aging?* Aging (Albany NY), 2009. 1(2): p. 182-90.

192. Blazkova, H., et al., *Bacterial intoxication evokes cellular senescence with persistent DNA damage and cytokine signalling.* J Cell Mol Med, 2010. 14(1-2): p. 357-67.

193. Bartkova, J., et al., *Oncogene-induced senescence is part of the tumorigenesis barrier imposed by DNA damage checkpoints.* Nature, 2006. 444(7119): p. 633-7.

194. Wang, Y., X. Zang, and P. Chen, *High expression of p16INK4a and low expression of Bmi1 are associated with endothelial cellular senescence in the human cornea.* Mol Vis, 2012. 18: p. 803-15.

12. Publications

Oncogene (2010) 29, 273–284

www.nature.com/onc

ORIGINAL ARTICLE

Cytokine expression and signaling in drug-induced cellular senescence

Z Novakova[1,2,6], S Hubackova[1], M Kosar[1], L Janderova-Rossmeislova[2,7], J Dobrovolna[2,8], P Vasicova[3], M Vancurova[1], Z Horejsi[4,9], P Hozak[2], J Bartek[1,5] and Z Hodny[1,2]

[1]*Department of Genome Integrity, Institute of Molecular Genetics, v.v.i., Academy of Sciences of the Czech Republic, Prague, Czech Republic;* [2]*Department of Biology of Cell Nucleus, Institute of Molecular Genetics, v.v.i., Academy of Sciences of the Czech Republic, Prague, Czech Republic;* [3]*Laboratory of Cell Reproduction, Institute of Microbiology, v.v.i., Academy of Sciences of the Czech Republic, Prague, Czech Republic;* [4]*Department of Molecular Virology, Institute of Molecular Genetics, v.v.i., Academy of Sciences of the Czech Republic, Prague, Czech Republic and* [5]*Department of Cell Cycle and Cancer, and Centre for Genotoxic Stress Research, Institute of Cancer Biology, Danish Cancer Society, Copenhagen, Denmark*

Cellular senescence guards against cancer and modulates aging; however, the underlying mechanisms remain poorly understood. Here, we show that genotoxic drugs capable of inducing premature senescence in normal and cancer cells, such as 5-bromo-2′-deoxyuridine (BrdU), distamycin A (DMA), aphidicolin and hydroxyurea, persistently activate Janus kinase–signal transducer and activator of transcription (JAK/STAT) signaling and expression of interferon-stimulated genes (ISGs), such as *MX1*, *OAS*, *ISG15*, *STAT1*, *PML*, *IRF1* and *IRF7*, in several human cancer cell lines. JAK1/STAT-activating ligands, interleukin 10 (IL10), IL20, IL24, interferon γ (IFNγ), IFNβ and IL6, were also expressed by senescent cells, supporting autocrine/paracrine activation of JAK1/STAT. Furthermore, cytokine genes, including proinflammatory IL1, tumor necrosis factor and transforming growth factor families, were highly expressed. The strongest inducer of JAK/STAT signaling, cytokine production and senescence was BrdU combined with DMA. RNA interference-mediated knockdown of JAK1 abolished expression of ISGs, but not DNA damage signaling or senescence. Thus, although DNA damage signaling, p53 and RB activation, and the cytokine/chemokine secretory phenotype are apparently shared by all types of senescence, our data reveal so far unprecedented activation of the IFNβ–STAT1–ISGs axis, and indicate a less prominent causative role of IL6-JAK/STAT signaling in genotoxic drug-induced senescence compared with reports on oncogene-induced or replicative senescence. These results highlight shared and unique features of drug-induced cellular senescence, and implicate induction of cancer secretory phenotype in chemotherapy.
Oncogene (2010) **29,** 273–284; doi:10.1038/onc.2009.318; published online 5 October 2009

Keywords: cytokines; JAK/STAT signaling; interleukins; cellular senescence; 5-bromo-2′-deoxyuridine; distamycin A

Introduction

Human cells proliferating *in vitro* randomly withdraw from the cell cycle and enter a state termed replicative cellular senescence (Hayflick and Moorhead, 1961). This complex phenotype is characterized by persistent cell cycle arrest, morphological and functional features (Campisi, 2005), including profound changes in cell secretory phenotype (Kuilman and Peeper, 2009). Replicative senescence is primarily caused by telomeric DNA attrition, which can be accelerated, for example, by oxidative stress (von Zglinicki, 2002). The progression towards replicative senescence is accompanied by gradual increase of the tumor suppressor p53, cyclin-dependent kinase inhibitors, $p21^{WAF1/CIP1}$ (p21) and $p16^{INK4a}$ (p16), and decline of growth-promoting factors such as c-Fos (Bringold and Serrano, 2000). The absence or abrogation of senescence is frequently observed under conditions compromising the function of p53 and RB tumor suppressor pathways, consistent with their key roles in cell cycle arrest and development of the senescent phenotype (Campisi, 2005; Mallette and Ferbeyre, 2007).

Of late, several forms of premature senescence independent of the proliferative history and telomere shortening have been described (Schmitt, 2007). Oncogene-induced senescence can be elicited by exposure of cells to aberrant mitogenic or oncogenic signals, such as mutational activation or overexpression of Ras, mos, cdc6 (cell division cycle 6), cyclin E, STAT5 (signal transducer and activator of transcription 5), etc.

Correspondence: Dr Z Hodny, Department of Genome Integrity, Institute of Molecular Genetics ASCR, v.v.i., Videnska 1083, 142 20 Prague, Czech Republic.
E-mail: hodny@img.cas.cz or Dr J Bartek, Institute of Cancer Biology, and Centre for Genotoxic Stress Research, Danish Cancer Society, Strandboulevarden 49, DK-2100 Copenhagen ∅, Denmark.
E-mail: jb@cancer.dk
[6]Current address: Biology of Reproduction Department, Institute of Animal Science, Prague, Czech Republic.
[7]Current address: Department of Sports Medicine, 3rd Faculty of Medicine, Charles University, Prague, Czech Republic.
[8]Current address: Department of Microbiology and Immunology, Hospital for Special Surgery, Weill Medical College of Cornell University, New York, NY, USA.
[9]Current address: DNA Damage Response Laboratory, Cancer Research UK, Clare Hall Laboratories, South Mims, UK.
Received 8 September 2008; revised 9 August 2009; accepted 2 September 2009; published online 5 October 2009

(Serrano *et al*., 1997; Bartkova *et al*., 2006; Di Micco *et al*., 2006; Collado *et al*., 2007; Mallette *et al*., 2007). Chronic subtoxic doses of stress-inducing compounds such as ethanol or H_2O_2 can cause stress-induced senescence (Toussaint *et al*., 2002). Drug-induced senescence can be promoted by a variety of chemically and functionally unrelated DNA-damaging anticancer agents, such as doxorubicin (Chang *et al*., 1999), camptothecin (Han *et al*., 2002), 5-aza-2′-deoxycytidine (Timmermann *et al*., 1998; Kulaeva *et al*., 2003), aphidicolin (APH) and hydroxyurea (HU) (Yogev *et al*., 2006), or halogenated nucleotide analogs such as 5-bromo-2′-deoxyuridine (BrdU) (Michishita *et al*., 1999; Minagawa *et al*., 2005). Despite the fact that oncogenic or stress stimuli do not promote telomere shortening, prematurely senescent cells share similar characteristics with cells undergoing replicative senescence. Overall, cellular senescence represents a universal growth arrest program, which can be triggered by diverse stimuli.

Importantly, markers characteristic of cells undergoing senescence *in vitro* were also found in preinvasive lesions of multiple types of human tumors (Michaloglou *et al*., 2005; Bartkova *et al*., 2006; Di Micco *et al*., 2006; Collado *et al*., 2007; Acosta *et al*., 2008; Kuilman *et al*., 2008), supporting a view that cellular senescence acts as a tumorigenesis barrier (Sager, 1991; Halazonetis *et al*., 2008). On the other hand, senescent cells in tissues have also been suggested to facilitate tumor growth (Krtolica *et al*., 2001; Campisi, 2005; Parrinello *et al*., 2005) through secreted factors that can promote tumorigenesis. For example, the ability of some cytokines to induce DNA damage during their chronic administration *in vitro* (Moiseeva *et al*., 2006) indicates their potential contribution to genome destabilization due to local effects of secreted compounds. Such vicious circle would also explain the coincidence of chronic inflammation (to which the secretion of proinflammatory cytokines by senescent cells can contribute) with predisposition to malignancy (Coussens and Werb, 2002; Lin and Karin, 2007). To elucidate these issues, new insights into cytokine secretion under various senescence-promoting conditions and its influence on pathophysiology of senescent cells are needed. To contribute to such efforts, we have examined the effects of several genotoxic, senescence-inducing compounds, such as halogenated deoxyuridines, thymidine, camptothecin, distamycin A (DMA), HU and APH, on cytokine/chemokine signaling and its potential role in premature cellular senescence.

Results

BrdU and DMA synergistically activate and induce STAT1

Long-term administration of BrdU causes premature cellular senescence in various cell lines (Michishita *et al*., 1999; Minagawa *et al*., 2005), synergistically with DMA, an AT-binding ligand (Suzuki *et al*., 2002). Similar to other types of senescence, BrdU + DMA-induced senescence (BDIS) is also accompanied by elevation of PML nuclear bodies (Janderova-Rossmeislova *et al*., 2007). While searching for a stimulus capable of activating the interferon-regulated PML gene during premature senescence (Chelbi-Alix *et al*., 1995), we found elevated levels of activated forms of STAT1 in cells undergoing BDIS. STAT1 phosphorylated on tyrosine 701 and serine 727 gradually increased during long-term treatment of HeLa cells with the senescence-inducing mixture of BrdU/DMA (each 10 μM; Figure 1a). The presence of both STAT1 forms was clearly observable at day 4, peaking between days 6 and 8 and then slowly decaying, accompanied by elevation of total STAT1 (Figure 1a). In contrast, the increase of total and Tyr701/Ser727-phosphorylated STAT1 was almost undetectable when either drug was used separately (Figure 1b; only day 6 of the treatment is shown). Even 10-fold higher concentration of BrdU (100 μM) did not outreach the effect of combined BrdU + DMA (Figure 1b), indicating synergistic action of both drugs on STAT1 expression and phosphorylation. Similar to HeLa cells, synergistic induction and activation of STAT1 with BrdU and DMA was found in A549 (Figure 1c) and U2OS cells (Figure 1d). However, in H1299 cells, DMA alone, but not BrdU even at high concentrations, induced total STAT1 and Tyr701/Ser727 phosphorylation (Supplementary Figure 1a), whereas MDA-MB-468 and HS913T cells were less sensitive to both drugs at concentrations effective in other cell lines (Supplementary Figures 1b and c).

5-Bromo-2′-deoxyuridine + DMA-treated HeLa cells displayed the activation of STAT1 concomitantly with proliferation arrest (Supplementary Figure 2g), enhanced senescence-associated β-galactosidase positivity (Supplementary Figures 1d and e), and induction and activation of tumor suppressors and cell cycle inhibitors (increased levels of p53, p21, phosphorylation of serine 15 of p53 and hypophosphorylation of RB; Supplementary Figure 2a). However, U2OS cells treated with 100 μM BrdU developed senescence-like phenotype with all markers present (Supplementary Figures 1f, g, 2c and i), yet without simultaneous activation of STAT1, indicating that STAT1 activation is not a universal feature of cellular senescence (Figure 1d).

Next, we examined how general is STAT1 activation in response to diverse genotoxic compounds. When halogenated nucleoside derivative 5-chloro-2′-deoxyuridine was used instead of BrdU, it synergized with DMA and activated STAT1 similar to BrdU (Supplementary Figure 1h). Other genotoxic compounds known to induce DNA replication stress and senescence in cancer cells, such as APH, HU ((Yogev *et al*., 2006), Supplementary Figures 1i–l), thymidine and camptothecin ((Han *et al*., 2002; Engstrom and Kmiec, 2007), data not shown) also activated and induced STAT1. APH or HU used individually at concentrations inducing an obvious senescent phenotype in HeLa cells induced phosphorylation of STAT1 at both sites and induction of total STAT1 to levels (Figure 1e) higher than that induced by BrdU or DMA alone, but not to the level induced by combined BrdU + DMA. Unexpectedly,

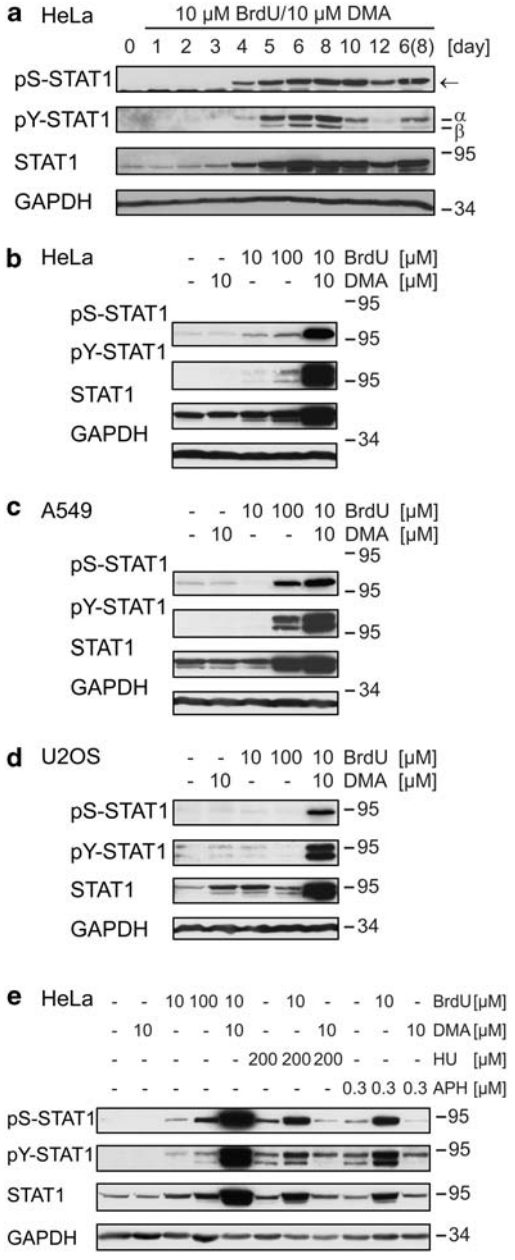

Figure 1 Genotoxic drugs induce expression and phosphorylation of signal transducer and activator of transcription 1 (STAT1) in various cell lines. (**a**) Immunoblotting analysis of a time-course of STAT1 expression and its phosphorylation on serine 727 (pS, specific band is marked by arrow) and tyrosine 701 (pY; α, β: STAT1 α and β isoforms detected) in HeLa cells treated by 10 μM 5-bromo-2′-deoxyuridine (BrdU) and 10 μM distamycin A (DMA). Note that increased expression and phosphorylation of STAT1 remained stable for next 2 days of cultivating in the absence of BrdU + DMA in culture medium (last lane). Immunoblot detection of total and phosphorylated forms of STAT1 in HeLa (**b**), A549 (**c**) and U2OS (**d**) cells after 6 days of treatment. (**e**) Immunoblot comparison of the effect of BrdU, DMA, hydroxyurea, aphidicolin and their combinations on STAT1 expression and phosphorylation. GAPDH (glyceraldehyde 3-phosphate dehydrogenase) was used as a loading control.

other AT-binding agents, such as the distamycin-related netropsin or the DNA intercalator Hoechst33258, showed no or weak effects on STAT1 (Supplementary Figure 1h). APH (0.3 μM) and HU (200 μM) combined with 10 μM BrdU or 10 μM DMA had additive, rather than synergistic effects on STAT1 phosphorylation (Figure 1e). Thus, STAT1 is activated by diverse chemical inducers of senescence in a cell line-dependent manner. To gain further insights into the biology of this phenomenon, we selected the synergistic combination of BrdU + DMA.

Cytokine expression in HeLa cells exposed to BrdU + DMA

As activation of STAT1 can be achieved by paracrine/autocrine signaling of diverse cytokines through membrane receptors, we next considered such scenario. The presence of secreted cytokines was supported by the ability of the medium conditioned by senescent HeLa cells to induce interferon-stimulated proteins, PML and STAT1, in untreated HeLa cells (Figure 2a). Moreover, using the RT^2 Profiler PCR Array System (SuperArray Bioscience Corp., Frederic, MD, USA) ('Interferons and receptors' and 'Common cytokines'; see Supplementary Materials and methods), we found increased transcript levels of several cytokine species, including a transforming growth factor family member inhibinβ A (~1400-fold), interleukin 8 (IL8) (~400-fold), IL24 (~300-fold), IL6 (~150-fold), a TNF (tumor necrosis factor) family member CD70 (TNFSF7; ~130-fold), transforming growth factor-α (~100-fold), IL1β (~40-fold), interferon β (IFNβ) (~15-fold) and IFNγ (more than threefold) (Tables 1 and 2; Supplementary Tables 1 and 2). We conclude that mRNA levels of several cytokines, including ligands capable of receptor-mediated activation of STAT1 (IFNβ, IFNγ, IL6, IL20, IL24 (Commins *et al*., 2008)), were indeed elevated in BDIS.

STAT1-activating ligands IFNβ and IL6 are secreted by senescent HeLa cells

The expression of IFNβ, the major STAT1-activating ligand, was confirmed in separate time-course experiments. Whereas IFNβ mRNA was induced 2.6-fold and 47-fold in BrdU- and DMA-treated HeLa cells, respectively, the BrdU + DMA combination caused a gradual increase of IFNβ mRNA to 268-fold elevation by day 6, as assessed by quantitative reverse transcription PCR (Figure 2b), consistent with synergistic effects of the combined treatment. The IFNβ mRNA in cells treated with high BrdU (100 μM) alone increased less, yet significantly (16-fold by day 6; Figure 2b). The BrdU + DMA-induced elevation of IFNβ mRNA was also reproduced in A549 cells (Figure 2c). Finally, enhanced IFNβ protein in culture medium of BrdU + DMA-treated HeLa cells was detected by ELISA (enzyme-linked immunosorbent assay) (Figure 2d) upon a 6-day culture, compared with parallel controls without BrdU/DMA.

Interleukin 6, though not the dominant inducer of STAT1, can contribute to STAT1 activation (Qing and Stark, 2004). We assessed secretion of the IL6 protein after treatment of HeLa cells with DMA or BrdU + DMA by immunoblotting (Figure 3a) and cytometric

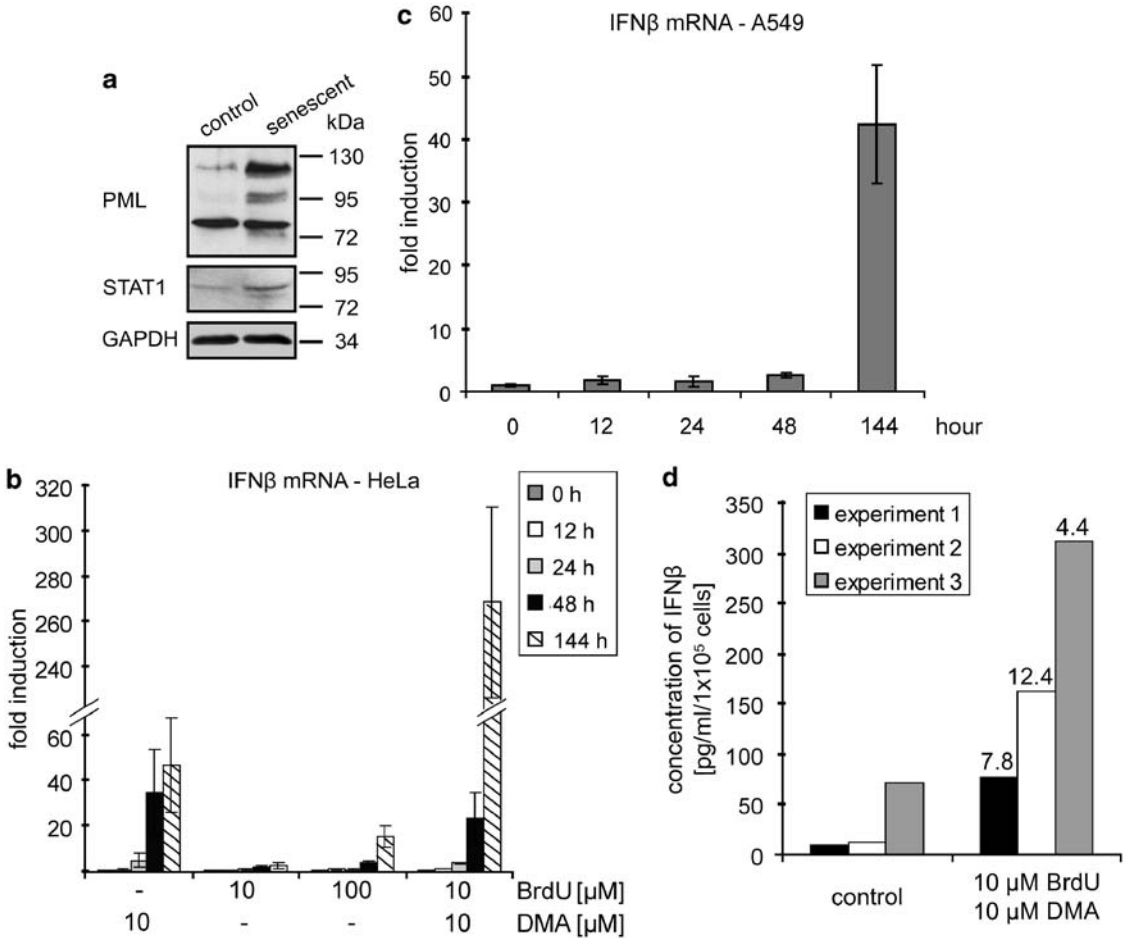

Figure 2 5-Bromo-2′-deoxyuridine plus distamycin A (BrdU + DMA) treatment induces expression of interferon-β (IFNβ). (**a**) Immunoblot detection of PML and signal transducer and activator of transcription 1 (STAT1) in control HeLa cells grown for 4 days in normal medium (control) and medium conditioned by BrdU + DMA-treated, senescent HeLa cells (senescent; for details see Supplementary Materials and methods). GAPDH (glyceraldehyde 3-phosphate dehydrogenase) serves as loading control. IFNβ mRNA levels quantified by quantitative reverse transcription PCR in HeLa cells (**b**) treated by BrdU and DMA and in A549 cells (**c**) treated by the combination of 10 μM BrdU and 10 μM DMA for specified time periods. The values representing average from two (**b**) and three (**c**) independent experiments are shown as a fold induction relative to control; error bars represent standard error. (**d**) Enzyme-linked immunosorbent assay (ELISA) of IFNβ secreted into medium by control and BrdU + DMA-senescent HeLa cells. Three independent experiments are shown separately, as the last experiment was processed with a different lot of ELISA kit. The values represent the concentration of IFNβ relative to the volume of cultivation medium per 100 000 cells; the numbers shown above the columns represent fold induction relative to control.

'bead array' system, in comparison to IL8, another interleukin produced during oncogene-induced senescence ((Acosta *et al*., 2008; Kuilman *et al*., 2008); Figures 3b and c). Increased concentrations of IL6 and IL8 were detected in the culture medium of HeLa cells treated with BrdU + DMA (10 μM) for 6 days compared with controls. Elevated STAT3 and its Tyr705 phosphorylation indicated the autocrine/paracrine IL6-like activity in BDIS cultures (Figure 3a).

To discriminate the specific contribution of BrdU *versus* DMA to IL6 gene expression (Figure 3d), we followed the dynamics of IL6 mRNA after exposure of HeLa cells to either BrdU or DMA. Compared with rapid elevation of IL6 mRNA after 4 h of DMA treatment (data not shown), which reached the highest levels (~60-fold) on day 6 (Figure 3e), BrdU induced the expression of IL6 only modestly (~threefold) and with delayed kinetics (after 48 h, Figure 3e). Thus, analogous to IFNβ, DMA has a dominant role in the IL6 induction, and the synergy of DMA and BrdU in the induction of IL6 expression correlates with their synergy to induce senescence.

We conclude that the BrdU + DMA-inducible activation of STAT1 is associated with expression and secretion of IFNβ and IL6, ligands capable of activating the Janus kinase (JAK)/STAT signaling pathway.

Expression of interferon-stimulated genes is elevated in cancer cells exposed to BrdU and DMA

The enhanced expression and activation of STAT1, and production of IFNβ by drug-induced senescent HeLa cells indicated the activity of the interferon-mediated JAK/STAT signaling. To examine whether the

Table 1 List of ISGs with transcripts upregulated by 10 μM BrdU + DMA

UniGene	*Description*	*Fold ind.*	P-*value*
Hs.517307	Myxovirus (influenza virus) resistance 1	1740.15	0.0003
Hs.632586	Chemokine (C–X–C motif) ligand 10	503.20	0.0005
Hs.20315	Interferon-induced protein with tetratricopeptide repeats 1	170.66	0.0004
Hs.512234	Interleukin 6	151.69	0.0025
Hs.47338	Interferon-induced protein with tetratricopeptide repeats 3	96.67	0.0007
Hs.458485	ISG15 ubiquitin-like modifier	91.77	0.0000
Hs.523847	Interferon, α-inducible protein 6	58.28	0.0004
Hs.163173	Interferon induced with helicase C domain 1	46.37	0.0012
Hs.532634	Interferon, α-inducible protein 27	42.52	0.0007
Hs.458414	Interferon-induced transmembrane protein 1 (9–27)	41.64	0.0006
Hs.401013	Interferon regulatory factor 4	28.25	0.0022
Hs.524760	2′,5′-oligoadenylate synthetase 1	25.55	0.0004
Hs.437609	Interferon-induced protein with tetratricopeptide repeats 2	21.41	0.0000
Hs.166120	Interferon regulatory factor 7	12.91	0.0094
Hs.62192	Coagulation factor III (thromboplastin, tissue factor)	11.71	0.0006
Hs.145150	SP110 nuclear body protein	11.31	0.0015
Hs.632790	Interleukin 3 receptor-α	8.66	0.0090
Hs.436061	Interferon regulatory factor 1	7.92	0.0003
Hs.380250	Interferon-γ-inducible protein 16	7.70	0.0041
Hs.82316	Interferon-induced protein 44	5.94	0.0089
Hs.591742	Interleukin 7 receptor	5.92	0.0006
Hs.224645	Pyrin and HIN domain family, member 1	5.45	0.0057

Abbreviations: BrdU, 5-bromo-2′-deoxyuridine; DMA, distamycin A; Fold ind., fold induction of the transcript, relative to control; ISG, interferon-stimulated gene.

Table 2 List of cytokines with transcripts upregulated by 10 μM BrdU + DMA

UniGene	*Description*	*Fold ind.*	P-*value*
Hs.583348	Inhibin-βA (activin A)	1408.55	0.0008
Hs.624	Interleukin 8	421.68	0.0004
Hs.411311	Interleukin 24	314.08	0.0039
Hs.512234	Interleukin 6 (interferon-β2)	140.56	0.0023
Hs.501497	CD70 molecule	129.34	0.0003
Hs.170009	Transforming growth factor-α	115.36	0.0000
Hs.272373	Interleukin 20	49.18	0.0028
Hs.473163	Bone morphogenetic protein 7 (osteogenic protein 1)	43.71	0.0003
Hs.126256	Interleukin 1-β	42.22	0.0090
Hs.478275	Tumour necrosis factor (ligand) superfamily, member 10	40.64	0.0000
Hs.591873	Interleukin 7	40.09	0.0010
Hs.1573	Growth differentiation factor 5 (cartilage-derived morphogenetic protein-1)	39.81	0.0008
Hs.241570	Tumour necrosis factor (TNF superfamily, member 2)	38.45	0.0003
Hs.181097	Tumour necrosis factor (ligand) superfamily, member 4	32.33	0.0031
Hs.856	Interferon-γ	27.76	0.0005
Hs.1722	Interleukin 1-α	19.29	0.0028
Hs.370414	Nodal homolog (mouse)	10.85	0.0012
Hs.211238	Interleukin 1 family, member 9	10.02	0.0011
Hs.960	Interleukin 9	8.06	0.0012
Hs.591402	Colony-stimulating factor 1 (macrophage)	5.98	0.0005
Hs.121507	Bone morphogenetic protein 3 (osteogenic)	5.84	0.0088

Abbreviations: BrdU, 5-bromo-2′-deoxyuridine; DMA, distamycin A; Fold ind.,fold induction of the transcript, relative to control.

transcription targets of the pathway are induced, we compared mRNA levels of 84 interferon-stimulated genes (ISGs) using RT^2 Profiler PCR Array System ('Interferon and Receptors'), which covers several known targets of IFN type I and II signaling. A total of 22 genes that showed more than fivefold elevation of mRNA in BrdU + DMA-treated HeLa cells (at day 6) compared with controls are listed in Table 1. The most upregulated gene was MX1 (~1700-fold), which is consistent with its strong and exclusive IFN type I inducibility (Ronni *et al*., 1998). The expression of MX1 was confirmed in time-course experiments at mRNA and protein levels (Supplementary Figures 3a–c). Elevated mRNAs of additional well-known interferon-inducible genes, including chemokine ligand 10 (~500-fold), the ubiquitin-like modifier ISG15 (~90-fold) and 2′,5′-oligoadenylate synthetase 1 (~25-fold), were also found (Table 1).

In addition, prolonged expression of IFNβ in senescent cells suggested involvement of transcription factors participating in late interferon response (interferon regulatory factors, IRFs), which can maintain

sustained expression of type I IFNs in a positive regulatory loop under conditions such as viral infection (Honda *et al*., 2005). Indeed, as indicated by 'Interferon RT PCR profiler array' data set, three members of the IRF family (IRF1, 4 and 7) were upregulated at the mRNA level (Table 1). Among them, IRF1 and IRF7, can be directly involved in stimulation of the IFNβ gene (Kim and Maniatis, 1997). We confirmed their expression at the mRNA and protein levels in time-course experiments when BrdU and DMA were used either simultaneously or separately. Gradual increase of IRF1 mRNA to 42-fold and 10-fold elevation (Figure 4a) accompanied by increased IRF1 protein levels (Figures 4c and d) was detected in HeLa cells exposed to 10 μM BrdU + DMA and 100 μM BrdU for 6 days, respectively. DMA and BrdU, when used separately, increased the level of IRF1 mRNA by eightfold and twofold after 6 days, respectively. A 120-fold increase of IRF7 mRNA was observed by day 6 using the combined BrdU + DMA, and 22-fold using 100 μM BrdU alone (Figure 4b). DMA and BrdU (each 10 μM) used separately increased the level of IRF7 mRNA by 24-fold and 1.6-fold after 6 days, respectively. The increase of IRF7 mRNA levels was also accompanied by the elevation of IRF7 protein (Figures 4c and d). Initial increases (over twofold) of both gene transcripts were detected already by 24-h BrdU + DMA treatment. The onset of IRF1 protein induction by 24-h BrdU + DMA treatment correlated with the induction of IFNβ expression (Figure 2b), indicating that IRF1 occurs in early phases of interferon gene induction and, together with IRF7, can participate in the persistent activity of the IFN-JAK/STAT pathway in cells undergoing BDIS. In addition, we found elevated IRF1 in HeLa cells brought to senescence using camptothecin, etoposide (see also Pamment *et al*., 2002), doxorubicin, APH and HU (data not shown).

Overall, the upregulation of transcripts of several ISGs indicated that BrdU + DMA-induced activity of interferon-JAK/STAT signaling results in corresponding gene expression.

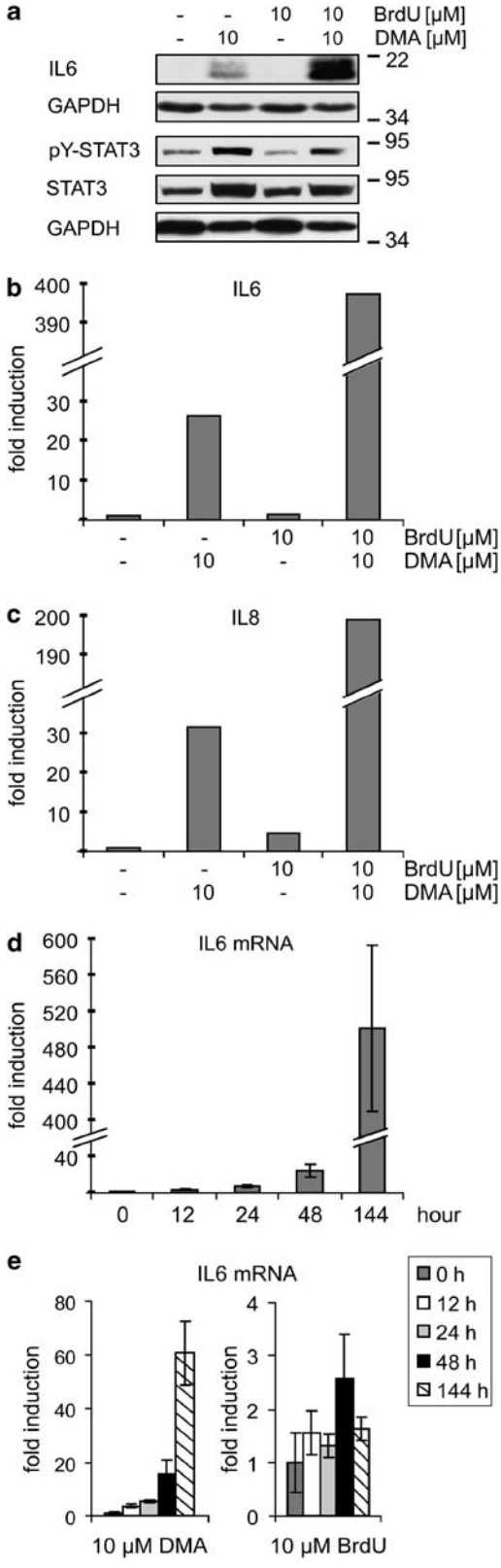

Figure 3 Induction of interleukin-6 (IL6) and IL8 expression during 5-bromo-2′-deoxyuridine plus distamycin A (BrdU + DMA)-evoked senescence. (**a**) Immunoblot detection of IL6 levels, the level of signal transducers and activators of transcription 3 (STAT3) and its Tyr705 phosphorylation status in HeLa cells treated with BrdU and DMA. GAPDH (glyceraldehyde 3-phosphate dehydrogenase) was used as the loading control. Estimation of IL6 (**b**) and IL8 (**c**) in medium conditioned by HeLa cells treated with BrdU and DMA, using the FACS bead array. Quantitative real time reverse transcription PCR quantification of IL6 mRNA levels in HeLa cells exposed to 10 μM BrdU + 10 μM DMA (**d**) and the two drugs used separately (**e**). The values representing average of three independent experiments are shown as fold induction relative to control; error bars represent standard error.

BrdU + DMA-induced expression of ISGs requires JAK1

To prove that activated JAK1/STAT1 signaling induced by BrdU + DMA is indeed instrumental for the induction of ISGs, we knocked down JAK1, the receptor-associated kinase responsible for STAT1 activation, using lentiviral transduction of HeLa cells with vectors carrying short hairpin RNAs (shRNA; Supplementary Materials and methods). Four JAK1-specific

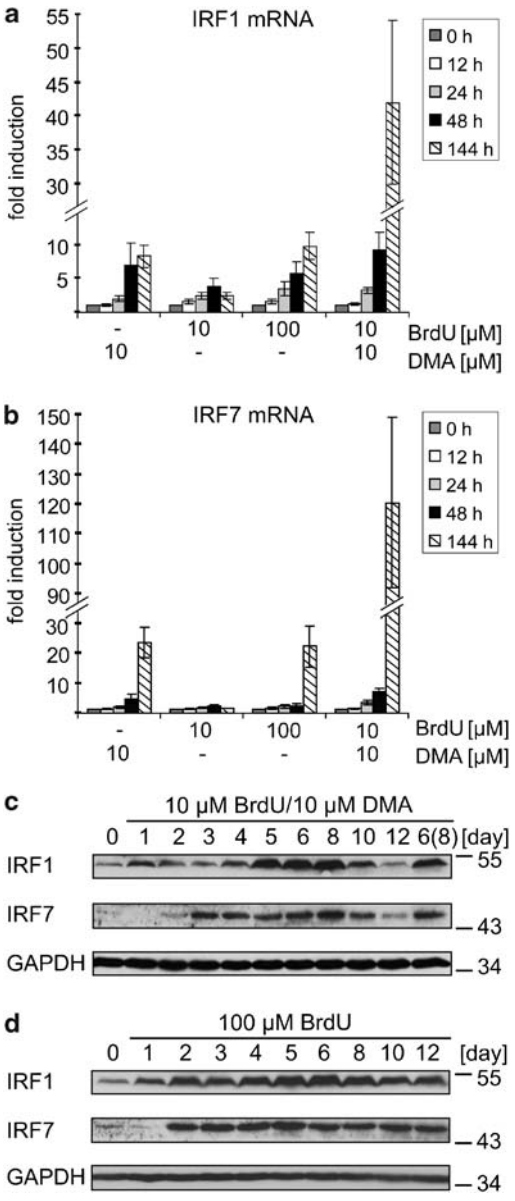

Figure 4 HeLa cells treated with 5-bromo-2′-deoxyuridine plus distamycin A (BrdU + DMA) exhibit increased expression of interferon regulatory factor 1 (IRF1) and IRF7. IRF1 (**a**) and IRF7 (**b**) mRNA levels quantified by quantitative reverse transcription PCR in BrdU + DMA-treated HeLa cells. The average values representing three independent experiments are given as fold induction relative to control. Error bars represent standard error. Immunoblot analysis of IRF1 and IRF7 protein levels in HeLa cells treated with 10 μM BrdU plus 10 μM DMA (**c**) or 100 μM BrdU (**d**) for various time intervals. Note that elevated levels of IRF1 and IRF7 observed at day 6 remained unchanged for the next 2 days after removal of both drugs from the culture medium (see the last lane in **c**). GAPDH (glyceraldehyde 3-phosphate dehydrogenase) was used as a loading control.

shRNAs showed different efficiency of JAK1 knockdown (Figures 5a and b), which correlated well with the extent of suppression of total and activated STAT1 and several ISGs (that is, IRF1 and MX1, Figure 5c and Supplementary Figure 3c). Thus, the induction of ISGs during development of BDIS depends on active JAK1/STAT1 signaling.

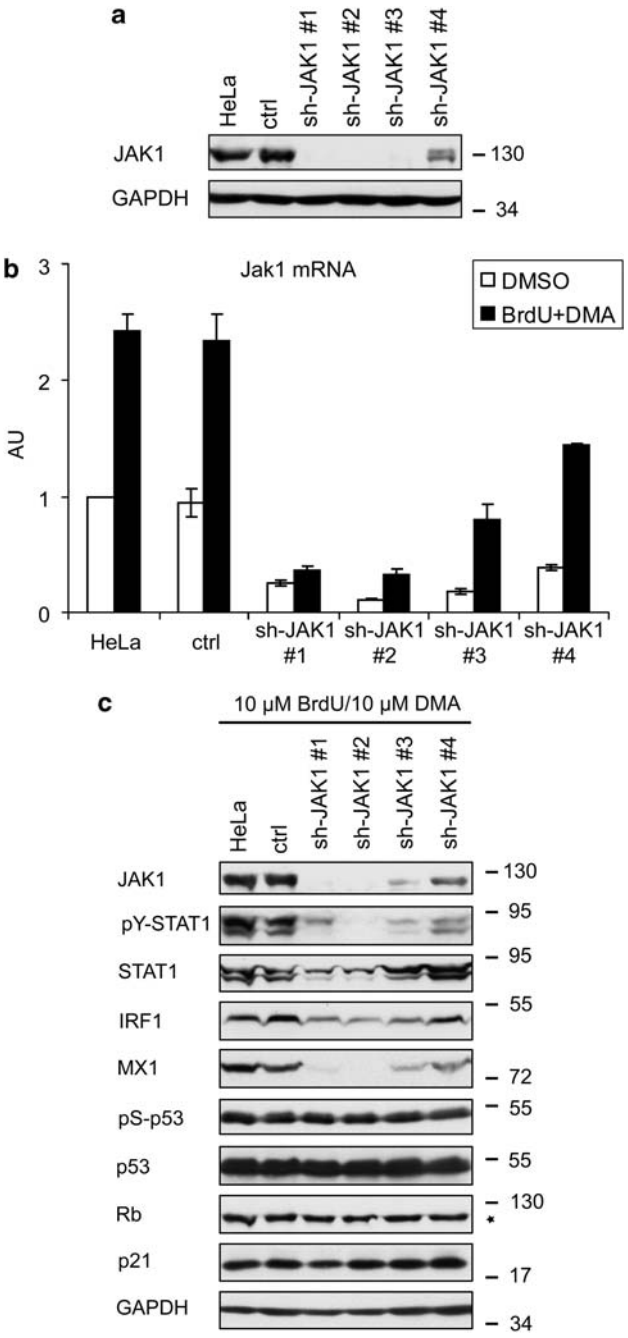

Figure 5 Inhibition of Janus kinase 1 (JAK1) expression aborts signal transducers and activators of transcription 1 (STAT1) activation and expression of interferon-stimulated genes (ISGs), but not DNA damage signaling. (**a**) Immunoblot analysis of JAK1 expression levels affected by short hairpin RNAs (shRNAs) directed against JAK1 (JAK#1, #2, #3, #4) in HeLa cells. (**b**) Real-time quantitative reverse transcription PCR estimation of knockdown efficiency of shRNAs directed against JAK1 (shJAK1 #1, #2, #3, #4). The average values representing three independent experiments are given as arbitrary units relative to control. Error bars represent standard error. (**c**) Immunoblot detection of STAT1 expression and activity, p21, Rb (hypophosphorylated Rb–asterisk), total and serine 15-phosphorylated p53 (pS-p53) and expression of ISGs (IRF1 and MX1) after a 6-day treatment with 5-bromo-2′-deoxyuridine plus distamycin A (BrdU + DMA) in HeLa cells transduced by shRNAs specific for JAK1 (shJAK1 #1, #2, #3, #4) and empty vector (ctrl). GAPDH (glyceraldehyde 3-phosphate dehydrogenase) was used as a loading control.

IL6 and JAK1 are not essential for drug-induced DNA damage signaling and BDIS

DNA damage signaling is a feature shared by all types of senescence (Campisi and d'Adda di Fagagna, 2007; Mallette and Ferbeyre, 2007; Halazonetis *et al*., 2008), and given the recent reports on oncogene-induced and replicative senescence (Kuilman and Peeper, 2009), complemented by our present data on drug-induced senescence, cytokine/chemokine secretion may represent another universal aspect of cellular senescence. Given that downregulation of IL6 by RNA interference rescued cells from oncogene-induced senescence (Kuilman *et al*., 2008), we examined whether this causal relationship is also involved in BDIS. Surprisingly, even a substantial shRNA-mediated depletion of IL6 (shIL#1: >90% for protein; Figure 6a and 85% for mRNA; Figure 6b), validated by the loss of potential of the corresponding HeLa-conditioned medium to support IL6-dependent growth of mouse hybridoma B9 cells (>90%; Supplementary Figure 4a), had no effect on receptor-dependent phosphorylation of STAT1 and STAT3, activation of 'senescence markers' (p21, Rb, p53, pS15p53; Figure 6a) and the development of BDIS (Supplementary Figures 4b–i). Furthermore, we found only marginal elevation of CCAAT-enhancer-binding protein β (C/EBPβ) mRNA in BDIS (Supplementary Figure 4j), contrary to the robust C/EBPβ increase reportedly underlying the IL6-C/EBPβ-positive feedback loop that drives $BRAF^{E600}$ oncogene-induced senescence (Kuilman *et al*., 2008). These results indicate that the IL6-C/EBPβ regulatory circuit is not essential for BDIS.

Furthermore, inhibition of JAK1-dependent signaling through JAK1-specific shRNA had no effect on development of BDIS (Supplementary Figures 5a–i). Even inhibition of four kinases of the JAK family (JAK1, JAK2, JAK3, Tyk2) with the specific JAK inhibitor I (2-(1,1-dimethylethyl)-9-fluoro-3,6-dihydro-7H-benz[h]-imidaz[4,5-f]isoquinolin-7-one), had no effect on activation of p21 and development of senescence itself (Figure 6c; Supplementary Figures 5j–m). Consistently, with preserved senescence, the extent of drug-induced DNA damage signaling, monitored by Ser15-phosphorylated p53 (Figures 5c and 6c), or focus formation of DNA damage markers γH2AX or 53BP1 in cells

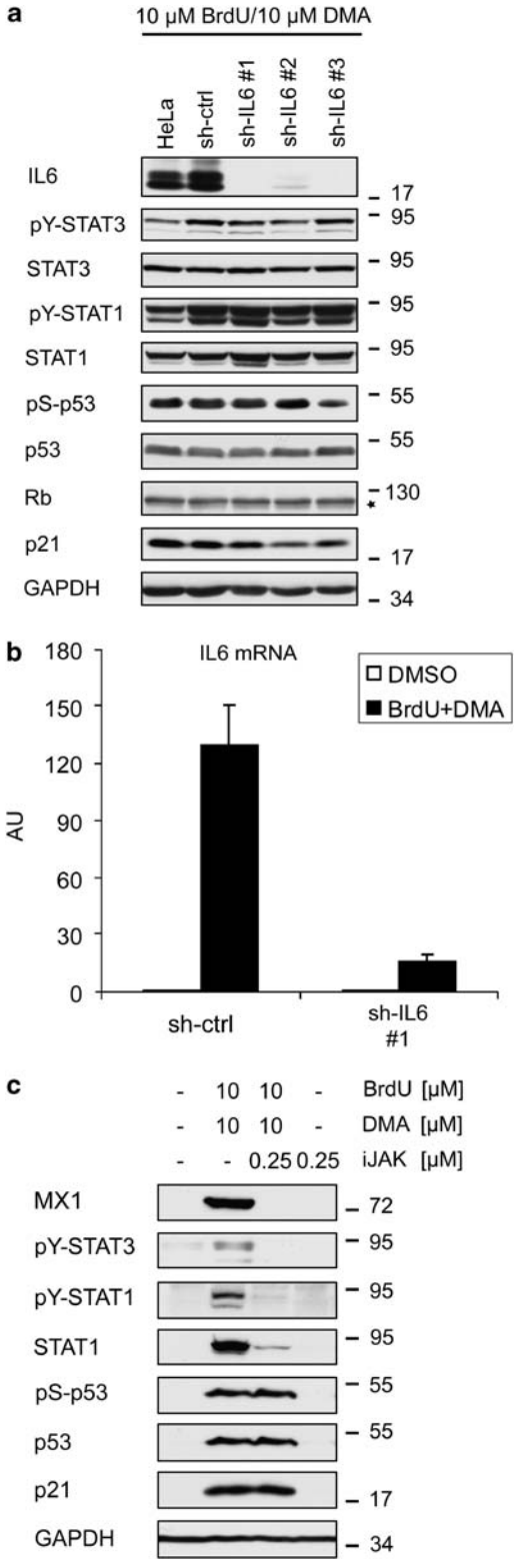

Figure 6 Inhibition of IL6 expression does not affect induction of expression and activation of signal transducers and activators of transcription 3 (STAT3), STAT1 and tumor suppressors after 5-bromo-2′-deoxyuridine plus distamycin A (BrdU + DMA) treatment. (**a**) Immunoblot detection of STAT3 and STAT1 expression and phosphorylation (pY-STAT3 and pY-STAT1), p53 and serine 15-phosphorylated p53 (pS-p53), p21 and Rb (hypophosphorylated Rb–asterisk) after 6 days of treatment with BrdU + DMA (10 μM) in HeLa cells transduced by short hairpin RNAs (shRNAs) specific for IL6 (shIL6 #1, #2, #3) and nonsense shRNA (sh-ctrl). GAPDH (glyceraldehyde 3-phosphate dehydrogenase) was used as a loading control. (**b**) Real-time quantitative reverse transcription PCR estimation of knockdown efficiency of shRNA directed against IL6 (shIL6 #1). The average values representing three independent experiments are given as arbitrary units relative to control. Error bars represent standard error. (**c**) Immunoblot detection of STAT3 and STAT1 phosphorylation (pY-STAT3 and pY-STAT1), MX1, p53 and serine 15-phosphorylated p53 (pS-p53), and p21 after 6 days of treatment with BrdU + DMA (10 μM) in HeLa cells treated with the chemical Janus kinase inhibitor I (iJAK).

treated by genotoxic drugs (data not shown), remained unaffected after JAK1 knockdown or JAK1 activity inhibition. Importantly, the JAK/STAT signaling was effectively abolished under such conditions, as documented by gross reduction of the most sensitive downstream readout, the MX1 expression (Figures 5c and 6c).

Altogether, these results indicate that IL6-C/EBPβ- and JAK1-mediated signaling is not required for the drug-induced DNA damage response and senescence.

Discussion

Cellular senescence is a biological phenomenon involved in major pathophysiological processes such as tumorigenesis and aging (Campisi, 2005; Collado *et al*., 2007). Our present study contributes several findings that help better understand premature senescence induced in tumor cells by diverse genotoxic compounds used in various clinical applications including cancer chemotherapy.

First, we report induction of a secretory phenotype that accompanied such senescence, characterized by prolonged activation of the JAK1/STAT1 signaling pathway and long-term upregulation of several ISGs including tumor suppressors, IRF1, PML, STAT1, mda-7/IL24, and additional cytokines, such as pro-inflammatory IL1α/β, IL6, IL8, TNFSF7 and TNFα. Our results extend recent broadly analogous findings on replicative senescence and oncogene-induced premature senescence (Acosta *et al*., 2008; Kuilman *et al*., 2008), and indicate that such secretory phenotype is shared by all major types of senescence. In addition, the spectrum of induced cytokines/chemokines we observed is significantly broader than those reported for other senescence scenarios, and the involvement of the IFNβ–STAT1–ISGs axis seems to be so far unprecedented.

Regulation of IFN-dependent signaling is complex (Shuai and Liu, 2005), yet the gradual onset and long-term persistence of IFNβ–JAK/STAT signaling seen in our drug-treated cells indicates engagement of positive regulatory loops reminiscent of those operating in virus-infected cells (Honda *et al*., 2005). According to such model, virally activated IRFs (IRF7 and IRF3) drive the expression of IFNs, the secretion of which enables the establishment of a positive regulatory loop through autocrine/paracrine mechanisms. The activation of the IFN type I JAK/STAT signaling results in transcriptional induction of IRFs and IFN genes whose products then close and amplify the loop. A similar mechanism might explain the persistent induction of ISGs (including IRF1 and IRF7) also in later phases of BrdU + DMA-induced secretory phenotype reported here. Surprisingly, IFNβ, but none of several IFNα species tested here, were induced in drug-exposed cells (Supplementary Table 1), suggesting that expression of IFN type I genes, IFNβ and IFNα, is differentially regulated in drug-induced senescence.

Another observation we made is the variability in terms of senescence and cytokine signaling responses, depending on the cancer cell line and genotoxic drug used. The former variability likely reflects the diverse genetic backgrounds in our models, particularly the status of the p53 and RB tumor suppressors whose defects (in MDA-MB-468 and HS913T cells) correlated with rather poor responses compared with p53/RB-proficient U2OS and A549 cells. RB and p53 are critical for proper execution of senescence (Collado *et al*., 2007; Mallette and Ferbeyre, 2007) and their defects are often accompanied by enhanced constitutive DNA damage (DiTullio *et al*., 2002), also because such tumors breached the anticancer barrier of DNA damage checkpoints and senescence (Mallette and Ferbeyre, 2007; Halazonetis *et al*., 2008). The fact that HeLa cells responded relatively well to genotoxic drugs may reflect BrdU/DMA-induced degradation of the papilloma virus oncoproteins E6 and E7 (Suzuki *et al*., 2001), thereby liberating the endogenous p53 and RB functions, and hence promoting the senescence response.

The latter variability, seen in response to the eight genotoxic compounds and their combinations used here, might be attributable to the distinct modes of drug–DNA interactions, or the types and extent of DNA lesions they cause. In any case, our results on differential abilities of genotoxic drugs to induce complex secretory phenotypes should be kept in mind when applying such compounds in neurological examinations (such as BrdU) and especially chemotherapy (several of the drugs used here).

From the mechanistic point of view, the key phosphorylations of STAT1 detected in our experiments, on Tyr701 and Ser727, are critical for STAT1 translocation into the cell nucleus and maximal transcriptional activation, respectively (van Boxel-Dezaire *et al*., 2006). STAT1 phosphorylation by JAK/Tyk kinases can be triggered by several cytokines and growth factors, for example, IL6, IL10 and growth hormones, but it is dominantly activated by interferons (Imada and Leonard, 2000), the production of which in response to drugs was revealed by our present study. Recently, IL6 and IL8 have been causally implicated in the induction and maintenance of oncogene-induced senescence (Acosta *et al*., 2008; Kuilman *et al*., 2008). Our data confirm and extend these studies, by showing that both IL6 and IL8 are produced in drug-induced senescence also. In contrast to the abolishment of BRAF-oncogene-induced senescence by RNA interference-mediated IL6 depletion (Kuilman *et al*., 2008), however, neither IL6 nor the JAK1/STAT1 signaling proved to be strictly required for the senescence phenotype induced by genotoxic drugs examined here. The lack of impact is unlikely to be attributable to insufficient knockdown, as IL6 was depleted to undetectable levels (over 90%) and the JAK1 knockdown abolished the downstream events of the JAK/STAT pathway such as MX1 induction. We propose that the secretory phenotype may have a less critical role in the chemically induced premature senescence compared with some other types of cellular senescence. This conclusion is further supported by the

fact that in some drug/cell line combinations reported here, the senescence phenotype occurred in the absence of pronounced JAK/STAT signaling.

We believe that the major driving force behind the genotoxic drug-induced senescence is the activated DNA damage response machinery, evoked by the DNA lesions caused by the drugs we use. Furthermore, DNA damage signaling was not affected by blocking either IL6 or JAK/STAT signaling here (Figures 5, 6 and data not shown), again supporting the notion that DNA damage checkpoints activate p53 and RB, and likely other pathways that impose the proliferation arrest characteristic of senescence. DNA damage signaling also contributes to other types of senescence, including replicative and oncogene-induced cellular senescence (Campisi and d'Adda di Fagagna, 2007; Mallette and Ferbeyre, 2007; Halazonetis *et al*., 2008), and the severity of cell phenotype depends on the threshold of DNA damage and/or 'oncogenic stress' involved (Bartek *et al*., 2007). We speculate that the more stringent requirement for cytokine/chemokine signaling in some other types of senescence may reflect the cooperative effects of the relatively modest degree of DNA damage evoked by BRAF oncogene, for example, that requires IL6 signaling to boost the intrinsic antiproliferative pathways to fully evoke and maintain senescence (Kuilman *et al*., 2008). In contrast, the extent of DNA damage generated by genotoxic drugs or some other senescence-inducing stimuli, including more potent oncogenes or telomere attrition, might be sufficient to reach the threshold required to trigger senescence.

Redundancy among ligands or signaling modules - in diverse senescence scenarios may also affect the biological outcome of the knockdown experiments. Thus, whereas the dramatic impact of depleting a single cytokine/chemokine ligand or receptor on oncogene-induced senescence (Acosta *et al*., 2008; Kuilman *et al*., 2008) implies very little or no redundancy in such secretory network signaling, the lack of impact on IL6 depletion in our experiments can be explained by multiple ligands capable of activating the signaling pathway (Figure 6c), consistent with a broad spectrum of cytokines/chemokines elevated in response to genotoxic drugs. Regardless of their requirement for establishment of senescence, the autocrine/paracrine effects of cytokines in our present experiments contributed to the senescence-associated gene expression pattern, as was shown by induction of many ISGs in senescent cells, and to their gross reduction upon JAK1 knockdown. We hope that our results will inspire further research into drug-induced secretory phenotypes, particularly *in vivo*, in clinical settings in which such drugs are applied for various diagnostic and therapeutic purposes. As the secreted signaling molecules also exert diverse cell non-autonomous effects, such as immunomodulation (Campisi, 2005), and genes such as IFNβ or mda-7/IL24 or MX1 that were found elevated in our present study harbor potent tumor suppressor functions (Kaynor *et al*., 2002; Fisher, 2005; Mushinski *et al*., 2009), their drug-induced expression may affect the outcome of cancer chemotherapy.

Materials and methods

Chemicals and antibodies
BrdU, DMA, netropsin, Hoechst33258, HU, APH and TriReagent were from Sigma (St Louis, MO, USA) and 5-chloro-2′-deoxyuridine from MPBiomedicals (Eschwege, Germany). The antibodies used are listed in Supplementary Materials and methods.

Cell culture
A549 and U2OS cells were cultured in Dulbecco's modified Eagle's medium supplemented with 10% fetal bovine serum, and HeLa were cultured in the same medium supplemented with 5% fetal bovine serum. Cells were kept at 37 °C under 5% CO_2 atmosphere. For additional cell culture information see Supplementary Materials and methods.

Induction of cellular senescence
On the basis of pilot experiments, 100 μM BrdU or a combination of 10 μM BrdU with 10 μM DMA (dissolved in dimethyl sulfoxide) were chosen for routine administration to reach senescence within 6 days of the treatment. Culture medium with fresh additives was changed every second day. STAT1 phosphorylation and IRF1 and IRF7 expression were estimated on HeLa cells treated with 10 μM BrdU or 10 μM DMA for 6 days, followed by thorough medium change and 2-day culture without drugs.

Quantitative real-time reverse transcription PCR
Total RNA was isolated using TriReagent according to the manufacturer's protocol. For IFNβ transcripts, purified RNA was treated with 80 U/ml DNase (TURBO DNA-free Kit, Applied Biosystems, Foster City, CA, USA) for 40 min at 37 °C. First strand cDNA was synthesized from 200 ng of RNA with random hexamer primers using TaqMan Reverse Transcription Reagents (Applied Biosystems). Quantitative reverse transcription PCR was performed in ABI Prism 7300 (Applied Biosystems) using SYBR Green I or Power SYBR Green I Master Mix (Applied Biosystems) with the primers shown in Supplementary Materials and methods. The relative cDNA amount was estimated by standard curve, data normalized to GAPDH (glyceraldehyde 3-phosphate dehydrogenase).

Determination of cytokine secretion
HeLa cells were treated with 10 μM BrdU or 10 μM DMA for 6 days with medium change every second day. The conditioned medium was collected at day 6 and the number of cells per each dish counted. The concentration of IFNβ in culture medium was estimated using Human IFNβ ELISA kit (PBL Biomedical Laboratories, Piscataway, USA). Absorbance (450 nm) was measured by reader Tecan Sunrise (Grödig, Austria). The concentration of IFNβ was derived from standard curve and expressed as picograms per milliliter medium per 100 000 cells. IL6 and IL8 were estimated by 'FACS bead array' using FlowCytomix Human Simplex Kit (BMS8213FF and BMS8204FF, respectively, Bender MedSystems, Wien, Austria) on flow cytometer LSRII (BD Biosciences, San Jose, USA) according to manufacturer's protocol.

Transduction of shRNA
Specific shRNAs were introduced into HeLa cells using lentiviruses. In brief, HEK293T cells were transfected by one shRNA-coding lentiviral expression vector and two lentiviral packaging vectors (pMD2.G, psPAX2, Addgene, www.addgene.org) using calcium phosphate transfection. After 2 days, supernatant was removed and viral particles precipitated for 24 h by

PEG-it virus precipitation solution (System Biosciences, Mountain View, CA, USA). HeLa cells were infected with viral particles by application of supernatant for 48 h. Transduced HeLa cells were selected using puromycin during 6 days. The list of shRNAs used is shown in Supplementary Materials and methods.

Conflict of interest

The authors declare no conflict of interest.

Acknowledgements

We thank Ondřej Horváth and Michal Koc for assistance, and Jan Frič and Ondřej Staněk for help with ELISA. This work was supported by the Grant Agency of the Academy of Sciences of the Czech Republic (Project IAA500390501), the Grant Agency of the Czech Republic (Project 204/08/1418), the European Commission (project TRIREME), Grant LC545 of the Ministry of Education, Youth and Sports of the Czech Republic, and the Institutional Grant (Project AV0Z5039906).

References

Acosta JC, O'Loghlen A, Banito A, Guijarro MV, Augert A, Raguz S *et al*. (2008). Chemokine signaling via the CXCR2 receptor reinforces senescence. *Cell* **133**: 1006–1018.

Bartek J, Lukas J, Bartkova J. (2007). DNA damage response as an anti-cancer barrier: damage threshold and the concept of 'conditional haploinsufficiency'. *Cell Cycle* **6**: 2344–2347.

Bartkova J, Rezaei N, Liontos M, Karakaidos P, Kletsas D, Issaeva N *et al*. (2006). Oncogene-induced senescence is part of the tumorigenesis barrier imposed by DNA damage checkpoints. *Nature* **444**: 633–637.

Bringold F, Serrano M. (2000). Tumor suppressors and oncogenes in cellular senescence. *Exp Gerontol* **35**: 317–329.

Campisi J. (2005). Senescent cells, tumor suppression, and organismal aging: good citizens, bad neighbors. *Cell* **120**: 513–522.

Campisi J, d'Adda di Fagagna F. (2007). Cellular senescence: when bad things happen to good cells. *Nat Rev Mol Cell Biol* **8**: 729–740.

Collado M, Blasco MA, Serrano M. (2007). Cellular senescence in cancer and aging. *Cell* **130**: 223–233.

Commins S, Steinke JW, Borish L. (2008). The extended IL-10 superfamily: IL-10, IL-19, IL-20, IL-22, IL-24, IL-26, IL-28, and IL-29. *J Allergy Clin Immunol* **121**: 1108–1111.

Coussens LM, Werb Z. (2002). Inflammation and cancer. *Nature* **420**: 860–867.

Di Micco R, Fumagalli M, Cicalese A, Piccinin S, Gasparini P, Luise C *et al*. (2006). Oncogene-induced senescence is a DNA damage response triggered by DNA hyper-replication. *Nature* **444**: 638–642.

DiTullio Jr RA, Mochan TA, Venere M, Bartkova J, Sehested M, Bartek J *et al*. (2002). 53BP1 functions in an ATM-dependent checkpoint pathway that is constitutively activated in human cancer. *Nat Cell Biol* **4**: 998–1002.

Engstrom JU, Kmiec EB. (2007). Manipulation of cell cycle progression can counteract the apparent loss of correction frequency following oligonucleotide-directed gene repair. *BMC Mol Biol* **8**: 9–25.

Fisher PB. (2005). Is mda-7/IL-24 a 'magic bullet' for cancer? *Cancer Res* **65**: 10128–10138.

Halazonetis TD, Gorgoulis VG, Bartek J. (2008). An oncogene-induced DNA damage model for cancer development. *Science* **319**: 1352–1355.

Han Z, Wei W, Dunaway S, Darnowski JW, Calabresi P, Sedivy J *et al*. (2002). Role of p21 in apoptosis and senescence of human colon cancer cells treated with camptothecin. *J Biol Chem* **277**: 17154–17160.

Hayflick L, Moorhead PS. (1961). The serial cultivation of human diploid cell strains. *Exp Cell Res* **25**: 585–621.

Honda K, Yanai H, Takaoka A, Taniguchi T. (2005). Regulation of the type I IFN induction: a current view. *Int Immunol* **17**: 1367–1378.

Chang BD, Broude EV, Dokmanovic M, Zhu H, Ruth A, Xuan Y *et al*. (1999). A senescence-like phenotype distinguishes tumor cells that undergo terminal proliferation arrest after exposure to anticancer agents. *Cancer Res* **59**: 3761–3767.

Chelbi-Alix MK, Pelicano L, Quignon F, Koken MH, Venturini L, Stadler M *et al*. (1995). Induction of the PML protein by interferons in normal and APL cells. *Leukemia* **9**: 2027–2033.

Imada K, Leonard WJ. (2000). The Jak-STAT pathway. *Mol Immunol* **37**: 1–11.

Janderova-Rossmeislova L, Novakova Z, Vlasakova J, Philimonenko V, Hozak P, Hodny Z. (2007). PML protein association with specific nucleolar structures differs in normal, tumor and senescent human cells. *J Struct Biol* **159**: 56–70.

Kaynor C, Xin M, Wakefield J, Barsoum J, Qin XQ. (2002). Direct evidence that IFN-beta functions as a tumor-suppressor protein. *J Interferon Cytokine Res* **22**: 1089–1098.

Kim TK, Maniatis T. (1997). The mechanism of transcriptional synergy of an *in vitro* assembled interferon-beta enhanceosome. *Mol Cell* **1**: 119–129.

Krtolica A, Parrinello S, Lockett S, Desprez PY, Campisi J. (2001). Senescent fibroblasts promote epithelial cell growth and tumorigenesis: a link between cancer and aging. *Proc Natl Acad Sci USA* **98**: 12072–12077.

Kuilman T, Michaloglou C, Vredeveld LC, Douma S, van Doorn R, Desmet CJ *et al*. (2008). Oncogene-induced senescence relayed by an interleukin-dependent inflammatory network. *Cell* **133**: 1019–1031.

Kuilman T, Peeper DS. (2009). Senescence-messaging secretome: SMSing cellular stress. *Nat Rev Cancer* **9**: 81–94.

Kulaeva OI, Draghici S, Tang L, Kraniak JM, Land SJ, Tainsky MA. (2003). Epigenetic silencing of multiple interferon pathway genes after cellular immortalization. *Oncogene* **22**: 4118–4127.

Lin WW, Karin M. (2007). A cytokine-mediated link between innate immunity, inflammation, and cancer. *J Clin Invest* **117**: 1175–1183.

Mallette FA, Ferbeyre G. (2007). The DNA damage signaling pathway connects oncogenic stress to cellular senescence. *Cell Cycle* **6**: 1831–1836.

Mallette FA, Gaumont-Leclerc MF, Ferbeyre G. (2007). The DNA damage signaling pathway is a critical mediator of oncogene-induced senescence. *Genes Dev* **21**: 43–48.

Michaloglou C, Vredeveld LCW, Soengas MS, Denoyelle C, Kuilman T, van der Horst CMAM *et al*. (2005). BRAFE600-associated senescence-like cell cycle arrest of human naevi. *Nature* **436**: 720–724.

Michishita E, Nakabayashi K, Suzuki T, Kaul SC, Ogino H, Fujii M *et al*. (1999). 5-Bromodeoxyuridine induces senescence-like phenomena in mammalian cells regardless of cell type or species. *J Biochem (Tokyo)* **126**: 1052–1059.

Minagawa S, Nakabayashi K, Fujii M, Scherer SW, Ayusawa D. (2005). Early BrdU-responsive genes constitute a novel class of senescence-associated genes in human cells. *Exp Cell Res* **304**: 552–558.

Moiseeva O, Mallette FA, Mukhopadhyay UK, Moores A, Ferbeyre G. (2006). DNA damage signaling and p53-dependent senescence after prolonged {beta}-interferon stimulation. *Mol Biol Cell* **17**: 1583–1592.

Mushinski JF, Nguyen P, Stevens LM, Khanna C, Lee S, Chung EJ *et al*. (2009). Inhibition of tumor cell motility by the interferon-inducible GTPase MxA. *J Biol Chem* **284**: 15206–15214.

Pamment J, Ramsay E, Kelleher M, Dornan D, Ball KL. (2002). Regulation of the IRF-1 tumour modifier during the response to

genotoxic stress involves an ATM-dependent signalling pathway. *Oncogene* **21**: 7776–7785.

Parrinello S, Coppe JP, Krtolica A, Campisi J. (2005). Stromal-epithelial interactions in aging and cancer: senescent fibroblasts alter epithelial cell differentiation. *J Cell Sci* **118**: 485–496.

Qing Y, Stark GR. (2004). Alternative activation of STAT1 and STAT3 in response to interferon-gamma. *J Biol Chem* **279**: 41679–41685.

Ronni T, Matikainen S, Lehtonen A, Palvimo J, Dellis J, Van Eylen F *et al*. (1998). The proximal interferon-stimulated response elements are essential for interferon responsiveness: a promoter analysis of the antiviral MxA gene. *J Interferon Cytokine Res* **18**: 773–781.

Sager R. (1991). Senescence as a mode of tumor suppression. *Environ Health Perspect* **93**: 59–62.

Serrano M, Lin AW, McCurrach ME, Beach D, Lowe SW. (1997). Oncogenic ras provokes premature cell senescence associated with accumulation of p53 and p16INK4a. *Cell* **88**: 593–602.

Shuai K, Liu B. (2005). Regulation of gene-activation pathways by PIAS proteins in the immune system. *Nat Rev Immunol* **5**: 593–605.

Schmitt CA. (2007). Cellular senescence and cancer treatment. *Biochim Biophys Acta* **1775**: 5–20.

Suzuki T, Michishita E, Ogino H, Fujii M, Ayusawa D. (2002). Synergistic induction of the senescence-associated genes by 5-bromodeoxyuridine and AT-binding ligands in HeLa cells. *Exp Cell Res* **276**: 174–184.

Suzuki T, Yaginuma M, Oishi T, Michishita E, Ogino H, Fujii M *et al*. (2001). 5-Bromodeoxyuridine suppresses position effect variegation of transgenes in HeLa cells. *Exp Cell Res* **266**: 53–63.

Timmermann S, Hinds PW, Munger K. (1998). Re-expression of endogenous p16ink4a in oral squamous cell carcinoma lines by 5-aza-2′-deoxycytidine treatment induces a senescence-like state. *Oncogene* **17**: 3445–3453.

Toussaint O, Royer V, Salmon M, Remacle J. (2002). Stress-induced premature senescence and tissue ageing. *Biochem Pharmacol* **64**: 1007–1009.

van Boxel-Dezaire AHH, Rani MRS, Stark GR. (2006). Complex modulation of cell type-specific signaling in response to type i interferons. *Immunity* **25**: 361–372.

von Zglinicki T. (2002). Oxidative stress shortens telomeres. *Trends Biochem Sci* **27**: 339–344.

Yogev O, Anzi S, Inoue K, Shaulian E. (2006). Induction of transcriptionally active Jun proteins regulates drug-induced senescence. *J Biol Chem* **281**: 34475–34483.

Supplementary Information accompanies the paper on the Oncogene website (http://www.nature.com/onc)

Supplementary materials and methods

Chemicals and antibodies

X-Gal was purchased from Fluka (Buchs, Switzerland). Human recombinant IL6 was purchased from Peprotech (New Jersey, USA) and JAK Inhibitor I (2-(1,1-dimethylethyl)-9-fluoro-3,6-dihydro-7H-benz[h]-imidaz[4,5-f]isoquinolin-7-one) from Calbiochem (Beeston, UK). Following antibodies were used: anti-PML rabbit serum, polyclonal sera against IRF1 (sc-13041), IRF7 (H-246) and p16 (H-156), rabbit serum C-20 against STAT3 (all from Santa Cruz Biotechnology, Santa Cruz, CA, USA), mouse monoclonal antibodies against STAT1 and phosphoserine 727 of STAT1 (EXBIO, Prague, Czech Republic), rabbit polyclonal serum against phosphotyrosine 701 of STAT1, anti-phosphoTyr705-STAT3 mouse monoclonal antibody and anti-phosphoSer15-p53 rabbit serum (Cell Signalling Technology, Danvers, MA, USA), anti-IL6 goat serum (R&D Systems, Minneapolis, MN, USA), mouse monoclonal antibody 6G5 against GAPDH (Acris Antibodies GmbH, Hiddenhausen, Germany), mouse monoclonal antibody against JAK1 (#05-1154; Millipore, Billerica, MA, USA), anti-MX1 mouse monoclonal antibody gifted by dr. Otto Haller (Institute for medical microbiology and hygiene, Freiburg, Germany), human autoimmune serum reactive with PCNA provided by dr. Kafkova (Institute of Rheumatology, Prague, Czech Republic), mouse monoclonal antibody against Rb (BD Pharmingen, San Diego, CA, USA), anti-p21 monoclonal antibody (DSC60; (Thullberg *et al.*, 2000); and Transduction Laboratories, Lexington; KY, USA), polyclonal serum against p53 obtained from dr. Vojtesek (Masaryk memorial cancer institute, Brno, Czech Republic). Secondary antibody conjugated with ALEXA 568 was purchased from Molecular Probes (Eugene, OR, USA).

Cell cultures

MDA-MB-468 and HS913T cells were cultured in Dulbecco's modified Eagle's medium supplemented with 10% fetal bovine serum (FBS), and H1299 were grown in RPMI-1640/10% FBS. Mouse hybridoma B9 cells (Deutsche Sammlung von Mikroorganismen und Zellkulturen GmbH, Braunschweig, Germany) were cultured in RPMI-1640 supplemented with 10% FBS, 50 μM mercaptoethanol and IL6 (100 pg/ml). Cells were kept at 37°C under 5% CO_2 atmosphere and 95% humidity.

Estimation of cellular senescence *in vitro*

Senescence associated-β-galactosidase assay was performed according to (Dimri *et al.*, 1995) with modifications described in (Serrano *et al.*, 1997). Images were captured by fluorescence microscope (Leica DMRXA or Leica DM6000B, Leica Microsystems, Wetzlar, Germany) equipped with digital camera, contrast of images was adjusted in Adobe Photoshop software.

Estimation of cytokine production

To assess a biological activity of cytokines secreted by senescent cells into cultivation medium, HeLa cells were driven into senescence by cultivation in 10 μM BrdU/10 μM DMA for 6 days. The cultivation medium was then removed, the cells thoroughly washed with fresh medium and cultivated in fresh drug-free medium for next 4 days with exchange at second day. The medium conditioned by senescent cells was removed at day 2 and 4 and transferred to normal proliferating HeLa cells. Control cells were treated in the same way by the medium conditioned by normal HeLa cell culture. After 4 days of cultivation in conditioned medium, cultures were harvested for further analysis of PML and STAT1 expression by immunoblotting.

Estimation of IL6 biological activity

To test the biological activity of IL6 secreted by senescent HeLa cells and the decrease of IL6 upon the knock-down mediated via IL6-specific short hairpin RNA, growth dependency of mouse hybridoma B9 cells on the presence of IL6 was exploited (Helle *et al.*, 1988). HeLa cells, either wild-type (untreated), or transduced with short hairpin non-sense (control) or IL6-specific shRNA (IL6 #1), were treated for 6 days with BrdU+DMA (10 μM). Cultivation medium (10% FBS/DMEM) was changed every second day with fresh drugs replenished. At day 6, medium was removed, the cells were thoroughly washed with fresh medium and cultivated in fresh drug-free 10% FBS/RPMI-1640 medium for the next 24 hours. The conditioned media were then transferred in increasing dilutions to mouse hybridoma B9 cells seeded in triplicate at the density of 25 000 cells/ml in 24 well plate. The dilution of medium conditioned by untreated HeLa cells, the addition of which no longer supported growth of B9 cells, was estimated as approximately 1:4000. This dilution was selected as the standard for subsequent comparative estimation of IL6 biological activity of conditioned media from

senescent HeLa cells treated with either control or IL6-specific shRNA, in the B9 cell growth assay. As positive or negative controls, B9 cells were cultivated with or without addition of recombinant IL6 (100 pg). 50-µl aliquots of B9 cell suspension cultures were taken every 24 hours for several days, and cell growth (cell count) and viability were measured after staining with Hoechst 33258 (Invitrogene, Carlsbad, CA, USA) by flow cytometer (BD LSRII, BD, Franklin Lakes, NJ, USA). Each experiment was performed in triplicate.

Primers used in qRT-PCR

GAPDH, 5'-GTCGGAGTCAACGGATTTGG-3', 5'-AAAAGCAGCCCTGGTGACC-3';
IRF-1, 5'-CTGGCACATCCCAGTGGAA-3', 5'-CATCCTCATCTGTTGTAGCTTCAGA-3';
IFNβ, 5'-AACTTTGACATCCCTGAGGAGATT-3', 5'-GCGGCGTCCTCCTTCTG-3';
IRF-7, 5'-CCCCCATCTTCGACTTCAGA-3', 5'-CAGGACCAGGCTCTTCTCCTT-3';
IL6, 5'-AGCCCTGAGAAAGGAGACATGTA-3', 5'-TCTGCCAGTGCCTCTTTGC-3';
MX1, 5'-CTCCCACTCCCTGAAATCTG-3', 5'-GAGCTGTTCTCCTGCACCTC-3'.
JAK1, 5′-GGATAACATCAGCTTCATGCTAAA-3′, 5′-CACCAGCAGGTTGGAGA TTT-3′;
C/EBPbeta, 5′-ACCCACGTGTAACTGTCAGCC-3′, 5′-TCAACAGCAACAAGCCCGT-3′

Determination of expression of interferon stimulated genes and cytokines by RT^2 Profiler PCR Array System

Total RNA was isolated using TriReagent and applied on RNeasy minicolumns (Qiagen, GmbH, Hilden, Germany). Briefly, cells were harvested into 1 vol TriReagent, 1/5 vol chloroform was then added. Following the addition of chloroform, the aqueous phase containing RNA was mixed with 2 volumes of 70% ethanol and applied onto RNeasy minicolumns according to the manufacturer's protocol. To eliminate contamination by genomic DNA, RNA was treated with 80 U/ml DNase for 40 minutes at 37°C. Quality of RNA was estimated by capillary electrophoresis using Agilent 2100 Bioanalyzer (Agilent Technologies, Santa Clara, CA, USA). RT-PCR was performed as described in previous paragraph. The mRNA levels of 84 ISGs and 84 cytokine genes were measured by the RT^2 Profiler PCR Array System ("Interferons and Receptors" cat. no. APHS-064 and "Common Cytokines" cat. no. APHS-021, SuperArray Bioscience Corp., Frederic, MD, USA) in ABI Prism 7300 using Power SYBR Green I Master Mix. The relative quantity of cDNA was

calculated by the $\Delta\Delta C_t$ method using five normalization genes: β-2-microglobulin, hypoxanthine phosphoribosyltransferase 1, ribosomal protein L13a, glyceraldehydes-3-phosphate dehydrogenase and actin. The results shown in Table 1, Table 2, Suppl. Table 1 and Suppl. Table 2 were acquired from one experiment, in which every gene was measured twice for every condition; p value was calculated by t-test from the values of duplicate measurements. Only genes which are induced more than 5-fold and their p value is less than 0.01 are listed in the Table 1 and 2.

SDS-PAGE and Western blotting

Cells were harvested into ice-cold PBS supplemented with inhibitors of proteases (1 mM AEBSF, 1 μg/ml leupeptin, 1 μg/ml pepstatin; Serva) and cocktail of phosphatase inhibitors (Sigma), centrifuged at 400×*g* for 5 minutes at 4°C and lysed in 62.5 mM Tris pH 6.8, 10% glycerol, 2% SDS. Then concentration of proteins was estimated by BCA method (Pierce Biotechnology Inc, Rockford, USA). 100 mM DTT and 0.01% bromphenol was added to lysates before separation in polyacrylamide gels by SDS-PAGE. The same protein amount was loaded into each well. Proteins were then electrotransferred onto nitrocellulose membrane using semi-dry blotting and detected by specific antibodies combined with horseradish peroxidase-conjugated secondary antibodies (goat anti-rabbit, goat anti-mouse, Bio-Rad, Hercules, CA, USA, rabbit anti-goat, Santa Cruz Biotechnology). Proteins were detected by ECL (Pierce Biotechnology). GAPDH was used as a marker of equal loading. Adobe Photoshop software was used for contrast adjustment of images.

Indirect immunofluorescence

Cells grown on glass cover slips were fixed by 4% paraformaldehyde and then permeabilized by 0.2% Triton X-100 for 15 minutes at RT. Cells were incubated with diluted primary antibody overnight at 4°C. The incubation with secondary antibodies was performed for 1 hour at RT. To counterstain nuclei cover slips were stained with DAPI (Sigma, St. Louis, MO, USA) for 20 minutes then mounted in Vectashield (Vector Laboratories, Burlingame, CA, USA) and viewed by fluorescence microscope (Leica DM6000B). Images were processed in Adobe Photoshop software.

The list of shRNAs used

Knockdown vectors containing shRNAs were purchased from OpenBiosystems (Huntsville, AL, USA) and Sigma (St. Louis, MO, USA). Non sense shRNA sequences (sh-ctrl; sequences were not provided by producer) or empty vectors (ctrl) were used as a negative control shRNA.

JAK1:
Control: shRNA (sh-ctrl) tagged with GFP – pGIPZ lentiviral shRNAmir
Jak1-specific shRNA (sh-Jak1) tagged by GFP – pGIPZ vector
sh-Jak1 #1
CCCATGGAAATGTGTGTACTAATAGTGAAGCCACAGATGTA
TTAGTACACACATTTCCATGGA

Control: empty pLKO.1 vector, Addgene, plasmid 10879
Jak1-specific shRNA (sh-Jak1) in LKO vector (Sigma)
shJAK1 #2
TRCN0000121275 (Sigma)
CCGGCGTTCTCTACTACGAAGTGATCTCGAGATCACTTCGTAGTAGAGAACGTTTT
TG
shJAK1 #3
TRCN0000003102 (Sigma)
CCGGGAGACTTCCATGTTACTGATTCTCGAGAATCAGTAACATGGAAGTCTCTTTT
T
shJAK1 #4
TRCN0000003104 (Sigma)
CCGGCTGAGCTACTTGGAGGATAAACTCGAGTTTATCCTCCAAGTAGCTCAGTTTT
T

IL6:
Control: shRNA (sh-ctrl) tagged with GFP – pGIPZ lentiviral shRNAmir
IL6-specific shRNA (sh-IL6) tagged by GFP – pGIPZ vector
sh-IL6 #1
AGCAAAGAATCTAGATGCAATATAGTGAAGCCACAGATGTA
TATTGCATCTAGATTCTTTGCC

sh-IL6 #2
CGGACATGACAACTCATCTCATTAGTGAAGCCACAGATGTA
ATGAGATGAGTTGTCATGTCCT
sh-IL6 #3
CCCTCAGATTGTTGTTGTTAATTAGTGAAGCCACAGATGTA
ATTAACAACAACAATCTGAGGT

Supplementary references

Dimri GP, Lee X, Basile G, Acosta M, Scott G, Roskelley C *et al* (1995). A biomarker that identifies senescent human cells in culture and in aging skin in vivo. *Proc Natl Acad Sci U S A* **92:** 9363-7.

Helle M, Boeije L, Aarden LA (1988). Functional discrimination between interleukin 6 and interleukin 1. *Eur J Immunol* **18:** 1535-40.

Serrano M, Lin AW, McCurrach ME, Beach D, Lowe SW (1997). Oncogenic ras provokes premature cell senescence associated with accumulation of p53 and p16INK4a. *Cell* **88:** 593-602.

Thullberg M, Welcker M, Bartkova J, Kjerulff AA, Lukas J, Hogberg J *et al* (2000). Monoclonal antibody probes for p21WAF1/CIP1 and the INK4 family of cyclin-dependent kinase inhibitors. *Hybridoma* **19:** 63-72.

Supplementary Figure 1

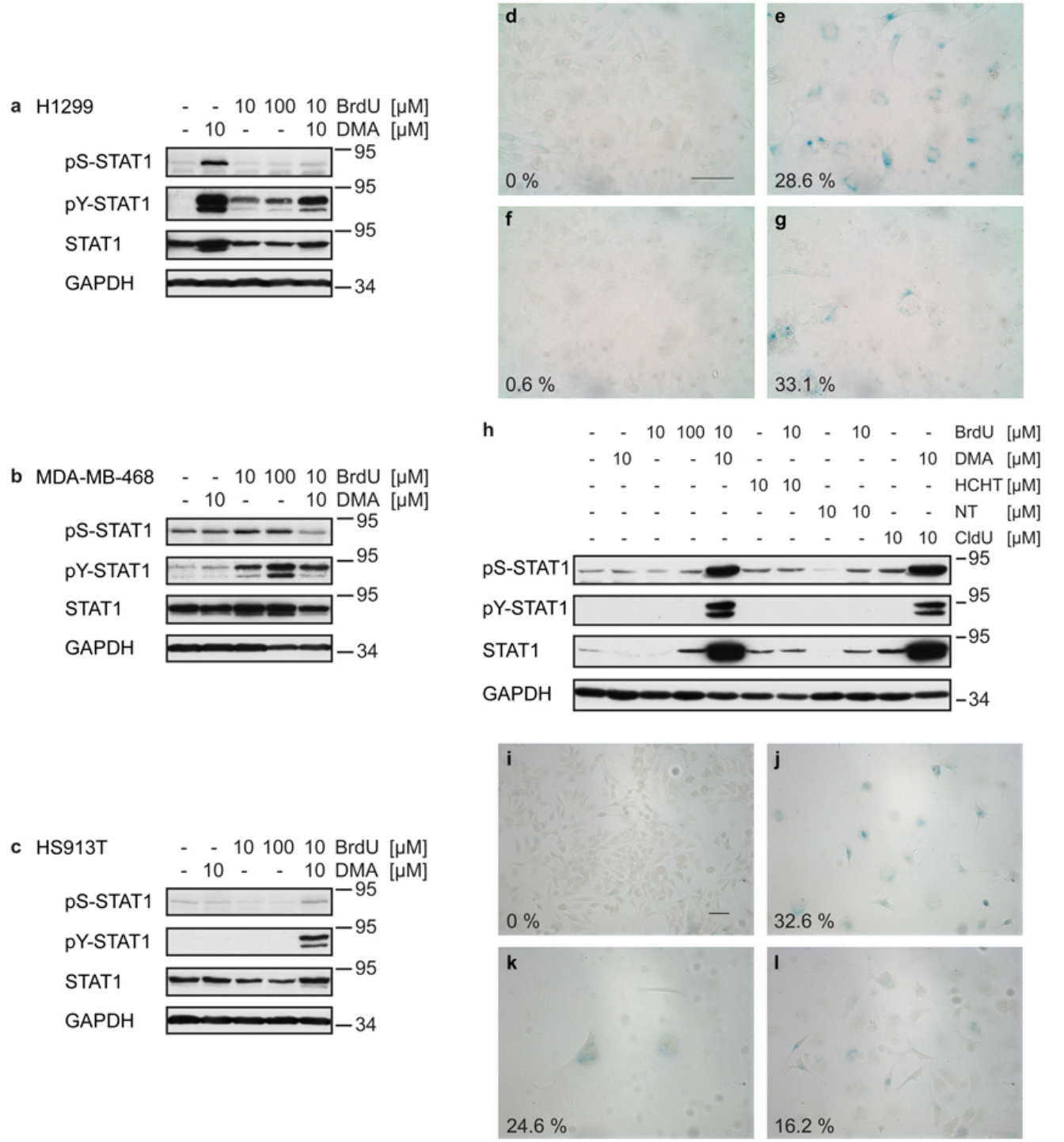

Supplementary Figure 1. Activation of STAT1 by senescence-inducing drugs.
The level of total STAT1 and its activated forms phosphorylated on serine727 (pS) and tyrosine701 (pY) detected by immunoblot in H1299 (a), MDA-MB-468 (b) and HS913T (c) cells after 6 days of treatment. Senescence associated-β-galactosidase (SA-β-gal) assay of HeLa cells treated for 6 days with vehicle (d) or 10 μM DMA/10 μM BrdU (e) and U2OS cells treated for 6 days with vehicle (f) or 100 μM BrdU (g); bar, 50 μm. (h) Immunodetection of STAT1 expression and phosphorylation in HeLa cells treated for 6 days by various genotoxic drugs and their combination. GAPDH was used as loading control. Senescence induced by 6-day treatment of vehicle (i), 10 μM DMA/10 μM BrdU (j), 0.3 μM APH (k) or 200 μM HU (l) was detected by SA-β-gal assay in HeLa cells; bar 50 μm. Representation of SA-β-gal-positive cells in culture is shown in percentage (counted from at least 500 cells).

Supplementary Figure 2

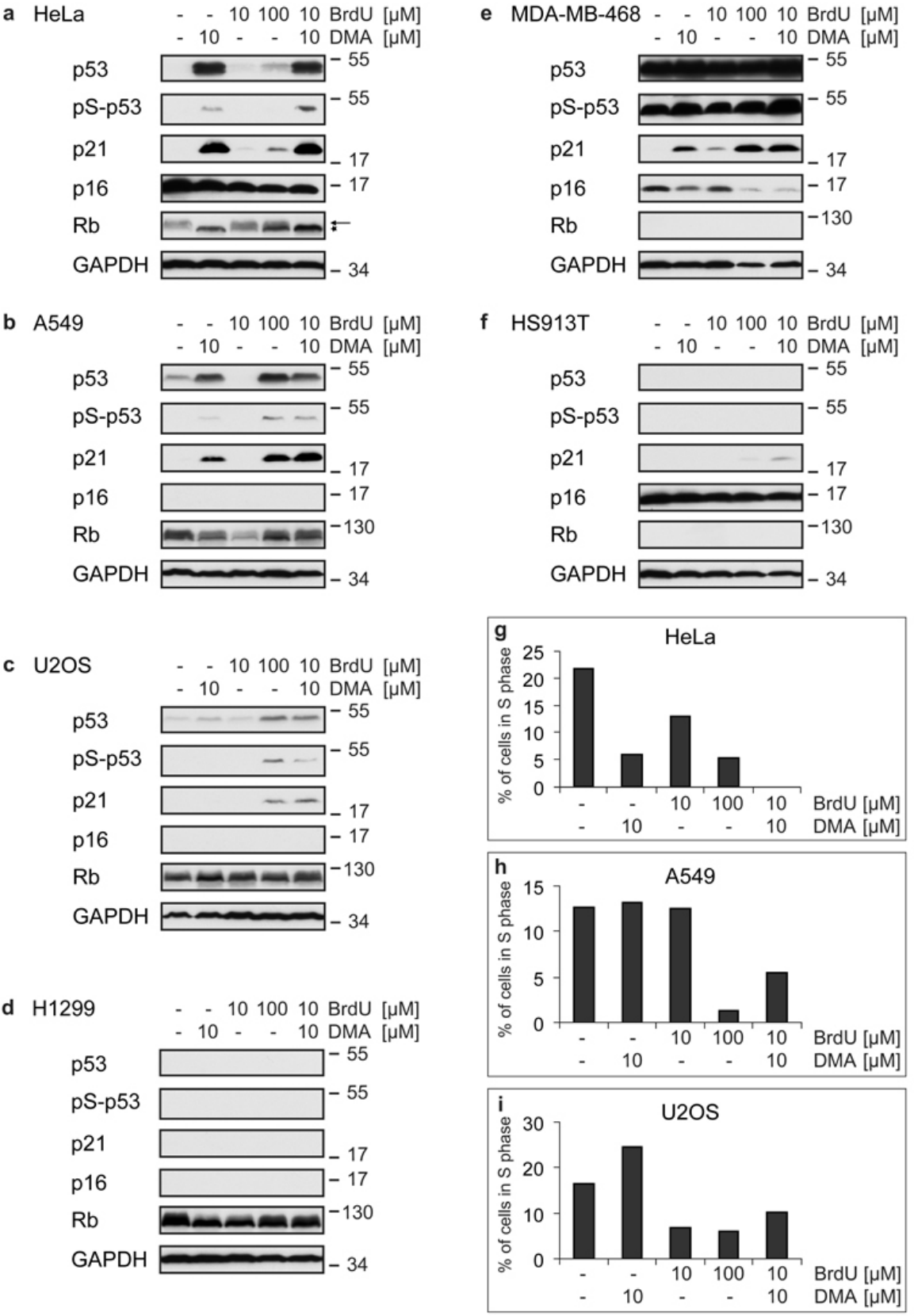

Supplementary Figure 2. Level of tumor suppressors and rate of proliferation after BrdU and DMA treatment in several cell lines.

Immunodetection of p53 and its serin-15-phosphorylated form (pS-p53), p21 and p16 expression level and expression and phosphorylation status of Rb (phosphorylated Rb – arrow, hypophosphorylated Rb – asterisk) in HeLa (a), A549 (b), U2OS (c), H1299 (d), MDA-MB-468 (e) and HS93T(f) cell lines after 6 days of treatment. All immunoblots were processed in one experiment, exposure time of each protein was the same for all cell lines shown. GAPDH was used as a loading control. Proliferation rate in HeLa (g), A549 (h) and U2OS (i) cultures after 6 day-treatment was estimated by S phase specific pattern of PCNA in at least 200 cells per culture.

Supplementary Figure 3

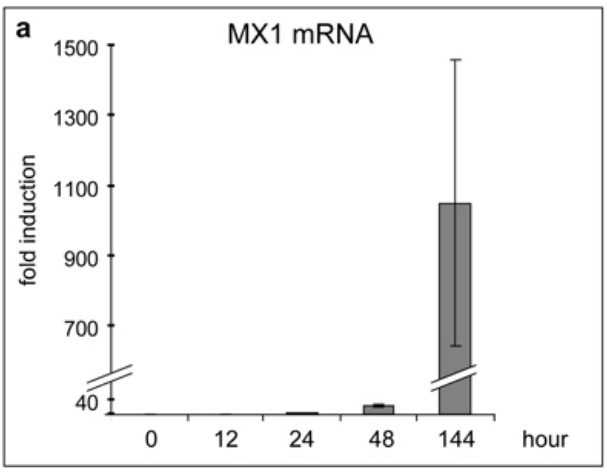

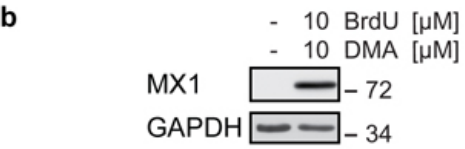

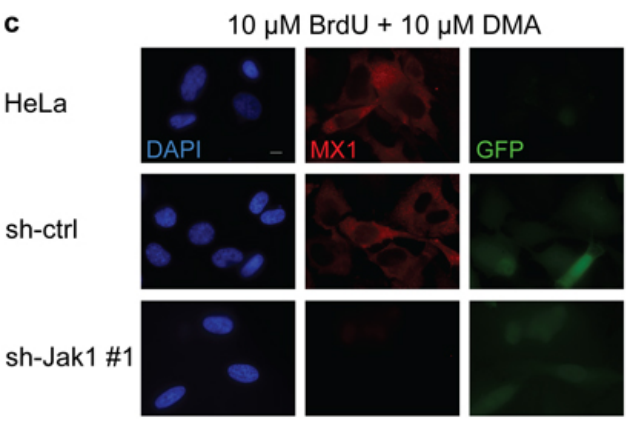

Supplementary Figure 3. BrdU+DMA-treatment increases mRNA and protein level of MX1. (a) Time course of MX1 mRNA level quantified by qRT-PCR in HeLa cells during treatment with combination of 10 μM BrdU and 10 μM DMA. (b) Immunoblot detection of MX1 expression level in HeLa cells after 6 days of BrdU+DMA treatment. GAPDH was used as a loading control. (c) Immunofluorescent detection of MX1 and GFP (anti-MX1 antibody in red, GFP in green as marker of transduction, DAPI in blue) in HeLa cells non-transduced or transduced by non-sense shRNA (sh-ctrl) or Jak1-specific shRNA (sh-Jak1 #1) which were treated for 6 days with 10 μM BrdU + 10 μM DMA. Representative micro-graphs are shown; bar, 10 μm.

Supplementary Figure 4

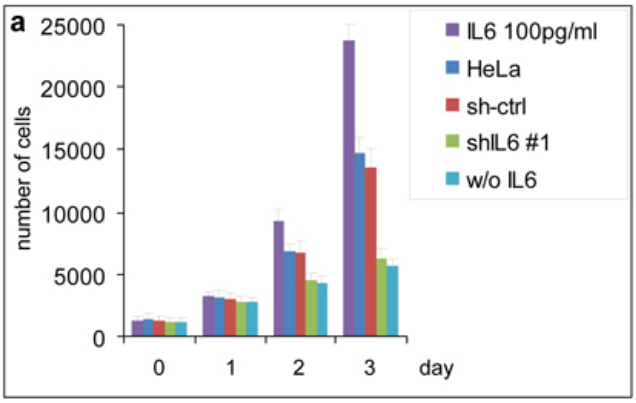

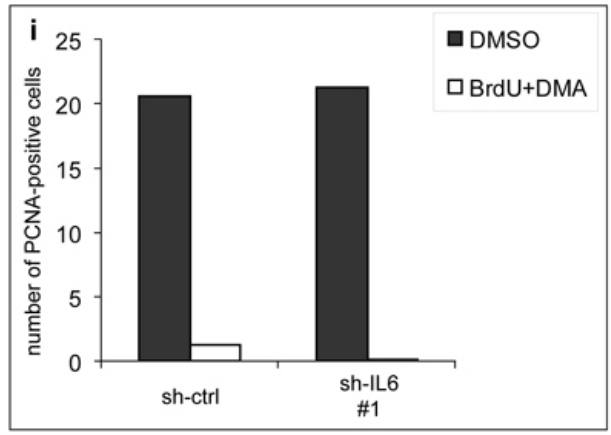

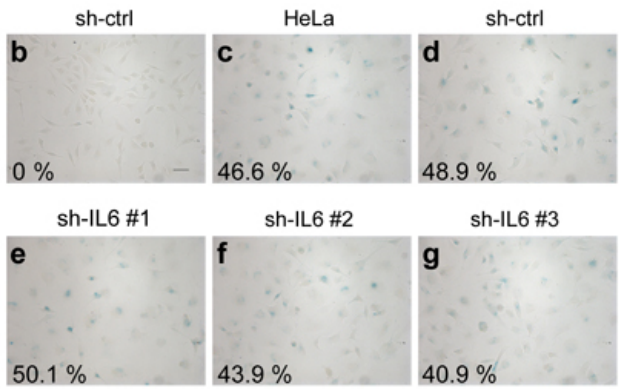

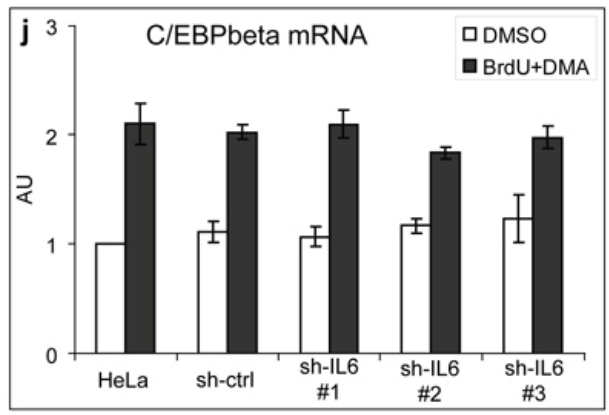

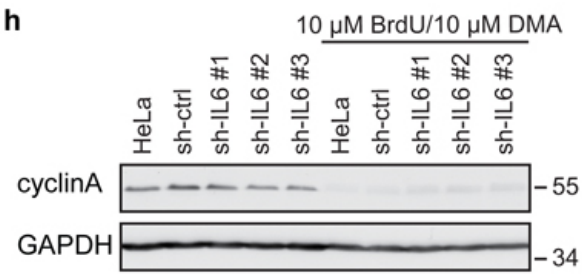

Supplementary Figure 4. Depletion of IL6 does not protect HeLa cells from BrdU+DMA-induced senescence. (a) Growth response of mouse hybridoma B9 cells to medium supplemented with (IL6 100 pg/ml) or without IL6 (w/o IL6), with 1:4000 dilution of conditioned medium from non-transduced (HeLa), non sense short hairpin RNA transduced (sh-ctrl) and shIL6#1 (shIL6 #1) transduced BrdU+DMA-treated HeLa cells. Average from three independent experiments is shown. Error bars represent standard deviation.

Representation of senescence associated-β-galactosidase-positive cells (shown in percentage; counted from at least 270 cells) in HeLa cells non-infected (HeLa; c) and infected with non-sense shRNA (sh-ctrl; b and d) and IL6-specific shRNA #1, #2 and #3 (sh-IL6; e, f and g) after 6-day treatment with vehicle (b) or 10 μM DMA/10 μM BrdU (c, d, e, f and g); bar 50 μm. Proliferation in HeLa cells containing IL6-specific short haipin RNAs after 6 day-treatment was estimated by immunodetection of cyclin A (h; GAPDH was used as a loading control), and by S phase specific pattern of PCNA (i; counted in at least 200 cells). qRT-PCR analysis of C/EBPbeta mRNA level in HeLa cells non-infected (HeLa) and infected with non-sense shRNA (sh-ctrl) and IL6-specific shRNA #1, #2 and #3 (j). The values representing average from three independent experiments are shown as arbitrary units relative to control; error bars represent standard error.

Supplementary Figure 5

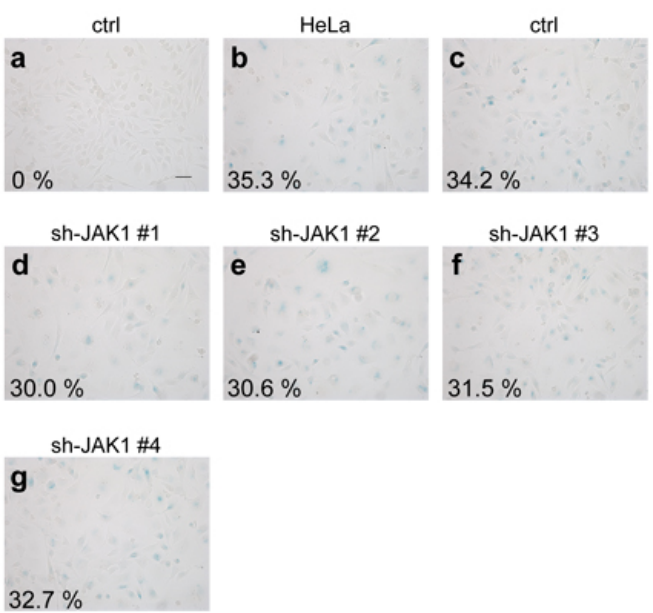

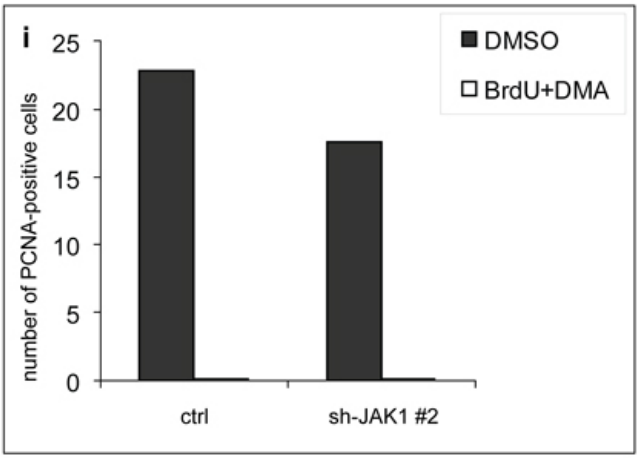

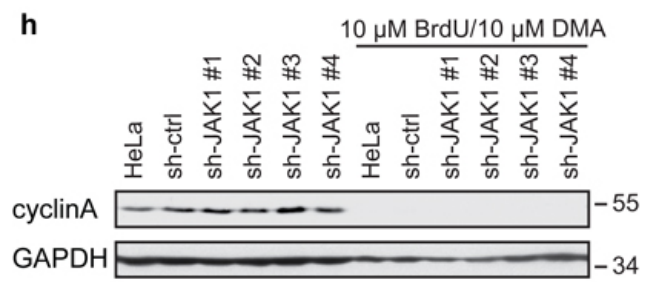

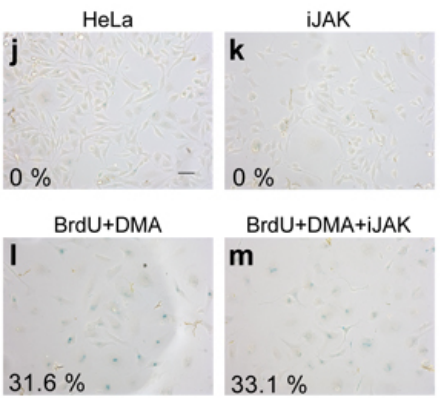

Supplementary Figure 5. Depletion of JAK1 does not protect HeLa cells from BrdU+DMA-induced senescence. (a-g) Representation of senescence associated-β-galactosidase-positive cells (shown in percentage; counted from 300 cells) in HeLa cells non-infected (HeLa; b) and infected with empty vector (ctrl; a and c) and JAK1-specific shRNA #1, #2, #3 and #4 (sh-Jak1; d, e, f and g) after 6-day treatment with vehicle (a) or 10 μM DMA/10 μM BrdU (b, c, d, e, f and g); bar, 50 μm. Proliferation of HeLa cells containing JAK1-specific RNA after 6 day-treatment was estimated by immunodetection of cyclin A (h; GAPDH was used as a loading control), and by S phase specific pattern of PCNA (i; counted in at least 200 cells). Presence of senescence associated-β-galactosidase-positive cells in HeLa cell cultures treated by vehicle (HeLa; j), 0.25 μM inhibitor of JAK kinases (iJAK; k), 10 μM BrdU+10 μM DMA (BrdU+DMA; l) and by their combination (BrdU+DMA+iJAK; m) is shown in percentage (counted from 300 cells); bar, 50 μm.

Supplementary tables

Supplementary Table 1. Induction of mRNA levels of 84 genes measured by RT^2 Profiler PCR Array "Interferons and Receptors" in HeLa cells treated by 10 μM BrdU+DMA

UniGene	Description	Fold ind.	p value
Hs.12341	Adenosine deaminase, RNA-specific	1.57	0.0072
Hs.129966	Ciliary neurotrophic factor receptor	0.53	0.4613
Hs.287729	Cytokine receptor-like factor 2	1.44	0.5400
Hs.520937	Colony stimulating factor 2 receptor, alpha, low-affinity	3.77	0.0033
Hs.524517	Colony stimulating factor 3 receptor	0.74	0.6650
Hs.632586	Chemokine (C-X-C motif) ligand 10	503.20	0.0005
Hs.501452	Epstein-Barr virus induced gene 3	78.25	0.0119
Hs.62192	Coagulation factor III (thromboplastin, tissue factor)	11.71	0.0006
Hs.61232	Interleukin 20 receptor beta	2.11	0.0040
Hs.458485	ISG15 ubiquitin-like modifier	91.77	0.0000
Hs.523847	Interferon, alpha-inducible protein 6	58.28	0.0004
Hs.380250	Interferon, gamma-inducible protein 16	7.70	0.0041
Hs.532634	Interferon, alpha-inducible protein 27	42.52	0.0007
Hs.14623	Interferon, gamma-inducible protein 30	2.55	0.0584
Hs.632258	Interferon-induced protein 35	7.81	0.0115
Hs.82316	Interferon-induced protein 44	5.94	0.0089
Hs.389724	Interferon-induced protein 44-like	2.31	0.0045
Hs.163173	Interferon induced with helicase C domain 1	46.37	0.0012
Hs.20315	Interferon-induced protein with tetratricopeptide repeats 1	170.66	0.0004
Hs.500491	Interferon-induced protein with tetratricopeptide repeats 1-like	0.71	0.4277
Hs.437609	Interferon-induced protein with tetratricopeptide repeats 2	21.41	0.0000
Hs.47338	Interferon-induced protein with tetratricopeptide repeats 3	96.67	0.0007
Hs.458414	Interferon induced transmembrane protein 1 (9-27)	41.64	0.0006
Hs.174195	Interferon induced transmembrane protein 2 (1-8D)	2.60	0.0042
Hs.37026	Interferon, alpha 1	0.95	0.9341
Hs.93907	Interferon, alpha 14	0.43	0.3744
Hs.211575	Interferon, alpha 2	0.10	0.0031
Hs.113211	Interferon, alpha 21	0.54	0.0398
Hs.1510	Interferon, alpha 4	0.44	0.6780
Hs.37113	Interferon, alpha 5	0.37	0.1013
Hs.533470	Interferon, alpha 6	0.75	0.4855
Hs.73890	Interferon, alpha 8	0.12	0.0370
Hs.529400	Interferon (alpha, beta and omega) receptor 1	0.78	0.0836
Hs.642682	Interferon (alpha, beta and omega) receptor 2	0.35	0.0115
Hs.93177	Interferon, beta 1, fibroblast	14.77	0.0234

Hs.441972	Interferon epsilon 1	0.30	0.0024
Hs.856	Interferon, gamma	3.16	0.0070
Hs.520414	Interferon gamma receptor 1	1.13	0.4053
Hs.634632	Interferon gamma receptor 2 (interferon gamma transducer 1)	1.24	0.1355
Hs.591083	Interferon, kappa	0.42	0.0244
Hs.73010	Interferon, omega 1	1.69	0.0021
Hs.7879	Interferon-related developmental regulator 1	0.28	0.0049
Hs.315177	Interferon-related developmental regulator 2	0.37	0.0043
Hs.504035	Interleukin 10 receptor, alpha	3.82	0.2635
Hs.512211	Interleukin 10 receptor, beta	0.80	0.1310
Hs.591088	Interleukin 11 receptor, alpha	0.64	0.1344
Hs.674	Interleukin 12B (natural killer cell stimulatory factor 2, p40)	1.08	0.8703
Hs.496646	Interleukin 13 receptor, alpha 1	0.66	0.0367
Hs.168132	Interleukin 15	0.69	0.2246
Hs.445868	Interleukin 20 receptor, alpha	0.27	0.0158
Hs.210546	Interleukin 21 receptor	1.16	0.7055
Hs.126891	Interleukin 22 receptor, alpha 2	0.51	0.5644
Hs.567792	Interleukin 28A (interferon, lambda 2)	0.51	0.1763
Hs.221375	Interleukin 28 receptor, alpha (interferon, lambda receptor)	0.24	0.0088
Hs.406745	Interleukin 29 (interferon, lambda 1)	1.75	0.4158
Hs.474787	Interleukin 2 receptor, beta	1.22	0.6173
Hs.84	Interleukin 2 receptor, gamma	2.89	0.0061
Hs.55378	Interleukin 31 receptor A	1.07	0.9581
Hs.632790	Interleukin 3 receptor, alpha (low affinity)	8.66	0.0090
Hs.513457	Interleukin 4 receptor	3.03	0.0147
Hs.68876	Interleukin 5 receptor, alpha	1.39	0.4930
Hs.512234	Interleukin 6 (interferon, beta 2)	151.69	0.0025
Hs.591492	Interleukin 6 receptor	0.74	0.1583
Hs.591742	Interleukin 7 receptor	5.92	0.0006
Hs.406228	Interleukin 9 receptor	1.13	0.6663
Hs.436061	Interferon regulatory factor 1	7.92	0.0003
Hs.374097	Interferon regulatory factor 2	1.69	0.0044
Hs.515477	Interferon regulatory factor 2 binding protein 1	1.03	0.9276
Hs.350268	Interferon regulatory factor 2 binding protein 2	0.52	0.0058
Hs.75254	Interferon regulatory factor 3	1.69	0.1329
Hs.401013	Interferon regulatory factor 4	28.25	0.0022
Hs.521181	Interferon regulatory factor 5	4.04	0.0063
Hs.591415	Interferon regulatory factor 6	0.83	0.4743
Hs.166120	Interferon regulatory factor 7	12.91	0.0094
Hs.137427	Interferon regulatory factor 8	1.16	0.7909
Hs.519680	Immunity-related GTPase family, M	1.60	0.6211
Hs.23581	Leptin receptor	0.48	0.0377

Hs.82906	Myeloproliferative leukemia virus oncogene	1.17	0.5786
Hs.517307	Myxovirus (influenza virus) resistance 1	1740.15	0.0003
Hs.524760	2',5'-oligoadenylate synthetase 1, 40/46kDa	25.55	0.0004
Hs.75348	Proteasome (prosome, macropain) activator subunit 1 (PA28 alpha)	4.76	0.0003
Hs.224645	Pyrin and HIN domain family, member 1	5.45	0.0057
Hs.145150	SP110 nuclear body protein	11.31	0.0015
Hs.134602	Titin	0.49	0.3531
Hs.534255	Beta-2-microglobulin	2.09	0.0032
Hs.412707	Hypoxanthine phosphoribosyltransferase 1	0.24	0.0009
Hs.546356	Ribosomal protein L13a	0.45	0.0027
Hs.544577	Glyceraldehyde-3-phosphate dehydrogenase	0.27	0.0023
Hs.520640	Actin, beta	0.22	0.0022

Fold ind. = fold induction of the transcript, relative to control.

Supplementary Table 2. Induction of mRNA levels of 84 genes measured by RT^2 Profiler PCR Array "Common Cytokines" in HeLa cells treated by 10 μM BrdU+DMA

UniGene	Description	Fold ind.	p value
Hs.1274	Bone morphogenetic protein 1	0.90	0.1014
Hs.73853	Bone morphogenetic protein 2	2.33	0.0200
Hs.121507	Bone morphogenetic protein 3 (osteogenic)	5.84	0.0088
Hs.68879	Bone morphogenetic protein 4	3.54	0.0049
Hs.296648	Bone morphogenetic protein 5	0.08	0.0005
Hs.285671	Bone morphogenetic protein 6	0.25	0.0072
Hs.473163	Bone morphogenetic protein 7 (osteogenic protein 1)	43.71	0.0003
Hs.409964	Bone morphogenetic protein 8b (osteogenic protein 2)	1.28	0.0049
Hs.591402	Colony stimulating factor 1 (macrophage)	5.98	0.0005
Hs.1349	Colony stimulating factor 2 (granulocyte-macrophage)	1.76	0.4226
Hs.473877	Family with sequence similarity 3, member B	0.93	0.8268
Hs.2007	Fas ligand (TNF superfamily, member 6)	ND	-
Hs.11392	C-fos induced growth factor (vascular endothelial growth factor D)	0.25	0.0127
Hs.2171	Growth differentiation factor 10	ND	-
Hs.643604	Growth differentiation factor 11	0.65	0.0079
Hs.279463	Growth differentiation factor 2	ND	-
Hs.86232	Growth differentiation factor 3	1.17	0.4226
Hs.1573	Growth differentiation factor 5 (cartilage-derived morphogenetic protein-1)	39.81	0.0008
Hs.41565	Growth differentiation factor 8	10.23	0.0244
Hs.25022	Growth differentiation factor 9	0.46	0.0110
Hs.37026	Interferon, alpha 1	0.20	0.0006
Hs.211575	Interferon, alpha 2	2.31	0.1059
Hs.1510	Interferon, alpha 4	0.56	0.3301
Hs.37113	Interferon, alpha 5	ND	-
Hs.73890	Interferon, alpha 8	0.16	0.0401
Hs.93177	Interferon, beta 1, fibroblast	3.58	0.0137
Hs.856	Interferon, gamma	27.76	0.0005
Hs.591083	Interferon, kappa	0.54	0.0021
Hs.193717	Interleukin 10	3.43	ND
Hs.467304	Interleukin 11	4.16	0.0003
Hs.673	Interleukin 12A (natural killer cell stimulatory factor 1, p35)	0.90	0.6029
Hs.674	Interleukin 12B (natural killer cell stimulatory factor 2, p40)	0.42	0.1166
Hs.845	Interleukin 13	0.92	0.4226
Hs.17987	Taxilin alpha	1.36	0.0497
Hs.168132	Interleukin 15	0.18	0.0050
Hs.459095	Interleukin 16 (lymphocyte chemoattractant factor)	5.21	0.0229
Hs.41724	Interleukin 17A	ND	-

Hs.156979	Interleukin 17B	ND	-
Hs.278911	Interleukin 17C	0.66	0.4226
Hs.302036	Interleukin 25	ND	-
Hs.83077	Interleukin 18 (interferon-gamma-inducing factor)	2.23	0.0018
Hs.128395	Interleukin 19	0.86	0.6862
Hs.1722	Interleukin 1, alpha	19.29	0.0028
Hs.126256	Interleukin 1, beta	42.22	0.0090
Hs.306974	Interleukin 1 family, member 10 (theta)	0.96	0.4226
Hs.516301	Interleukin 1 family, member 5 (delta)	5.76	0.0134
Hs.278910	Interleukin 1 family, member 6 (epsilon)	ND	-
Hs.166371	Interleukin 1 family, member 7 (zeta)	0.74	0.1355
Hs.278909	Interleukin 1 family, member 8 (eta)	2.60	0.0166
Hs.211238	Interleukin 1 family, member 9	10.02	0.0011
Hs.89679	Interleukin 2	ND	-
Hs.272373	Interleukin 20	49.18	0.0028
Hs.567559	Interleukin 21	1.35	0.4756
Hs.287369	Interleukin 22	1.27	0.4226
Hs.411311	Interleukin 24	314.08	0.0039
Hs.694	Interleukin 3 (colony-stimulating factor, multiple)	ND	-
Hs.73917	Interleukin 4	0.91	0.4226
Hs.2247	Interleukin 5 (colony-stimulating factor, eosinophil)	0.79	0.1471
Hs.512234	Interleukin 6 (interferon, beta 2)	140.56	0.0023
Hs.591873	Interleukin 7	40.09	0.0010
Hs.624	Interleukin 8	421.68	0.0004
Hs.960	Interleukin 9	8.06	0.0012
Hs.407506	Inhibin, alpha	4.20	0.0377
Hs.583348	Inhibin, beta A (activin A, activin AB alpha polypeptide)	1408.55	0.0008
Hs.520187	Left-right determination factor 2	ND	-
Hs.36	Lymphotoxin alpha (TNF superfamily, member 1)	2.57	0.3500
Hs.376208	Lymphotoxin beta (TNF superfamily, member 3)	1.37	0.4226
Hs.370414	Nodal homolog (mouse)	10.85	0.0012
Hs.645488	Platelet-derived growth factor alpha polypeptide	2.01	0.0085
Hs.170009	Transforming growth factor, alpha	115.36	0.0000
Hs.645227	Transforming growth factor, beta 1	1.41	0.0316
Hs.133379	Transforming growth factor, beta 2	3.13	0.0018
Hs.592317	Transforming growth factor, beta 3	0.24	0.0056
Hs.241570	Tumor necrosis factor (TNF superfamily, member 2)	38.45	0.0003
Hs.81791	Tumor necrosis factor receptor superfamily, member 11b (osteoprotegerin)	0.64	0.0084
Hs.478275	Tumor necrosis factor (ligand) superfamily, member 10	40.64	0.0000
Hs.333791	Tumor necrosis factor (ligand) superfamily, member 11	2.65	0.0004
Hs.415839	Tumor necrosis factor (ligand) superfamily, member 12	1.05	0.6950
Hs.54673	Tumor necrosis factor (ligand) superfamily, member 13	1.40	0.0916
Hs.525157	Tumor necrosis factor (ligand) superfamily, member 13b	1.78	0.0925

Hs.129708	Tumor necrosis factor (ligand) superfamily, member 14	ND	-
Hs.181097	Tumor necrosis factor (ligand) superfamily, member 4	32.33	0.0031
Hs.501497	CD70 molecule	129.34	0.0003
Hs.494901	Tumor necrosis factor (ligand) superfamily, member 8	1.07	0.4226
Hs.534255	Beta-2-microglobulin	1.80	0.1156
Hs.412707	Hypoxanthine phosphoribosyltransferase 1	0.21	0.0009
Hs.546356	Ribosomal protein L13a	0.51	0.0266
Hs.544577	Glyceraldehyde-3-phosphate dehydrogenase	0.25	0.0015
Hs.520640	Actin, beta	0.23	0.0005

Fold ind. = fold induction of the transcript, relative to control.

Cell Cycle 9:15, 3085-3099; August 1, 2010; © 2010 Landes Bioscience

Regulation of the PML tumor suppressor in drug-induced senescence of human normal and cancer cells by JAK/STAT-mediated signaling

Sona Hubackova,[1] Zora Novakova,[1,2,†] Katerina Krejcikova,[1] Martin Kosar,[1] Jana Dobrovolna,[2,‡] Pavlina Duskova,[1,3,] Hana Hanzlikova,[1] Marketa Vancurova,[1] Peter Barath,[4] Jiri Bartek[1,3,5,*] and Zdenek Hodny[1,*]

[1]Department of Genome Integrity; and [2]Department of Biology of Cell Nucleus; Institute of Molecular Genetics; v.v.i., Academy of Sciences of the Czech Republic; Prague, Czech Republic; [3]Laboratory of Genome Integrity; Palacky University; Olomouc, Czech Republic; [4]Laboratory of Molecular Biology; Cancer Research Institute; Slovak Academy of Sciences; Bratislava, Slovakia; [5]Institute of Cancer Biology and Centre for Genotoxic Stress Research; Danish Cancer Society; Copenhagen, Denmark

[†]Current address: Biology of Reproduction Department; Institute of Animal Science; Prague, Czech Republic; [‡]Hospital for Special Surgery; Department of Microbiology and Immunology; Weill Medical College of Cornell University; New York, NY USA

Key words: PML, genotoxic stress, JAK/STAT signaling, interferons, DNA damage, cellular senescence, p53, tumor suppressor, cytokines

Abbreviations: 53BP1, p53 binding protein 1; APH, aphidicolin; ARF, alternate reading frame; ATM, ataxia telangiectasia mutated; ATR, ataxia telangiectasia and Rad3 related; BLM, bloom syndrome mutated; BrdU, 5-bromo-2'-deoxyuridine; CBP, CREB-binding protein; Chk2, checkpoint kinase 2; CHX, cycloheximide; CPT, camptothecin; DDR, DNA damage response; DMA, distamycin A; ET, etoposide; GAPDH, glyceraldehyde 3-phosphate dehydrogenase; HIPK2, homeodomain-interacting protein kinase 2; HIRA, histone repressor A; HP1, heterochromatin protein 1; IFN, interferon; iJAK, inhibitor of JAK kinases; IL, interleukin; IRF, interferon regulatory factor; ISGs, interferon-stimulated genes; ISRE, interferon-stimulated response element; JAK, janus kinase/just another kinase; mdm2, murine double minute 2; MXA, myxovirus resistance A; NBS1, nijmegen breakage syndrome 1; pRb, retinoblastoma protein; PML, promyelocytic leukemia protein; PML NBs, promyelocytic leukemia nuclear bodies; RARα, retinoic acid receptor alpha; RPA, replication protein A; SA-β-gal, senescence-associated beta-galactosidase; SAHF, senescence-associated heterochromatin foci; STAT, signal transducers and activators of transcription; SUMO, small ubiquitin-like modifier; TMD, thymidine; TRF1, telomeric repeat binding factor 1; Tyk2, tyrosine kinase 2

The Promyelocytic leukemia protein (PML) tumor suppressor is upregulated in several forms of cellular senescence, however the mechanism of its induction is elusive. Here we show that genotoxic drugs that induce senescence, such as 5-bromo-2'deoxyuridine (BrdU), thymidine (TMD), distamycin A (DMA), aphidicolin (APH), etoposide (ET) and camptothecin (CPT) all evoke expansion of PML nuclear compartment and its association with persistent DNA lesions in several human cancer cell lines and normal diploid fibroblasts. This phenomenon was accompanied by elevation of PML transcripts after treatment with BrdU, TMD, DMA and CPT. Chemical inhibition of all JAK kinases and RNAi-mediated knock-down of JAK1 suppressed PML expression, implicating JAK/STAT-mediated signaling in regulation of the PML gene. As PML protein stability remained unchanged after drug treatment, decreased protein turnover was unlikely to explain the senescence-associated increased abundance of PML. Furthermore, binding activity of Interferon Stimulated Response Element (ISRE) within the PML gene promoter, and suppression of reporter gene activity after deletion of ISRE from the PML promoter region suggested that drug-induced PML transcription is controlled via transcription factors interacting with this element. Collectively, our data show that upregulation of the PML tumor suppressor in cellular senescence triggered by diverse drugs including clinically used anti-cancer chemotherapeutics relies on stimulation of PML transcription by JAK/STAT-mediated signaling, possibly evoked by the autocrine/paracrine activities of senescence-associated cytokines.

*Correspondence to: Zdenek Hodny and Jiri Bartek; Email: hodny@img.cas.cz and jb@cancer.dk
Submitted: 05/24/10; Accepted: 05/26/10
Previously published online: www.landesbioscience.com/journals/cc/article/12521
DOI: 10.4161/cc.9.15.12521

Introduction

The PML tumor suppressor, a key component of a distinct nuclear compartment termed PML nuclear bodies (PML NBs),[1] is commonly downregulated in human tumors of diverse histogenesis and its loss is often associated with tumor progression.[2] While the absence of PML expression in tumors is rarely attributable to *PML* gene mutation or silenced transcription, such aberrantly low levels of PML mainly reflect enhanced protein turnover.[2] Furthermore, individuals carrying chromosomal translocation t(15;17)(q22;q21), which results in loss of PML function due to reciprocal fusion of *PML* and *RARα* genes, are predisposed to acute promyelocytic leukemia.[3] Consistent with PML tumor-suppressor activity, mice lacking PML are tumor-prone.[4]

Although the exact biochemical basis of PML antitumor properties is unclear, PML and intact PML NBs are involved in several tumor-suppressive pathways regulating apoptosis and cellular senescence. Senescence is promoted and/or maintained by several mechanisms including derepression of the INK4a/ARF locus encoding the p16^{INK4a} and ARF tumor suppressors, and persistent activation of the DNA damage response (DDR) machinery in response to activated oncogenes, telomere attrition or diverse genotoxic insults.[5-7]

Owing to the irreversible cell cycle arrest in response to oncogenic events, cellular senescence appears to serve as an anti-tumor barrier,[8-10] the failure of which may allow progression of early lesions to full malignancy.[11] Causally involved in the establishment and maintenance of the senescent phenotype in human cells are two cell cycle inhibitory tumor suppressor pathways, p53/p21$^{waf1/cip1}$ and p16INK^{INK4a}/pRb.[10,12,13] PML participates in both these pathways, consistent with its proapoptotic and growth suppressive properties.[14] Thus, PML facilitates acetylation, protein stabilization and phosphorylation-mediated activation of p53.[15,16] Furthermore, the *PML* gene is a direct transcriptional target of p53,[17] implicating PML in a positive feedback loop controlling p53 activity. In concert with pRb, PML and PML NBs facilitate formation of chromatin-dense nuclear structures known as senescence-associated heterochromatin foci (SAHF) involved in oncogene- and etoposide-induced senescence.[13] PML NBs are required for SAHF formation, and the histone chaperone HIRA and HP1 proteins pass transiently through PML NBs to become activated for SAHF-associated chromatin remodeling.[18-20]

Consistent with anti-tumor properties of PML and its role in the pro-senescence pathways, multiplication of PML nuclear compartment was observed in replicative,[21] oncogene-,[15,22,23] bacterial toxin-[24] and hydroxyurea-induced senescence.[25] Thus the induction of PML appears to be shared by most, if not all, forms of cellular senescence. In addition, overexpression of PML itself (specifically PML isoform IV) was able to induce senescence in human and mouse primary fibroblasts,[26] and ablation of the *PML* gene was sufficient to bypass oncogene-induced senescence in mouse[15] but apparently not in human cells.[23] Presumably, the enhancement of PML levels in senescent cells reflects transcriptional induction[23] and/or protein stabilization,[2,27] however the precise molecular mechanisms of PML induction during cellular senescence remain to be elucidated.

In various biological settings not involving cellular senescence, *PML* transcription is known to be controlled by interferons (IFNs[28-31]), cytokines that regulate antiviral, antiproliferative and immunological responses.[32] The two types of IFNs, type I (represented by IFNα family, IFNβ, IFNω and IFNτ) and type II (represented by IFNγ only) bind to their specific plasma membrane receptors, thereby initiating a cascade of events known as the JAK/STAT (Janus kinase/signal transducer and activator of transcription) signaling pathway. Besides IFNs, several other cytokines, such as IL6, IL10 and IL24 are capable of activating different branches of JAK/STAT signaling via their own receptors.[33] The binding of IFNα/β to the receptor triggers autophosphorylation-mediated activation of JAK1 and Tyk2 kinases which phosphorylate transcription factors STAT1 and STAT2. Activated STATs homodimerize or heterodimerize to form two distinct transcription activator complexes: a) IFNα-activated factor (AAF, identical to IFNγ-activated factor, GAF), a homodimer of STAT1 and IFN-stimulated gene factor 3 (ISGF3), a heterotrimeric complex of STAT1, STAT2 and IRF9 (interferon regulatory factor 9, named also p48 or ISGFγ). AAF/GAF and ISGF3 bind to specific DNA sequences, the IFNγ-activated sequence (GAS) and the IFN-stimulated response element (ISRE), respectively. Through these mechanisms JAK/STAT signaling—the primary IFN response—results in transcriptional induction of hundreds of IFN-stimulated genes (ISGs[30]) that include also growth/tumor suppressors interferon regulatory factor 1 (IRF1), STAT1 and p53.[34]

Intriguingly, enhanced expression and/or secretion of cytokines including IFNs were reported for cells undergoing senescence in response to diverse oncogenic and DNA damaging stimuli.[35-41] Significantly, cytokine secretion and cellular senescence can still be evoked even in malignant cells, for example by exposure to certain genotoxic insults,[35] a notion that has potential therapeutic implications. In an attempt to provide more mechanistic insights into the emerging links between increased PML and cytokine signaling in cellular senescence, we set out to investigate the regulation of PML abundance and the potential role of JAK/STAT signaling in series of human normal and cancer cell types undergoing senescence upon exposure to genotoxic drugs, model scenarios relevant for both cell physiology and cancer treatment.

Results

PML NBs, PML protein and transcript levels are enhanced after genotoxic stress. To elucidate the mechanism of PML increase in drug-induced senescence, we first quantified the numbers of PML NBs during senescence induced by BrdU and DMA (used either separately or simultaneously) in HeLa cells (**Fig. 1A–F**). The synergistic effect of the two drugs on the development of senescence (estimated as senescence-associated β-galactosidase staining, SA-β-gal; **Suppl. Fig. 1A–E**) was associated with potentiated elevation of PML NBs number when compared to single use of either drug. Concomitant with upregulation of PML NBs,

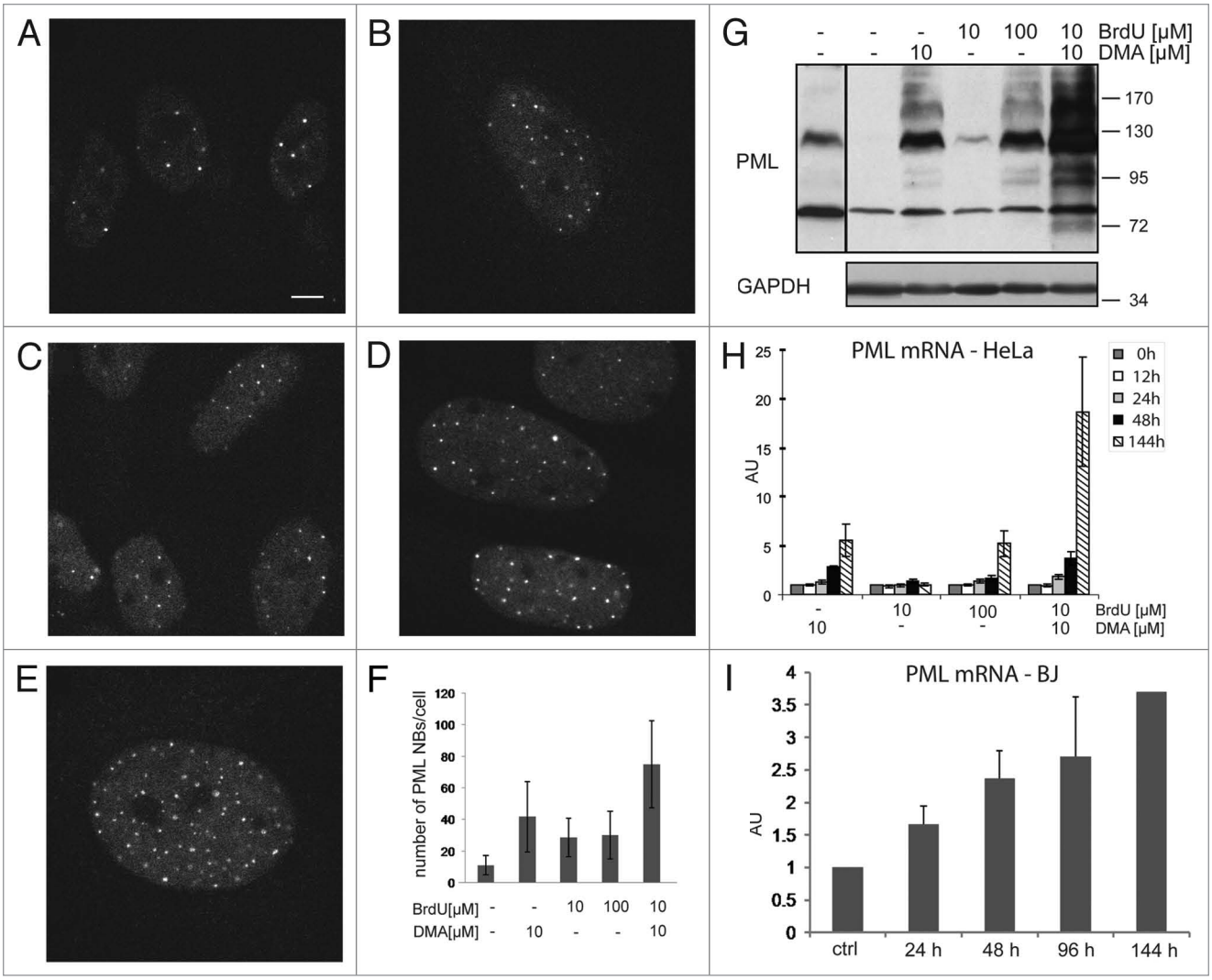

Figure 1. BrdU/DMA induces expression of PML and increased numbers of PML NBs in HeLa cells. Immunofluorescence detection of PML NB induction in untreated HeLa cells (A), treated for six days by 10 μM DMA (B), 10 μM BrdU (C), 100 μM BrdU (D) or 10 μM BrdU/DMA (E). (F) Graphical summary of numbers of PML NBs per cell in HeLa cells treated for six days with BrdU, DMA or their combination. (G) Immunoblot detection of PML protein after six-day treatment with BrdU, DMA or their combination. To show basal level of PML, longer exposition of the film is included for control cells (first line). GAPDH was used as a loading control. (H) mRNA levels of PML quantified by qRT-PCR in HeLa cells treated with BrdU, DMA or their combination for specified time period. The values represent average of three independent experiments and are shown as a fold induction relative to control; error bars represent standard error. GAPDH was used as a reference gene. (I) PML mRNA levels quantified by qRT-PCR in BJ cells treated with CPT for specified time period. The values represent average of three independent experiments (in case of day 6 there was only one experiment) and are shown as a fold induction relative to control; error bars represent standard error. Actin was used as a reference gene.

a marked increase of PML protein level was detected after 6-day exposure of HeLa cells to BrdU alone (100 μM) or BrdU combined with DMA (both 10 μM) (**Fig. 1G**; note also the increase of high-molecular, >130 kDa, likely SUMO-2/3-modified, forms of PML[42]). Furthermore, the levels of PML mRNA were assessed by quantitative real time RT-PCR (qRT-PCR) after exposure to BrdU, DMA or their combination. PML mRNA levels increased gradually from day 1 to day 6, reaching levels more than 15 times higher (for BrdU/DMA-treatment) than those in control untreated cells (**Fig. 1H**).

Next, we examined whether other senescence-evoking compounds such as aphidicolin (APH[43]), thymidine (TMD[44]), etoposide (ET[45]) and camptothecin (CPT[46-48]) are able to induce expansion of the PML nuclear compartment. Interestingly, different cell lines responded to the various drugs by different degrees of senescence induction, and after titration experiments we chose for further analyses those combinations of compound(s) that induced the commonly accepted hallmarks of premature senescence (proliferation arrest, SA-β-gal positivity, cell enlargement and spreading) in particular cellular models (**Table 1 and Suppl. Figure 1F–M**). Analogous to BrdU and DMA, these additional drugs also caused significant elevation of PML NBs (**Suppl. Fig. 2**) and PML protein (**Fig. 3**) at the time of fully developed senescence in HeLa cells (in most cases by day 6; as assessed morphologically and by SA-β-gal staining; **Suppl. Fig. 1**). PML mRNA levels were also significantly elevated after treatment with

Table 1. List of drug-induced senescent cell models used

Cell line	Compound	Concentration	Treatment duration
HeLa	bromodeoxyuridine	10 μM	6 days
HeLa	bromodeoxyuridine	100 μM	6 days
HeLa	distamycin A	10 μM	6 days
HeLa	bromodeoxyuridine	10 μM	6 days
	distamycin A	10 μM	
HeLa	camptothecin	0.5 μM	6 days
U2OS	thymidine	2.5 mM	6 days
U2OS	aphidicolin	0.3 μM	5 days
U2OS	etoposide	5 μM	6 days
BJ	camptothecin	0.5 μM	6 days
HCT-116	thymidine	2.5 mM	6–9 days

CPT in BJ fibroblasts (**Fig. 1I**), and in U2OS cells treated with TMD (**Suppl. Fig. 3A**), ET and APH (not shown).

To determine whether protein stabilization also contributes to the observed elevation of PML (as the presence of PML high-molecular forms might indicate), HeLa cells were treated with 100 μM BrdU for 4 days and de novo protein synthesis was then blocked by cycloheximide (CHX; 100 μg/ml) for 6 or 24 hours. In both control and BrdU-treated cells, the levels of PML protein remained almost unchanged after 24 h of CHX exposure (**Suppl. Fig. 3B**), indicating high stability of the PML protein independently of the senescence state in HeLa cells. High stability of PML protein regardless of senescence induction was also observed in U2OS cells exposed to various concentrations of CHX up to 100 μg/ml (**Suppl. Fig. 3C**). The efficiency of translation inhibition by CHX was documented by complete abrogation of IFNα-stimulated expression of PML. These results do not support a major role of enhanced PML protein stability in drug-induced senescence.

Collectively, our data indicate that the elevation of PML NBs and PML protein levels during genotoxic stress-induced senescence in several human cell types are accompanied by increase of *PML* gene transcripts, rather than a pronounced stabilization at the protein level.

PML NBs co-associate with foci of persistent DNA damage. Previous studies on spatial relationship between PML NBs and the sites of DNA damage (specifically markers of DNA double strand breaks) showed that PML co-localized with foci that persisted for prolonged periods of time after ionizing radiation.[49,50] This contrasts with data on acute foci formed immediately after DNA damage induction, where no such co-localization was found (Ref. 51 and J. Lukas, personal communication). Consistently, here we observed only rare co-localization of PML with DNA damage foci generated with most drugs before day 4 of treatment (data not shown), while the frequency of such co-localization gradually increased at later time points (see **Figure 2A** for BrdU/DMA-treatment of HeLa cells; PML NBs are detected by antibody against Sp100, another structural marker of PML NBs[1]). Analogous but earlier (from day 2 onwards) co-localization of PML with DNA damage foci was observed after CPT treatment in BJ cells (**Fig. 2C**), which corresponded to faster onset of senescence in these settings (data not shown). Interestingly, TMD evoked co-association (adjacent localization) rather than co-localization of PML NBs with the 53BP1-decorated DNA damage foci (**Fig. 2B**). In HeLa cells, specific filiform PML structures co-localizing with γH2AX foci were frequently formed after CPT treatment (**Fig. 2D**). Moreover, BLM helicase, which is involved in the maintenance of genome stability[52,53] and co-localizes with both DNA damage foci[54] and PML NBs,[55-57] changed its nuclear distribution in BrdU-treated HeLa cells. In untreated cells, BLM showed a diffuse nucleoplasmic staining pattern and only rare co-localization with PML NBs (**Fig. 2E**). However, in cells treated with BrdU (100 μM) for 5 days, BLM accumulated in large spots co-localizing frequently with PML NBs (**Fig. 2E**). In contrast, PML NBs did not co-localize or co-associate with TRF1, a marker of telomeric chromatin, at least in BrdU-treated (500 μM) HeLa cells (**Fig. 2F**).

These results show that PML NBs, multiplied in number by drug-induced genotoxic stress in senescent cells, frequently co-localize with persistent DNA lesions likely representing DNA double strand breaks. Although the function of PML and PML NBs at the sites of DNA damage has not been deciphered yet, our present findings indicate a potential role of PML nuclear compartment in the processing and/or repair of chronic, difficult-to-repair DNA lesions known to accompany cellular senescence.[58]

Simultaneous activation of JAK/STAT signaling and DNA damage response in drug-induced senescence. Treatment of human cells with BrdU and DMA induces a complex cytokine response including secretion of interferon beta (IFNβ), activation of JAK/STAT1/3 signaling pathways and enhanced expression of interferon stimulated genes such as MXA, STAT1, IRF1 and IRF7.[35] In our present experiments, not only BrdU and DMA, but also APH, TMD, ET and CPT, irrespective of their distinct mechanisms of DNA damage induction, all activated JAK/STAT1/3 signaling, as detected by phosphorylated forms of STAT1 and STAT3 (STAT1pY701 and STAT3pY705) (**Fig. 3**). Such similar responses suggest a common underlying mechanism that activates this signaling pathway after genotoxic stress.

As expected for DNA damaging drugs, activation of the ATM/Chk2/p53 axis (monitored here by activated Chk2 kinase phosphorylated at threonine 68,[59]), formation of DNA damage foci (detected with 53BP1 antibody[60] or with the antibody recognizing histone H2AX phosphorylated at serine 139, known as γH2AX[61]), elevation of p53 (both total protein and the serine 15-phosphorylated form[62,63]), induction of the p53 transcriptional target $p21^{waf/cip}$ (p21,[64]) and the development of cellular senescence (assayed morphologically and by SA-β-gal staining), were the effects common to all these compounds (**Figs. 2 and 3 and Suppl. Fig. 1**).

These results confirmed that premature senescence induced by different genotoxic drugs is accompanied by activation of the ATM/Chk2/p53/p21 DNA damage checkpoint pathway as well as by the activation of JAK/STAT1/3 signaling.

Enhancement of PML nuclear compartment in drug-induced senescence is dependent on JAK1/STAT signaling.

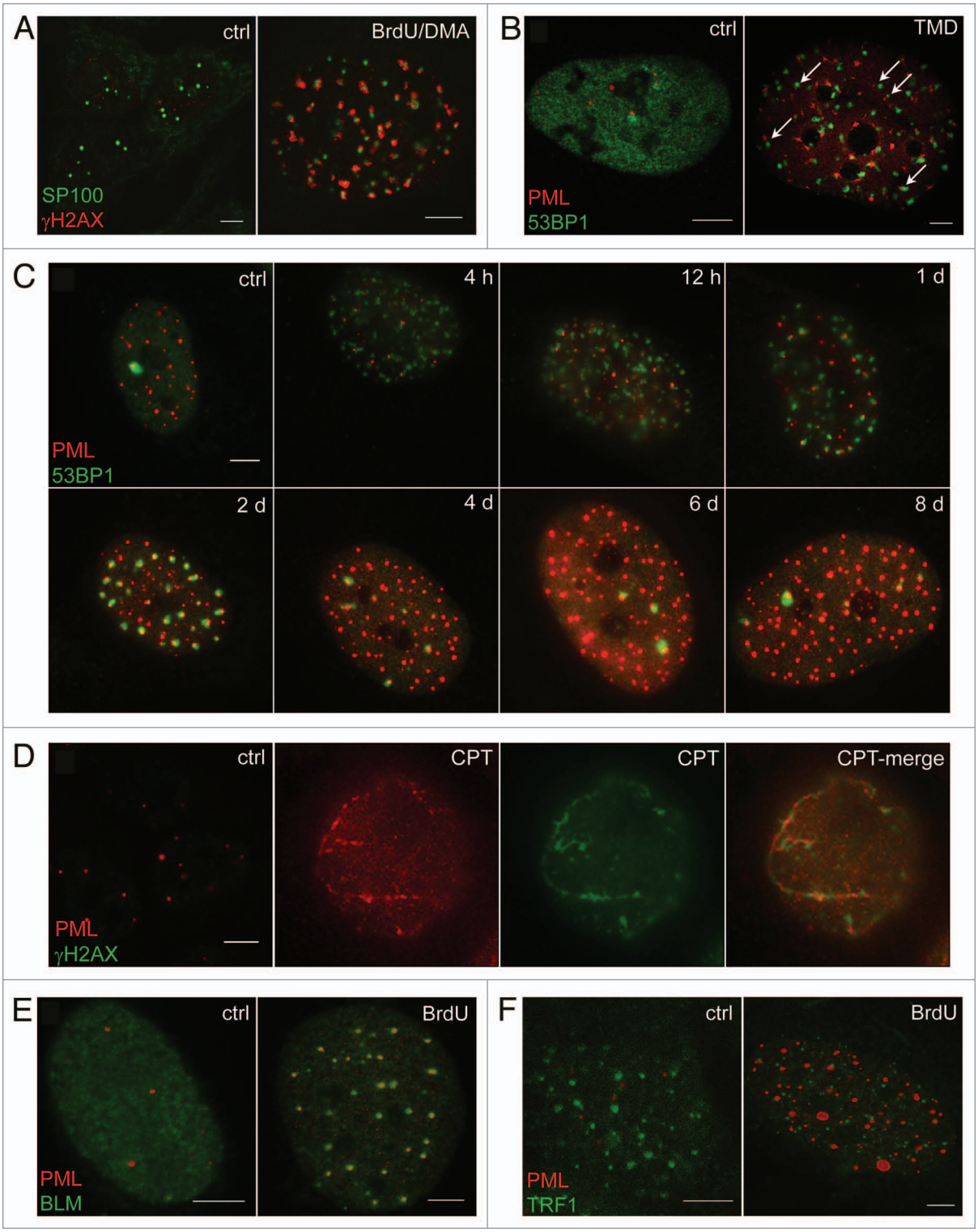

Figure 2. PML NBs co-associate with DNA damage foci. Immunofluorescence detection of Sp100 and γH2AX in control HeLa cells or HeLa cells treated for eight days with a combination of BrdU and DMA (A). Immunofluorescence detection of PML and 53BP1 in untreated U2OS cells or cells treated for six days with TMD (B). Time course detection of PML and 53BP1 in BJ cells treated with CPT for 4 and 12 hours and for 1, 2, 4, 6 and 8 days (C). Co-localization of PML filiform structures with γH2AX in control HeLa cells or treated for six days with CPT (D). Immunofluorescence detection of nuclear distribution of BLM helicase in control and 100 μM BrdU-treated cells for five days (E). Detection of PML and TRF1 in control HeLa cells or after treatment with 500 μM BrdU for six days (F). Bar, 5 μm.

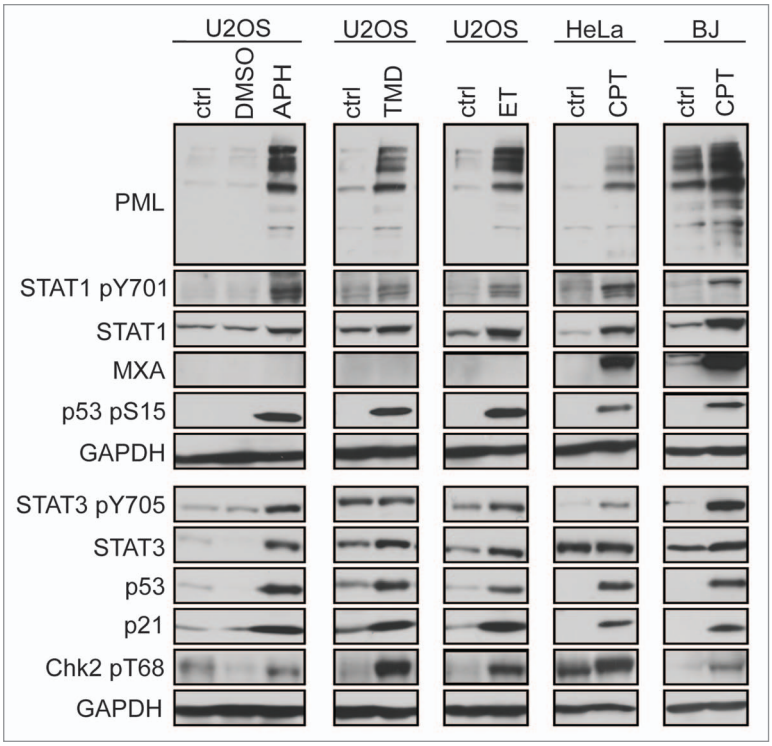

Figure 3. DNA damage response, activation of JAK/STAT signalling pathway and PML induction in drug-induced senescence. Immunoblot detection of activated markers of JAK/STAT signaling (detected as phosphorylated STAT1 tyrosine 701 and STAT3 tyrosine 705) and induced levels of ISGs (PML, STAT1, STAT3) in U2OS, HeLa and BJ cells treated for six days by different drugs promoting senescence (TMD, APH, ET, CPT). DMSO, as a solvent vehicle, was used as one control. As markers of activated DNA damage response served phosphorylated p53 serine 15, Chk2 threonine 68, and increased levels of total p53 and p21. GAPDH was used as a loading control.

As interferon-induced PML expression[31] is regulated via interferon response elements located in the *PML* gene promoter,[65] we tested whether the JAK/STAT signaling pathway known to act through these elements may be responsible for the expansion of nuclear PML compartment during drug-induced genotoxic stress. First, we utilized chemical inhibition of JAK family kinases with 2-(1,1-dimethylethyl)-9-fluoro-3,6-dihydro-7H-benz[h]-imidaz[4,5-f]isoquinolin-7-one (iJAK). Simultaneous exposure of HeLa cells to BrdU/DMA and iJAK at a concentration inhibitory for all JAK kinases (i.e., JAK1, JAK2, JAK3 and Tyk2) significantly impaired, although did not entirely block, the increase of PML NBs (**Suppl. Fig. 4A–D**) and PML levels (**Fig. 4A**; especially the low mobility forms of PML) normally induced by such drug treatment. Very similar effects of JAK kinase inhibition on the JAK/STAT signaling pathway (STAT1 pY701 and STAT3 pY705), expression of ISGs (STAT1 and STAT3) and PML were observed after treatment of U2OS cells with TMD or HeLa cells with CPT (**Fig. 4B and C**). Notably, iJAK treatment showed only negligible, if any, effect on PML protein levels induced by etoposide (**Fig. 4B**). Similar differences were observed also at PML mRNA levels (not shown).

As the phosphorylation cascade of JAK/STAT signaling pathways is dominated by the activity of JAK1 kinase, we performed a stable knock-down of JAK1 kinase in HeLa cells using lentiviral transduction of short hairpin RNA (see JAK1 mRNA levels for two most effective hairpins #2 and #3; **Fig. 4E**). Four of five independent shJAK1s (i.e., #1, #2, #3 and #5) resulted in a decrease of PML protein (**Fig. 4D**) and mRNA levels (**Fig. 4F**) accompanied by a decrease of tyrosine 701 phosphorylated STAT1 (**Fig. 4D**) and MXA mRNA (**Fig. 4G**) used here to document the JAK1 inhibition. Again, the loss of low-molecular forms of PML was more pronounced, likely reflecting higher stability of posttranslationally modified PML protein species. Importantly, chemical inhibition of JAK kinases suppressed the phosphorylation of STAT3 and STAT1 and elevation of PML levels in cells exposed to pro-senescence treatment by *Haemophilus ducreyi* cytolethal distending toxin (data not shown), indicating that the JAK kinase dependent expression of PML is not limited to drug-induced senescence.

Taken together, enhancement of PML nuclear compartment and PML transcript levels during drug-induced senescence require activity of the JAK1 kinase.

***PML* gene induction in drug-induced senescence is regulated via an ISRE element in the *PML* gene promoter.** IFN type I and type II induction of *PML* gene was mapped to two DNA binding elements of the PML proximal promoter, ISRE (+605/+618) and GAS (+363/+374; numbered relative to transcription start[65]), respectively. To assess whether the elevation of PML is indeed mediated by JAK/STAT signaling at the transcription level, and if so, whether this is mediated via either of the two reported IFN-sensitive DNA response elements, a 1.44 kbp Hind III fragment of the proximal *PML* gene promoter region driving a luciferase reporter[65] was transfected into U2OS cells and luciferase activity was measured after 3-day exposure to the pro-senescence BrdU/DMA combination (**Fig. 5A**) or thymidine (not shown). Indeed, the reporter gene activity was enhanced after treatment with either BrdU/DMA or TMD. Furthermore,

Figure 4 (See opposite page). Inhibition of JAK kinases inhibits PML expression. Immunoblot analyses of JAK/STAT pathway activation and PML induction after inhibition of JAK kinases by the JAK kinase inhibitor I (iJAK) after six days of treatment with a combination of BrdU and DMA in HeLa cells (A); with TMD or ET in U2OS cells (B); and with CPT in HeLa cells (C). (D) Immunoblot detection of total and tyrosine 701 phosphorylated STAT1, serine 15 phosphorylated p53 and PML levels after a 6-day treatment with BrdU + DMA in HeLa cells transduced by shRNA specific for JAK1 (shJAK1 #1, #2, #3, #4, #5) or empty vector (non sense). GAPDH was used as a loading control. (E) Knock-down efficiency of two shRNAs directed against JAK1 (shJAK1 #2 and #3) estimated as JAK1 mRNA levels by real time qPCR in HeLa cells treated for six days with a combination of BrdU and DMA. The average values representing three independent experiments are given as arbitrary units relative to control. Error bars represent standard error. PML (F) and MXA (G) gene mRNA levels estimated by RT-qPCR in HeLa cells transfected with shRNA specific for JAK1 (shJAK1#2 and #3) and treated for six days with a combination of BrdU and DMA. The average values from two (for MXA) or three (for PML) independent experiments are given as arbitrary units relative to control. Error bars represent standard error.

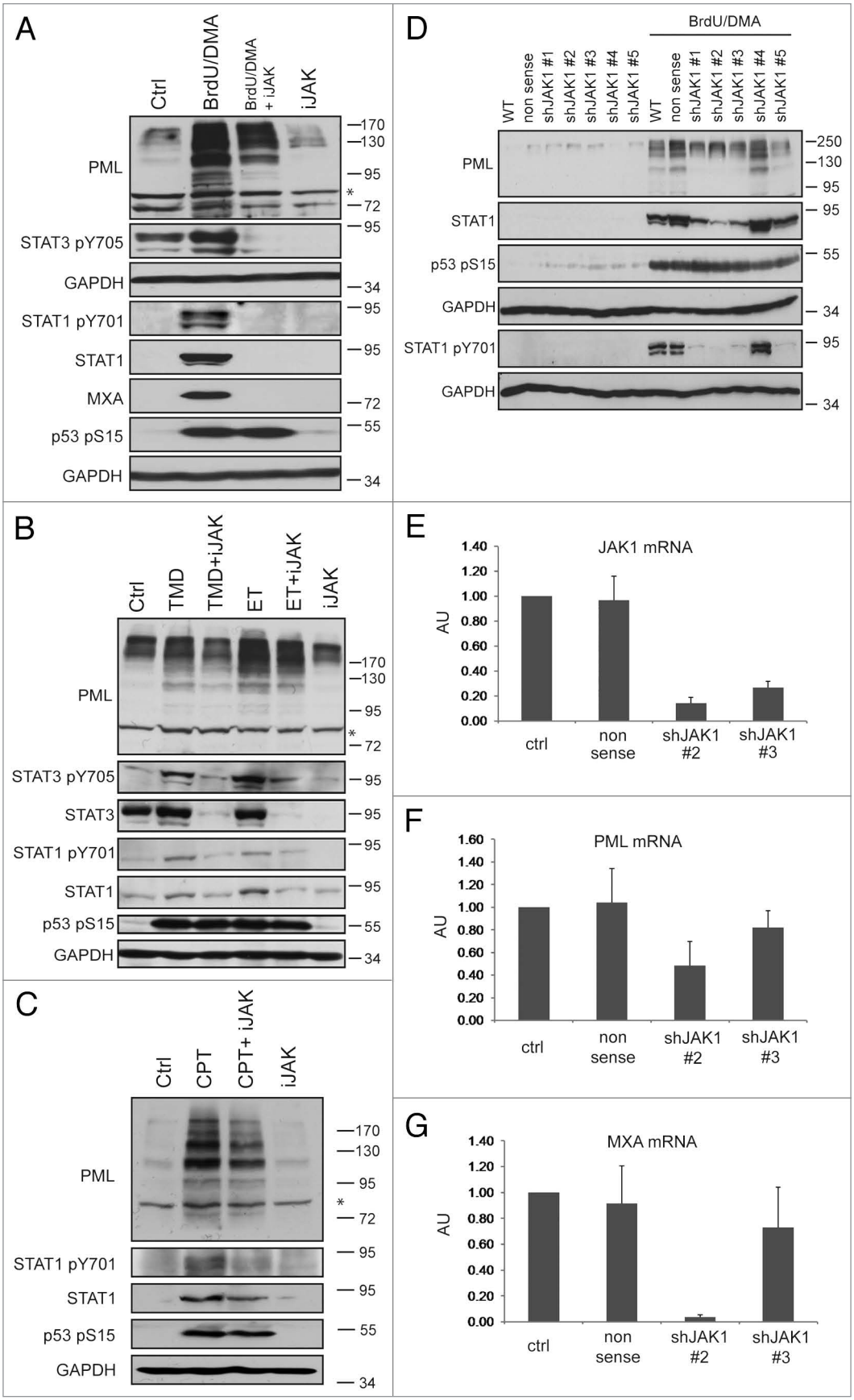

Figure 4. For figure legend, see page 3090.

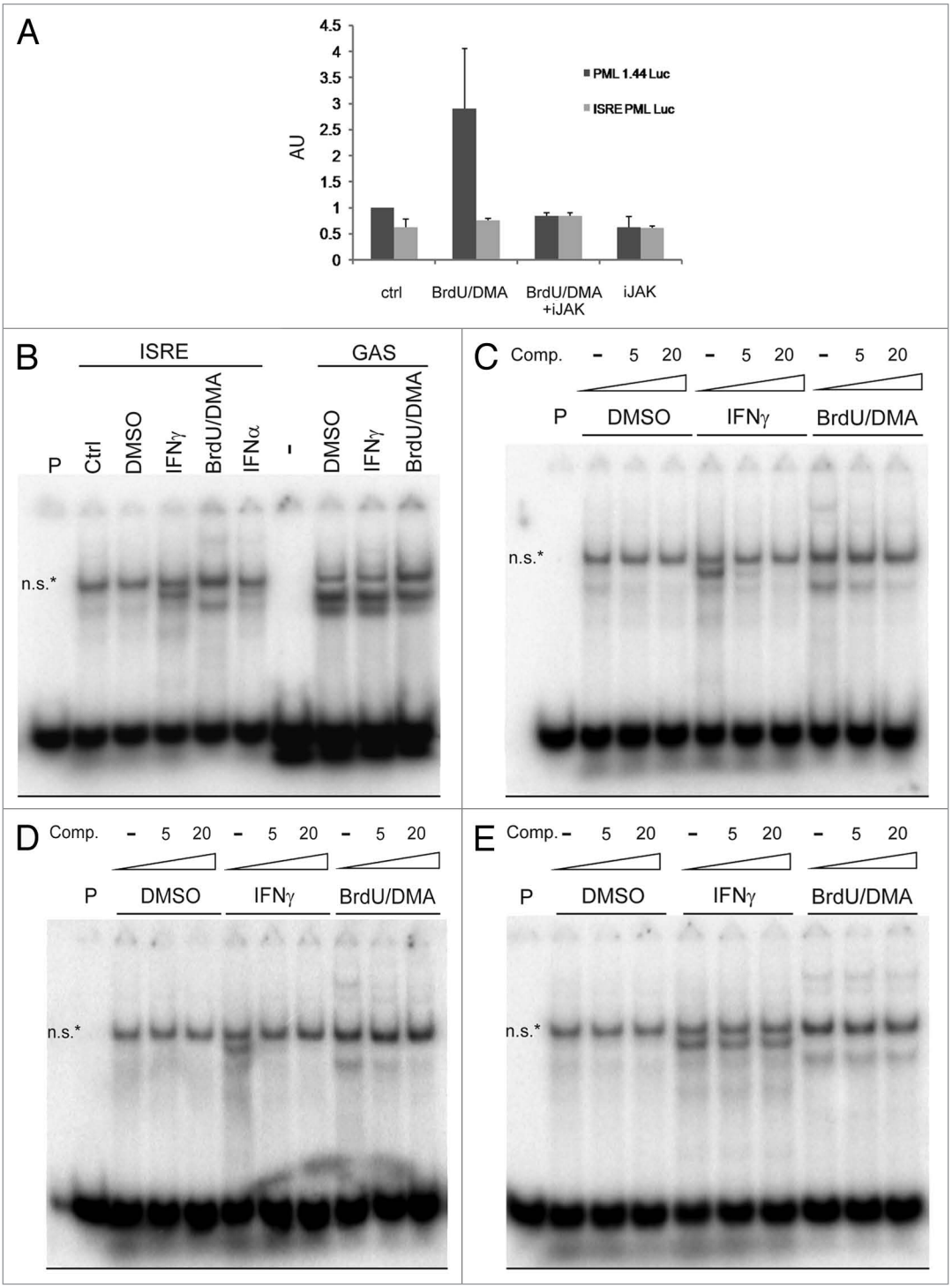

Figure 5. *PML* transcription after genotoxic stress is dependent on intact ISRE element of PML promoter gene. (A) Luciferase reporter gene activity under the control of *PML* gene promoter (PML 1.44 Luc) in U2OS cells with intact or deleted ISRE DNA binding site (ISRE PML Luc). Cells were treated for three days in the presence or absence of BrdU/DMA and JAK kinase inhibitor I (iJAK). The average values representing three independent experiments are given as arbitrary units relative to control. Error bars represent standard error. (B) Gel retardation assay using ISRE and GAS oligonucleotide probes derived from the PML promoter. HeLa cells were treated with BrdU/DMA for six days and with 1,000 U/ml IFNα or 100 U/ml IFNγ for 24 hours. DMSO was used as a vehicle control for BrdU/DMA treatment. Competition of PML ISRE binding activity with 5-fold and 20-fold molar excess of non-labelled PML ISRE oligonucleotide (C), wild-type (D) or mutated MXA ISRE oligonucleotide (E). n.s.*, nonspecific binding.

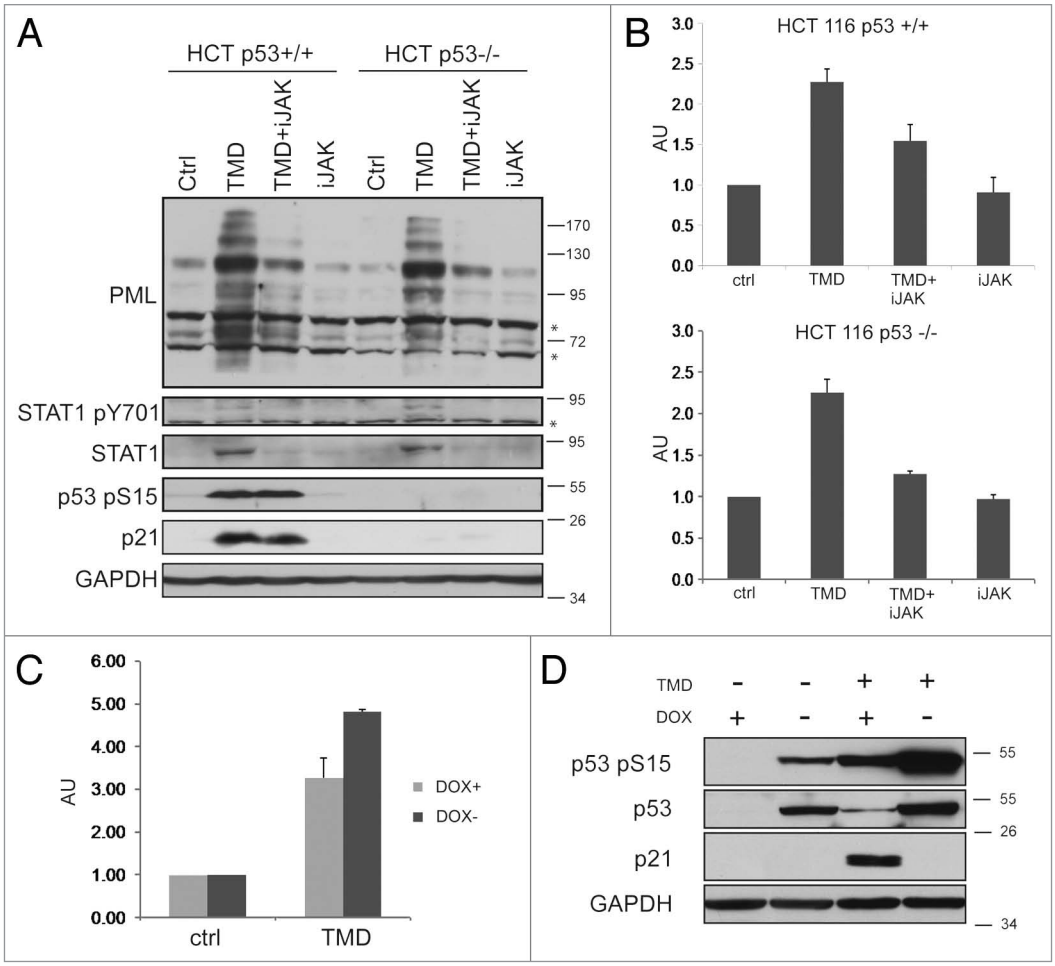

Figure 6. JAK/STAT-induced PML expression is independent of p53. (A) Immunoblot detection of PML in p53 wild-type and p53 negative HCT-116 cells treated with thymidine for 6 days. iJAK inhibitor was used for the same time to inhibit signaling through JAK/STAT pathways in both p53 wt and p53 negative cells. Effect of this inhibitor is shown by changes in activation of STAT1 and its total level. Effect of knock-out is shown by level of p53, p21 and phosphorylation of p53 on serine 15. GAPDH was used as loading control. (B) PML mRNA levels estimated by RT-qPCR in HCT-116 cells with or without p53 treated for six days with TMD alone or in combination with iJAK. The average values representing two independent experiments are given as arbitrary units relative to control. Error bars represent standard error. Actin was used as a reference gene. (C) PML mRNA levels estimated by RT-qPCR in U2OS cells expressing dominant negative p53 under tetracycline control (Off-system) treated for six days with/out TMD and doxycycline (DOX^+/DOX^-). The average values representing two independent experiments are given as arbitrary units relative to control. Error bars represent standard error. GAPDH was used as reference gene. (D) Immunoblot detection of p53, its form phosphorylated at serine 15 (pS15p53) and $p21^{waf/cip}$ obtained at the same experimental setting as in (C). GAPDH was used as loading control. Representative blot of three independent experiments is shown. *, nonspecific signal

the activity of the PML-Luc reporter induced by either treatment was impaired in cells concomitantly exposed to the JAK kinase inhibitor (**Fig. 5A**), thereby documenting that the genotoxic stress-induced JAK/STAT signaling controls PML promoter activity.

The responsiveness of the PML-Luc reporter was abolished by deletion of the short fragment of the PML promoter bearing the ISRE element, indicating that the deleted ISRE sequence is directly involved in the transcriptional induction of the *PML* gene upon exposure of cells to genotoxic stress (**Fig. 5A**). To confirm the participation of ISRE in regulation of PML gene transcription, we followed the DNA binding activity specific to ISRE in nuclear extracts prepared from BrdU/DMA-treated HeLa cells by a gel retardation assay. Specific gel migration shift was seen only when using the PML-ISRE but not the PML-GAS probe (**Fig. 5B**). The DNA probe-protein complex was sensitive to competition with cold PML-ISRE and MXA-ISRE oligonucleotides but not to mutated MXA-ISRE (**Fig. 5C–E**), thereby confirming the specificity of the ISRE DNA-protein complex.

In conclusion, these data indicate a direct regulatory role of JAK-mediated pathways in genotoxic stress-induced *PML* gene transcription. The ISRE element located in the *PML* gene proximal regulatory region was identified as the DNA binding element participating in JAK/STAT-mediated transcription of PML under genotoxic stress conditions.

The JAK/STAT pathway controls PML transcription during genotoxic stress independently of p53. Since a recent study reported that PML transcription in oncogene-induced senescence

is mediated by p53,[17] we wished to assess this important notion in our drug-induced senescence models. As expected, p53 was stabilized and activated (as deduced from total and Ser15-phosphorylated levels of p53) during premature senescence induced by all drugs tested (**Figs. 2A and 4A–D**). Therefore, we investigated further whether PML expression induced via JAK/STAT signaling depends on transcriptional activity of p53. First, isogenic human cell lines HCT-116 with intact wild-type (HCT-116 $p53^{+/+}$) or deleted p53 (HCT-116 $p53^{-/-}$,[66]) were exposed to TMD in the presence or absence of iJAK and the PML protein and mRNA levels were evaluated. The comparable increase of both PML protein (**Fig. 6A**) and mRNA levels (**Fig. 6B**) in p53 positive as well as negative cell lines indicated independence of PML expression on active p53. Chemical inhibition of JAK kinases by iJAK inhibitor led in both cases to substantial suppression of PML protein and mRNA, confirming again the dominant involvement of JAK/STAT signaling in PML expression. Second, data obtained with U2OS cells conditionally expressing (in a tetracycline-repressible manner) a dominant-negative form of p53 (U2OS p53DD[67]) and exposed to TMD did not show any dependence of PML expression on transcription activity of p53 (**Fig. 6C**). This negative result contrasted sharply with parallel examination of the known p53 transcription target $p21^{waf/cip}$ whose induction in response to TMD was abolished by expression of the dominant-negative p53 (**Fig. 6D**).

We conclude from these experiments that induction of PML in response to at least some genotoxic drugs via the JAK/STAT signaling is not dependent on transcriptional activity of p53.

Discussion

The PML protein is an important positive regulator of cellular senescence and a tumor suppressor commonly lost in human cancer.[2] The role of PML and PML NBs in the senescence barrier against activated oncogenes, tumor progression and likely other pathophysiological settings that involve senescence, such as wound healing, inflammation and aging,[68] provide a strong stimulus to elucidate the regulation and function of PML. Our present study contributes to better understanding of PML biology by providing novel insights into regulation of PML and abundance and subcellular localization of PML NBs in cellular senescence evoked by exposure of human normal as well as cancerous cells to a range of genotoxic drugs that are used for various purposes in both research and clinical practice. Specifically, our results show that response to genotoxic drugs includes senescence-associated elevation of PML and PML NBs, and indicate that this phenomenon is mainly attributable to enhanced *PML* gene expression. In addition, we demonstrate that this positive regulatory mechanism involves cytokine-activated JAK/STAT signaling pathways, and reflects activation of PML transcription through an ISRE element within the proximal *PML* gene promoter. Finally, we also provide evidence that this mode of regulation is independent of the p53 tumor suppressor, while at the cellular level, the PML NBs become closely associated with persistent sites of DNA damage occupied by active DDR signaling machinery that has been causally linked to cellular senescence.[8,69]

Genotoxic agents enhance PML nuclear compartment and PML mRNA levels. PML NBs' numbers vary throughout the cell cycle and under diverse growth conditions such as heat-shock or viral infection, reflecting the abundance of the PML protein.[70] We have shown here that the number of PML NBs in human normal fibroblasts and several cancer cell lines increased significantly following the induction of senescence by exposure to drugs including BrdU, thymidine, distamycin A, etoposide, aphidicolin and camptothecin. This general finding is reminiscent of PML NBs multiplication reported for oncogenic *Ras*-induced senescent human diploid fibroblasts,[23] in replicatively senescent human mesenchymal stem cells,[21] hydroxyurea-treated IMR90 fibroblasts[25] and in cytolethal distending toxin-induced senescence in several human normal and cancer cell types,[24] suggesting that the expansion of PML NBs represents a potentially universal marker of cellular senescence in vitro. Our data show that multiplication of PML NBs is accompanied by elevated PML protein and transcript levels, but not enhanced protein stabilisation. The latter finding differs from a report on a shorter PML protein half-life[27] that was however measured only in virally transformed HEK293 and mouse 3T3 cells, and only for one, an ill-defined, isoform of PML, in contrast to our analysis of global PML abundance. Thus, we suggest that PML protein turnover may depend on the cell origin and individual PML isoforms, and it was not a regulatory factor in our experiments on a panel of human cell types undergoing drug-induced senescence. Altogether, our data show that the multiplication of PML NBs after genotoxic stress is a common feature of drug-induced cellular senescence and it can be attributed to enhanced expression of the *PML* gene.

PML NBs co-associate with persistent DNA damage foci. There is accumulating evidence that some types of cellular senescence are promoted by specific forms of DNA damage characterized by persistent DDR signaling,[71] possibly due to either inhibition of DNA repair as in case of telomeric regions or due to irreparability of certain DNA lesions. Such lesions can be followed microscopically as long-term persisting DNA damage foci positive for modified histone H2AX[61] and other markers of DNA double strand breaks such as 53BP1.[60] Inhibition of DDR emanating from these lesions results in bypass of senescence.[11,72,73] It is presently thought therefore that such permanent DDR signaling is a prerequisite for promotion and long-term maintenance of the senescent state.[8,74]

We showed here that DNA damage foci in advanced stage of chemical senescence frequently colocalize with PML NBs (**Fig. 2**), which is consistent with previous studies using ionizing radiation as a source of DNA damage.[49,50] PML NBs serve as depots for proteins involved in DDR, such as ATM, ATR, BLM, Chk2, Rad51, Rad52, RPA, Mre11 and NBS1, and undergo dynamic re-structuring after irradiation, including recruitment of DNA repair factors.[75] Moreover, some components of the DDR machinery are post-translationally modified directly in PML NBs, such as p53.[76,77] Thus the formation of PML NBs in the near proximity of the sites of persisting DNA lesions might reflect chronic, futile attempts to repair the problematic lesions.

Upon DNA damage induced by BrdU in our present experiments, the nucleoplasmic pool of the RecQ helicase BLM was

lost and BLM accumulated at the persistent DNA damage foci together with PML NBs (**Fig. 2E**). Importantly, sumoylation of BLM was reported to direct this helicase to PML NBs, and this was proposed to negatively regulate BLM function in DNA repair.[54] While the role of PML NBs in drug-induced senescence remains to be elucidated, it is tempting to speculate that the observed accumulation of PML and PML NBs in the vicinity of the DNA lesions in senescent cells may have some repressive effect on DNA repair, possibly through sequestering some of the DDR components.

PML expression in drug-induced senescence requires JAK1/STAT signaling and ISRE-mediated transcription. The *PML* gene promoter binds transcription factors of the STAT family activated by interferon signaling[65] and these factors are activated during drug-induced senescence in association with production of cytokines including IFNβ.[35] Given that the activation of STATs proceeds via cytokine receptor-associated kinases of JAK family, here we employed chemical inhibition of JAK kinases and indeed demonstrated that the JAK kinase activity is involved in PML expression in senescence triggered by BrdU/DMA, thymidine or camptothecin, but not etoposide. The latter scenario might reflect activation of PML expression via some additional mechanism(s) such as the NFκB pathway, which is strongly induced by etoposide and could operate through NFκB DNA-binding elements located in the PML promoter (our unpublished data). Moreover, inhibition of the JAK1 kinase expression by short hairpin RNAs further supported the involvement of JAK1 kinase in PML expression after BrdU-treatment. It should be emphasized that besides IFNs type I and II, JAK1 is activated by several cytokines/cytokine receptors[78] including IL6, IL7 and IL10, which we and others found expressed after genotoxic stress.[35,39] Which of the numerous cytokines produced by senescent cell is involved in activation of JAK1/STAT signaling pathway(s) and expression of PML is a complex task for future studies.

We have also mapped the PML promoter region required for transmitting JAK/STAT signaling under DNA-damaging conditions. Stadler and collaborators identified two DNA binding elements, ISRE and GAS, which mediate induction of PML promoter/reporter gene constructs by IFNs, both elements being located in the first untranslated exon of the *PML* gene.[65] Our present results from gel retardation assays demonstrated the presence of ISRE but not GAS binding activity in nuclear extracts prepared from BrdU/DMA-treated senescent cells. Together with the fact that ISRE was specifically required in our reporter assays, these results strongly implicate the ISRE DNA binding element in genotoxic stress-induced PML transcription.

As to the transcription factors involved, the ISRE consensus sequence is recognized not only by STATs but also by transcription factors of the interferon regulatory factor family such as IRF1,[79] whose expression/activation is regulated by interferons.[30] Since overexpression of IRF1 leads to elevated PML transcripts,[80] increased levels of IRF1 found after drug treatment[35] may contribute to JAK/STAT-dependent PML expression in our present study. Moreover, ATM-dependent stabilization of IRF1 was reported after etoposide treatment,[81] and precise characterization of transcription factor(s) responsible for ISRE-dependent PML expression needs further clarification.

The roles of DDR and p53 in JAK/STAT-controlled PML expression and relevance to cancer. The genotoxic drugs employed in our study are widely used in biomedicine, and therefore it is of interest to better understand their biological and molecular effects on both normal and cancer cells. Not surprisingly, all genotoxic drugs in our experiments evoked DNA damage signaling and activated/stabilized p53. Based on reported dependence of PML expression on p53 in mouse embryonal fibroblasts during *Ras*-induced senescence,[17] we tested whether p53 is instrumental for the observed JAK/STAT-dependent expression of PML in drug-induced senescence. Utilizing p53 positive and negative HCT-116 cell lines,[66] we clearly show independence of PML expression on p53 status after treatment with thymidine, etoposide and aphidicolin. The same conclusion can be drawn from the alternative approach using tetracycline-regulated dominant negative expression of p53 in U2OS cells treated with thymidine as a representative example. As to upstream signaling to the JAK/STAT cascade, one candidate that deserves attention is the reported cytokine-independent route via activation of the c-Abl kinase by ATM-mediated phosphorylation in response to ionizing radiation.[82] Thus, phosphorylation of STAT1 via the ATM/c-Abl axis might represent an initial event in the activation of JAK/STAT signaling after genotoxic stress. Activated STAT1 could then transactivate ISGs including interferons and PML.

While answering some questions, our present data also identify some issues that remain to be elucidated in the future. Among these is the elucidation of the precise DDR (sub)pathway(s) that results in the enhanced JAK/STAT signaling to PML promoter, and the identity of the transcription factors involved. Another critical issue is identification of the key cytokines that serve as ligands upstream of the observed JAK/STAT-induced signaling. A plethora of chemokines and cytokines have been implicated in development and maintenance of cellular senescence[83] including their autocrine/paracrine secretion by cells undergoing drug-induced senescence.[35] It is also apparent that at least one other pathway contributes to PML transcriptional regulation under basal growth conditions as well as in IFNα-treated[84] or genotoxic drug-treated cells, as inhibition of JAK/STAT signaling impaired, but did not entirely eliminate, PML expression in such experiments.

From a broader perspective, our present findings are relevant for cancer biology and mechanisms behind biological responses to chemotherapy. Importantly, drug-induced senescence, unlike most other types of cellular senescence, can be evoked also in tumor cells. Our present results provide mechanistic insights into the regulation of PML nuclear compartment during genotoxic stress and highlight the emerging significance of autocrine/paracrine stimulation in the development of senescent phenotype and the so-called "bystander" effects (reviewed in ref. 85) observed under various conditions including radiotherapy or chemotherapy. We hope that the identification of the critical role of JAK/STAT signaling and ISRE-mediated transcription as important aspects of PML expression in drug-induced senescence will

stimulate further work on the cytokines and other elements of this pathway that might represent a candidate therapeutic target to optimize chemotherapy.

Materials and Methods

Chemicals and antibodies. 5-bromo-2'-deoxyuridine, cycloheximide, etoposide, camptothecin, aphidicolin, thymidine and TriReagent were purchased from Sigma (St. Louis, MO), distamycin A was obtained from Dr. Perrotta (Chemper, Prato, Italy), X-Gal from Fluka (Buchs, Switzerland) and IFNα-2b from Schering Plough (Kenilworth, NJ). JAK inhibitor I was purchased from Merck KGaA (Darmstadt, Germany).

The following antibodies were used: mouse monoclonal (mAb) antibody PG-M3 against PML (for immunofluorescence), rabbit polyclonal antibody against PML (for immunoblots), polyclonal serum against IRF1 (sc-13041), polyclonal serum against STAT3 (clone C-20), rabbit polyclonal antibody against 53BP1 (H300), all from Santa Cruz Biotechnology (Santa Cruz, CA), mouse mAb antibody against STAT1 (EXBIO, Prague, Czech Republic), rabbit polyclonal serum against phosphotyrosine 701 of STAT1, phosphoserine 15 of p53 and phosphothreonine of Chk2, mouse mAb against phosphotyrosine 705 of STAT3 (Cell Signaling Technology, Danvers, MA), mouse mAb antibody against MXA (a gift from G. Koch, University of Freiburg, Germany), mouse mAb antibody against JAK1 and γH2AX (Millipore, Billerica, MA), rabbit polyclonal serum against BLM (gift from Norma F. Neff, New York Blood Center, New York, NY), rabbit polyclonal serum against TRF1 (T. de Lange, The Rockefeller University, NY) and mouse mAb antibody against GAPDH (GeneTEX, Irvine, CA). For immunofluorescence, secondary antibodies anti-mouse IgG antibody conjugated with Cy3 (Jackson ImmunoResearch Laboratories, West Grove, PA) and anti-rabbit IgG antibody Alexa 488 (Invitrogene, Carlsbad, CA) were used.

Cell cultures. Human cancer cell lines HeLa, U2OS and HCT-116 and BJ normal human fibroblasts (at population doublings between 25 and 45) were cultured in Dulbecco's modified Eagle's medium (D-MEM) supplemented with 10% foetal bovine serum (FBS). Cells were kept at 37°C under 5% CO_2 atmosphere and 95% humidity.

Induction and assay of cellular senescence in vitro. In pilot experiments, cells were treated with various concentrations of individual drugs to select best conditions leading to senescence. 100 μM BrdU or a combination of 10 μM BrdU with 10 μM DMA (dissolved in DMSO), 0.5 μM camptothecin, 0.3 μM aphidicolin (dissolved in DMSO), 5 μM etoposide and 2.5 mM thymidine were chosen as the most suitable for routine administration to reach senescence within 6 days of the treatment in the majority of cells within the given cell population. For chemical inhibition of JAK kinases, 0.25 μM JAK inhibitor I was used simultaneously with the appropriate senescence-inducing chemicals. Culture medium with fresh additives was changed every second day (every third day in case of thymidine-treated U2OS cells without tetracycline system). Cells treated with the JAK inhibitor I alone were passaged every two days. To avoid the known sensitivity of BrdU-treated cells to light-induced DNA damage, cells were exposed to light only for minimal time periods necessary for handling. Senescence associated-β-galactosidase assay was performed as described[86] with modifications described in.[87] Images were captured in bright field by a fluorescence microscope (Leica DMRXA, Germany) equipped with digital camera.

Indirect immunofluorescence. Cells grown on glass coverslips were fixed by 4% formaldehyde and permeabilized by 0.1% Triton X-100 in two consecutive steps, each for 20 minutes at RT. After washing with PBS, cells were incubated with diluted primary antibodies for 1 hour at RT and then extensively washed with PBS/0.1% Tween 20. The incubation with secondary antibodies was performed for 1 hour at RT. To counterstain nuclei, coverslips were mounted in Mowiol containing 4',6-diamidino-2-phenylindole (DAPI; Sigma, St. Louis, MO, USA) and viewed by a confocal microscope (Leica TCS SP, Weltzlar, Germany) or by a fluorescence microscope (Leica DMRXA, Germany). Minimum of 100 cells on confocal micrographs for each treatment was used for statistical evaluation of PML NB numbers.

Quantitative real time RT-PCR (qRT-PCR). Total RNA samples were isolated using TriReagent according to the manufacturer's protocol. Purified RNA was treated with 80 U/ml DNase (TURBO DNA-free Kit, Ambion, Applied Biosystems, Foster City, CA, USA) for 30 minutes at 37°C. First strand cDNA was synthesized from 200 ng of RNA sample with random hexamer primers using TaqMan Reverse Transcription Reagents (Applied Biosystems). qRT-PCR was performed in ABI Prism 7300 (Applied Biosystems) using SYBR Green I Master Mix (Applied Biosystems) with the following set of primers:

PML (designed to encompass PML exons common to all isoforms): 5'-CCG CAA GAC CAA CAA CAT CTT-3', 5'-CAG CGG CTT GGA ACA TCC T-3'; GAPDH: 5'-CTC CCA CTC CCT GAA ATC TG-3', 5'-GAG CTG TTC TCC TGC ACC TC-3'; MXA: 5'-CTC CCA CTC CCT GAA ATC TG-3', 5'-GAG CTG TTC TCC TGC ACC TC-3'; JAK1: 5'-GGA TAA CAT CAG CTT CAT GCT AAA-3', 5'-CAC CAG CAG GTT GGA GAT TT-3'; Actin: 5'-AGG CAC CAG GGC GTG AT-3', 5'-TCG CCC ACA TAG GAA TCC TT-3'. The relative quantity of cDNA was estimated by ΔΔCt, data were normalized to GAPDH or actin.

SDS-PAGE and western blotting. Cells were harvested into Laemmli SDS sample lysis buffer supplemented with a cocktail of protease inhibitors (EDTA free, Roche Diagnostics, Mannheim, Germany) with 1 μg/ml leupeptin (Serva, Heidelberg, Germany) and a cocktail of phosphatase inhibitors (Roche Diagnostics, Mannheim, Germany), sonicated and centrifuged at 16,000 x g for 10 min. Concentration of proteins was estimated by the BCA method (Pierce Biotechnology Inc., Rockford, IL). 100 mM DTT and 0.01% bromphenol was added to lysates before separation in polyacrylamide gels by SDS-PAGE (9% gels were used for most of the proteins, 14% gels for p21 and Chk2 pT68). The same protein amount (35 μg) was loaded into each well (except BJ lysates—25 μg). Proteins were electrotransferred onto a nitrocellulose membrane using wet or semidry transfer and detected by specific antibodies combined with horseradish peroxidase-conjugated secondary antibodies

(goat anti-rabbit, goat anti-mouse, Bio-Rad, Hercules, CA). Peroxidase activity was detected by ECL (Pierce Biotechnology Inc.). GAPDH was used as a marker of equal loading.

Gel retardation assay. Gel retardation assays were essentially done as described.[88] In brief, 1 μg of nuclear extracts from HeLa cells (prepared with Nuclear Extraction Kit, Marligen, Rockville, MD) treated with or without BrdU/DMA for 6 days was incubated with ^{32}P-end-labeled double-stranded oligonucleotides corresponding to the ISRE (+605/+618) and GAS binding site (+363/+374) of the PML promoter[65] in binding buffer (4 mM HEPES, 70 mM KCl, 5 mM $MgCl_2$, 5% glycerol, 1 mM DTT, 100 μM $ZnSO_4$, pH 7.9) for 20 min at room temperature. Nuclear extracts prepared from cells treated with IFNα (24 hours) or IFNγ (24 hours) were used as controls. For competition assays, the competitor DNA was added 10 min prior to addition of labelled probes. DNA-protein complexes were then resolved by electrophoresis on a 6% acrylamide gel in 1x TBE buffer (89 mM Tris-base, 89 mM boric acid, 2 mM EDTA, pH 8.0). The gels were blotted on filter paper and exposed to phosphoimager screens (Fuji) and/or X-ray films. Sequences of double-strand DNA oligonucleotides used are listed below:

PML ISRE forward: 5'-ATC TAA ACC GAG AAT CGA AAC TAA GCT G-3'; PML ISRE reverse: 5'-CAG CTT AGT TTC GAT TCT CGG TTT AGA T-3'; PML GAS forward: 5'-TCC CGC TTT ACC GTA AGT CAG CGG-3'; PML GAS reverse: 5'-CCG CTG ACT TAC GGT AAA GCG GGA-3'; MXA ISRE wt forward: 5'-AGC TTG GTC TGT GAG TTT CAT TTC TTC GCC A-3'; MXA ISRE wt reverse: 5'-TGG CGA AGA AAT GAA ACT CAC AGA CCA AGC T-3'; MXA ISRE mut forward: 5'-AGC TTG GTC TGT GAG GCG CAG CGC TTC GCC A-3'; MXA ISRE mut reverse: 5'-TGG CGA AGC GCT GCG CCT CAC AGA CCA AGC T-3' (mutated bases are underlined).

Transduction of shRNA. Specific shRNAs were introduced into HeLa cells using lentiviruses as described in our previous article.[35] shRNA used are listed below:

#1 5'-CCG GGA CAG TCA CAA GAC TTG TGA ACT CGA GTT CAC AAG TCT TGT GAC TGT CTT TTT G-3'

#2 5'-CCG GCG TTC TCT ACT ACG AAG TGA TCT CGA GAT CAC TTC GTA GTA GAG AAC GTT TTT G-3'

#3 5'-CCG GGA GAC TTC CAT GTT ACT GAT TCT CGA GAA TCA GTA ACA TGG AAG TCT CTT TTT-3'

#4 5'-CCG GCT GAG CTA CTT GGA GGA TAA ACT CGA GTT TAT CCT CCA AGT AGC TCA GTT TTT-3'

#5 5'-CCG GGC CTT AAG GAA TAT CTT CCA ACT CGA GTT GGA AGA TAT TCC TTA AGG CTT TTT G-3'

Estimation of PML promoter activity. The Bluescript II SK$^+$ plasmid containing the PML promoter fragment (-809/+633) in front of a luciferase reporter gene (PML 1.44-Luc) was a gift from H. de Thé.[65] ΔISRE PML-Luc was made by deletion of a 34-bp fragment (595/628) containing the ISRE element using adjacent Bgl II and Nco I restriction sites. To measure luciferase activity, cells were seeded at 6 x 10^4 per well in 12-well plates one day before transfection. 450 ng of PML 1.44-Luc or ΔISRE PML-Luc with 50 ng of vector containing Renilla luciferase under thymidine kinase promoter (pRL-TK) were transfected to each well using FuGENE 6 (Roche Diagnostics, Mannheim, Germany). 24 h after transfection, senescence-inducing drugs with or without iJAK were added for the following 72 hours and then cell lysates were harvested according to the manufacturer's protocol (the same as for the dual luciferase assay). For the dual luciferase assay, luciferase activities were quantified with a luminometer (GloMax®-Multi Microplate Multimode Reader, Turner Biosystems, CA) using The Dual-Luciferase Reporter Assay System (Promega, Madison, WI).

Acknowledgements

We thank to Lenka Janderová-Rossmeislová, Markéta Cernohorská and Vladimír Cermák for technical support and helpful discussions. This study was supported by Grant Agency of the Academy of Sciences of the Czech Republic (Project No. IAA500390501), Grant Agency of the Czech Republic (Projects No. 204/08/1418 and No. 301/08/0353), Institutional Grant (Project No. AV0Z5039906), the Danish Cancer Society, the Danish National Research Foundation, the Czech Ministry of Education (MSM6198959216), Novo Nordisk (R153-A12997) and the European Commission 7th Framework Programme (Projects Infla-Care and TRIREME).

Note

Supplementry materials can be found at:
www.landesbioscience.com/supplement/HubackovaCC9-15-sup.pdf

References

1. Ascoli CA, Maul GG. Identification of a novel nuclear domain. J Cell Biol 1991; 112:785-95.
2. Gurrieri C, Capodieci P, Bernardi R, Scaglioni PP, Nafa K, Rush LJ, et al. Loss of the tumor suppressor PML in human cancers of multiple histologic origins. J Natl Cancer Inst 2004; 96:269-79.
3. Stone RM, O'Donnell MR, Sekeres MA. Acute myeloid leukemia. Hematology Am Soc Hematol Educ Program 2004; 98-117.
4. Wang ZG, Delva L, Gaboli M, Rivi R, Giorgio M, Cordon-Cardo C, et al. Role of PML in cell growth and the retinoic acid pathway. Science 1998; 279:1547-51.
5. Toussaint O, Royer V, Salmon M, Remacle J. Stress-induced premature senescence and tissue ageing. Biochem Pharmacol 2002; 64:1007-9.
6. Collado M, Blasco MA, Serrano M. Cellular senescence in cancer and aging. Cell 2007; 130:223-33.
7. Mallette FA, Ferbeyre G. The DNA damage signaling pathway connects oncogenic stress to cellular senescence. Cell Cycle 2007; 6:1831-6.
8. d'Adda di Fagagna F. Living on a break: cellular senescence as a DNA-damage response. Nat Rev Cancer 2008; 8:512-22.
9. Sager R. Senescence as a mode of tumor suppression. Environ Health Perspect 1991; 93:59-62.
10. Campisi J. Cellular senescence as a tumor-suppressor mechanism. Trends Cell Biol 2001; 11:27-31.
11. Bartkova J, Rezaei N, Liontos M, Karakaidos P, Kletsas D, Issaeva N, et al. Oncogene-induced senescence is part of the tumorigenesis barrier imposed by DNA damage checkpoints. Nature 2006; 444:633-7.
12. Brown JP, Wei W, Sedivy JM. Bypass of senescence after disruption of p21$^{CIP1/WAF1}$ gene in normal diploid human fibroblasts. Science 1997; 277:831-4.
13. Narita M, Nunez S, Heard E, Lin AW, Hearn SA, Spector DL, et al. Rb-mediated heterochromatin formation and silencing of E2F target genes during cellular senescence. Cell 2003; 113:703-16.
14. Gottifredi V, Prives C. p53 and PML: new partners in tumor suppression. Trends Cell Biol 2001; 11:184-7.
15. Pearson M, Carbone R, Sebastiani C, Cioce M, Fagioli M, Saito S, et al. PML regulates p53 acetylation and premature senescence induced by oncogenic Ras. Nature 2000; 406:207-10.
16. Louria-Hayon I, Grossman T, Sionov RV, Alsheich O, Pandolfi PP, Haupt Y. The promyelocytic leukemia protein protects p53 from Mdm2-mediated inhibition and degradation. J Biol Chem 2003; 278:33134-41.
17. de Stanchina E, Querido E, Narita M, Davuluri RV, Pandolfi PP, Ferbeyre G, et al. PML is a direct p53 target that modulates p53 effector functions. Mol Cell 2004; 13:523-35.

18. Zhang R, Poustovoitov MV, Ye X, Santos HA, Chen W, Daganzo SM, et al. Formation of MacroH2A-containing senescence-associated heterochromatin foci and senescence driven by ASF1a and HIRA. Dev Cell 2005; 8:19-30.
19. Zhang R, Chen W, Adams PD. Molecular dissection of formation of senescence-associated heterochromatin foci. Mol Cell Biol 2007; 27:2343-58.
20. Ye X, Zerlanko B, Zhang R, Somaiah N, Lipinski M, Salomoni P, et al. Definition of pRB- and p53-dependent and -independent steps in HIRA/ASF1a-mediated formation of senescence-associated heterochromatin foci. Mol Cell Biol 2007; 27:2452-65.
21. Janderova-Rossmeislova L, Novakova Z, Vlasakova J, Philimonenko V, Hozak P, Hodny Z. PML protein association with specific nucleolar structures differs in normal, tumor and senescent human cells. J Struct Biol 2007; 159:56-70.
22. Jiang WQ, Ringertz N. Altered distribution of the promyelocytic leukemia-associated protein is associated with cellular senescence. Cell Growth Differ 1997; 8:513-22.
23. Ferbeyre G, de Stanchina E, Querido E, Baptiste N, Prives C, Lowe SW. PML is induced by oncogenic ras and promotes premature senescence. Genes Dev 2000; 14:2015-27.
24. Blazkova H, Krejcikova K, Moudry P, Frisan T, Hodny Z, Bartek J. Bacterial intoxication evokes cellular senescence with persistent DNA damage and cytokine signaling. J Cell Mol Med 2009; 14:357-67.
25. Bourdeau V, Baudry D, Ferbeyre G. PML links aberrant cytokine signaling and oncogenic stress to cellular senescence. Front Biosci 2009; 14:475-85.
26. Bischof O, Kirsh O, Pearson M, Itahana K, Pelicci PG, Dejean A. Deconstructing PML-induced premature senescence. EMBO J 2002; 21:3358-69.
27. Scaglioni PP, Yung TM, Cai LF, Erdjument-Bromage H, Kaufman AJ, Singh B, et al. A CK2-dependent mechanism for degradation of the PML tumor suppressor. Cell 2006; 126:269-83.
28. Lavau C, Marchio A, Fagioli M, Jansen J, Falini B, Lebon P, et al. The acute promyelocytic leukaemia-associated PML gene is induced by interferon. Oncogene 1995; 11:871-6.
29. Korioth F, Gieffers C, Maul GG, Frey J. Molecular characterization of NDP52, a novel protein of the nuclear domain 10, which is redistributed upon virus infection and interferon treatment. J Cell Biol 1995; 130:1-13.
30. Der SD, Zhou A, Williams BR, Silverman RH. Identification of genes differentially regulated by interferon alpha, beta or gamma using oligonucleotide arrays. Proc Natl Acad Sci USA 1998; 95:15623-8.
31. Chelbi-Alix MK, Pelicano L, Quignon F, Koken MH, Venturini L, Stadler M, et al. Induction of the PML protein by interferons in normal and APL cells. Leukemia 1995; 9:2027-33.
32. Platanias LC. Mechanisms of type-I- and type-II-interferon-mediated signaling. Nat Rev Immunol 2005; 5:375-86.
33. Commins S, Steinke JW, Borish L. The extended IL-10 superfamily: IL-10, IL-19, IL-20, IL-22, IL-24, IL-26, IL-28 and IL-29. J Allergy Clin Immunol 2008; 121:1108-11.
34. Takaoka A, Hayakawa S, Yanai H, Stoiber D, Negishi H, Kikuchi H, et al. Integration of interferon-alpha/beta signaling to p53 responses in tumour suppression and antiviral defence. Nature 2003; 424:516-23.
35. Novakova Z, Hubackova S, Kosar M, Janderova-Rossmeislova L, Dobrovolna J, Vasicova P, et al. Cytokine expression and signaling in drug-induced cellular senescence. Oncogene 2010; 29:273-84.
36. Kuilman T, Michaloglou C, Vredeveld LC, Douma S, van Doorn R, Desmet CJ, et al. Oncogene-induced senescence relayed by an interleukin-dependent inflammatory network. Cell 2008; 133:1019-31.
37. Acosta JC, O'Loghlen A, Banito A, Guijarro MV, Augert A, Raguz S, et al. Chemokine signaling via the CXCR2 receptor reinforces senescence. Cell 2008; 133:1006-18.
38. Coppe JP, Patil CK, Rodier F, Sun Y, Munoz DP, Goldstein J, et al. Senescence-associated secretory phenotypes reveal cell-nonautonomous functions of oncogenic RAS and the p53 tumor suppressor. PLoS Biol 2008; 6:2853-68.
39. Rodier F, Coppe JP, Patil CK, Hoeijmakers WA, Munoz DP, Raza SR, et al. Persistent DNA damage signaling triggers senescence-associated inflammatory cytokine secretion. Nat Cell Biol 2009; 11:973-9.
40. Mariotti M, Castiglioni S, Bernardini D, Maier J. Interleukin 1alpha is a marker of endothelial cellular senescent. Immun Ageing 2006; 3:4.
41. Katakura Y, Nakata E, Tabira Y, Miura T, Teruya K, Tsuchiya T, et al. Decreased tumorigenicity in vivo when transforming growth factor beta treatment causes cancer cell senescence. Biosci Biotechnol Biochem 2003; 67:815-21.
42. Vertegaal ACO, Andersen JS, Ogg SC, Hay RT, Mann M, Lamond AI. Distinct and overlapping sets of SUMO-1 and SUMO-2 target proteins revealed by quantitative proteomics. Mol Cell Proteomics 2006; 5:2298-310.
43. Marusyk A, Wheeler LJ, Mathews CK, DeGregori J. p53 mediates senescence-like arrest induced by chronic replicational stress. Mol Cell Biol 2007; 27:5336-51.
44. Engstrom JU, Kmiec EB. Manipulation of cell cycle progression can counteract the apparent loss of correction frequency following oligonucleotide-directed gene repair. BMC Mol Biol 2007; 8:9.
45. te Poele RH, Okorokov AL, Jardine L, Cummings J, Joel SP. DNA damage is able to induce senescence in tumor cells in vitro and in vivo. Cancer Res 2002; 62:1876-83.
46. Cheng HL, Chang SM, Cheng YW, Liu HJ, Chen YC. Characterization of the activities of p21$^{Cip1/Waf1}$ promoter-driven reporter systems during camptothecin-induced senescence-like state of BHK-21 cells. Mol Cell Biochem 2006; 291:29-38.
47. Roberson RS, Kussick SJ, Vallieres E, Chen S-YJ, Wu DY. Escape from therapy-induced accelerated cellular senescence in p53-null lung cancer cells and in human lung cancers. Cancer Res 2005; 65:2795-803.
48. Han Z, Wei W, Dunaway S, Darnowski JW, Calabresi P, Sedivy J, et al. Role of p21 in apoptosis and senescence of human colon cancer cells treated with camptothecin. J Biol Chem 2002; 277:17154-60.
49. Carbone R, Pearson M, Minucci S, Pelicci PG. PML NBs associate with the hMre11 complex and p53 at sites of irradiation induced DNA damage. Oncogene 2002; 21:1633-40.
50. Dellaire G, Kepkay R, Bazett-Jones DP. High resolution imaging of changes in the structure and spatial organization of chromatin, gamma-H2A.X and the MRN complex within etoposide-induced DNA repair foci. Cell Cycle 2009; 8:3750-69.
51. Mirzoeva OK, Petrini JH. DNA damage-dependent nuclear dynamics of the Mre11 complex. Mol Cell Biol 2001; 21:281-8.
52. Yankiwski V, Noonan JP, Neff NF. The C-terminal domain of the Bloom syndrome DNA helicase is essential for genomic stability. BMC Cell Biol 2001; 2:11.
53. Cheok CF, Bachrati CZ, Chan KL, Ralf C, Wu L, Hickson ID. Roles of the Bloom's syndrome helicase in the maintenance of genome stability. Biochem Soc Trans 2005; 33:1456-9.
54. Eladad S, Ye TZ, Hu P, Leversha M, Beresten S, Matunis MJ, et al. Intra-nuclear trafficking of the BLM helicase to DNA damage-induced foci is regulated by SUMO modification. Hum Mol Genet 2005; 14:1351-65.
55. Gharibyan V, Youssoufian H. Localization of the Bloom syndrome helicase to punctate nuclear structures and the nuclear matrix and regulation during the cell cycle: comparison with the Werner's syndrome helicase. Mol Carcinog 1999; 26:261-73.
56. Bischof O, Kim SH, Irving J, Beresten S, Ellis NA, Campisi J. Regulation and localization of the Bloom syndrome protein in response to DNA damage. J Cell Biol 2001; 153:367-80.
57. Davalos AR, Kaminker P, Hansen RK, Campisi J. ATR and ATM-dependent movement of BLM helicase during replication stress ensures optimal ATM activation and 53BP1 focus formation. Cell Cycle 2004; 3:1579-86.
58. Dellaire G, Bazett-Jones DP. Beyond repair foci: subnuclear domains and the cellular response to DNA damage. Cell Cycle 2007; 6:1864-72.
59. Matsuoka S, Rotman G, Ogawa A, Shiloh Y, Tamai K, Elledge SJ. Ataxia telangiectasia-mutated phosphorylates Chk2 in vivo and in vitro. Proc Natl Acad Sci USA 2000; 97:10389-94.
60. Schultz LB, Chehab NH, Malikzay A, Halazonetis TD. p53 binding protein 1 (53BP1) is an early participant in the cellular response to DNA double-strand breaks. J Cell Biol 2000; 151:1381-90.
61. Rogakou EP, Pilch DR, Orr AH, Ivanova VS, Bonner WM. DNA double-stranded breaks induce histone H2AX phosphorylation on serine 139. J Biol Chem 1998; 273:5858-68.
62. Shieh SY, Ikeda M, Taya Y, Prives C. DNA damage-induced phosphorylation of p53 alleviates inhibition by MDM2. Cell 1997; 91:325-34.
63. Siliciano JD, Canman CE, Taya Y, Sakaguchi K, Appella E, Kastan MB. DNA damage induces phosphorylation of the amino terminus of p53. Genes Dev 1997; 11:3471-81.
64. Noda A, Ning Y, Venable SF, Pereira-Smith OM, Smith JR. Cloning of senescent cell-derived inhibitors of DNA synthesis using an expression screen. Exp Cell Res 1994; 211:90-8.
65. Stadler M, Chelbi-Alix MK, Koken MH, Venturini L, Lee C, Saib A, et al. Transcriptional induction of the PML growth suppressor gene by interferons is mediated through an ISRE and a GAS element. Oncogene 1995; 11:2565-73.
66. Bunz F, Dutriaux A, Lengauer C, Waldman T, Zhou S, Brown JP, et al. Requirement for p53 and p21 to sustain G_2 arrest after DNA damage. Science 1998; 282:1497-501.
67. Thullberg M, Welcker M, Bartkova J, Kjerulff AA, Lukas J, Hogberg J, et al. Monoclonal antibody probes for p21$^{WAF1/CIP1}$ and the INK4 family of cyclin-dependent kinase inhibitors. Hybridoma 2000; 19:63-72.
68. Adams PD. Healing and hurting: molecular mechanisms, functions and pathologies of cellular senescence. Mol Cell 2009; 36:2-14.
69. Bartek J, Lukas J, Bartkova J. DNA damage response as an anti-cancer barrier: damage threshold and the concept of 'conditional haploinsufficiency'. Cell Cycle 2007; 6:2344-7.
70. Bernardi R, Pandolfi PP. Structure, dynamics and functions of promyelocytic leukaemia nuclear bodies. Nat Rev Mol Cell Biol 2007; 8:1006-16.
71. von Zglinicki T, Saretzki G, Ladhoff J, d'Adda di Fagagna F, Jackson SP. Human cell senescence as a DNA damage response. Mech Ageing Dev 2005; 126:111-7.
72. d'Adda di Fagagna F, Reaper PM, Clay-Farrace L, Fiegler H, Carr P, Von Zglinicki T, et al. A DNA damage checkpoint response in telomere-initiated senescence. Nature 2003; 426:194-8.
73. Di Micco R, Fumagalli M, Cicalese A, Piccinin S, Gasparini P, Luise C, et al. Oncogene-induced senescence is a DNA damage response triggered by DNA hyper-replication. Nature 2006; 444:638-42.

74. Halazonetis TD, Gorgoulis VG, Bartek J. An oncogene-induced DNA damage model for cancer development. Science 2008; 319:1352-5.
75. Dellaire G, Bazett-Jones DP. PML nuclear bodies: dynamic sensors of DNA damage and cellular stress. Bioessays 2004; 26:963-77.
76. D'Orazi G, Cecchinelli B, Bruno T, Manni I, Higashimoto Y, Saito S, et al. Homeodomain-interacting protein kinase-2 phosphorylates p53 at Ser 46 and mediates apoptosis. Nat Cell Biol 2002; 4:11-9.
77. Hofmann TG, Moller A, Sirma H, Zentgraf H, Taya Y, Droge W, et al. Regulation of p53 activity by its interaction with homeodomain-interacting protein kinase-2. Nat Cell Biol 2002; 4:1-10.
78. Ihle JN, Kerr IM. Jaks and Stats in signaling by the cytokine receptor superfamily. Trends in Genetics 1995; 11:69-74.
79. Bandyopadhyay SK, Leonard GT Jr, Bandyopadhyay T, Stark GR, Sen GC. Transcriptional induction by double-stranded RNA is mediated by interferon-stimulated response elements without activation of interferon-stimulated gene factor 3. J Biol Chem 1995; 270:19624-9.
80. Dror N, Rave-Harel N, Burchert A, Azriel A, Tamura T, Tailor P, et al. Interferon regulatory factor-8 is indispensable for the expression of promyelocytic leukemia and the formation of nuclear bodies in myeloid cells. J Biol Chem 2007; 282:5633-40.
81. Pamment J, Ramsay E, Kelleher M, Dornan D, Ball KL. Regulation of the IRF-1 tumour modifier during the response to genotoxic stress involves an ATM-dependent signaling pathway. Oncogene 2002; 21:7776-85.
82. Baskaran R, Wood LD, Whitaker LL, Canman CE, Morgan SE, Xu Y, et al. Ataxia telangiectasia mutant protein activates c-Abl tyrosine kinase in response to ionizing radiation. Nature 1997; 387:516-9.
83. Kuilman T, Peeper DS. Senescence-messaging secretome: SMS-ing cellular stress. Nat Rev Cancer 2009; 9:81-94.
84. Vlasakova J, Novakova Z, Rossmeislova L, Kahle M, Hozak P, Hodny Z. Histone deacetylase inhibitors suppress IFN{alpha}-induced upregulation of promyelocytic leukemia protein. Blood 2007; 109:1373-80.
85. Wright EG. Manifestations and mechanisms of non-targeted effects of ionizing radiation. Mutat Res 2010; 687:28-33.
86. Dimri GP, Lee X, Basile G, Acosta M, Scott G, Roskelley C, et al. A biomarker that identifies senescent human cells in culture and in aging skin in vivo. Proc Natl Acad Sci USA 1995; 92:9363-7.
87. Serrano M, Lin AW, McCurrach ME, Beach D, Lowe SW. Oncogenic ras provokes premature cell senescence associated with accumulation of p53 and $p16^{INK4a}$. Cell 1997; 88:593-602.
88. Li R, Hodny Z, Luciakova K, Barath P, Nelson BD. Sp1 activates and inhibits transcription from separate elements in the proximal promoter of the human adenine nucleotide translocase 2 (ANT2) gene. J Biol Chem 1996; 271:18925-30.

Suppl.Fig.1

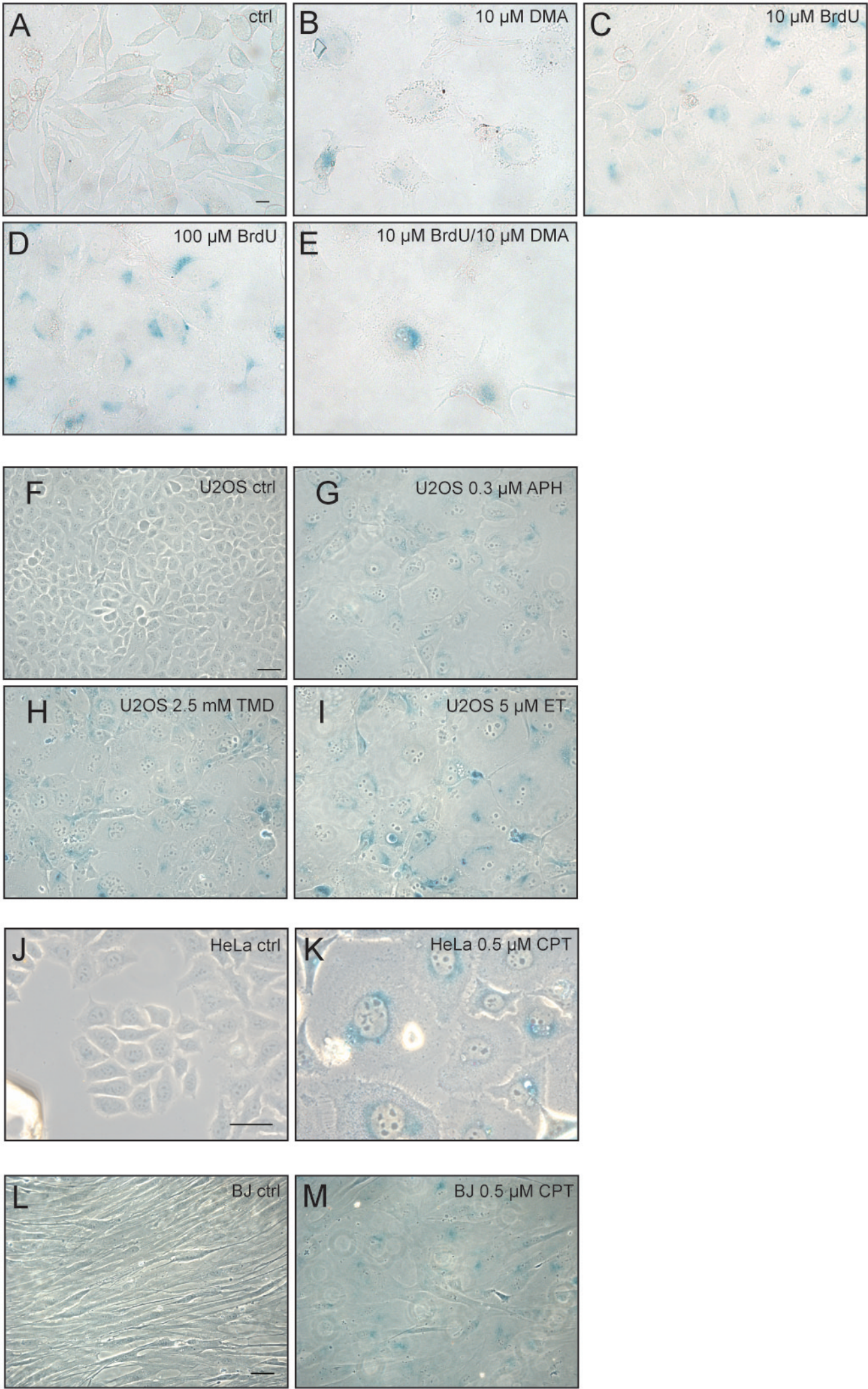
A
ctrl
B
10 μM DMA
C
10 μM BrdU
D
100 μM BrdU
E
10 μM BrdU/10 μM DMA
F
U2OS ctrl
G
U2OS 0.3 μM APH
H
U2OS 2.5 mM TMD
I
U2OS 5 μM ET
J
HeLa ctrl
K
HeLa 0.5 μM CPT
L
BJ ctrl
M
BJ 0.5 μM CPT

Suppl.Fig. 2

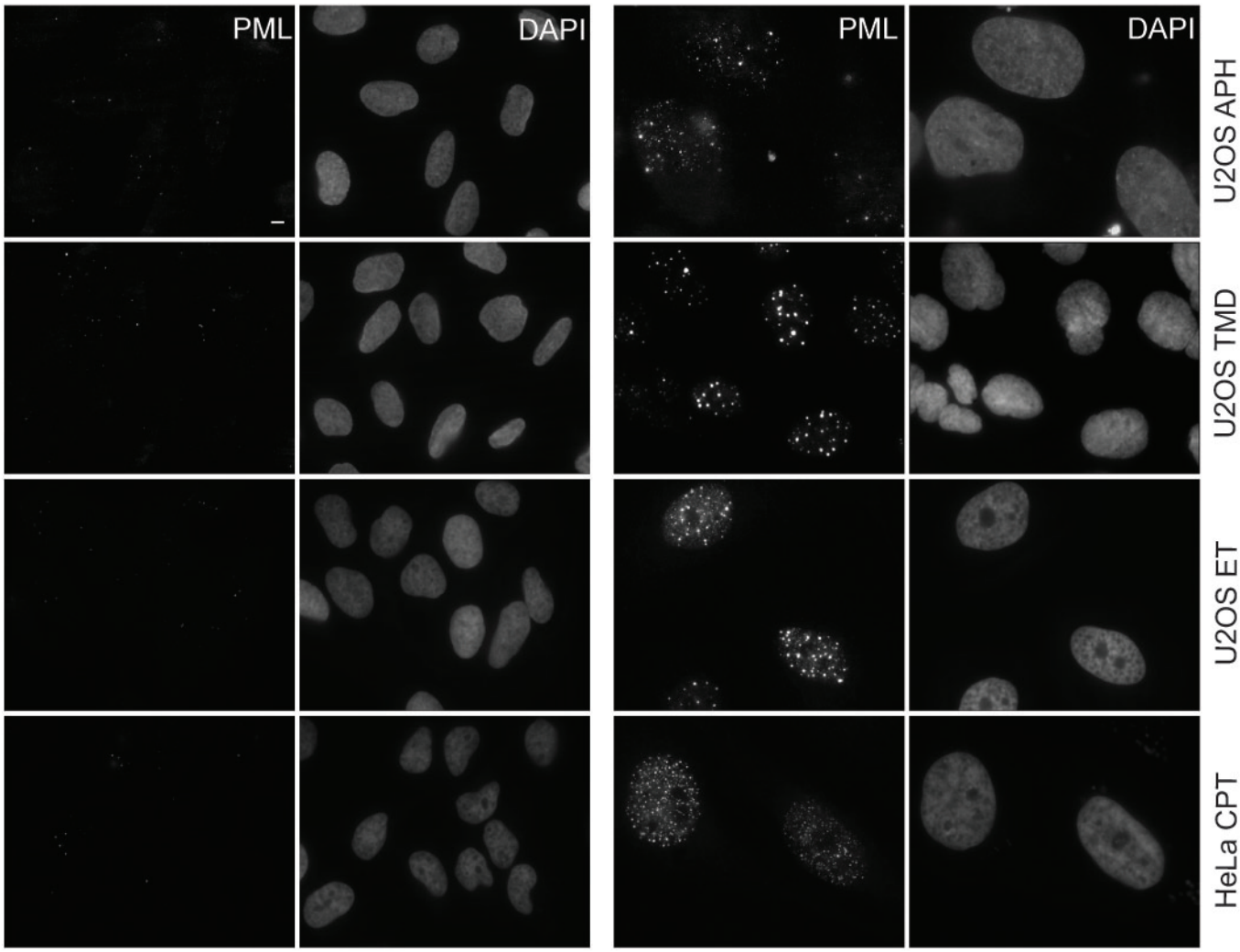
PML
DAPI
PML
DAPI
U2OS ctrl
U2OS ctrl
U2OS ctrl
HeLa ctrl
U2OS APH
U2OS TMD
U2OS ET
HeLa CPT

x

Suppl.Fig.3

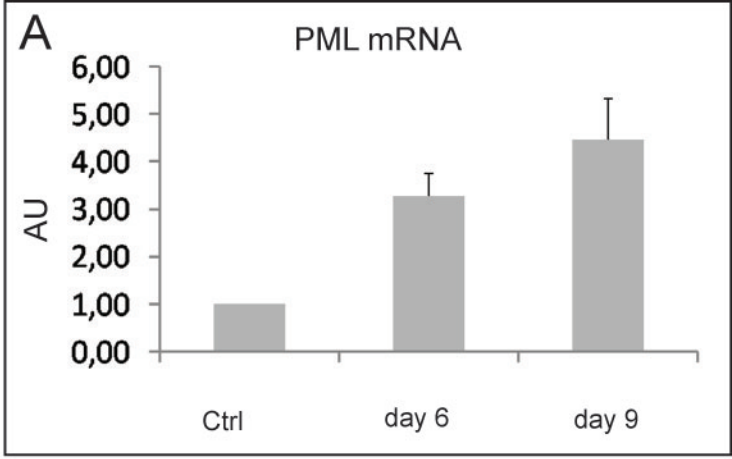
A
PML mRNA
AU
6,00
5,00
4,00
3,00
2,00
1,00
0,00
Ctrl
day 6
day 9

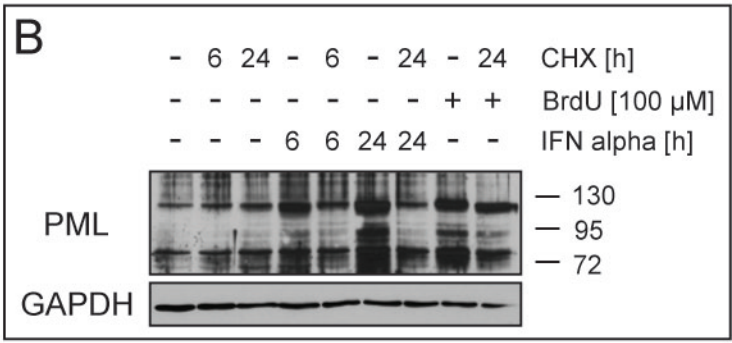
B
- 6 24 - 6 - 24 - 24 CHX [h]
- - - - - - - + + BrdU [100 µM]
- - - 6 6 24 24 - - IFN alpha [h]
PML
GAPDH
130
95
72

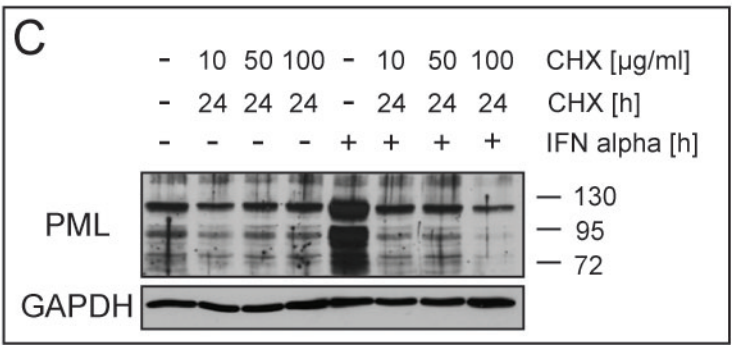
C
- 10 50 100 - 10 50 100 CHX [µg/ml]
- 24 24 24 - 24 24 24 CHX [h]
- - - - + + + + IFN alpha [h]
PML
GAPDH
130
95
72

Suppl.Fig4

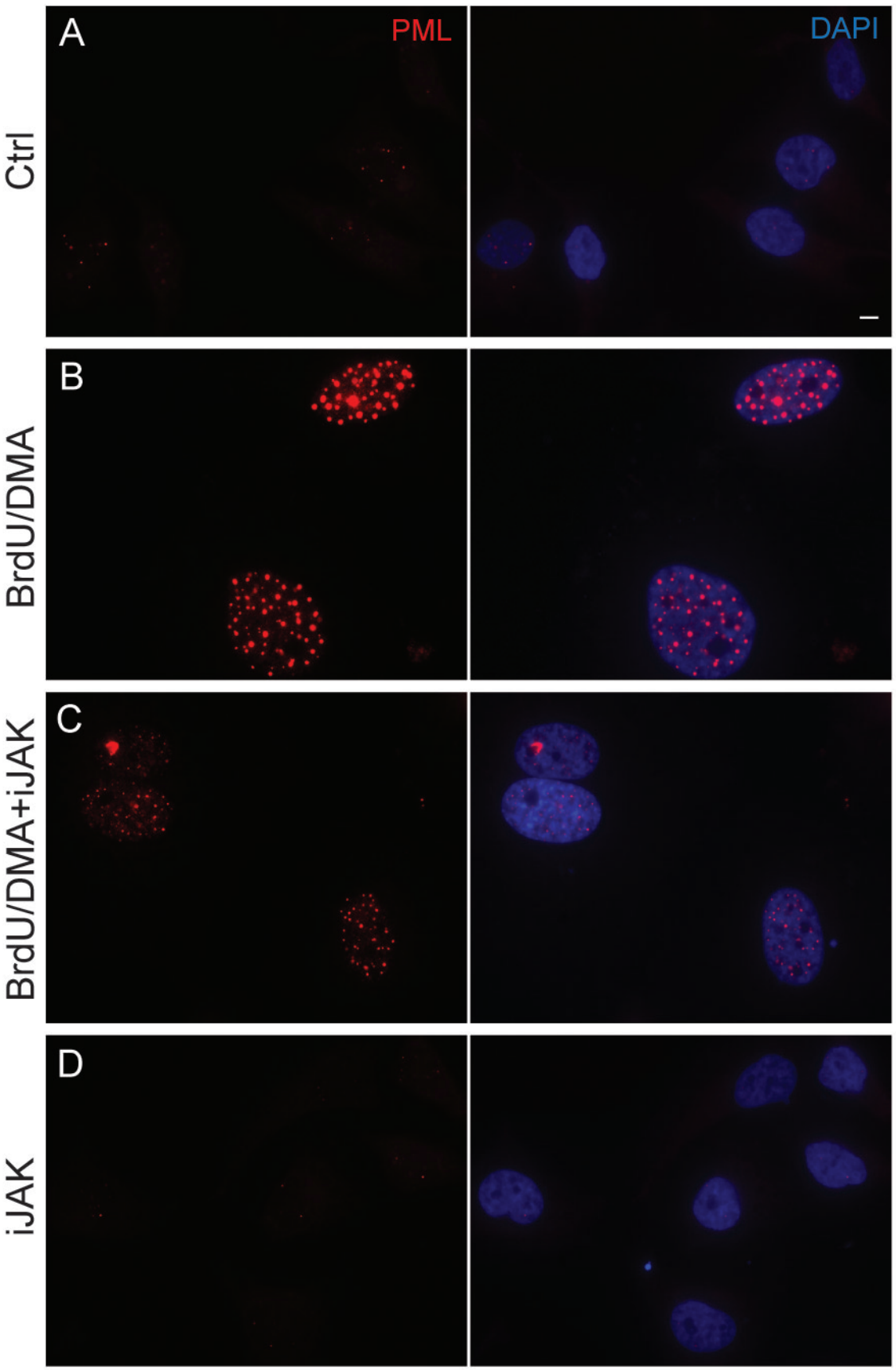

Supplementary Figure 1.

Senescence associated-B-galactosidase assay (SA-B-gal) of HeLa cells treated six days with vehicle (a), 10 μM DMA (b), 10 μM BrdU (c), 100 μM BrdU (d), or 10 μM BrdU/DMA (e); U2OS cells treated six days with vehicle (f), 0.3 μM APH (g), 2.5 mM TMD (h) or 5 μM ET (i); HeLa cells treated six days with vehicle (j) or 0.5 μM CPT (k); BJ cells treated with vehicle (l) or 0.5 μM CPT (m)

Supplementary Figure 2. Elevation of PML NB in drug-induce senescence

Immunofluorescent detection of PML NB in U2OS cells treated six days with 0.3 μM APH, 2.5 mM TMD or 5 μM ET in comparison to control cells and HeLa cells treated with 0.5 μM CPT in comparison to appropriate control cells.

Supplementary Figure 3.

(a) mRNA levels of PML quantified by qRT-PCR in U2OS cells treated by TMD for specified time period. GAPDH was used as a reference gene. (b) Immunoblot detection of PML protein stability in HeLa cells treated with cycloheximide for 6 or 24 hours alone or in combination with BrdU and DMA or IFNalpha in comparison to untreated control. (c) Immunoblot detection of PML protein stability in HeLa cells treated with different doses of cycloheximide for 24 hours with or without IFN alpha treatment.

Supplementary Figure 4. Reduction of PML NB after inhibition of JAK kinases in HeLa cells

Immunofluorescent detection of PML NB in HeLa cells treated for six days with combination of BrdU and DMA (b) or BrdU/DMA and JAK kinase inhibitor I (iJAK) (c) in comparison to control cells (a) and cells treated only with iJAK (d).

THE JOURNAL OF BIOLOGICAL CHEMISTRY VOL. 287, NO. 32, pp. 26702–26714, August 3, 2012

Interleukin 6 Signaling Regulates Promyelocytic Leukemia Protein Gene Expression in Human Normal and Cancer Cells*[S]

Received for publication, October 25, 2011, and in revised form, June 13, 2012 Published, JBC Papers in Press, June 18, 2012, DOI 10.1074/jbc.M111.316869

Sona Hubackova[‡1], **Katerina Krejcikova**[‡], **and Jiri Bartek**[‡§2], **and Zdenek Hodny**[‡3]

From the [‡]*Department of Genome Integrity, Institute of Molecular Genetics, v.v.i., Academy of Sciences of the Czech Republic, 14220 Prague, Czech Republic and* [§]*Danish Cancer Society Research Center, DK-2100 Copenhagen, Denmark*

Background: PML is a tumor suppressor involved in response to viral and genotoxic stress.
Results: Depletion of IL6 siRNA-mediated knockdown of STAT3 or NEMO suppresses PML gene expression.
Conclusion: PML is regulated via IL-6-dependent JAK-STAT3 and PI3K-NFκB signaling pathways in an autocrine/paracrine manner.
Significance: Paracrine regulation of PML gene expression is a part of tissue adaptation to local stress.

Tumor suppressor PML is induced under viral and genotoxic stresses by interferons and JAK-STAT signaling. However, the mechanism responsible for its cell type-specific regulation under non-stimulated conditions is poorly understood. To analyze the variation of PML expression, we utilized three human cell types, BJ fibroblasts and HeLa and U2OS cell lines, each with a distinct PML expression pattern. Analysis of JAK-STAT signaling in the three cell lines revealed differences in levels of activated STAT3 but not STAT1 correlating with PML mRNA and protein levels. RNAi-mediated knockdown of STAT3 decreased PML expression; both STAT3 level/activity and PML expression relied on IL6 secreted into culture media. We mapped the IL6-responsive sequence to an ISRE(−595/−628) element of the PML promoter. The PI3K/Akt/NFκB branch of IL6 signaling showed also cell-type dependence, being highest in BJ, intermediate in HeLa, and lowest in U2OS cells and correlated with IL6 secretion. RNAi-mediated knockdown of NEMO (NF-κ-B essential modulator), a key component of NFκB activation, suppressed NFκB targets LMP2 and IRF1 together with STAT3 and PML. Combined knockdown of STAT3 and NEMO did not further promote PML suppression, and it can be bypassed by exogenous IL6, indicating the NF-κB pathway acts upstream of JAK-STAT3 through induction of IL6. Our results indicate that the cell type-specific activity of IL6 signaling pathways governs PML expression under unperturbed growth conditions. As IL6 is induced in response to various viral and genotoxic stresses, this cytokine may regulate autocrine/paracrine induction of PML under these pathophysiological states as part of tissue adaptation to local stress.

Promyelocytic (PML)[4] nuclear bodies (NBs) are complex structures of mammalian nuclei comprising more than 100 proteins of various function including important cell cycle and cell fate regulators and factors involved in response to DNA damage (1). PML, a scaffold protein required for structural maintenance of PML NBs, is considered a tumor suppressor (for review, see *e.g.* Refs. 2 and 3), as loss of PML gene integrity by chromosomal translocation and gene fusion is linked to pathogenesis of acute promyelocytic leukemia (4) and mice with ablation of PML are tumor-prone (5). Importantly, PML expression is frequently deregulated in many human solid tumors (6–8). Early stages of epithelial tumors feature higher levels of PML than normal tissue cells, whereas advanced invasive tumor stages are associated with down-regulation of PML. Interestingly, Koken *et al.* (8) reported a high abundance of PML in tumor stroma regardless of tumor stage, especially in the vascular component. These expression patterns indicate decreased expression or loss of PML during acquisition of the invasive phenotype and involvement of a paracrine mechanism in PML induction (8). The latter notion is consistent with several studies showing that PML is inducible by cytokines, namely type I and type II interferons (9–12).

The mechanism of tumor-suppressive function of PML is not completely understood. In general, PML plays a role in cellular senescence and apoptosis (for reviews, see *e.g.* Refs. 13 and 14). Some effects of PML can be linked directly to PML protein itself, whereas others can be attributed to the function of PML nuclear compartment, which is built with the aid of PML tetramers. Soluble PML can bind to p53, a transcription factor mediating DNA damage response, senescence, and apoptosis, and facilitates acetylation, stabilization, and phosphorylation-mediated activation of p53 (15, 16). Moreover, as a direct transcriptional target of p53, PML is implicated in a positive feedback loop controlling p53 activity (17). Furthermore, PML and PML NBs cooperate with pRb in formation of chromatin-dense nuclear structures known as senescence-associated heterochromatin foci (18–21) observed in some forms of cellular

* This work was supported by Grant Agency of the Czech Republic (Project 204/08/1418), Institutional Grant (Project RVO 68378050), the Danish Cancer Society, the Danish National Research Foundation, the Czech Ministry of Education (MSM6198959216), Novo Nordisk (R153-A12997), and the European Commission 7th Framework Programme (Projects Infla-Care, Biomedreg and TRIREME).
[S] This article contains supplemental Figs. 1 and 2.
[1] Supported in part by the Faculty of Science, Charles University, Prague, Czech Republic.
[2] To whom correspondence may be addressed. E-mail: jb@cancer.dk.
[3] To whom correspondence may be addressed. Tel.: 420-24106-3151; Fax: 420-24106-2289; E-mail: hodny@img.cas.cz.

[4] The abbreviations used are: PML, promyelocytic leukemia protein; NBs, nuclear body; ISRE, interferon-stimulated response element; NFκB, nuclear factor κB; qRT-PCR, quantitative real time RT-PCR; rhIL6, recombinant human IL6; NEMO, NF-κ-B essential modulator.

senescence (22). Multiplication of PML NBs is observed in almost all types of cellular senescence (13, 15, 23–26). The elevation of PML in senescent cells is mediated at the transcription level (25) via activated Janus kinase/signal transducer and transcription activator (JAK/STAT) signaling (27) and/or post-translationally in some cell types (28).

Several groups including ours reported that various genotoxic stresses leading to activation of DNA damage response induce expression of a complex cytokine network (for reviews, see Refs. 29–31), which can also include type I and type II interferons (32). Activated JAK/STAT signaling accompanying lasting DNA damage response during drug-induced premature senescence contributes to multiplication of nuclear PML compartment through modulation of PML transcript level (33). Notably, PML NBs were found to quickly reassemble after DNA damage and to co-associate with persistent DNA lesions (33–35), implicating PML NBs in metabolism of damaged DNA (36). Importantly, persistent DNA damage response activity and development of cellular senescence is a feature characteristic for early stages of human tumorigenesis (37–41). Collectively, these findings suggest that under conditions of genotoxic stress the PML compartment is regulated at least in part in an autocrine/paracrine manner via secreted cytokines activating the JAK/STAT signaling pathway. Although we reported previously that JAK/STAT signaling (33) directly modulates PML transcription, the key cytokine responsible for PML activation was not determined due to a wide spectrum of cytokines produced by senescent cells.

In contrast to our understanding of PML gene induction during genotoxic stress, regulation of PML transcription under unstressed conditions is currently unclear. Despite that it has been known for almost two decades that various normal and malignant human cell types both *in vitro* and *in vivo* harbor variable numbers of PML nuclear bodies (42), the underlying mechanism responsible for such differences is unknown. In addition, the number of PML NBs noticeably differs even among individual cells in a given cell population (43) partly reflecting cell cycle dependence (8) or proliferative age (see *e.g.* Ref. 23).

In this study we address some of the open questions about PML regulation and show that expression of PML under unperturbed cell culture conditions is partially dependent on IL6, whose level of secretion is cell type-dependent. In general, IL6 is a functionally pleiotropic cytokine produced by many cell types in response to injury, inflammation, and infection. IL6 is an important regulator of cell proliferation and survival, and it is involved in regenerative and inflammatory processes (for review, see Ref. 44). Such functions of IL6 are mediated via its binding to membrane-bound or -soluble α-subunit IL6 receptor. IL6-IL6 receptor complexes then associate at the cellular membrane with two molecules of gp130 subunit followed by gp130 homodimer formation, which results in activation of kinases JAK1, JAK2, and TYK2. These events trigger engagement of phosphatase Src homology domains containing tyrosine phosphatase-2 (SHP-2) and subsequent initiation of signaling cascades including JAK/STAT-3, phosphoinositide 3-kinase (PI3K)-protein kinase B/Akt (PKB/Akt) and ras/raf/mitogen-activated protein kinase pathway (MAPK) (for review, see *e.g.* Refs. 44 and 45). Our present results also show that activities of both the JAK/STAT and PI3K/Akt pathways correlate with PML expression, which in turn is IL6-inducible. Furthermore, down-regulation of key components of either of the two signaling pathways leads to suppression of PML levels. We conclude that IL6 signaling represents an important determinant of regulation of the PML nuclear compartment.

EXPERIMENTAL PROCEDURES

Antibodies—The following antibodies were used: mouse monoclonal antibody PG-M3 against PML (for immunofluorescence), rabbit polyclonal antibodies against PML (for immunoblots), STAT5, phosphotyrosine 694 of STAT5, STAT3 (clone C-20), NEMO, and p53 (all from Santa Cruz Biotechnology (Santa Cruz, CA)); mouse monoclonal antibody against phosphotyrosine 705 of STAT3, rabbit polyclonal antibodies against phosphotyrosine 701 of STAT1, phosphoserine 15 of p53, rabbit monoclonal antibodies against phosphoserine 473 of Akt and against total Akt (all from Cell Signaling Technology (Danvers, MA); mouse monoclonal antibody against GAPDH (GeneTEX, Irvine, CA); mouse monoclonal antibody against phosphoserine 139 of histone H2AX (Millipore, Billerica, MA); mouse monoclonal antibody against total STAT1 (SM2 clone, Exbio, Vestec, Czech Republic). For immunofluorescence, secondary antibodies anti-mouse IgG antibody conjugated with Cy3 (Jackson ImmunoResearch Laboratories, West Grove, PA) and anti-rabbit IgG antibody Alexa 488 (Invitrogen) were used.

Cell Cultures—Human cancer cell lines HeLa (cervix carcinoma), U2OS (osteosarcoma), and BJ normal human fibroblasts (at population doublings between 30 and 45) were cultured in Dulbecco's modified Eagle's medium supplemented with 10% fetal bovine serum. Cells were kept at 37 °C under 5% CO_2 atmosphere and 95% humidity.

Indirect Immunofluorescence—Cells grown on glass coverslips were fixed by 4% formaldehyde and permeabilized by 0.1% Triton X-100 in two consecutive steps, each for 15 min at room temperature. After washing with PBS, cells were incubates in 10% FBS (diluted in PBS) for 30 min to block unspecific signal. After this step cells were incubated with diluted primary antibodies for 1 h at room temperature and then extensively washed with PBS, 0.1% Tween 20. The incubation with secondary antibodies was performed for 1 h at room temperature. To counterstain nuclei, coverslips were mounted in Mowiol containing 4′,6-diamidino-2-phenylindole (Sigma) and viewed by a fluorescence microscope (Leica DMRXA).

Quantitative Real Time RT-PCR (qRT-PCR)—Total RNA samples were isolated using the RNeasy Mini kit (Qiagen, MD) according to the manufacturer's protocol. First strand cDNA was synthesized from 200 ng of total RNA with random hexamer primers using TaqMan Reverse Transcription Reagents (Applied Biosystems). qRT-PCR was performed in ABI Prism 7300 (Applied Biosystems) using SYBR Green I Master Mix (Applied Biosystems) with the following set of primers: PML (designed to encompass PML exons common to all isoforms), 5′-CCG CAA GAC CAA CAA CAT CTT-3′, 5′-CAG CGG CTT GGA ACA TCC T-3′; actin, 5′-AGG CAC CAG GGC GTG AT-3′, 5′-TCG CCC ACA TAG GAA TCC TT-3′; STAT3, 5′-CTT TGA GAC CGA GGT GTA TCA CC-3′,

5′-GGT CAG CAT GTT GTA CCA CAG G-3′; NEMO, 5′-GGT GGA GCA CCT GAA GAG AT-3′, 5′-CAG AGC CTG GCA TTC CTT AG-3′; IL6, 5′-AGC CCT GAG AAA GGA GAC ATG TA-3′, 5′-TCT GCC AGT GCC TCT TTG C-3′; IRF1, 5′- AAA AGG AGC CAG ATC CCA AGA-3′, 5′-CAT CCG GTA CAC TCG CAC AG-3′; LMP2, 5′-TGT GCA CTC TCT GGT TCA GC-3′, 5′-GGA GGT TCC TCC AGT TCT ATC C-3′; CTNNB1, 5′-CAC AAG CAG AGT GCT GAA GGT G-3′, 5′-GAT TCC TGA GAG TCC AAA GAC AG-3′. The relative quantity of cDNA was estimated by ΔΔCt, and data were normalized to β-actin. Samples were measured in triplicate.

SDS-PAGE and Immunoblotting—Cells were harvested into Laemmli SDS sample lysis buffer, sonicated, and centrifuged at 16,000 × *g* for 10 min. Proteins concentration was estimated by the BCA method (Pierce). 100 mM DTT and 0.01% bromphenol was added to lysates before separation in polyacrylamide gels by SDS-PAGE (9% gels were used). The same protein amount (25 μg for BJ cells, 35 μg for other cell lines; in experiments with cell line comparison, 25 μg of protein was used) was loaded into each well. Proteins were electrotransferred onto a nitrocellulose membrane using wet transfer and detected by specific antibodies combined with horseradish peroxidase-conjugated secondary antibodies (goat anti-rabbit, goat anti-mouse; Bio-Rad). Peroxidase activity was detected by ECL (Pierce). GAPDH was used as a marker of equal loading.

Estimation of PML Promoter Activity—The Bluescript II SK+ plasmid containing the PML promoter fragment (−809/+633) in front of a luciferase reporter gene (PML 1.44-Luc) was a gift from H. de Thé (27). ΔISRE PML-Luc was made by deletion of a 34-bp fragment (−595/−628) containing the ISRE element using adjacent BglII and NcoI restriction sites. To measure luciferase activity, cells were seeded at 6×10^4 per well in 12-well plates 1 day before transfection. 450 ng of PML 1.44-Luc or ΔISRE PML-Luc with 50 ng of vector containing Renilla luciferase under thymidine kinase promoter (pRL-TK) were transfected to each well using FuGENE 6 (Roche Diagnostics). 24 h after transfection cell lysates were harvested according to the manufacturer's protocol. For the dual luciferase assay, luciferase activities were quantified with a luminometer (GloMax®-Multi Microplate Multimode Reader, Turner Biosystems, CA) using the Dual Luciferase Reporter Assay System (Promega, Madison, WI). The values are given as ratios of PML-Luc and pRL-TK luminescence (arbitrary units).

Determination of Cytokines in Cultivation Media—The conditioned medium from cells was collected 24 h after fresh medium was changed, and the numbers of cells per each dish were counted. The concentrations of IL6 and IL1β were estimated by a FACS bead array using FlowCytomix Human Simplex kit (IL6-BMS8213FF, IL1β-BMS8224FF; Bender MedSystems, Wien, Austria) on flow cytometer LSRII (BD Biosciences) according to the manufacturer's protocol.

Estimation of IL6 Biological Activity—To test the effectiveness of IL6 depletion mediated via IL6 antibody (2 μg/ml; goat polyclonal antibody; R&D Systems, Inc., Minneapolis, MN), growth dependence of mouse hybridoma B9 cells on the presence of IL6 was utilized (46). The conditioned media from BJ and HeLa cells incubated for 2 and 4 days, respectively, with IL6 antibody were transferred in a 1:1 dilution with fresh medium to mouse hybridoma B9 cells seeded in triplicate at a density of 25,000 cells/ml on 24-well plates. As positive or negative controls, B9 cells were cultivated with or without the addition of recombinant IL6 (100 pg/ml, Peprotech, NJ), respectively. 50-μl aliquots of B9 cell cultures were removed after 3 days, and cell growth and viability were measured after staining with Hoechst 33258 (Invitrogen) by flow cytometer (BD LSRII, BD Biosciences). To test for antibody toxicity in B9 cells, goat polyclonal antibody against HP1γ (Santa Cruz) was used at a concentration 2 μg/ml.

siRNA-mediated Gene Knockdown—Specific siRNAs were introduced into cells using Lipofectamine™ RNAiMAX (Invitrogen). Non-sense siRNA sequences were used as negative control siRNAs. siRNA was used are shown (non-sense siRNA sequences and siSTAT3 (Ambion); si NEMO (Dharmacon)): siSTAT3, #1 (5′-GGCUGGACAAUAUCAUUGAtt-3′), #2 (5′-GCCUCAAGAUUGACCUAGAtt-3′), #3 (5′-GCACCUUCCUGCUAAGAUUtt-3′); siNEMO, a mix of four siRNAs (no sequence available).

Chromatin Immunoprecipitation—Chromatin immunoprecipitation was performed as described previously (47, 48). Briefly, untreated BJ, HeLa, U2OS, and IL6-treated HeLa (5 ng/ml for 0, 0.5, 1, and 6 h) and U2OS (5 ng/ml for 48 h) were fixed (5×10^6 cells/sample) with 1% formaldehyde for 15 min, and the reaction was stopped with 0.125 M glycine. Cells were lysed in radioimmune precipitation cell lysis buffer (150 mM NaCl, 1% Nonidet P-40, 0.5% deoxycholate, 0.1% SDS, 50 mM Tris, pH 8, 5 mM EDTA) for 10 min on ice. All buffers were supplemented with protease inhibitors (Complete EDTA-free, Roche Diagnostics). Samples were sonicated 33 times for 10 s with 50-s pause at 23% amplitude (Digital Sonifier 450, Branson Ultrasonics Corp.) in an ice bath. Protein concentration was adjusted to 1 mg/ml with radioimmune precipitation assay buffer. A part of each lysate was saved as a control reaction input. Lysates were precleared with protein A/G UltraLink Resin beads (Thermo Scientific) pre-equilibrated in radioimmune precipitation assay buffer. Precleared samples were then incubated with individual antibodies (STAT3, clone C-20, and STAT5; Santa Cruz) overnight at 4 °C followed by incubation with A/G UltraLink Resin beads for 3 h at 4 °C. The same total protein amount was used for each reaction. Immunocomplexes bound on beads were washed twice with radioimmune precipitation assay buffer, four times with LiCl buffer (100 mM Tris-HCl, pH 8.0, 1 mM EDTA, 500 mM LiCl, 0.5% Nonidet P-40, 0.5% sodium deoxycholate), and twice with TE buffer (10 mM Tris-HCl, pH 8.0, 1 mM EDTA). Protein-DNA complexes were eluted with 0.1 M Tris-HCl, pH 8.0, 1 mM EDTA, and 1% SDS, de-cross-linked in the presence of 200 mM NaCl for 5 h at 65 °C, and then treated with proteinase K (20 μg/sample) for 30 min at 45 °C. DNA was extracted with phenol/chloroform, precipitated, and PCR-amplified. The following primers encompassing ISRE element in PML promoter were used: 5-TCAAGGGACTCAGCCAACTGG-3 and 5-GAGGCATGGTGGGCTCCT-3.

Statistical Analysis—Data were expressed as the means ± S.E. Analysis of variance was used for statistical evaluation of the data. p value<0.05 was expressed as significant difference.

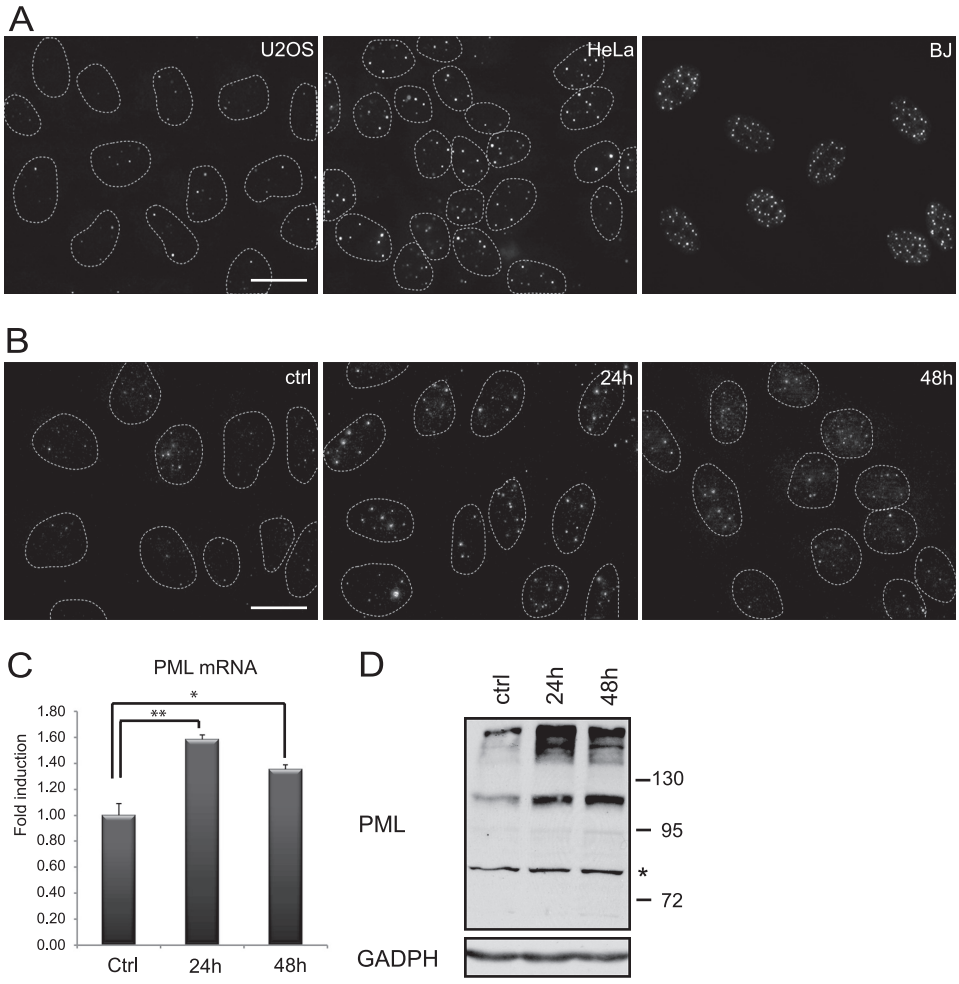

FIGURE 1. **PML and PML NBs are controlled by paracrine signaling.** *A*, immunofluorescence detection of PML NBs in untreated U2OS, HeLa, and BJ cells cultured under standard conditions is shown. Immunofluorescence detection of PML NBs (*B*) and mRNA levels of PML (*C*) were quantified by qRT-PCR in U2OS cells treated 24 and 48 h with conditioned medium from BJ cells (diluted 1:1 with fresh medium). The values represent the average of two independent experiments performed in triplicate and are given as -fold induction of PML mRNA levels relative to control U2OS cells treated with conditioned medium from U2OS cells (diluted 1:1 with fresh medium); *error bars* represent S.E. *Asterisks* (*) and (**) represent *p* values <0.05 and <0.01, respectively. β-Actin was used as a reference gene. *Bar*, 15 μm. *D*, shown is immunoblot detection of PML in U2OS cells after 24 and 48 h of treatment with conditioned medium from BJ cells (diluted 1:1 with fresh medium). Bands with lower mobility than 130 kDa represent unmodified PML isoforms. A nonspecific band is marked by *asterisk*. GAPDH was used as a loading control.

RESULTS

PML NBs, PML Protein, and Transcript Level Are Modulated in a Paracrine Manner—In our previous work we showed that PML gene transcription is regulated in an autocrine manner via cytokine-activated JAK/STAT signaling pathways in human normal and cancer cell lines exposed to various genotoxic compounds (33). To provide further insight into PML gene regulation, we asked whether autocrine/paracrine signaling determines PML levels also in naïve cells grown under unperturbed conditions *in vitro*. First, we selected three human cell types that feature low (U2OS cells, 3–4 PML NBs), medium (HeLa cells, 7–8 PML NBs), and high (BJ cells, PD 35, >30 PML NBs) numbers of PML NBs per nucleus, respectively, when grown under standard conditions (see Fig. 1*A* for PML NBs immunofluorescence staining). Next, we exposed U2OS cells with low content of PML NB to culture medium conditioned by BJ fibroblasts (population doubling 38) for 1 and 2 days and examined the number of PML NBs (Fig. 1*B*). We found an increase of the number of PML NBs in U2OS cells exposed to BJ-conditioned media. This intriguing result was further corroborated by the elevated PML mRNA examined by real time RT-qPCR (Fig. 1*C*) and elevated PML protein determined by immunoblotting (Fig. 1*D*). Both protein and mRNA levels of PML significantly increased in U2OS cells exposed to preconditioned media already after 24 h. These data indicate that the variation of basal PML gene expression seen in various cell types under normal cell culture conditions depends on signaling molecules secreted into culture media, consistent with the hypothesis that autocrine/paracrine mechanisms contribute to regulation of the PML compartment.

Activity of IL6-JAK/STAT Signaling Is Cell Type-dependent and Correlates with PML Expression—As reported previously, PML transcription is regulated by interferon-stimulated JAK/STAT signaling (27, 33). Therefore, we next compared the basal activity of JAK/STAT1/3/5 signaling in U2OS, HeLa, and BJ cells. The level of activated STAT1 (detected as STAT1 phosphorylated at tyrosine 701) was undetectable in all three cell types, yet it was inducible upon IFNγ treatment in all three cell

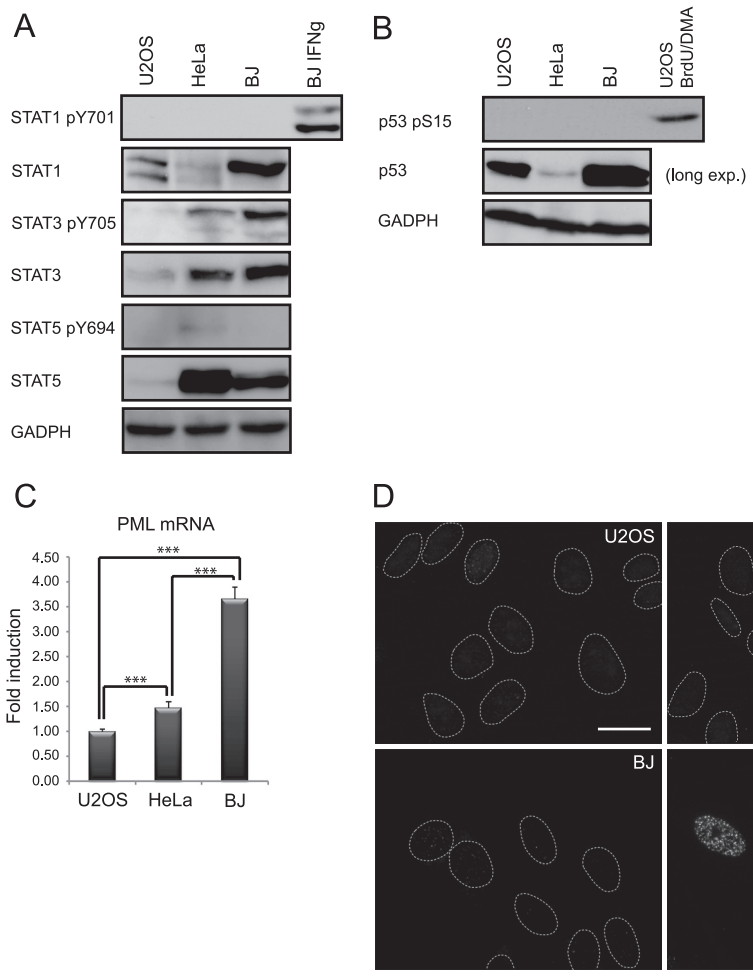

E

[pg/ml/100 000 cells]	U2OS	HeLa	BJ
IL6	<1.2	66.3	371.7
IL1b	0.36	0.57	1.4

FIGURE 2. **Cell type-dependent differences in IL6-STAT3 activity and expression of PML.** *A*, shown is immunoblot detection of total STAT1, STAT3, STAT5, tyrosine 701-phosphorylated STAT1, tyrosine 705-phosphorylated STAT3, and tyrosine 694-phosphorylated STAT5 in U2OS, HeLa, and BJ cells cultivated at standard conditions and BJ exposed to IFNγ (10 IU/ml) for 24 h (included as a positive control of STAT1 activation); GAPDH was used as a loading control. *B*, shown is immunoblot detection of total and p53 serine 15-phosphorylated p53 in U2OS, HeLa, and BJ cultivated at standard conditions; U2OS cell treated with a combination of 10 μM BrdU and 10 μM distamycin A (*BrdU/DMA*) are included as positive control; GAPDH was used as a loading control. *C*, PML mRNA levels were detected by real time qRT-PCR in U2OS, HeLa, and BJ cells cultivated at standard conditions. The values represent the average of two independent experiments performed in triplicate and are given as the -fold induction of PML mRNA levels relative to U2OS; β-catenin (CTNNB1) was used as a reference gene. *Asterisks* (***) represent a p value <0.005. *D*, shown is immunofluorescence detection of endogenous level of γH2AX, a marker of DNA damage response, in U2OS, HeLa, and BJ cells. BJ treated for 4 days with camptothecin (*BJ CPT*) were used as a positive control of γH2AX formation. *Bar*, 15 μm. *E*, shown is an estimation of IL6 and IL1β in medium of U2OS, HeLa, and BJ cells measured by FACS beads.

types (Fig. 2*A*, only BJ is shown). The level of activated STAT5 (detected as STAT5-phosphorylated at tyrosine 694) was also almost undetectable in all three cell lines (Fig. 2*A*). In contrast, basal levels of activated STAT3 (phosphorylated at tyrosine 705) were detectable, highest in BJ, and lowest in U2OS cells (Fig. 2*A*), correlating with PML mRNA levels (Fig. 2*C*) and the number of PML NBs (Fig. 1*A*) in these cell types. Because p53 was reported as a candidate inducer of PML (17) and endogenous stress can activate p53, we assessed the basal level of the activated form of p53 (detected with antibody against p53 phosphorylated at serine 15). Serine 15-phosphorylated p53 was very low-to-undetectable in all three cell types (see Fig. 2*B*) consistent with low levels of endogenous DNA damage assessed by nuclear foci of serine 139-phosphorylated histone H2AX (γH2AX), a surrogate marker of DNA damage signaling (49), in contrast to elevated γH2AX in positive control cells treated by camptothecin (Fig. 2*D*). Interestingly, the concentration of the inductor of the JAK/STAT3 pathway, IL6, when measured in conditioned media of each of the three cell types was highest in BJ, lower in HeLa, and below the detection limit (1.2 pg/ml of assay used; see "Experimental Procedures") in U2OS cells, correlating again with levels of activated STAT3 and the number of PML NBs (Fig. 2*E*). Intriguingly, IL6 levels correlated with IL1β, which was reported to induce IL6 (Ref. 50;

Fig. 2*E*). Thus the positive correlation between expression of PML NBs and levels of secreted IL6 and phosphorylated STAT3 in different cell lines suggested a role of activated IL6-JAK/STAT3 signaling in regulation of basal PML gene expression.

Down-regulation of IL6/STAT3 Signaling Results in Suppression of PML Gene Expression—To test directly whether IL6-JAK/STAT3 signaling is involved in PML gene regulation, siRNA-mediated knockdown of STAT3 was performed in BJ cells, and the effect of such STAT3 depletion on PML expression was estimated. Three independent specific STAT3 siRNAs were tested (see supplemental Fig. 1*A*), and siSTAT3 #2 was selected for further experiments. STAT3 siRNA transfection resulted in almost complete knockdown of STAT3 at mRNA (>90%) and protein levels by 48 h after transfection (Fig. 3, *A* and *B*). This was accompanied by a substantial decrease of numbers of PML NBs (Fig. 3*C*) and PML protein levels (Fig. 3*B*) and suppression of PML mRNA (Fig. 3*D*). To analyze whether the effect of activated STAT3 on PML gene expression is mediated via secreted IL6, BJ-conditioned medium was depleted for IL6 with a specific antibody (51). The effectiveness of IL6 depletion was verified utilizing growth dependence of murine hybridoma B9 cells on human IL6 (46). Both recombinant human IL6 (rhIL6)-supplemented (100 pg/ml) and BJ-conditioned media stimulated proliferation of B9 cells, whereas IL6-depleted BJ-conditioned or rhIL6-negative (control) medium had no effect on growth of B9 cells (supplemental Fig. 1*B*). Substitution of IL6 antibody by a control-unrelated antibody (to HP1) had no effect on the ability of BJ-conditioned media to support growth of B9 cells, thereby excluding any potential cytostatic effects of neutralizing antibodies (supplemental Fig. 1*B*). In BJ cells, the level of activated STAT3 (Fig. 3*E*) as well as PML mRNA (Fig. 3*F*) was decreased after 2 days of cultivation in medium depleted of IL6. A similar effect of IL6 neutralization on PML level was reproduced in HeLa cells (see supplemental Fig. 1*C*). Likewise, HeLa conditioned medium but not its IL6-depleted form supported growth of B9 cells (supplemental Fig. 1*D*). Furthermore, stimulation of HeLa with exogenous rhIL6 (5000 pg/ml) led to increase of activated and total STAT3 levels after 30 min post-stimulation and persisted for at least additional 6 h (Fig. 3*G*). This was accompanied by elevation of PML transcript, the increased level of which was clearly observed after 1 h of IL6 treatment (Fig. 3*H*). Notably, the same treatment of U2OS cells led to a delayed response; the increase of activated and total STAT3 was not observable until 48 h of IL6 exposure (supplemental Fig. 1*E*) followed by elevation of PML mRNA transcript (supplemental Fig. 1*F*). Stimulation of U2OS and HeLa cells with IL6 also increased the number of PML NBs (Fig. 3*I* and data not shown). Altogether, these findings indicate that IL6 and STAT3 are involved in regulation of basal PML gene expression.

PML Gene Induction by IL6-STAT3 Is Regulated via an ISRE Element in the PML Gene Promoter—Previously, the main IFN-JAK/STAT signaling-responsive regulatory site of PML gene promoter has been mapped to a DNA binding element of the PML proximal promoter, ISRE (+605/+618; numbered relative to transcription start; Ref. 27). We found that deletion of the ISRE element within the 1.44-kbp HindIII fragment of the proximal PML gene promoter regions driving a luciferase reporter led to a significant decrease of basal reporter gene activity (Fig. 4*A*). Moreover, depletion of culture medium with the IL6 neutralizing antibody resulted in a decrease of luciferase reporter gene activity driven with promoter containing wild type ISRE element, whereas the reporter gene activity of construct with deleted ISRE element remained unchanged irrespective of IL6 depletion (Fig. 4*B*). On the other hand, the increase of luciferase activity in HeLa cells treated with IL6 was observed after 1 h for wild type ISRE but not for PML promoter with deleted ISRE (Fig. 4*C*). These results further support the role of the ISRE DNA binding site in response to IL6. To prove direct binding of STAT3 to human PML ISRE binding site *in vivo*, we performed chromatin immunoprecipitation (ChIP). As shown in Fig. 4*D*, treatment of HeLa (for 0.5, 1, and 6 h) and U2OS cells (48 h) with IL6 resulted in increased binding of STAT3 to the PML gene regulatory region-containing ISRE sequence in comparison to the non-stimulated state. No increase of STAT5 binding to PML ISRE was observed in HeLa cells treated with IL6 (supplemental Fig. 1, *G* and *H*). Note that STAT3 binding in unperturbed BJ, HeLa, and U2OS correlated with basal levels of PML expression in these cell types.

Comparison of the PML ISRE sequence with the sequence of STAT3 consensus binding site derived from previously identified STAT3 binding sequences on STAT3-regulated genes, as listed in Table 3 in Ehret *et al.* (52), showed a good match (supplemental Fig. 1*I*). Collectively, these findings indicated that PML gene expression is directly regulated by an IL6-activated signaling pathway and STAT3 as transcription activator directly binding to the PML gene promoter.

NFκB Signaling Contributes to IL6-STAT3-mediated PML Expression—Besides the JAK/STAT3 pathway, IL6 stimulates the PI3K/Akt-PKB/ κB kinase/NFκB signaling cascade through activation of JAK kinases (53). Therefore, to investigate the mechanism controlling both PML gene expression and activity of the IL6-STAT3 pathway, we focused on NFκB signaling, as IL6 can regulate its own expression through a positive feedback loop involving NFκB (see *e.g.* Ref. 54). Notably, the levels of the active serine 473-phosphorylated form of Akt kinase were proportional to levels of IL6, activated STAT3, and PML in the three cell types tested (supplemental Fig. 2*A*). RNAi-mediated down-regulation of NEMO, the γ-subunit of IκB kinase required for kinase activity of the complex and activation of NFκB (55), depleted (>90%) NEMO mRNA (see Fig. 5, *A* and *G*, and supplemental Fig. 2*E*) and protein (Fig. 5*B*) in BJ cells 2 days after siRNA transfection. To assess the impact of NEMO knockdown, we estimated mRNA levels of known NFκB targets LMP2 and IRF1, both of which were decreased (supplemental Fig. 2, *B* and *C*). Importantly, we found that the levels of PML mRNA (Fig. 5*C*) and PML protein (Fig. 5*B*) were also decreased in such NEMO-depleted cells. The resulting decrease of PML protein on immunoblot was relatively modest, as expected from the long half-life of PML (>24 h; see Ref. 33). NEMO knockdown was also accompanied by a decrease of total and activated STAT3 (Fig. 5*B*). As IL6 is one of the transcriptional targets of NFκB, we estimated its transcript and protein levels after NEMO depletion. As expected, both IL6 mRNA (Fig. 5*D*) and protein (supplemental Fig. 2*F*) were decreased, consistent with reduction of NFκB activity and explaining the concomitant

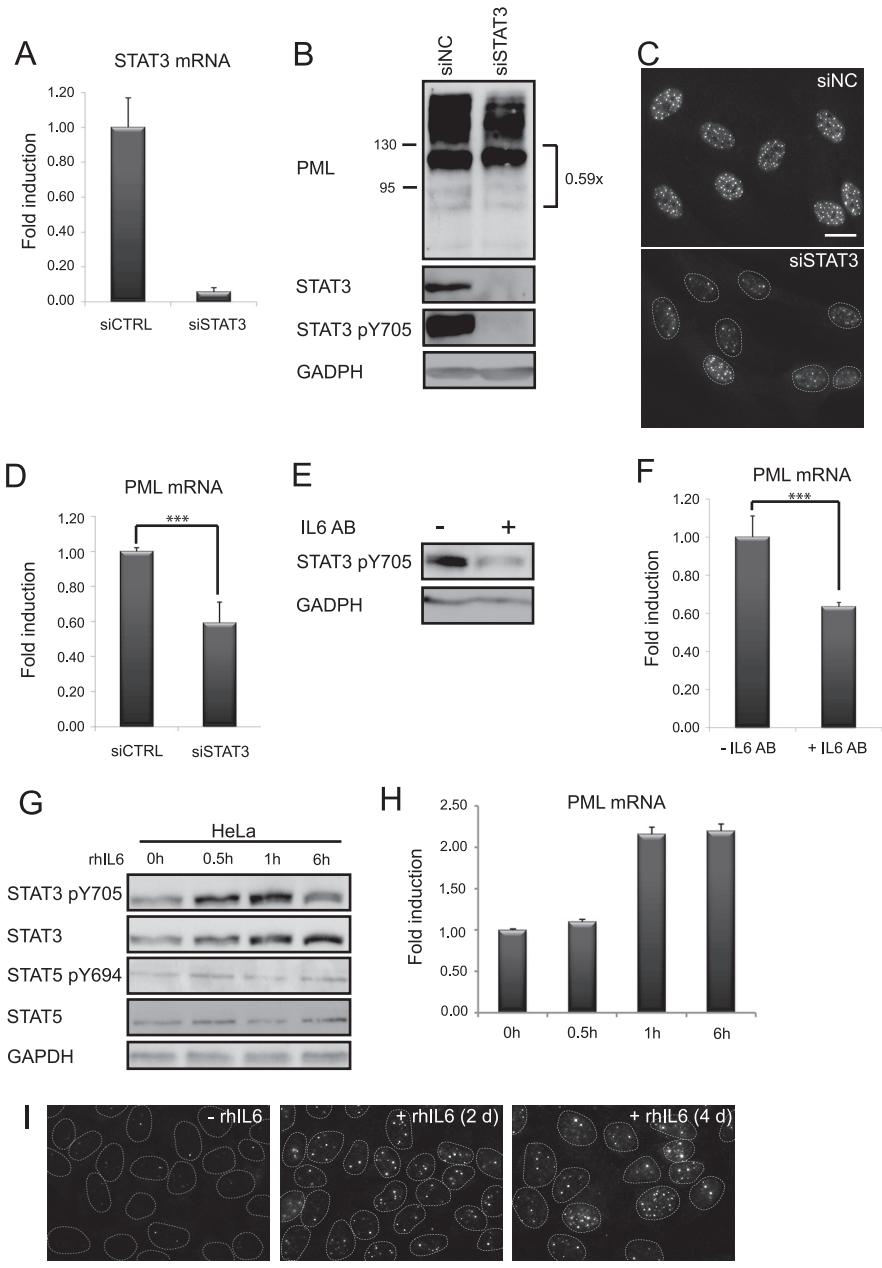

FIGURE 3. **IL6-STAT3 pathway modulates basal PML gene expression.** *A*, shown is efficiency of STAT3 knockdown by specific siRNA detected on mRNA given as the -fold induction of PML mRNA levels relative to BJ transfected with control nonspecific siRNA (β-actin was used as a reference gene). *B*, shown is protein level by immunoblot detection of PML, total, and activated STAT3 in BJ cells 2 days after transfection. Ratios of major unmodified PML isoforms and GAPDH, estimated by densitometric analysis, are given on the *right side of the PML immunoblot*. Shown is down-regulation of PML after STAT3 knockdown, estimated at protein levels by immunofluorescence detection of PML NBs (*C*) and on mRNA levels by qRT-PCR in BJ cells (*D*) 2 days after transfection. The values represent the average of three independent experiments performed in triplicate and are given as -fold induction of PML mRNA levels relative to BJ transfected with control nonspecific siRNA. *Bar*, 15 μm. *E*, shown is down-regulation of STAT3 activity measured as tyrosine 705-phosphorylated STAT3 2 days after depletion of IL6 from medium by IL6 antibody (IL6 AB, 2 μg/ml ; antibody was at all times in the medium) in BJ cells; GAPDH was used as a loading control. *F*, down-regulation of PML mRNA levels was estimated by real time qRT-PCR in BJ cells 2 days after depletion of IL6 from medium by IL6 antibody (*AB*). The values represent the average of three independent experiments performed in triplicate and are given as -fold induction of PML mRNA levels relative to BJ without IL6 depletion; β-actin was used as a reference gene. *Asterisks* (***) represent p values < 0.005. *G*, time-course response of total and activated STAT3 and STAT5 levels was detected by immunoblotting as tyrosine 705-phosphorylated STAT3 and tyrosine 694-phosphorylated STAT5 in HeLa cells treated with IL6 (5000 pg/ml). *H*, time course response of PML mRNA levels in HeLa cells treated with IL6 (5000 pg/ml) estimated by RT-qPCR. The values represent the average of two independent experiments performed in triplicate and are given as -fold induction of PML mRNA levels relative to untreated HeLa cells. *I*, induction of PML protein levels was detected as PML NBs by indirect immunofluorescence in U2OS cells after a 2- and 4-day exposure to recombinant human IL6 (rhIL6; 1000 pg/ml). *Bar*, 15 μm.

decrease of STAT3 activation. The effect of NEMO down-regulation on STAT3 activation and PML mRNA levels was bypassed by the addition of rhIL6 into culture medium during siRNA treatment (see "Experimental Procedures" for details; Fig. 5, *E* and *F*). However, the addition of rhIL6 had no significant effect on mRNA levels of NEMO itself and the known NFκB target IRF1 (Fig. 5, *G* and *H*). Thus, to test whether NFκB signaling acts upstream of or in parallel to IL6-STAT3 signaling to control PML gene expression, the double knockdown of STAT3 and NEMO in BJ cells was performed and analyzed. We

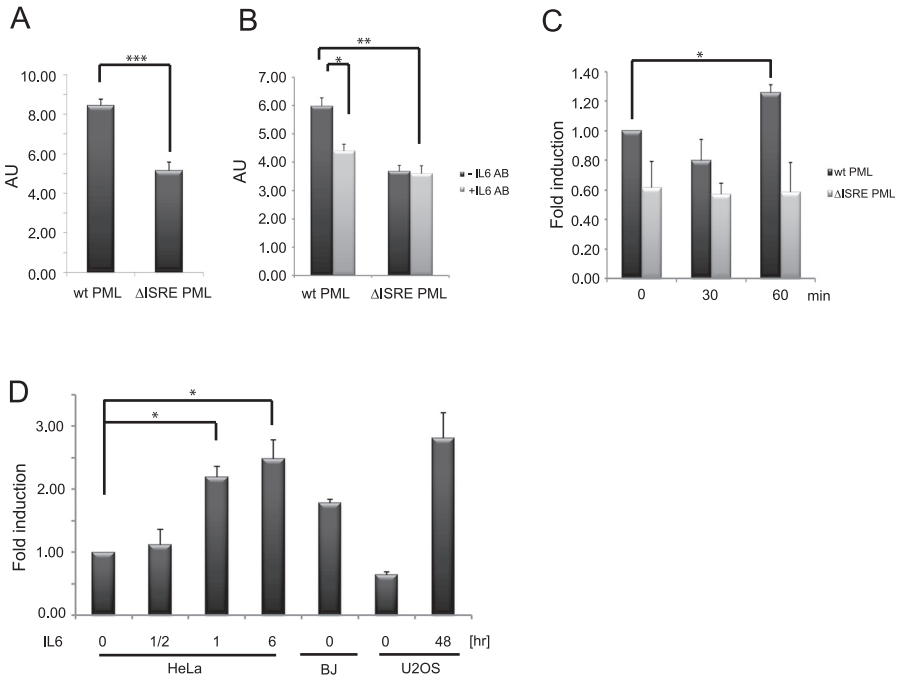

FIGURE 4. **ISRE element of PML promoter gene is involved in basal transcription of PML gene.** Shown is luciferase reporter gene activity under the control of PML gene promoter (−809 bp/+633 bp relative to transcription start) in HeLa cells with an intact or deleted (−595 bp/−628 bp) ISRE DNA binding site (cells were harvested 24 h after transfection; the average values representing three independent experiments are given as arbitrary units (*AU*); *error bars* represent S.E.) (*A*), with or without IL6-depleting antibody (*IL6 AB*; 2 μg/ml; average values representing two independent experiments are given as arbitrary units; *error bars* represent S.E.) (*B*), and with or without IL6 treatment (5000 pg/ml; average values representing two independent experiments are given as -fold induction; *error bars* represent S.E.) (*C*). *Asterisks* (*, **, and ***) represent *p* values <0.05, <0.01, and <0.005, respectively. *D*, shown is evaluation of STAT3 binding to PML ISRE element in untreated BJ, HeLa, and U2OS cells and in HeLa and U2OS cells treated with IL6 for 0.5, 1, and 6 h in HeLa and 48 h in U2OS cells, respectively, quantified with RT-qPCR after chromatin immunoprecipitation. The values quantified with RT-qPCR represent average of two independent experiments performed in triplicate and are expressed as -fold induction relative to HeLa untreated cells.

observed no additive or synergistic effects of the combined STAT3/NEMO knockdown on the number of PML NBs and PML mRNA (Fig. 5, *I* and *J*; for knockdown efficiency, see supplemental Fig. 2, *D* and *E*), indicating that the NFκB pathway acts upstream of the IL6-STAT3 signaling module. We interpret these data as evidence for a role of NFκB signaling in control of a previously unrecognized IL6-dependent autocrine/paracrine loop that maintains activity of the IL6-STAT3 pathway and PML level.

DISCUSSION

PML is a multifunctional protein that belongs to the family of interferon-stimulated genes. Expression of PML is stimulated by interferons of type I and II (9–12), which are produced during cellular responses to viral infection (for review, see Ref. 56) and some genotoxic insults (32, 33). Response of PML to both types of interferons is mediated via transcription factors STAT1 and STAT2 (27), and it is suppressed by inhibitors of histone deacetylases (47). Besides STAT1 and STAT2, overexpression of STAT5a led to elevation of PML NBs (57). In addition to this mode of transcriptional regulation, Shtutman *et al.* (58) showed that overexpression of β-catenin induces PML, indicating that Wnt signaling can participate in regulation of PML gene expression. Furthermore, De Stanchina *et al.* (17) reported that induction of PML during oncogenic Ras signaling depends on intact Arf and p53 and that PML is a direct target of p53. None of these studies, however, has addressed the mechanism of constitutive expression of this important antiviral and tumor suppressor protein. Here we show that the variation of PML content in different cell types propagated under standard cell culture conditions relies on constitutive activity of IL6-dependent signaling and thus is regulated in autocrine/paracrine manner. Analysis of two IL6-dependent signaling pathways, JAK/STAT3 and Akt/NFκB, by experimental manipulation of key components revealed responses of PML transcript and protein levels. Our data also indicate a functional cross-talk of the two pathways through a positive regulatory loop consisting of self-regulated expression of IL6 via Akt/NFκB (see the scheme supplemental Fig. 2*G*).

Although the role of IL6 as a signaling molecule that mobilizes organism-protective systems including innate and acquired immunity is well established, the precise functions of PML and PML NBs in cellular stress responses are not well understood. There is accumulating evidence that PML is involved in response to 1) viral infections and 2) genotoxic stress (for review, see Ref. 59). Importantly, both types of response result in induction of IL6, suggesting a potential physiologically significant link between IL6 signaling and PML.

PML and Viral Infections—Interferons are produced in virus-infected cells and regulate cellular antiviral responses via controlling expression of a large number of interferon-stimulated genes, which then interfere with critical processes of viral replication cycle. Importantly, overexpression of PML can establish resistance to infection by some viruses (such as RNA vesicular stomatitis virus and influenza virus) through prevent-

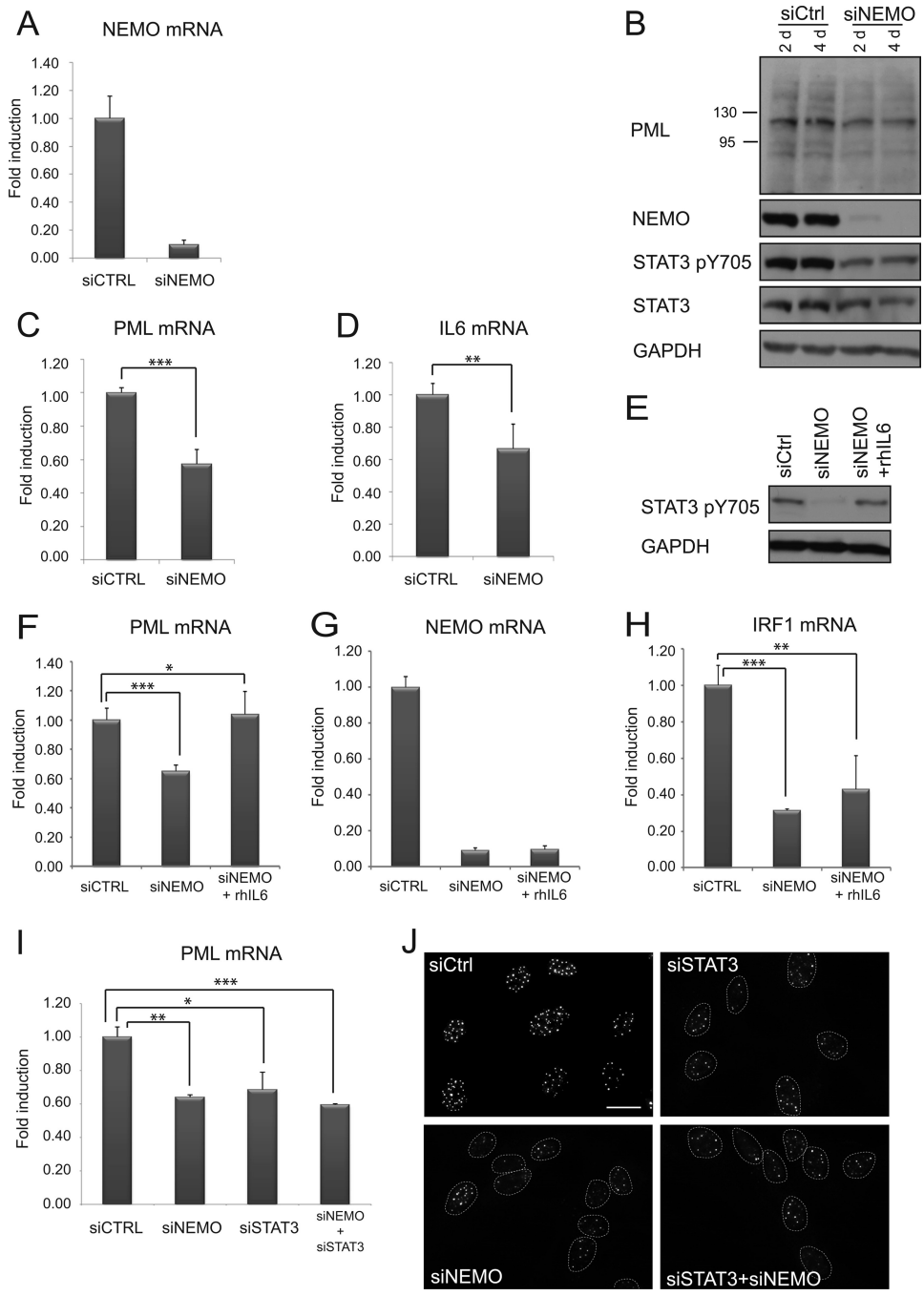

FIGURE 5. **NFκB pathway controls PML expression through regulation of IL6 level.** *A*, shown is efficiency of NEMO knockdown by specific siRNA detected on mRNA level 2 days after transfection in BJ. *B*, down-regulation of PML, NEMO, and the activated and total form of STAT3 in BJ detected on immunoblot 2 and 4 days after transfection of NEMO siRNA; GAPDH was used as loading control. Down-regulation of PML (D) and IL6 mRNA (*D*) levels quantified by qRT-PCR in BJ cells 2 days after NEMO knockdown is shown. The values represent the average of three independent experiments and are given as the -fold induction relative to BJ cells transfected with control nonspecific siRNA; *error bars* represent S.E. β-Actin was used as a reference gene. *E*, shown is immunoblot detection of the STAT3-activated form after NEMO knockdown and NEMO knockdown with the addition of recombinant human IL6 protein (5000 pg/ml) into medium of BJ cells. Shown is down-regulation of PML (*F*), NEMO (*G*), and IRF1 (*H*) mRNA levels 2 days after NEMO knockdown and NEMO knockdown with the addition of recombinant human IL6 protein (5000 pg/ml) quantified by real time qRT-PCR in BJ cells. The values represent the average of two independent experiments and are shown as -fold induction relative to BJ cells transfected with control nonspecific siRNA; *error bars* represent S.E.; β-actin was used as a reference gene. Shown is down-regulation of PML mRNA (*I*) and protein levels detected as PML NBs (*J*) 2 days after NEMO, STAT3, or combined NEMO and STAT3 knockdown by specific siRNAs in BJ cells. The mRNA values represent the average of two independent experiments and are shown as -fold induction relative to BJ cells transfected with control nonspecific siRNA; *error bars* represent S.E. β-Actin was used as a reference gene. *Bar*, 15 μm. *Asterisks* (*, **, and ***) represent *p* value <0.05, <0.01, and <0.005, respectively.

ing their replication by interference with viral mRNA and protein synthesis (60). The role of PML in protection against viral infection is indirectly supported also by the existence of some viruses that developed mechanisms to bypass (or even take advantage of) PML function (for review, *e.g.* see Ref. 61). Remarkably, infection of cells with certain (mainly DNA) viruses including herpes simplex virus type-1 (HSV-1) and human cytomegalovirus (HCMV) results in disruption of PML

NBs (62), which is mediated by virally encoded proteins ICP0 of HSV-1 (63) and IE1 of HCMV (Ref. 64; for review, see Ref. 65), respectively. Both viral proteins ICP0 and IE1 reduce SUMOylation of PML, which is a prerequisite for PML NBs formation (66). A nucleus entering viral capsid proteins can sequester PML before disaggregation (67), and PML NBs disruption is linked to formation of viral DNA replication compartments containing PML liberated from PML NBs (68–71). Moreover, HSV-1 infection is accompanied by proteasome-dependent degradation of PML (72). Importantly, oncogenic viruses, such as hepatitis C virus HCV inactivate the PML tumor-suppressive pathway and thus block activation of p53 (73).

PML and Genotoxic Stress—Intriguingly, the common theme of response to viral infections and DNA damage is dynamic redistribution of PML NBs and associated proteins to sites of viral genomes and DNA damage, respectively (for review, see Ref. 59). The first indirect evidence of PML involvement in response to genotoxic stress came from the findings that NBS1 and MRE11, components of the Mre11-Rad50-NBS1 complex that senses, signals, and partly processes DNA double strand breaks, are present in PML NBs (74, 75). Lately, Carbone *et al.* (34) showed the increase of PML and PML NBs after ionizing irradiation accompanied by delayed but gradual colocalization of PML NBs with sites of persistent DNA breaks. The colocalization of PML NBs with late DNA damage foci was confirmed in other studies utilizing genotoxic drugs as DNA-damaging agents (33, 35) or bacterial toxins (26).[5] As mentioned above, the common denominator of these two types of stresses (viral and genotoxic) is activation of a complex cytokine network including induction and secretion of IL6 (26, 32, 76–78). In our previous work we showed that both JAK/STAT1/2 and JAK/STAT3 signaling is involved in stress-induced PML gene transcription (32, 33). One of the key questions raised by those studies was which other cytokines in addition to interferons induce PML (13). Until now, however, the critical ligand activating the STAT3 pathway remained unidentified due to a wide spectrum of genotoxic stress-induced cytokines.

The IL6-STAT3 Pathway Controls Basal PML Gene Expression—With the goal to identify the mechanism of PML transcription under unperturbed cell culture conditions, we employed three cell types (BJ, HeLa, and U2OS) that differ in constitutive numbers of PML NBs, PML mRNA, and protein levels. Remarkably, medium conditioned with PML NB high content BJ cells induced PML mRNA, protein, and PML NBs in U2OS with low content PML NBs, indicating autocrine/paracrine signaling as a main mode of regulation of PML "basal" transcription. As we observed no differences in endogenous DNA damage response (determined as the activation of p53 and presence of γH2AX/53BP1 foci) or activity in stress signaling (as judged from the T180/Y182 activated form of p38MAPK; data not shown) under our culture conditions, we excluded the effect of activated p53 on PML transcription. However, when analyzing the activity of JAK/STAT1/2, JAK/STAT5, and JAK/STAT3 pathways, we noticed cell type-specific differences in the level of activated STAT3 but not STAT1 and STAT5. Moreover, we found marked cell type-dependent variation in the amount of STAT3-activating ligand IL6 secreted into culture media, which correlated well not only with activated STAT3 but also with numbers of PML NBs, PML protein, and mRNA levels. Importantly, both media supplemented with human recombinant IL6- or BJ cells-conditioned media containing IL6 resulted in induction of PML and PML NBs in U2OS or HeLa cells. In addition, both depletion of IL6 in culture medium with IL6 neutralizing antibody and siRNA-mediated knockdown of STAT3 led to a decrease of STAT3 active form, PML mRNA and PML NBs in BJ cells.

The responsiveness to IL6 can be modulated by the level of expression of its cognate receptor IL6 receptor and other components of this signaling pathway. This is supported by a kinetic study of STAT3 activation in HeLa and U2OS cells by IL6 that was accompanied by a proportional response of STAT3-dependent PML transcription in these two types of cells. Although the response of HeLa cells to exogenous IL6 was fast, as is expected for this type of signaling, there was a significant delay in STAT3 tyrosine 705 phosphorylation and related STAT3 and PML gene induction in U2OS cells. We suggest that the basis for such a difference is the initial "constitutive" level of STAT3 at the time of exogenous IL6 addition, being relatively high in HeLa but low in U2OS cells. Such effect can reflect the existence of positive feedback (see below), which contributes to accumulation of components of the signaling pathway thus progressively amplifying the cell response to an ongoing stimulus.

As shown previously, deletion of PML ISRE element led to a decrease of luciferase reporter gene activity in cells exposed to type I interferons (27). Our findings summarized on Fig. 4, including chromatin immunoprecipitation to prove direct binding of STAT3 to the PML gene regulatory region *in vivo*, indicate that IL6-mediated STAT3 signaling controls PML transcription through the same DNA binding element, which comprises a nucleotide sequence similar to the common consensus binding site of STAT transcription factors (52). In fact, the PML ISRE element resembles STAT3 consensus better than that of STAT1 (79) (see supplemental Fig. 1*E*). Altogether, our data indicate that IL6 controls PML gene expression under unperturbed cell culture conditions via JAK/STAT3 signaling and direct binding of STAT3 to the PML regulatory region.

Role of Akt-NFκB Signaling in IL6-mediated Induction of PML—The activation of IL6 receptor transmits signal to three pathways: (i) JAK/STAT3, (ii) PKB/Akt, and (iii) ras/raf/MAPK. Because IL6 gene expression is directly controlled via NFκB (80), we hypothesized that IL6 transcription and production is under IL6 self-control in a positive feedback loop via activation of the Akt-NFκB pathway. Indeed, the active form of kinase Akt correlated with secreted IL6 in the three cell types tested here, being highest in BJ and undetectable in U2OS. siRNA mediated knockdown of a key component of NFκB activation, the γ-subunit of IκB kinase NEMO, resulted in suppression of IL6 protein and mRNA levels and activated STAT3 and PML mRNA and protein levels. We cannot exclude the possibility that PML transcription is at least in part directly regulated by NFκB, as several putative NFκB binding sites are present in the proximal PML promoter. However, the fact that knockdown of NEMO and down-regulation of NFκB signaling (con-

[5] S. Hubackova, K. Krejcikova, J. Bartek, and Z. Hodny, unpublished results.

firmed with decreased expression of known NFκB targets IRF1 and LMP2; (81, 82) can be bypassed by the addition of recombinant IL6 suggests that NFκB signaling is not acting in parallel but rather upstream of STAT3 signaling via modulation of IL6 production. Indeed, the combined knockdown of NEMO and STAT3 did not result in either additive or synergistic effects, thereby further supporting our conclusion that both modules operate in succession along the same signaling pathway.

The cell type-specific nature of variation in constitutive IL6 signaling and resulting PML expression has not been addressed here except for the observed correlations of the analyzed parameters. This is an interesting question that deserves further research to identify key component(s) of a negative feedback, which sets the basal level of the IL6 signaling circuitry. Whether this putative negative feedback acts on regulation of IL1β signaling (50) as a potential upstream stimulus of IL6 induction under normal conditions should be further investigated.

Conclusion—In this study we demonstrated that interleukin 6 (also called interferon β2) regulates basal PML transcription via JAK/STAT3 and Akt/NFκB signaling, thus broadening the spectrum of cytokines involved in PML gene expression. We anticipate that this mechanism participates in part in PML gene regulation also in scenarios when cells in tissues encounter viral or genotoxic stress, which are accompanied by IL6 induction. This can be the underlying mechanism of elevated PML observed in initial stages of several human tumors (8). Notably, initial but not advanced tumor stages contain senescent cells (38), and there is evidence that all forms of cellular senescence are accompanied by production of IL6 (26, 32, 76–78, 83). The paracrine effects of IL6 can also explain the elevation of PML and PML NBs in tumor stroma and tumor endothelial cells (8). Given the involvement of PML in cellular stress responses, we propose that such paracrine component of PML gene induction is a part of tissue adaptation to local stress, aiming to alarm and prepare the surrounding intact cells to face the challenge of incoming damage to avoid further spreading of injury.

REFERENCES

1. Dellaire, G., and Bazett-Jones, D. P. (2007) Beyond repair foci. Subnuclear domains and the cellular response to DNA damage. *Cell Cycle* **6,** 1864–1872
2. Ruggero, D., Wang, Z. G., and Pandolfi, P. P. (2000) The puzzling multiple lives of PML and its role in the genesis of cancer. *Bioessays* **22,** 827–835
3. Bernardi, R., and Pandolfi, P. P. (2007) Structure, dynamics, and functions of promyelocytic leukaemia nuclear bodies. *Nat. Rev. Mol. Cell Biol.* **8,** 1006–1016
4. de Thé, H., Chomienne, C., Lanotte, M., Degos, L., and Dejean, A. (1990) The t(15;17) translocation of acute promyelocytic leukaemia fuses the retinoic acid receptor α gene to a novel transcribed locus. *Nature* **347,** 558–561
5. Wang, Z. G., Delva, L., Gaboli, M., Rivi, R., Giorgio, M., Cordon-Cardo, C., Grosveld, F., and Pandolfi, P. P. (1998) Role of PML in cell growth and the retinoic acid pathway. *Science* **279,** 1547–1551
6. Gurrieri, C., Capodieci, P., Bernardi, R., Scaglioni, P. P., Nafa, K., Rush, L. J., Verbel, D. A., Cordon-Cardo, C., and Pandolfi, P. P. (2004) Loss of the tumor suppressor PML in human cancers of multiple histologic origins *J. Natl. Cancer Inst.* **96,** 269–279
7. Gambacorta, M., Flenghi, L., Fagioli, M., Pileri, S., Leoncini, L., Bigerna, B., Pacini, R., Tanci, L. N., Pasqualucci, L., Ascani, S., Mencarelli, A., Liso, A., Pelicci, P. G., and Falini, B. (1996) Heterogeneous nuclear expression of the promyelocytic leukemia (PML) protein in normal and neoplastic human tissues. *Am. J. Pathol.* **149,** 2023–2035
8. Koken, M. H., Linares-Cruz, G., Quignon, F., Viron, A., Chelbi-Alix, M. K., Sobczak-Thépot, J., Juhlin, L., Degos, L., Calvo, F., and de Thé, H. (1995) The PML growth-suppressor has an altered expression in human oncogenesis. *Oncogene* **10,** 1315–1324
9. Lavau, C., Marchio, A., Fagioli, M., Jansen, J., Falini, B., Lebon, P., Grosveld, F., Pandolfi, P. P., Pelicci, P. G., and Dejean, A. (1995) The acute promyelocytic leukaemia-associated PML gene is induced by interferon. *Oncogene* **11,** 871–876
10. Korioth, F., Gieffers, C., Maul, G. G., and Frey, J. (1995) Molecular characterization of NDP52, a novel protein of the nuclear domain 10, which is redistributed upon virus infection and interferon treatment. *J. Cell Biol.* **130,** 1–13
11. Der, S. D., Zhou, A., Williams, B. R., and Silverman, R. H. (1998) Identification of genes differentially regulated by interferon α, β, or γ using oligonucleotide arrays. *Proc. Natl. Acad. Sci. U.S.A.* **95,** 15623–15628
12. Chelbi-Alix, M. K., Pelicano, L., Quignon, F., Koken, M. H., Venturini, L., Stadler, M., Pavlovic, J., Degos, L., and de Thé, H. (1995) Induction of the PML protein by interferons in normal and APL cells. *Leukemia* **9,** 2027–2033
13. Bourdeau, V., Baudry, D., and Ferbeyre, G. (2009) PML links aberrant cytokine signaling and oncogenic stress to cellular senescence *Front. Biosci.* **14,** 475–485
14. Krieghoff-Henning, E., and Hofmann, T. G. (2008) Role of nuclear bodies in apoptosis signaling. *Biochim. Biophys. Acta* **1783,** 2185–2194
15. Pearson, M., Carbone, R., Sebastiani, C., Cioce, M., Fagioli, M., Saito, S., Higashimoto, Y., Appella, E., Minucci, S., Pandolfi, P. P., and Pelicci, P. G. (2000) PML regulates p53 acetylation and premature senescence induced by oncogenic Ras. *Nature* **406,** 207–210
16. Louria-Hayon, I., Grossman, T., Sionov, R. V., Alsheich, O., Pandolfi, P. P., and Haupt, Y. (2003) The promyelocytic leukemia protein protects p53 from Mdm2-mediated inhibition and degradation. *J. Biol. Chem.* **278,** 33134–33141
17. de Stanchina, E., Querido, E., Narita, M., Davuluri, R. V., Pandolfi, P. P., Ferbeyre, G., and Lowe, S. W. (2004) PML is a direct p53 target that modulates p53 effector functions. *Mol. Cell* **13,** 523–535
18. Narita, M., Nũnez, S., Heard, E., Narita, M., Lin, A. W., Hearn, S. A., Spector, D. L., Hannon, G. J., and Lowe, S. W. (2003) Rb-mediated heterochromatin formation and silencing of E2F target genes during cellular senescence. *Cell* **113,** 703–716
19. Zhang, R., Poustovoitov, M. V., Ye, X., Santos, H. A., Chen, W., Daganzo, S. M., Erzberger, J. P., Serebriiskii, I. G., Canutescu, A. A., Dunbrack, R. L., Pehrson, J. R., Berger, J. M., Kaufman, P. D., and Adams, P. D. (2005) Formation of MacroH2A-containing senescence-associated heterochromatin foci and senescence driven by ASF1a and HIRA. *Dev. Cell* **8,** 19–30
20. Zhang, R., Chen, W., and Adams, P. D. (2007) Molecular dissection of formation of senescence-associated heterochromatin foci. *Mol. Cell. Biol.* **27,** 2343–2358
21. Ye, X., Zerlanko, B., Zhang, R., Somaiah, N., Lipinski, M., Salomoni, P., and Adams, P. D. (2007) Definition of pRB- and p53-dependent and -independent steps in HIRA/ASF1a-mediated formation of senescence-associated heterochromatin foci. *Mol. Cell. Biol.* **27,** 2452–2465
22. Kosar, M., Bartkova, J., Hubackova, S., Hodny, Z., Lukas, J., and Bartek, J. (2011) Senescence-associated heterochromatin foci are dispensable for cellular senescence, occur in a cell type- and insult-dependent manner and follow expression of p16(ink4a). *Cell Cycle* **10,** 457–468
23. Janderová-Rossmeislová, L., Nováková, Z., Vlasáková, J., Philimonenko, V., Hozák, P., and Hodný, Z. (2007) PML protein association with specific nucleolar structures differs in normal, tumor and senescent human cells. *J. Struct. Biol.* **159,** 56–70
24. Jiang, W. Q., and Ringertz, N. (1997) Altered distribution of the promyelocytic leukemia-associated protein is associated with cellular senescence. *Cell Growth Differ.* **8,** 513–522
25. Ferbeyre, G., de Stanchina, E., Querido, E., Baptiste, N., Prives, C., and Lowe, S. W. (2000) PML is induced by oncogenic ras and promotes premature senescence. *Genes Dev.* **14,** 2015–2027
26. Blazkova, H., Krejcikova, K., Moudry, P., Frisan, T., Hodny, Z., and Bartek,

J. (2010) Bacterial intoxication evokes cellular senescence with persistent DNA damage and cytokine signaling. *J. Cell. Mol. Med.* **14,** 357–367
27. Stadler, M., Chelbi-Alix, M. K., Koken, M. H., Venturini, L., Lee, C., Saïb, A., Quignon, F., Pelicano, L., Guillemin, M. C., and Schindler, C., (1995) Transcriptional induction of the PML growth suppressor gene by interferons is mediated through an ISRE and a GAS element. *Oncogene* **11,** 2565–2573
28. Scaglioni, P. P., Yung, T. M., Cai, L. F., Erdjument-Bromage, H., Kaufman, A. J., Singh, B., Teruya-Feldstein, J., Tempst, P., and Pandolfi, P. P. (2006) A CK2-dependent mechanism for degradation of the PML tumor suppressor. *Cell* **126,** 269–283
29. Coppé, J. P., Desprez, P. Y., Krtolica, A., and Campisi, J. (2010) The senescence-associated secretory phenotype. The dark side of tumor suppression. *Annu. Rev. Pathol.* **5,** 99–118
30. Kuilman, T., and Peeper, D. S. (2009) Senescence-messaging secretome, SMS-ing cellular stress. *Nat. Rev. Cancer* **9,** 81–94
31. Young, A. R., and Narita, M. (2009) SASP reflects senescence. *EMBO Rep.* **10,** 228–230
32. Novakova, Z., Hubackova, S., Kosar, M., Janderova-Rossmeislova, L., Dobrovolna, J., Vasicova, P., Vancurova, M., Horejsi, Z., Hozak, P., Bartek, J., and Hodny, Z. (2010) Cytokine expression and signaling in drug-induced cellular senescence. *Oncogene* **29,** 273–284
33. Hubackova, S., Novakova, Z., Krejcikova, K., Kosar, M., Dobrovolna, J., Duskova, P., Hanzlikova, H., Vancurova, M., Barath, P., Bartek, J., and Hodny, Z. (2010) Regulation of the PML tumor suppressor in drug-induced senescence of human normal and cancer cells by JAK/STAT-mediated signaling. *Cell Cycle* **9,** 3085–3099
34. Carbone, R., Pearson, M., Minucci, S., and Pelicci, P. G. (2002) PML NBs associate with the hMre11 complex and p53 at sites of irradiation induced DNA damage. *Oncogene* **21,** 1633–1640
35. Dellaire, G., Kepkay, R., and Bazett-Jones, D. P. (2009) High resolution imaging of changes in the structure and spatial organization of chromatin, γ-H2A.X, and the MRN complex within etoposide-induced DNA repair foci. *Cell Cycle* **8,** 3750–3769
36. Dellaire, G., and Bazett-Jones, D. P. (2004) PML nuclear bodies: dynamic sensors of DNA damage and cellular stress. *Bioessays* **26,** 963–977
37. Bartkova, J., Horejsí, Z., Koed, K., Krämer, A., Tort, F., Zieger, K., Guldberg, P., Sehested, M., Nesland, J. M., Lukas, C., Ørntoft, T., Lukas, J., and Bartek, J. (2005) DNA damage response as a candidate anti-cancer barrier in early human tumorigenesis. *Nature* **434,** 864–870
38. Bartkova, J., Rezaei, N., Liontos, M., Karakaidos, P., Kletsas, D., Issaeva, N., Vassiliou, L. V., Kolettas, E., Niforou, K., Zoumpourlis, V. C., Takaoka, M., Nakagawa, H., Tort, F., Fugger, K., Johansson, F., Sehested, M., Andersen, C. L., Dyrskjot, L., Ørntoft, T., Lukas, J., Kittas, C., Helleday, T., Halazonetis, T. D., Bartek, J., and Gorgoulis, V. G. (2006) Oncogene-induced senescence is part of the tumorigenesis barrier imposed by DNA damage checkpoints. *Nature* **444,** 633–637
39. Di Micco, R., Fumagalli, M., Cicalese, A., Piccinin, S., Gasparini, P., Luise, C., Schurra, C., Garre', M., Nuciforo, P. G., Bensimon, A., Maestro, R., Pelicci, P. G., and d'Adda di Fagagna, F. (2006) Oncogene-induced senescence is a DNA damage response triggered by DNA hyper-replication. *Nature* **444,** 638–642
40. Gorgoulis, V. G., Vassiliou, L. V., Karakaidos, P., Zacharatos, P., Kotsinas, A., Liloglou, T., Venere, M., Ditullio, R. A., Jr., Kastrinakis, N. G., Levy, B., Kletsas, D., Yoneta, A., Herlyn, M., Kittas, C., and Halazonetis, T. D. (2005) Activation of the DNA damage checkpoint and genomic instability in human precancerous lesions. *Nature* **434,** 907–913
41. Bartek, J., Lukas, J., and Bartkova, J. (2007) DNA damage response as an anti-cancer barrier. Damage threshold and the concept of "conditional haploinsufficiency." *Cell Cycle* **6,** 2344–2347
42. Stuurman, N., de Graaf, A., Floore, A., Josso, A., Humbel, B., de Jong, L., and van Driel, R. (1992) A monoclonal antibody recognizing nuclear matrix-associated nuclear bodies. *J. Cell Sci.* **101,** 773–784
43. Koken, M. H., Puvion-Dutilleul, F., Guillemin, M. C., Viron, A., Linares-Cruz, G., Stuurman, N., de Jong, L., Szostecki, C., Calvo, F., and Chomienne, C. (1994) The t(15;17) translocation alters a nuclear body in a retinoic acid-reversible fashion. *EMBO J.* **13,** 1073–1083
44. Scheller, J., Chalaris, A., Schmidt-Arras, D., and Rose-John, S. (2011) The pro- and anti-inflammatory properties of the cytokine interleukin-6. *Biochim. Biophys. Acta* **1813,** 878–888
45. Heinrich, P. C., Behrmann, I., Haan, S., Hermanns, H. M., Müller-Newen, G., and Schaper, F. (2003) Principles of interleukin (IL)-6-type cytokine signaling and its regulation. *Biochem. J.* **374,** 1–20
46. Aarden, L. A. (1989) Hybridoma growth factor. *Ann. N.Y. Acad. Sci.* **557,** 192–198, discussion 198–199
47. Vlasáková, J., Nováková, Z., Rossmeislová, L., Kahle, M., Hozák, P., and Hodny, Z. (2007) Histone deacetylase inhibitors suppress IFNα-induced up-regulation of promyelocytic leukemia protein. *Blood* **109,** 1373–1380
48. Carey, M., Peterson, C. L., and Smale, S. T. (2008) *Transcriptional Regulation in Eukaryotes: Concepts, Strategies, and Techniques*, 2 Ed., pp. 132–139, Cold Spring Harbor Laboratory Press, Cold Spring Harbor, NY
49. Rogakou, E. P., Pilch, D. R., Orr, A. H., Ivanova, V. S., and Bonner, W. M. (1998) DNA double-stranded breaks induce histone H2AX phosphorylation on serine 139. *J. Biol. Chem.* **273,** 5858–5868
50. Eda, H., Burnette, B. L., Shimada, H., Hope, H. R., and Monahan, J. B. (2011) Interleukin-1β-induced interleukin-6 production in A549 cells is mediated by both phosphatidylinositol 3-kinase and interleukin-1receptor-associated kinase-4. *Cell Biol. Int.* **35,** 355–358
51. Walter, M., Liang, S., Ghosh, S., Hornsby, P. J., and Li, R. (2009) Interleukin 6 secreted from adipose stromal cells promotes migration and invasion of breast cancer cells. *Oncogene* **28,** 2745–2755
52. Ehret, G. B., Reichenbach, P., Schindler, U., Horvath, C. M., Fritz, S., Nabholz, M., and Bucher, P. (2001) DNA binding specificity of different STAT proteins. Comparison of *in vitro* specificity with natural target sites. *J. Biol. Chem.* **276,** 6675–6688
53. Takahashi-Tezuka, M., Hibi, M., Fujitani, Y., Fukada, T., Yamaguchi, T., and Hirano, T. (1997) Tec tyrosine kinase links the cytokine receptors to PI 3-kinase probably through JAK. *Oncogene* **14,** 2273–2282
54. Matsusaka, T., Fujikawa, K., Nishio, Y., Mukaida, N., Matsushima, K., Kishimoto, T., and Akira, S. (1993) Transcription factors NF-IL6 and NF-κB synergistically activate transcription of the inflammatory cytokines, interleukin 6, and interleukin 8. *Proc. Natl. Acad. Sci. U.S.A.* **90,** 10193–10197
55. Tegethoff, S., Behlke, J., and Scheidereit, C. (2003) Tetrameric oligomerization of IκB kinase γ (IKKγ) is obligatory for IKK complex activity and NF-κB activation. *Mol. Cell. Biol.* **23,** 2029–2041
56. Biron, C. A. (1998) Role of early cytokines, including α, and β interferons (IFN-α/β) in innate and adaptive immune responses to viral infections. *Semin. Immunol.* **10,** 383–390
57. Mallette, F. A., Gaumont-Leclerc, M. F., Huot, G., and Ferbeyre, G. (2007) Myc down-regulation as a mechanism to activate the Rb pathway in STAT5A-induced senescence. *J. Biol. Chem.* **282,** 34938–34944
58. Shtutman, M., Zhurinsky, J., Oren, M., Levina, E., and Ben-Ze'ev, A. (2002) PML is a target gene of β-catenin and plakoglobin and coactivates β-catenin-mediated transcription. *Cancer Res.* **62,** 5947–5954
59. Everett, R. D. (2006) Interactions between DNA viruses, ND10 and the DNA damage response. *Cell. Microbiol.* **8,** 365–374
60. Chelbi-Alix, M. K., Quignon, F., Pelicano, L., Koken, M. H., and de Thé, H. (1998) Resistance to virus infection conferred by the interferon-induced promyelocytic leukemia protein. *J. Virol.* **72,** 1043–1051
61. Regad, T., and Chelbi-Alix, M. K. (2001) Role and fate of PML nuclear bodies in response to interferon and viral infections. *Oncogene* **20,** 7274–7286
62. Maul, G. G., Guldner, H. H., and Spivack, J. G. (1993) Modification of discrete nuclear domains induced by herpes simplex virus type 1 immediate early gene 1 product (ICP0) *J. Gen. Virol.* **74,** 2679–2690
63. Everett, R. D., and Maul, G. G. (1994) HSV-1 IE protein Vmw110 causes redistribution of PML. *EMBO J.* **13,** 5062–5069
64. Wilkinson, G. W., Kelly, C., Sinclair, J. H., and Rickards, C. (1998) Disruption of PML-associated nuclear bodies mediated by the human cytomegalovirus major immediate early gene product. *J. Gen. Virol.* **79,** 1233–1245
65. Sternsdorf, T., Grötzinger, T., Jensen, K., and Will, H. (1997) Nuclear dots. Actors on many stages. *Immunobiology* **198,** 307–331
66. Müller, S., and Dejean, A. (1999) Viral immediate-early proteins abrogate the modification by SUMO-1 of PML and Sp100 proteins, correlating with nuclear body disruption. *J. Virol.* **73,** 5137–5143

67. Puvion-Dutilleul, F., Venturini, L., Guillemin, M. C., de Thé, H., and Puvion, E. (1995) Sequestration of PML and Sp100 proteins in an intranuclear viral structure during herpes simplex virus type 1 infection. *Exp. Cell Res.* **221,** 448–461
68. Burkham, J., Coen, D. M., and Weller, S. K. (1998) ND10 protein PML is recruited to herpes simplex virus type 1 prereplicative sites and replication compartments in the presence of viral DNA polymerase. *J. Virol.* **72,** 10100–10107
69. Burkham, J., Coen, D. M., Hwang, C. B., and Weller, S. K. (2001) Interactions of herpes simplex virus type 1 with ND10 and recruitment of PML to replication compartments. *J. Virol.* **75,** 2353–2367
70. Everett, R. D., and Murray, J. (2005) ND10 components relocate to sites associated with herpes simplex virus type 1 nucleoprotein complexes during virus infection. *J. Virol.* **79,** 5078–5089
71. Everett, R. D., Rechter, S., Papior, P., Tavalai, N., Stamminger, T., and Orr, A. (2006) PML contributes to a cellular mechanism of repression of herpes simplex virus type 1 infection that is inactivated by ICP0. *J. Virol.* **80,** 7995–8005
72. Chelbi-Alix, M. K., and de Thé, H. (1999) Herpes virus induced proteasome-dependent degradation of the nuclear body-associated PML and Sp100 proteins. *Oncogene* **18,** 935–941
73. Herzer, K., Weyer, S., Krammer, P. H., Galle, P. R., and Hofmann, T. G. (2005) Hepatitis C virus core protein inhibits tumor suppressor protein promyelocytic leukemia function in human hepatoma cells. *Cancer Res.* **65,** 10830–10837
74. Lombard, D. B., and Guarente, L. (2000) Nijmegen breakage syndrome disease protein and MRE11 at PML nuclear bodies and meiotic telomeres. *Cancer Res.* **60,** 2331–2334
75. Mirzoeva, O. K., and Petrini, J. H. (2001) DNA damage-dependent nuclear dynamics of the Mre11 complex. *Mol. Cell. Biol.* **21,** 281–288
76. Kuilman, T., Michaloglou, C., Vredeveld, L. C., Douma, S., van Doorn, R., Desmet, C. J., Aarden, L. A., Mooi, W. J., and Peeper, D. S. (2008) Oncogene-induced senescence relayed by an interleukin-dependent inflammatory network. *Cell* **133,** 1019–1031
77. Acosta, J. C., O'Loghlen, A., Banito, A., Guijarro, M. V., Augert, A., Raguz, S., Fumagalli, M., Da Costa, M., Brown, C., Popov, N., Takatsu, Y., Melamed, J., d'Adda di Fagagna, F., Bernard, D., Hernando, E., and Gil, J. (2008) Chemokine signaling via the CXCR2 receptor reinforces senescence. *Cell* **133,** 1006–1018
78. Rodier, F., Coppé, J. P., Patil, C. K., Hoeijmakers, W. A., Muñoz, D. P., Raza, S. R., Freund, A., Campeau, E., Davalos, A. R., and Campisi, J. (2009) Persistent DNA damage signaling triggers senescence-associated inflammatory cytokine secretion. *Nat. Cell Biol.* **11,** 973–979
79. Horvath, C. M., Wen, Z., and Darnell, J. E., Jr. (1995) A STAT protein domain that determines DNA sequence recognition suggests a novel DNA-binding domain. *Genes Dev.* **9,** 984–994
80. Libermann, T. A., and Baltimore, D. (1990) Activation of interleukin-6 gene expression through the NF-κB transcription factor. *Mol. Cell. Biol.* **10,** 2327–2334
81. Rein, T., Müller, M., and Zorbas, H. (1994) *In vivo* footprinting of the IRF-1 promoter. Inducible occupation of a GAS element next to a persistent structural alteration of the DNA. *Nucleic Acids Res.* **22,** 3033–3037
82. Wright, K. L., White, L. C., Kelly, A., Beck, S., Trowsdale, J., and Ting, J. P. (1995) Coordinate regulation of the human TAP1 and LMP2 genes from a shared bidirectional promoter. *J. Exp. Med.* **181,** 1459–1471
83. Minamino, T., Yoshida, T., Tateno, K., Miyauchi, H., Zou, Y., Toko, H., and Komuro, I. (2003) Ras induces vascular smooth muscle cell senescence and inflammation in human atherosclerosis. *Circulation* **108,** 2264–2269

Suppl. Fig. 1

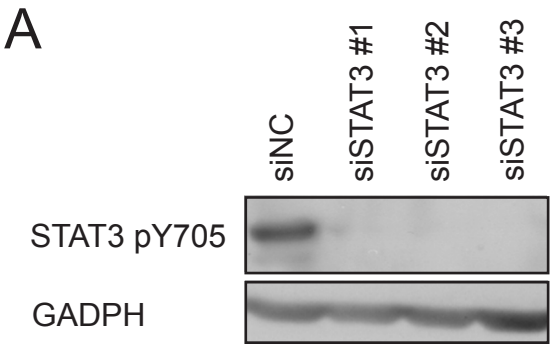

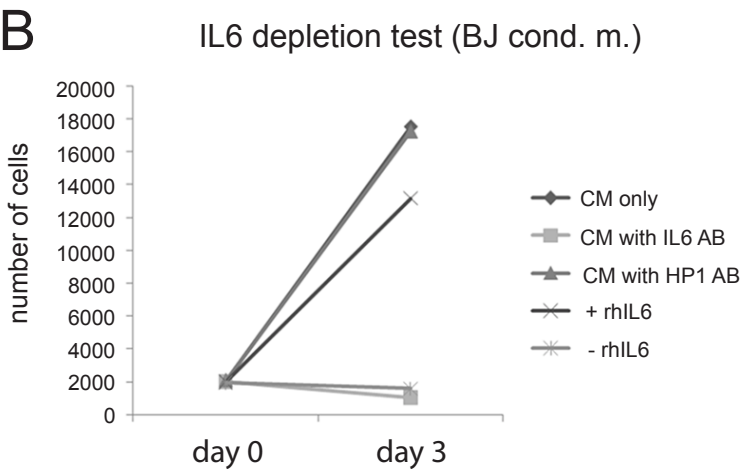

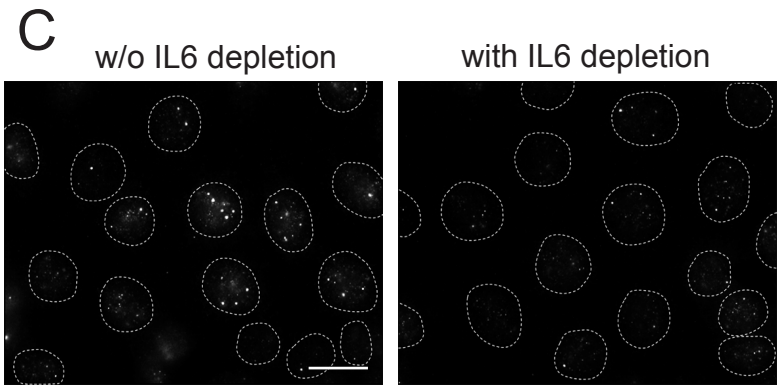

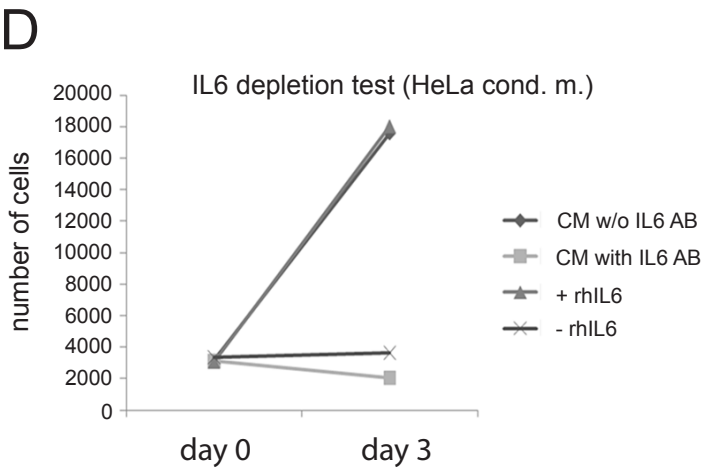

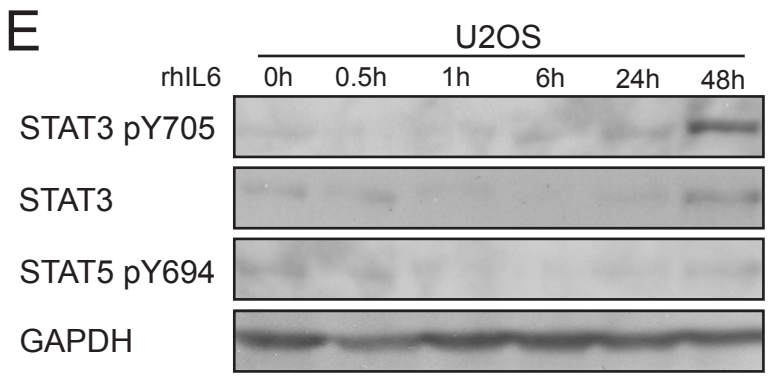

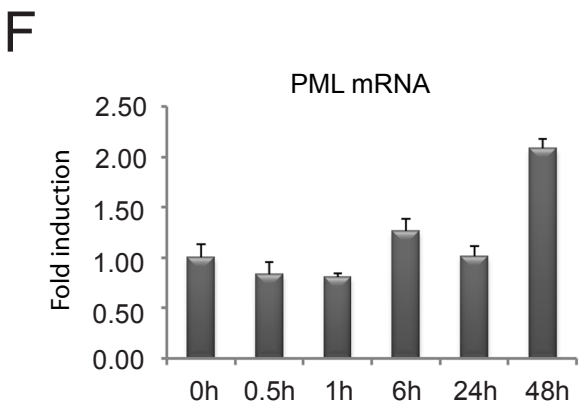

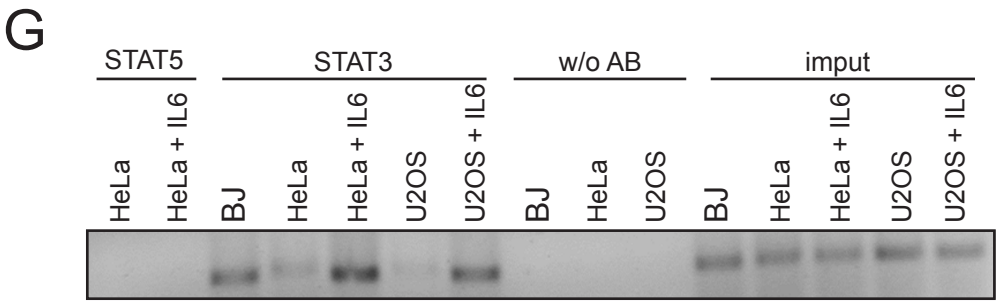

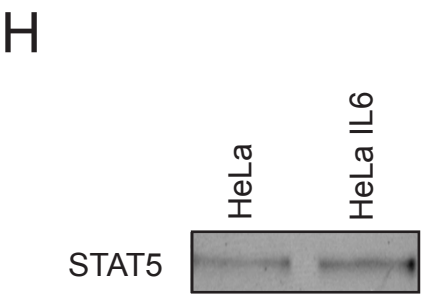

I

PML ISRE element (+595/+623):

AAACCGAGAATCGAAACTAAGCTGGGGT

STAT3 consensus site:

STAT1 consensus site:

Supplementary Figure 1.

(A) Immunoblot detection of STAT3 knock-down efficiency by three independent specific siRNAs. siSTAT3#2 was used in further experiments. GAPDH was used as loading control. (B) IL6-dependent proliferation assay of B9 mouse hybridoma cells. Estimation of IL6 activity in medium conditioned by BJ cells (CM) two days without or with IL6 depletion using IL6 antibody (2 μg/ml). B9 cells treated with rhIL6 (100 pg/ml) were used as a positive control (+rhIL6), B9 without rhIL6 addition were used as a negative control (-rhIL6). Medium conditioned by BJ cells two days with HP1 neutralizing antibody (2 μg/ml) was used as control of antibody cytotoxicity. (C) Down-regulation of PML detected as decrease of PML NBs in HeLa after four days depletion of IL6 from cultivation medium. Bar, 15 μm. (D) B9 proliferation assay as in (B) using medium conditioned by HeLa cells. (E) Immunoblot detection of STAT3 basal and activated level detected as tyrosine 705 phosphorylated STAT3 and tyrosine 694 phosphorylated STAT5 in U2OS cells after IL6 treatment (5000 pg/ml). GAPDH was used as loading control. (F) Elevation of PML gene expression in U2OS cells after treatment with IL6 (5000 pg/ml). The values represent average of two independent experiments performed in triplicates and are shown as a fold induction relative to untreated cells. (G) Evaluation of STAT3 binding to PML ISRE element in untreated BJ, HeLa and U2OS cells and in HeLa treated with IL6 for 6 h and U2OS for 48 h, quantified with gel eletrophoresis after chromatin immunoprecipitation. To exclude unspecific binding to G-Sepharose beads, ChIP in the absence of the antibody was performed (w/o AB). (H) Verification of suitability of STAT5 antibody for ChIP: immunoblot of STAT5 chromatin immunoprecipitate of Hela cells (untreated and treated with IL6 for 6 h) assayed with STAT5 antibody. (I) PML ISRE sequence is compared to STAT3 consensus binding site, which was calculated from data in Table III of reference (1) and to known STAT1/STAT2/IRF9 consensus binding site (2).

1. Ehret, G. B., Reichenbach, P., Schindler, U., Horvath, C. M., Fritz, S., Nabholz, M., and Bucher, P. (2001) *J Biol Chem* **276**, 6675-6688
2. Horvath, C. M., Wen, Z., and Darnell, J. E., Jr. (1995) *Genes Dev* **9**, 984-994

Suppl. Fig. 2

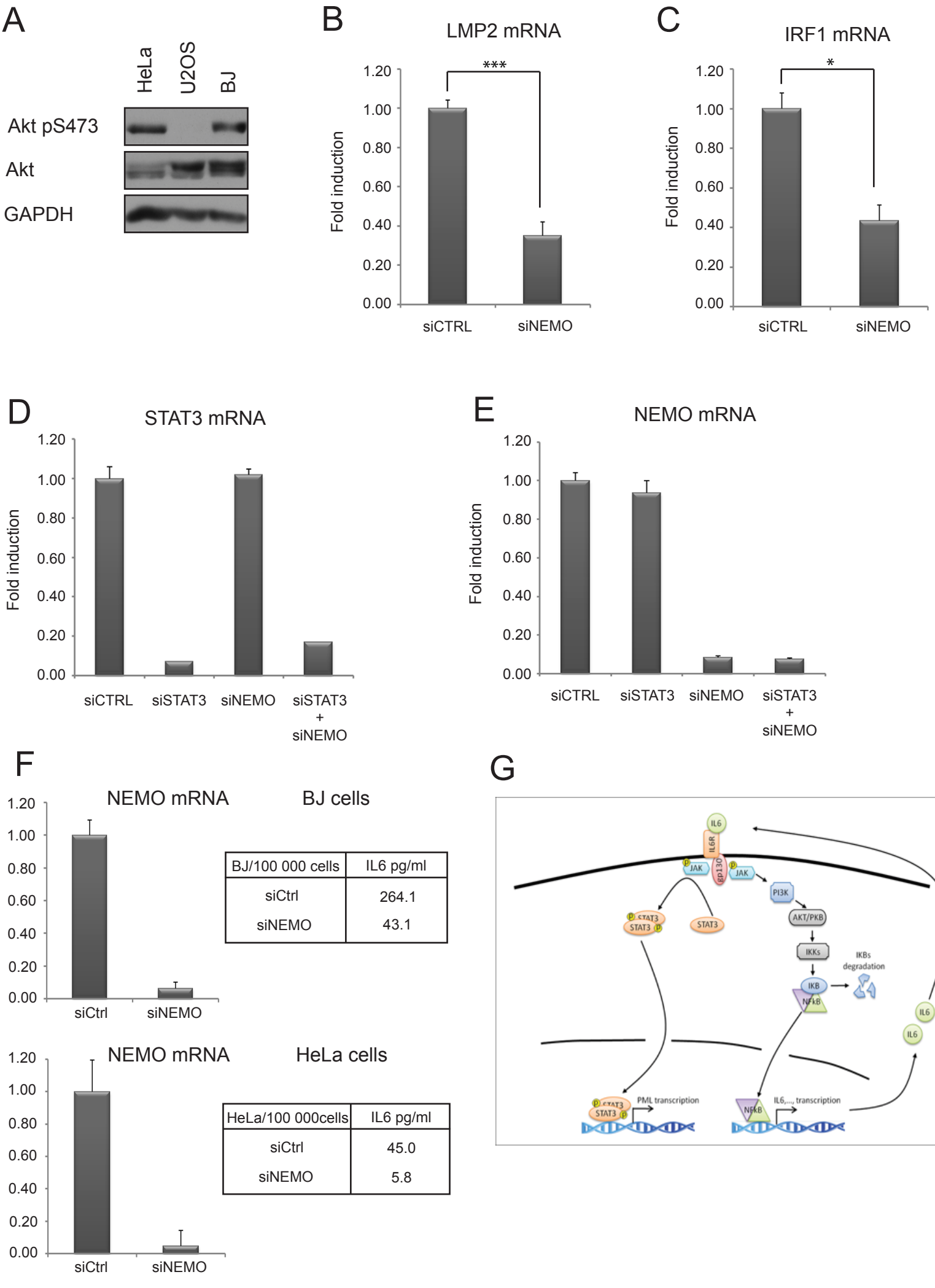
A
HeLa
U2OS
BJ
Akt pS473
Akt
GAPDH
B
LMP2 mRNA
***
Fold induction
1.20
1.00
0.80
0.60
0.40
0.20
0.00
siCTRL
siNEMO
C
IRF1 mRNA
*
Fold induction
1.20
1.00
0.80
0.60
0.40
0.20
0.00
siCTRL
siNEMO
D
STAT3 mRNA
Fold induction
1.20
1.00
0.80
0.60
0.40
0.20
0.00
siCTRL
siSTAT3
siNEMO
siSTAT3 + siNEMO
E
NEMO mRNA
Fold induction
1.20
1.00
0.80
0.60
0.40
0.20
0.00
siCTRL
siSTAT3
siNEMO
siSTAT3 + siNEMO
F
NEMO mRNA
BJ cells
Fold induction
1.20
1.00
0.80
0.60
0.40
0.20
0.00
siCtrl
siNEMO
BJ/100 000 cells
IL6 pg/ml
siCtrl
264.1
siNEMO
43.1
NEMO mRNA
HeLa cells
Fold induction
1.20
1.00
0.80
0.60
0.40
0.20
0.00
siCtrl
siNEMO
HeLa/100 000cells
IL6 pg/ml
siCtrl
45.0
siNEMO
5.8
G
IL6
IL6R
JAK
gp130
JAK
PI3K
AKT/PKB
STAT3
STAT3
IKKs
IKBs degradation
IKB
NFkB
IL6
IL6
PML transcription
IL6,... transcription

Supplementary Figure 2.

(A) Immunoblot detection of total and serine 473 phosphorylated Akt in U2OS, HeLa and BJ cells cultivated at standard conditions; GAPDH was used as loading control. (B) Down-regulation of LMP2 and (C) IRF1 mRNA levels quantified by qRT-PCR in BJ cells two days after NEMO knock-down. The values represent average of two independent experiments and are shown as the fold induction relative to BJ cells transfected with control non-specific siRNA; error bars represent standard error. β-actin was used as a reference gene. Asterisks (*) and (***) represent P-value <0.05 and <0.005, respectively. (D) Efficiency of STAT3 and (E) NEMO knock-down using specific siRNAs detected on mRNA levels by qRT-PCR in BJ cells two days after transfection. The values represent average of two independent experiments and are shown as the fold induction relative to BJ cells transfected with control non-specific siRNA; error bars represent standard error. β-actin was used as a reference gene. (F) Effect of siRNA mediated knock-down of NEMO (siNEMO) in HeLa and BJ cells on NEMO mRNA (left panels) and IL6 protein secreted into cultivation media (table on the right, values are expressed in pg/ml/100 000 cells) in comparison to non-specific siRNA (siNC) estimated 48 h after transfection. The values represent average of two independent experiments and are shown as the fold induction relative to BJ cells transfected with control non-specific siRNA; error bars represent standard error. (G) Model of activation of PML with IL6/STAT3 and NFκB pathway. Binding IL6 to its cognate receptor activates two pathways: i) activated JAK kinase phosphorylates STAT3 to allow its dimerization and translocation to the nucleus where STAT3 activates PML transcription; ii) kinase cascade of PI3K pathway phosphorylates IKK kinase and activate NFκB. NFκB redistributes to the nucleus and activates its target genes including IL6, resulting in activation of IL6 positive feedback loop.

Cell Cycle 10:3, 457-468; February 1, 2011; © 2011 Landes Bioscience

Senescence-associated heterochromatin foci are dispensable for cellular senescence, occur in a cell type- and insult-dependent manner, and follow expression of p16^{ink4a}

Martin Kosar,[1,2] Jirina Bartkova,[2] Sona Hubackova,[1] Zdenek Hodny,[1,*] Jiri Lukas[2] and Jiri Bartek[1,2,*]

[1]Department of Genome Integrity; Institute of Molecular Genetics v.v.i; Academy of Sciences of the Czech Republic; Prague, Czech Republic;
[2]Institute of Cancer Biology and Centre for Genotoxic Stress Research; Danish Cancer Society; Copenhagen, Denmark

Key words: activated Ras oncogene, replication stress, senescence-associated heterochromatin foci, hydroxyurea, etoposide, bacterial toxin, histone 3 trimethylated on lysine 9, DNA damage response

Abbreviations: BrdU, 5-bromo-2'-deoxyuridine; DAPI, 4',6-diamidino-2-phenylindole; DDR, DNA damage response; DOXO, doxorubicin; ET, etoposide; H3K9Me3, histone H3 (tri)methylated at lysine 9; HdCDT, *Haemophilus ducreyi* cytolethal distending toxin; HIRA, histone repressor A; HP1, heterochromatin protein 1; HU, hydroxyurea; pRb, retinoblastoma protein; PML, promyelocytic leukemia protein; SA-β-gal, senescence-associated beta-galactosidase; SAHF, senescence-associated heterochromatin foci

Cellular senescence, an irreversible proliferation arrest evoked by stresses such as oncogene activation, telomere dysfunction or diverse genotoxic insults, has been implicated in tumor suppression and aging. Primary human fibroblasts undergoing oncogene-induced or replicative senescence are known to form senescence-associated heterochromatin foci (SAHF), nuclear DNA domains stained densely by DAPI and enriched for histone modifications including lysine9-trimethylated histone H3. While cellular senescence occurs also in premalignant human lesions, it is unclear how universal SAHF formation is among various cell types, under diverse stresses and whether SAHF occur in vivo. Here, we report that human primary fibroblasts (BJ and MRC-5) and primary keratinocytes undergoing replicative senescence or premature senescence induced by oncogenic H-Ras, diverse chemotherapeutics and bacterial cytolethal distending toxin, show differential capacity to form SAHF. Whereas all tested cell types formed SAHF in response to activated H-Ras, only MRC-5, but not BJ fibroblasts or keratinocytes, formed SAHF under senescence induced by etoposide, doxorubicin, hydroxyurea, bacterial intoxication or telomere attrition. In addition, DAPI-defined SAHF were detected on paraffin sections of Ras-transformed cultured fibroblasts, but not human lesions at various stages of tumorigenesis. Overall, our results indicate that unlike the widely present DNA damage response marker γH2AX, SAHF is not a common feature of cellular senescence. Whereas SAHF formation is shared by diverse cultured cell types under oncogenic stress, SAHF are cell-type-restricted under genotoxin-induced and replicative senescence. Furthermore, while the DNA/DAPI-defined SAHF formation in cultured cells parallels enhanced expression of p16^{ink4a}, such 'prototypic' SAHF are not observed in tissues, including premalignant lesions, irrespective of enhanced p16^{ink4a} and other features of cellular senescence.

Introduction

Cellular senescence is a state of stable cell cycle arrest accompanied by a set of characteristic morphological and physiological features that distinguish senescent cells not only from proliferating cells, but also from arrested quiescent or terminally differentiated cells.[1,2] Such senescence-associated features typically include irreversible proliferation arrest, enlarged cellular morphology, expression of senescence-associated β-galactosidase activity (SA-β-gal),[3] enhanced nuclear heterochromatinization[4] and increased numbers of nuclear PML bodies,[5,6] as well as transcriptional changes and secretion of a spectrum of cytokines, proteases and growth factors, collectively referred to as the 'senescence-associated secretory phenotype'.[7-12] Additional functional markers of senescence reflect the underlying mechanistic basis of the senescent state, in particular constitutive DNA damage signaling.[13-16] Importantly, none of the listed individual features or 'markers' of cellular senescence is sufficiently specific or unique to unequivocally identify senescent cells on its own, and therefore a set of such markers, when expressed concomitantly, is currently applied to define senescence. This set of senescence features is generally regarded as being shared by cells undergoing replicative

*Correspondence to: Jiri Bartek and Zdenek Hodny; Email: jb@cancer.dk and hodny@img.cas.cz
Submitted: 12/30/10; Accepted: 12/30/10
DOI: 10.4161/cc.10.3.14707

senescence, due to telomere shortening towards the end of the cell's life span,[17-19] and the so-called premature senescence, due to more acute stressors such as oxidative stress and other DNA damaging insults[20,21] and activated oncogenes.[22] The efforts to identify markers,[23] and better understand the molecular basis of senescence, are mainly motivated by the important roles played by cellular senescence in both normal physiology and diverse pathologies. Such established and emerging biological roles of cellular senescence encompass suppression of tumorigenesis,[24-26] involvement in degenerative diseases and organismal aging,[2,27,28] responses to various medical treatments,[29] and contribution to tissue repair processes.[30]

Mechanistically, the onset and maintenance of the senescent state involve action of two major tumor suppressive pathways, p53-p21 and p16^{ink4a}-pRb.[31,32] Upstream signals that trigger these pathways commonly include, but may not be exclusively restricted to, persistent activity of the DNA damage response (DDR) machinery,[14,15] orchestrated by the major signaling modules of ATM-Chk2 and ATR-Chk1 kinases.[33] A functional biomarker that is used most often to detect activated DDR is a histone variant H2AX phosphorylated by ATM/ATR on serine 139, commonly known as γH2AX.[34] This nuclear marker is widely detected in cells undergoing diverse modes of senescence,[13-16,35] either as a predominantly focal pattern of γH2AX (reflecting mainly DNA double strand breaks and/or dysfunctional telomeres signaled primarily by activated ATM) or a more even global nuclear pattern of γH2AX (phosphorylated mainly by ATR in response to oxidative or replication stresses, for example). Another mechanistically important aspect of cellular senescence is the formation of chromatin structures called senescence-associated heterochromatin foci (SAHF).[36] These domains of facultative heterochromatin can be detected cytologically as compacted foci of DNA stained by DAPI. Whereas DAPI staining of nuclei of normal human cells is relatively uniform, senescent cells show up to 30–50 punctate DAPI-stained DNA foci.[4] The SAHF are formed by nuclease resistant compaction of chromatin,[4] and each focus apparently represents condensed chromatin of one chromosome.[37] SAHF also feature protein modifications typical of transcriptionally silent heterochromatin, such as lysine 9-trimethylated histone H3 (H3K9Me3).[4] A number of additional proteins are known to contribute to formation and/or maintenance of the SAHF, including histone chaperones HIRA and Asf1,[38] heterochromatin proteins 1 (HP1),[4] and high-mobility group A (HMGA) proteins,[39] histone variant macroH2A,[40] and pRb.[4] The p16^{ink4a}-pRB pathway appears to be required for SAHF formation,[4,38] and functionally SAHF have been implicated in transcriptional silencing of proliferation-promoting genes.[4] Thus, the under-phosphorylated, active pRb initiates chromatin silencing at E2F target genes exemplified by cyclin A,[4] which might then provide nucleation sites for large scale HIRA/ASF1a-mediated heterochromatinization.[41]

Despite the accumulating wealth of information about the formation and composition of SAHF, however, these structures have largely been studied only in a very few strains of cultured fibroblasts, and there is a striking paucity of data on their relevance for a broader spectrum of cell types, occurrence in senescence caused by various stimuli, and whether or not SAHF are applicable to studies in vivo. In this study, we have addressed some of these important open questions about SAHF biology. Specifically, we have examined whether SAHF form in multiple human cell types including primary fibroblasts and epithelial cells, and under conditions that lead to replicative senescence or premature senescence induced by activated Ras oncogene,[22] bacterial intoxication[42] and several genotoxic chemotherapeutics, respectively, all insults known to trigger cellular senescence. Furthermore, we took advantage of available tissues from characterized cohorts of premalignant and malignant human lesions, known to display (or lack) features of cellular senescence, including enhanced accumulation of heterochromatin markers HP1 and H3K9Me3 as well as γH2AX. The results of these analyses, as well as detection of γH2AX and levels of p16^{ink4a} in the diverse experimental settings, are presented below. Overall, our findings reveal unexpected selectivity of SAHF formation with respect to cellular context, challenge the possibility that SAHF might serve as a universal marker of senescence and raise questions about the nature and biological significance of such selectivity.

Results

SAHF formation is common in oncogene-induced senescence. As Ras-induced senescence was the initial scenario employed in the pioneering studies of Narita and Lowe to propose the SAHF concept,[4] we first assessed whether SAHF formation is shared by multiple types of human cells undergoing oncogene-induced senescence. To this end, we utilized a well established model of the oncogenic mutant H-Ras^{V12},[22] expressed in two types of human diploid primary fibroblasts (strains BJ and MRC-5) and primary human keratinocytes, respectively. In time course experiments, lentiviral transduction of H-Ras^{V12} led in all three cell types to widespread cellular senescence by day 12 after transduction, as judged by changes in morphology, enhanced SA-β-Gal staining (**Fig. 1**) and grossly diminished DNA replication indicated by inhibited incorporation of BrdU (**Sup. Table 1**). The formation of SAHF was monitored by DAPI DNA staining combined with immunofluorescence detection of the heterochromatin marker H3K9Me3 and HP1γ (**Fig. 1** and data not shown), features typically associated with SAHF.[4] The first detectable SAHF appeared at day 5 in all three cell types, with the highest percentage of the initially positive cells seen in MRC-5 (**Fig. 2A**). The initial differences in relative proportions of SAHF-positive cells among the three cell types became minimized by day 12, however, when no statistically significant differences in percentages of SAHF-positive cells were found (**Fig. 2A**). Of note, the proportions of SAHF-positive cells did not change during extended periods of cultivation until 250 days after oncogene transduction. Also, both the partial colocalization of DAPI-stained heterochromatin foci with H3K9Me3 (**Fig. 1**), and the observed percentages of SAHF-containing cells were consistent with results of a previous study analyzing Ras-induced senescence in IMR-90 cells, another strain of human diploid fibroblasts.[4]

Altogether, our data extend previous studies and indicate that the ability to form SAHF during oncogene-induced senescence

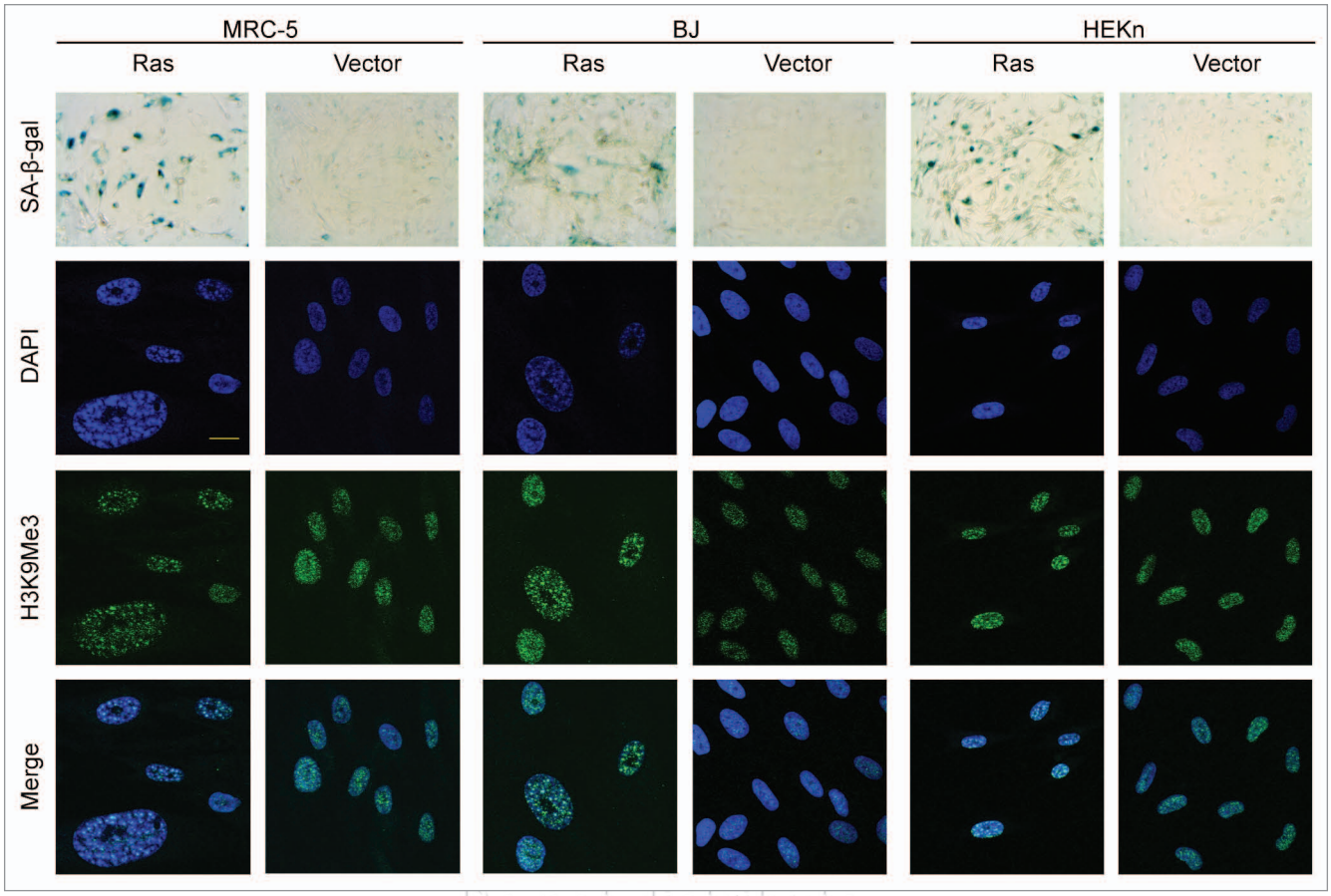

Figure 1. Senescence-associated heterochromatin foci accumulate in oncogene-induced senescence. MRC-5, BJ and HEKn cells containing H-ras^{V12} (Ras) or empty vector were stained for SA-β-gal activity, DAPI and H3K9Me3 at day 12, as indicated. Scale bar, 20 μm.

upon transformation with activated Ras is shared by various cell types, here represented by human fibroblast strains MRC-5 and BJ and primary keratinocytes.

SAHF formation in drug-induced premature senescence is cell type restricted. Several chemotherapeutic drugs including etoposide,[43] hydroxyurea[44] and doxorubicin[45,46] are known to induce premature senescence in human cells. To examine whether SAHF formation is a feature associated with drug-induced senescence, exponentially growing MRC-5, BJ and keratinocyte cultures were continually exposed to commonly used doses of hydroxyurea (HU; 600 μM), etoposide (ET; 10 μM) and doxorubicin (DOXO; 100 ng/ml), respectively, and the cells analyzed at days 2, 5, 8 and 12. Each of the agents induced robust senescence phenotypes by day 12 of drug exposure, in all three cell types (see **Sup. Fig. 1** for SA-β-Gal staining and **Sup. Table 1** for BrdU incorporation). The formation of SAHF was followed by DAPI staining and indirect immunofluorescence as described above for the Ras-induced senescence. In contrast to consistent heterochromatinization and SAHF formation during the Ras oncogene-induced senescence in all three cell types, drug-induced senescence was accompanied by SAHF formation only in MRC-5 cells, but not in BJ or keratinocytes treated with any of the three drugs (**Figs. 2 and 3**). This differential SAHF formation was not altered even when the experiments were prolonged until day 21 of drug exposure (data not shown). Among the three chemotherapeutics used, HU and ET were more potent inducers of SAHF in MRC-5 cells than DOXO, despite the fact that DOXO evoked robust cell cycle arrest and DNA damage, as monitored by BrDU incorporation and γH2AX, respectively (**Sup. Table 1**). Overall, the proportion of SAHF-positive cells among the drug-induced MRC-5 senescent cells was lower (approx. 20%) than in oncogene-induced MRC-5 senescent cells, despite a similar overall senescent phenotype was seen in settings with distinct senescence-inducing stimuli (**Figs. 2 and 3, Sup. Table 1 and Sup. Fig. 1**).

We conclude that unlike the universal occurrence of SAHF in oncogene-induced senescence, SAHF formation is restricted to only one of the three normal human cell types undergoing senescence evoked by several genotoxic drugs.

Restricted SAHF formation in replicative and bacterial toxin-induced senescence. To extend our study to other presently known forms of cellular senescence, we next examined SAHF formation during the most recently described senescence mode induced by bacterial intoxication,[42] and the traditionally most studied replicative senescence. First, we exposed MRC-5, BJ and keratinocytes to cytolethal distending toxin (HdCDT) prepared from *Haemophilus ducreyi*,[47] a scenario that we recently reported to induce cellular senescence in the subpopulations of various human cell types, both normal and cancer-derived, that

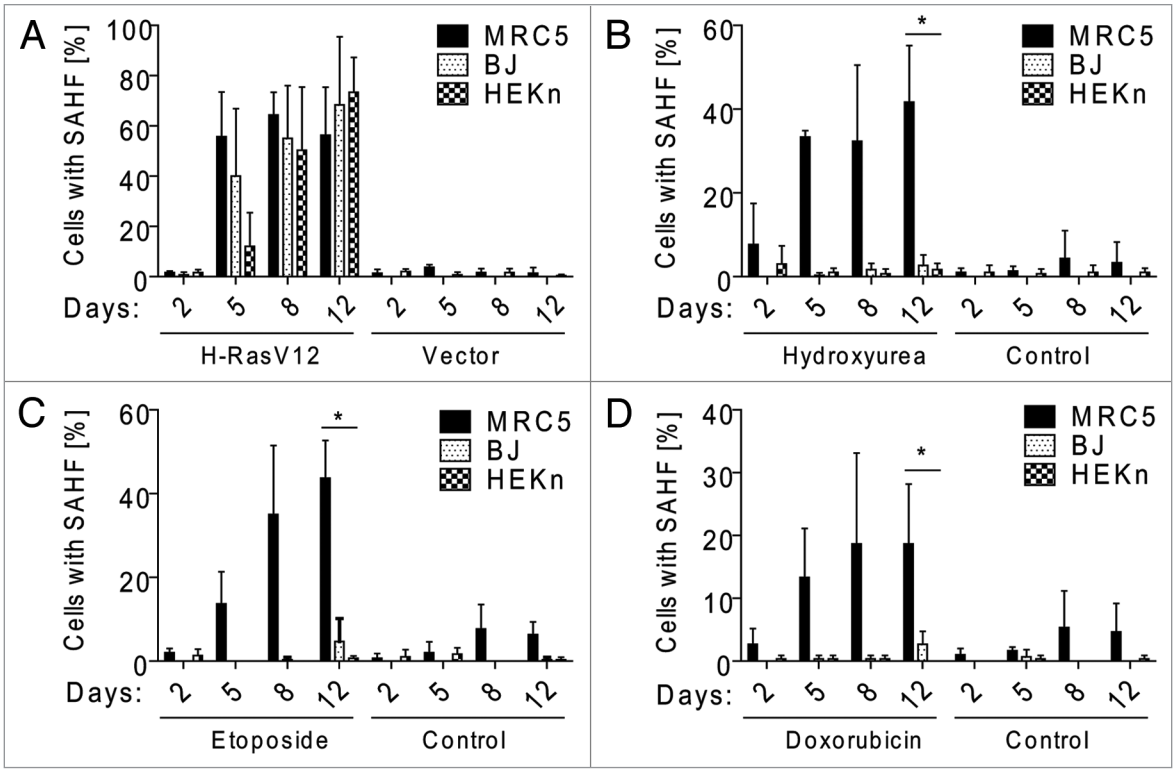

Figure 2. SAHF formation induced by different stimuli is cell-type-restricted. Scoring for percentage of MRC-5, BJ and HEKn cells containing SAHF (based on DAPI nuclear foci staining, see Material and Methods) at day 2, 5, 8 and 12 after transduction with H-ras^{V12} or empty vector (A), exposure to hydroxyurea (B), etoposide (C) or doxorubicin (D). Error bars represent the SD of three separate experiments. *$p < 0.05$ MRC-5 vs. BJ and HEKn, unpaired t-test.

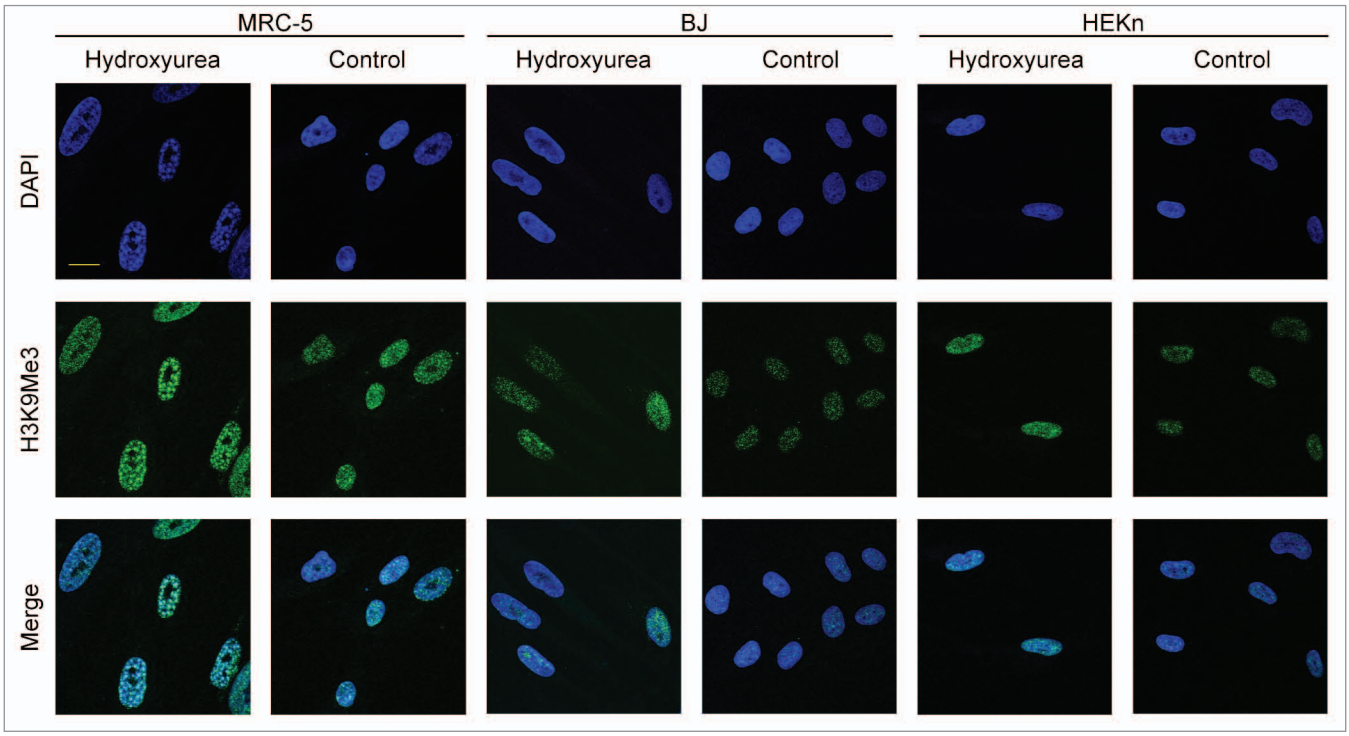

Figure 3. SAHF formation in drug-induced senescence. MRC-5, BJ and HEKn cells were exposed to hydroxyurea, etoposide or doxorubicin and stained for DAPI and H3K9Me at day 12, as indicated. Scale bar, 20 μm.

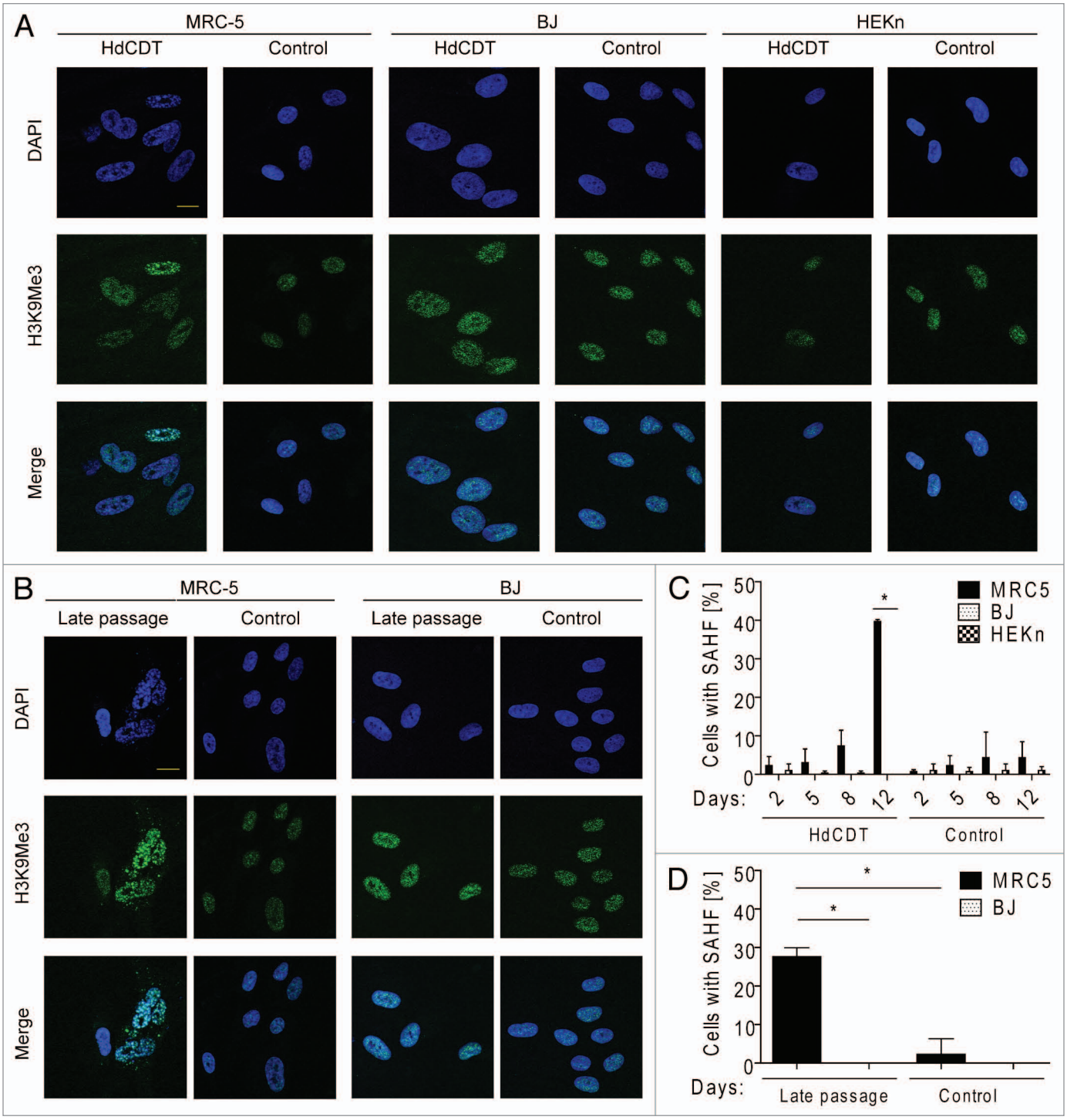

Figure 4. SAHF formation in replicative and bacterial toxin-induced senescence. Comparison of DAPI and H3K9Me staining in control and *Haemophilus ducreyi* CDT (HdCDT) senescent MRC-5, BJ and HEKn cells (A) and young (Control) versus late passages (senescence) of MRC-5 and BJ (B). Scale bars, 20 μm. Percentage of SAHF-positive cells scored in control and HdCDT-senescent MRC-5, BJ and HEKn cells (C) and young and late-passage, senescent MRC-5 and BJ (D). Error bars represent the SD of three separate experiments. *$p < 0.05$ HdCDT vs. control; late passage MRC-5 vs. late passage BJ; and late passage MRC-5 vs. young passage MRC5 and BJ; unpaired t-test.

survive the acute phase of bacterial intoxication.[42] Formation of DAPI-defined SAHF that colocalized with heterochromatin markers H3K9Me3 and HP1γ was observed in HdCDT-exposed senescent MRC-5 cells but not in similarly treated BJ cells and keratinocytes (**Fig. 4A and C** and data not shown), despite all tree cell types showed other features of senescence, including inhibited cell proliferation, enlarged morphology and SA-β-gal staining (**Sup. Fig. 1, Sup. Table 1** and data not shown).

Next, we compared the early-passage 'young' MRC-5 and BJ fibroblasts with their respective 'old' counterparts undergoing replicative senescence, for potential evidence of SAHF formation. As expected, neither fibroblast strain showed SAHF or senescence features at early passage (**Fig. 4B, Sup. Fig. 1 and Sup. Table 1**). Interestingly, the 'old,' senescent populations of MRC-5 cells displayed DAPI-stained DNA/SAHF foci accompanying other features of senescence in contrast to lack of SAHF formation in senescent BJ fibroblasts (**Fig. 4B and D**) despite the fact that both strains shared other recognized features of the senescent phenotype and the fact that the BJ cells reached the senescent state after more passages in vitro compared to MRC-5. To further validate the apparent differential ability to form SAHF under conditions of replicative senescence between MRC-5 and BJ fibroblasts, the latter cells were observed for additional 150 days after reaching their replicative senescence, still with no evidence of SAHF formation (data not shown).

Collectively, these experiments further support the notion that the ability to form SAHF does not necessarily correlate with the senescent state, here documented for replicative and toxin-evoked senescence, and that the MRC-5 cells are more prone to SAHF formation compared to other normal cell types including epithelial cells.

'Classical' DNA/DAPI-defined SAHF are not detected in human tissues and tumors. We have previously reported that cellular senescence observed in clinical specimens of premalignant human lesions is accompanied by enhanced heterochromatinization markers H3K9Me3 and HP1γ that correlated with active DNA damage signaling.[48] On the other hand, to our knowledge the issue of whether these features of senescence are also accompanied by the appearance of the classical DNA/DAPI-defined SAHF in such human specimens has not been investigated so far. To address this important issue, we first asked whether the classical SAHF can be detected on paraffin sections prepared from formalin fixed human fibroblasts undergoing oncogene-induced senescence upon lentiviral transduction of H-Ras^{V12} in vitro, pelleted and processed into tissue blocks in a manner mimicking the procedures routinely used in clinical pathology. As can be seen from the examples of Ras-transformed BJ fibroblasts, immunohistochemical examination of paraffin sections still revealed the DNA/DAPI-defined SAHF in such specimens (**Fig. 5A**), albeit at somewhat lower frequency compared to senescent BJ cells grown and analyzed directly on coverslips (**Fig. 1**). These results indicate that routine tissue processing might reduce, but not completely compromise the ability to detect SAHF on paraffin sections. Next, we used the same immunofluorescence detection technique to investigate a series of sections from formalin-fixed paraffin-embedded tissues of human urinary bladder tumors (n = 19), normal human bladder (n = 5) and colon (n = 16), and a cohort of the previously characterized colorectal adenomas (grade III, n = 38) and colon carcinomas (n = 44), for SAHF formation by DAPI staining and expression of H3K9Me3. In contrast to sections from paraffin embedded Ras-transformed BJ cells, no SAHF formation was observed on tissue sections of normal epithelial tissues, adenomas or carcinomas (**Fig. 5B** and data not shown). The apparent lack of DNA/DAPI-defined SAHF was not accompanied by analogous lack of heterochromatinization, as the variable nuclear expression patterns of H3K9Me3 and HP1γ markers were partly focal and the proteins expressed at higher levels among both adenomas and carcinomas as compared to normal mucosa (**Fig. 5B** and data not shown; reviewed in ref. 48). The apparent discrepancy between adenoma-associated senescence in vivo and the lack of classical DAPI-defined SAHF was further corroborated by analysis of 14 cases of human colorectal adenoma available as frozen tissue. Using frozen tissues allowed us not only to avoid the potential caveat of paraffin blocks, but also to assess senescence by the SA-β-gal assay directly on sections, an approach that is not feasible on archival paraffin sections. Consistent with the data obtained on paraffin sections, no clear evidence of the classical DNA/DAPI-defined SAFH was seen upon examination of these adenoma frozen sections, despite the positive variable and partly even focal, expression pattern of the heterochromatin markers HP1γ, H3K9Me3 and SA-β-gal activity (data not shown and **Sup. Material** reviewed in ref. 48).

Thus, while our data on immunofluorescence patterns of the H3K9Me3 and HP1γ markers in human tissues are consistent with previous reports on generally enhanced heterochromatinization in tumors, the observed heterochromatin domains appear to be distinct from the classical DNA/DAPI-defined SAHF observed in cell culture models undergoing senescence.

SAHF formation correlates with p16^{ink4a} accumulation and with the lack of proliferation. Taken together, the experimental data obtained with cultured senescent cells and the somewhat unexpected results from the analyses of the human tissue specimens raised some conceptually important questions that we decided to address by additional experiments.

First, considering the apparent overall lack of the classical SAHF formation in human tumors in vivo (this study), yet their shared occurrence in all examined cell types undergoing Ras-mediated, oncogene-induced senescence in vitro (this study and reviewed in ref. 4) and the proposed role of SAHF in silencing proliferation-associated genes such as cyclin A,[4] we asked whether classical SAHF structures might occur in human cultured proliferating cancer cell lines, known to harbor activated Ras and/or other potent oncogenes. As the cancer cell lines grow in vitro, where SAHF are induced by oncogenes and accompany senescence, SAHF formation/persistence in proliferating tumor cells might indicate some tumor-associated bypass of the SAHF-heterochromatinization barrier initially activated as part of the senescence program. To address this issue, we examined a panel of human carcinoma-derived cell lines, including T24, UMSCC-2, HN-5, HCT116, as well as the pre-malignant Hacat cells for SAHF formation. While T24 is a prototypic cancer cell line derived from a tumor harboring activated H-Ras oncogene, HCT116 is a colon cancer cell line matching our clinical colon carcinoma series, and the remaining three cell lines are derived from squamous carcinomas/keratinocytes to match our normal epithelial type examined above. As documented by the examples of fluorescence images (**Sup. Fig. 2**) and the summary of the data (**Sup. Table 2**), the individual cell lines showed pronounced differences in levels of H3K9Me3 and HP1γ, but no evidence of the DNA/DAPI-positive SAHF. These results support the

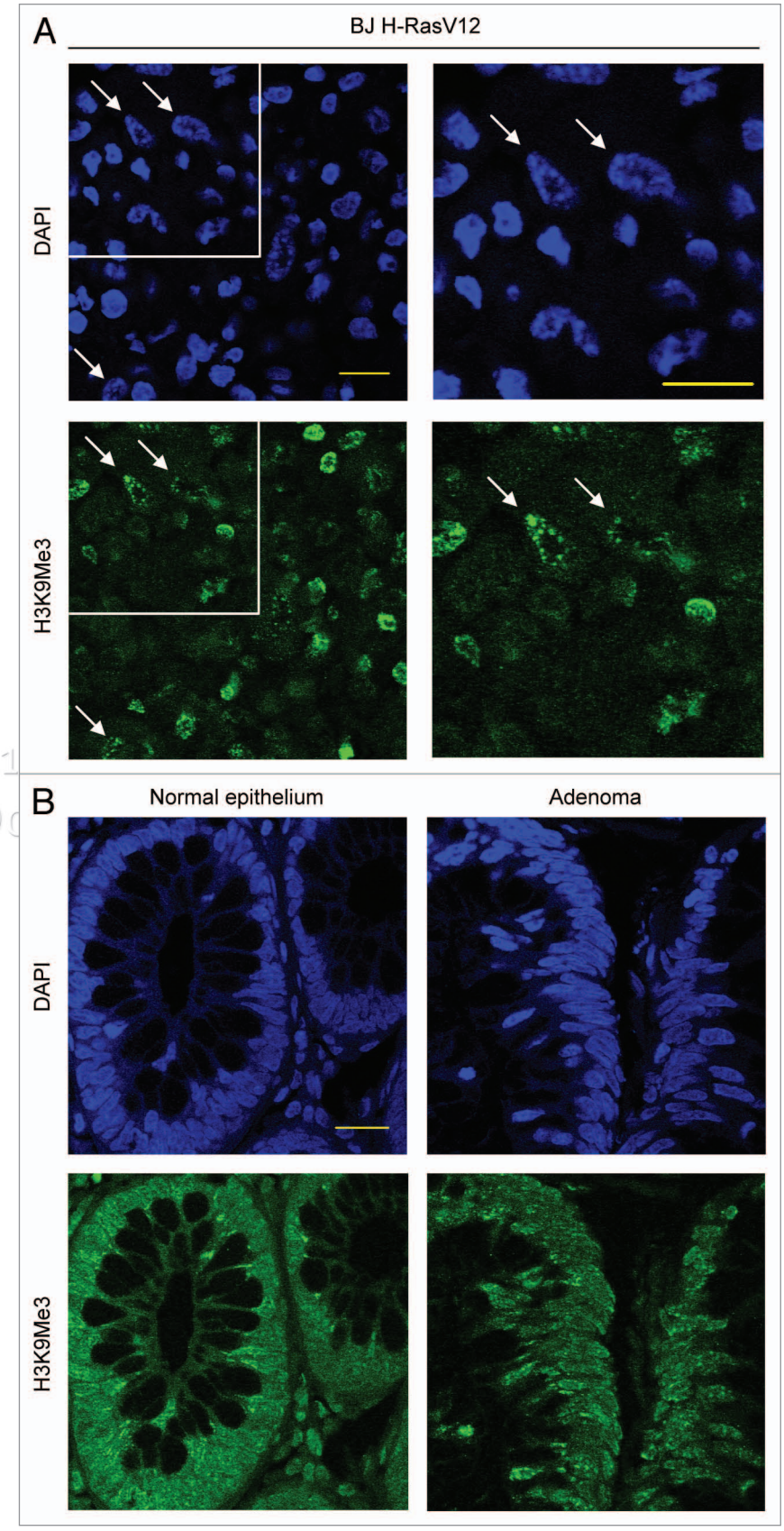

Figure 5. Analysis of SAHF on paraffin sections. (A) Paraffin sections of formalin-fixed pellets of senescent BJ cells with H-ras^{V12} expression: note a subset of cells with SAHF detectable both on DAPI and H3K9Me3 staining. (B) DAPI staining and H3K9Me3 immunohistochemistry on formalin-fixed, paraffin tissue section of normal human colon and grade III colon adenoma: While there are no typical DAPI-positive focal SAHF, the heterochromatin marker H3K9Me3 is positive, and shows some focal nuclear staining in a fraction of the adenoma cells. Scale bars, 20 μm.

conclusion based on the analysis of tumor sections (see above and reviewed in ref. 48), that the presence of elevated heterochromatin markers such as H3K9Me3 and HP1γ (even when forming distinct nuclear foci, see **Sup. Fig. 2**) is compatible with cancer cell proliferation. Furthermore, the data also show that unlike senescent, arrested cells, the proliferating cancer cells do not form the classical DNA/DAPI-defined SAHF, which are apparently distinct from the H3K9Me3/HP1γ-rich heterochromatin domains that do not necessarily reflect silencing of proliferation genes such as cyclin A, a protein highly expressed in all cell lines of our panel (data not shown).

The second, and arguably even more important question, is what molecular mechanistic features might dictate whether or not the classical DAPI/heterochromatin SAHF will form in distinct cell types under otherwise similar conditions and undergoing cellular senescence triggered by various stimuli. Given the distinct propensity to form SAHF among our three models of normal human cells, even under senescence conditions that share the features of inhibited proliferation, morphological changes, SA-β-gal activity and constitutive DNA damage signaling, we argued that the observed differences might reflect variable levels of the p16^{ink4a} CDK inhibitor, and hence the activation of the pRb pathway, whose role in SAHF formation has been documented.[4,38] Indeed, biochemical examination of p16^{ink4a} protein abundance in the two fibroblast strains, MRC-5 and BJ undergoing senescence induced by each of the six stimuli used in our present study, showed a perfect correlation between the observed SAHF formation and the enhanced level of p16^{ink4a} (**Fig. 6**). Specifically, in cell extracts of senescent BJ cells, robust induction of p16^{ink4a} was only apparent under Ras-induced senescence, the only condition associated with the occurrence of classical DNA/DAPI-defined SAHF in these cells. This contrasted with virtually undetectable levels of

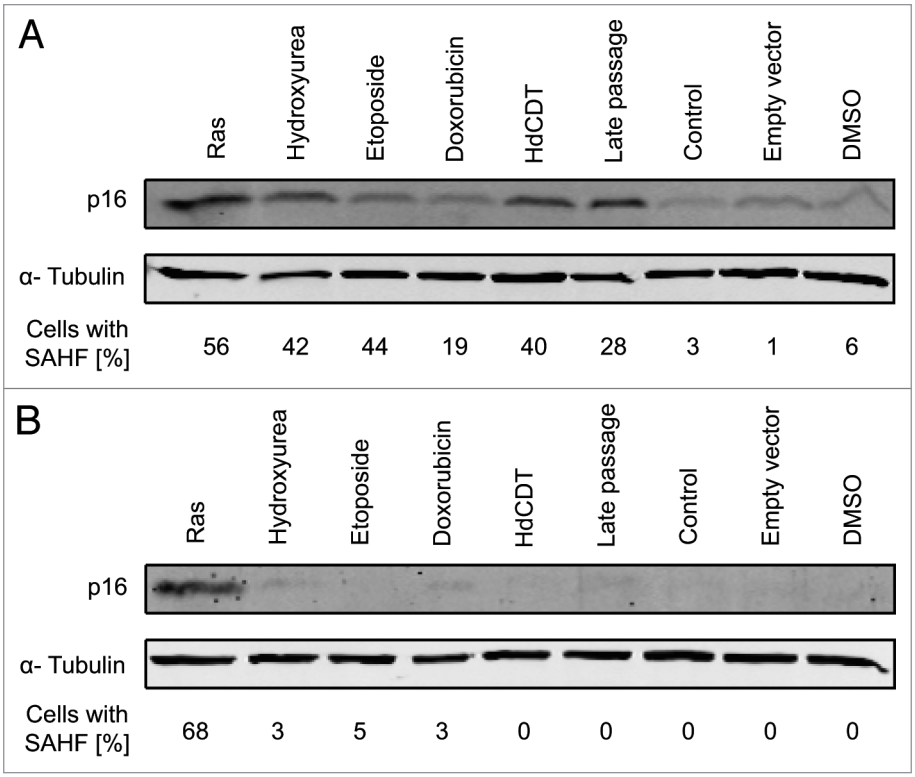

Figure 6. p16^{ink4a} levels correlate with SAHF formation. Abundance of p16^{ink4a} assayed by immunoblotting in cell extracts of MRC-5 (A) and BJ (B) fibroblasts at senescence (day 12) induced by activated Ras oncogene (Ras), hydroxyurea, etoposide, doxorubicin, HdCDT and exhaustive passaging (late passage) in comparison to a set of appropriate controls: empty vector for Ras; young (Control) and vehicle (DMSO) as counterparts for the other senescence stimuli. Percentage of SAHF-positive cells for the particular experiment is shown under each immunoblot.

p16^{ink4a} in BJ cells senescent in response to hydroxyurea, etoposide, doxorubicin, bacterial intoxication or replicative exhaustion (**Fig. 6B**). In contrast to BJ cells, and consistent with the degree of SAHF formation, extracts of MRC-5 cells undergoing senescence showed increased p16^{ink4a} in all six scenarios, albeit to different levels. Notably, the highest and lowest abundance of p16^{ink4a} were found in MRC-5 senescent after Ras and doxorubicin exposure, respectively (**Fig. 6A**). These results, as well as the intermediate levels found in the other four senescent scenarios, corresponded well with the relative proportions of cells featuring DNA/DAPI-defined SAHF among the total senescent cell population. These results are consistent with the proposed causal role of the p16^{ink4a}-pRb pathway in SAHF formation, and their significance is further discussed below.

Discussion

The major contribution of our present study of heterochromatin formation during cellular senescence is the systematic comparative analysis of various types of normal human cells exposed to multiple senescence-inducing stimuli, complemented by analysis of human tissues and tumors. As discussed below, we believe that our study provides new data relevant for several senescence-related aspects of human biology and pathology such as aging, barrier to tumorigenesis and response to chemotherapy. The key issues raised by our present findings are the pronounced variation of SAHF formation in a cell type- and senescence stimulus-dependent manner, an outstanding link of SAHF formation with oncogene-induced senescence, the fact that SAHF formation seems dispensable for multiple forms of cellular senescence, the close correlation of SAHF formation with enhanced expression of p16^{ink4a}, the limitations of SAHF as a potential marker of senescence in vivo, as well as the implications of our findings for the concept of heterochromatinization during cancer development and its relevance for therapy. Below, we discuss some of these conceptually important issues in the light of current mechanistic understanding of cellular senescence, including SAHF formation and their emerging significance for biomedicine.

First, our data strongly indicate that SAHF formation is not a universal component of the senescence program and, in fact, appears to be dispensable for multiple modes of cellular senescence, in various cell types. On one hand, we confirm and extend the findings[4,38-40] that some strains of human fibroblasts, here represented by MRC-5 cells, form SAHF during oncogene-induced as well as replicative senescence. More importantly, we show that under senescence induced by most stimuli, including several chemotherapeutic drugs, bacterial intoxication and replicative senescence, SAHF are absent in two of the three cell types used here, the BJ fibroblasts and normal keratinocytes. The latter cells are a mixed population of keratinocytes pooled from several donors, thereby excluding that any rare individual genetic variation or clonal selection events might account for the observed lack of 'classical' SAHF. While it is understandable that most studies on heterochromatinization to date focused on the mechanistic aspects of SAHF formation, such as the involvement of the pRb pathway, histone chaperones, chromatin modifications and remodeling and the impact of SAHF on transcriptional control of cell cycle-promoting genes,[4,37-40,49] these analyses mainly dealt with oncogene-induced senescence and are not sufficiently representative of cellular senescence in its multiple forms. We believe it is equally important to consider a wider spectrum of cellular models and place more emphasis on studies of epithelial cells, represented here by normal human keratinocytes. So far the cellular model predominantly used in the senescence field has been fibroblasts. While useful as a model, the biased focus on fibroblasts is not proportional to their significance in major human pathologies such as cancer, which targets most frequently epithelial cells. Apart from the conceptual significance of the grossly variable SAHF response among diverse

cell types, a more 'translational' implication of our present work is that SAFH may not represent a reliable common marker to identify cells undergoing senescence. This notion is further supported by our analyses of human tissues, suggesting that identification of senescent cells in situ through the DAPI-defined SAFH is not feasible.

Further to the potentially usable general markers of senescence, the mechanism that appears to be shared by all major types of senescence is the constitutive DNA damage signaling, often documented by the positivity of γH2AX.[13-16,48,50-52] While analysis of DDR was not a major focus of our present study, we did find elevated γH2AX in all three cell types, and under senescence induced by all six stimuli studied here, an observation that further supports the common involvement of DDR signaling and checkpoints in cellular senescence. Notably, we and others have documented that γH2AX and other functional markers of activated DDR can conveniently be assessed on tissue sections.[13,48,53-55] Although active DDR signaling per se obviously does not uniquely identify senescent cells, we believe that an appropriate combination of γH2AX with some additional cytochemically or histochemically detectable senescence feature(s) may provide a robust tool for assessment of senescence in vivo in the near future.

Another important aspect of our study is the close correlation of the ability to form SAHF and the increased level of $p16^{ink4a}$, a CDK inhibitor whose involvement in cellular senescence and also SAHF formation has been widely studied.[4,22,32,40,56-60] Our present findings are consistent with the proposed causal role of $p16^{ink4a}$ in SAHF formation,[4] and with the fact that ectopic overexpression of $p16^{ink4a}$ can induce SAHF formation in certain cellular context.[4] Also, based on immunohistochemical analysis of human tissues, high expression of $p16^{ink4a}$ has been proposed to serve as a marker to identify senescent cells in the skin of old individuals.[61] On the other hand, it is evident that elevated $p16^{ink4a}$ per se may be dispensable for induction of senescence, as documented by only partial correlation of heterochromatinization and $p16^{ink4a}$ levels in human premalignant lesions,[48] and here for example for the BJ fibroblasts senescent in response to various chemotherapeutics or bacterial intoxication. In fact, low levels of $p16^{ink4a}$ were reported for BJ cells undergoing replicative senescence.[32] It appears that in cells with low expression of $p16^{ink4a}$, senescence induction relies more on the p53-p21 axis, and possibly other mechanisms, likely including also DNA damage checkpoints, only some of which require p53. At the same time, the $p16^{ink4a}$-mediated senescence-associated proliferation arrest appears to be more robust and irreversible even upon depletion of p53, as compared to the possibly partially reversible arrest under $p16^{ink4a}$-low conditions, at least in replicative senescence.[32] One striking observation, emerging from earlier studies and corroborated by our present findings, is the robust induction of $p16^{ink4a}$ in response to oncogenic stress, even in cells such as BJ that do not respond by $p16^{ink4a}$ induction when undergoing senescence triggered by non-oncogenic stimuli. The overall picture emerging is that $p16^{ink4a}$, albeit not essential for every mode of cellular senescence, is critical for the formation of SAHF,[4] robust engagement of pRb and irreversible cell cycle arrest,[62,63] attributes that also underlie the role of the $p16^{ink4a}$-pRb pathway in tumor suppression.[64,65]

Last but not least, our data are relevant to the biological role of senescence as an intrinsic barrier against tumor progression.[66-69] In mechanistic terms, not only the upstream DDR signaling and the p53 pathway[2,4,51,54,55] but also the $p16^{ink4a}$-pRb pathway and heterochromatinization have been implicated in such anti-tumor barrier function.[26] In the light of our present results of enhanced H3K9Me3-positive heterochromatinization, yet without the 'classical' SAHF defined by DAPI-positive foci in human tumors, we speculate that there are at least two intriguing scenarios to consider for SAHF in tumorigenesis. First, enhanced heterochromatinization in vivo may help to block proliferation-driving genes such as the pRb/E2F target genes that become transcriptionally inhibited by SAHF during oncogene-induced senescence.[4,26] This would imply that the heterochromatin changes detected in vivo are functionally analogous to the 'classical' DAPI-positive SAHF, and contribute to the overall senescence-mediated decrease of cell proliferation, consistent with a tumor suppressive function of the H3K9Me3/HP1γ-rich heterochromatinization seen in human premalignant lesions (reviewed in ref. 48 and this study). If this were the case, then the question is how could advanced, invasive tumors in vivo and cancer cell lines proliferate despite expressing this type of heterochromatin, as is documented for both the clinical specimens as well as the cancer cell lines (reviewed in refs. 48, 70, 71 and this study). This apparent discrepancy might be reconciled if, during cancer progression, the downstream inhibitory impact of heterochromatin on proliferation-promoting genes was somehow bypassed or eliminated, similarly to p53 or Chk2 mutations undermine the DDR-imposed checkpoints originally activated in early lesions.[33,67,72] The net result (consistent with our observations on clinical material) would be persistent enhanced heterochromatinization also in invasive tumors, again analogous to persistent ATM/ATR activation and γH2AX positivity often seen in advanced tumors, despite the downstream checkpoint effectors have been blunted.[54] The other potential scenario, however, could reflect the recent studies on the inhibition of DDR by heterochromatin.[73,74] In this scenario, the altered yet enhanced heterochromatinization, perhaps in the configuration that lacks the DNA/DAPI foci, might help to limit the overall DDR signaling from the ongoing oncogene-induced replication stress and DNA damage[33,67,72] and thereby promote cancer survival by bypassing the DDR barrier. This scenario would explain the enhanced degree of heterochromatin reported for invasive human tumors[48,70] and the rapidly proliferating cancer cell lines (this study). The tumor-suppressive, pro-senescence role and the latter DDR-inhibitory, pro-survival role of enhanced heterochromatinization may not be mutually exclusive. These two heterochromatin states may target distinct sets of genes and differ from each other mechanistically in ways that we still do not understand. Furthermore, the diverse heterochromatin states may also be manifested differentially during different phases of tumor progression, in a context-dependent manner, with the pro-survival mode of heterochromatin being predominant in advanced lesions to limit the impact of DNA damage signaling and ensuing senescence or cell death pathways.

The understanding of heterochromatin biology including SAHF formation has advanced rapidly in recent years; however, it is also evident that many outstanding questions remain to be answered. Relevant to our present study, examples of such questions may include: (1) the potential existence of distinct SAHF structures, only one of which displays the typical DNA/DAPI-defined foci, and their impact on gene expression; (2) what is the contribution, if any, of oxidative stress in general, and high oxygen tension or other artificial conditions to SAHF formation, activation of the $p16^{ink4a}$-pRb pathway and cellular immortalization versus senescence; (3) potential distinct biological functions of heterochromatin, including effects on DDR, under various pathological conditions such as aging or cancer progression. On a positive note, one potential avenue to personalized treatment, based on genetic profiles, DDR and heterochromatin states, could be to modulate chromatin modifications such as methylation or acetylation, to synergize with endogenous DNA damage signaling that occurs in most tumors,[72] and/or with standard-of-care genotoxic therapies, to selectively sensitize and eliminate tumor cells.

Materials and Methods

Chemicals. Hydroxyurea (Sigma, # H8627) and doxorubicin (Sigma, # D1515) were dissolved in H_2O. Etoposide (Sigma, # E1383) was diluted in DMSO. Recombinant toxin from H. ducreyi was prepared by Dr. Frisan (Karolinska Institutet, Stockholm, Sweden). Preparation of CdtA, CdtB and CdtC subunits and reconstitution of the active holotoxin (HdCDT) was previously described in references 47 and 75.

Cell cultures. Normal human fibroblasts BJ and MRC-5 (both from ATCC and at population doublings between 27 and 37) were cultured in Dulbecco's modified Eagle's medium (D-MEM, Invitrogen, # 31966) supplemented with 10% foetal bovine serum (FBS, Invitrogen, # 10270-106) and penicillin/streptomycin (Invitrogen, # 15140122). Cells were kept at 37°C under 5% CO_2 atmosphere and 95% humidity. Neonatal Human Epidermal Keratinocytes (HEKn; Invitrogen, # C-001-5C) were cultured in EpiLife Medium (Invitrogen, # M-EPI-500-CA) supplemented with HKGS Kit (Invitrogen, # S-001-K) at population doublings between four and ten. HEKn were kept in a humidified atmosphere of 5% CO_2 and 3% O_2 at 37°C. To reach replicative senescence, MRC-5 cells were passaged until population doubling 48, while BJ cells required longer cultivation, until population doubling 86 under similar culture conditions.

Induction of premature cellular senescence in vitro. In pilot experiments, cells were treated with various concentrations of individual drugs to select best concentration leading to senescence. 600 μM hydroxyurea, 10 μM etoposide and 100 ng/ml doxorubicin were chosen as the most suitable for routine administration to reach senescence in the majority of cells within the given cell population. Culture medium with fresh additives was changed every 72 h. The 100% activity of bacterial toxin from *H. ducreyi* was estimated as the lowest cytopathic dose that caused complete irreversible G_2/M block of 'reference' HeLa cell strain 24 hours after intoxication.[42] For induction of senescence we used 'balanced' toxin dilutions to get optimal ratio of surviving cells to dead cells; i.e., 70% activity for BJ, MRC5 and HEKn. Medium was routinely changed 72 hours after a single HdCDT-administration. Cells were routinely harvested at day 12 or as specified.

Indirect immunofluorescence. For immunofluorescence microscopy, cells cultured on coverslips were fixed in 4% formaldehyde and permeabilized by 0.1% Triton X-100 in two consecutive steps, each for 15 minutes at RT, essentially as described in reference 76 and 77. After washing with PBS, cells were blocked for 30 minutes in 10% foetal calf serum. The following primary antibodies were used: mouse monoclonal antibody against histone H2A.X phosphorylated at serine 139 (γH2AX; Abcam, # ab22551, 1:500), rabbit polyclonal antibody against histone H3 trimethylated at lysine 9 (H3K9Me3, Milipore, # 07-442, 1:1,000) and mouse monoclonal antibody against heterochromatin protein-1γ (HP1γ, Chemicon, # MAB3450, 1:4,000). Incubation with primary antibodies was performed for 60 minutes at RT and then cells were washed with PBS. Secondary antibodies Alexa Fluor® 488 goat anti-rabbit (Invitrogen, #A11034, 1:500) and Alexa Fluor® 568 goat anti-mouse (Invitrogen, #A11031, 1:500) were then applied for 60 minutes at RT, followed by final wash in PBS. Coverslips were mounted in Vectashield Mounting Medium with DAPI (Vector Laboratories, # H-1200). Confocal images were acquired on LSM-510 (Carl Zeiss Microimaging Inc., Germany) equipped with Plan-Apochromat 63x/1.4 oil immersion objective, ZEN2009 software (Carl Zeiss Microimaging Inc., Germany) and with appropriate configurations for multiple color acquisition. For quantitative and comparative imaging, identical image acquisition parameters were used.

BrdU proliferation assay. Cells cultured on coverslips were incubated with 10 μM BrdU (Sigma, B5002) for 6 hours before fixation with 4% formaldehyde. After DNA denaturation in 2 M HCl for 30 minutes, cells were washed in PBS and incubated with mouse monoclonal antibody against BrdU (APbiotech, RPN20AB, 1:1,300) and stained as described above. Images were acquired on a widefield fluorescence microscope AxioObserver (Carl Zeiss Microimaging Inc., Germany) equipped with Plan Apochromat 20x/0.8 objective, camera Coolsnap HQ (Roper Scientific, Germany) and Metamorph software (Universal Imaging Corporation Ltd., Great Britain).

Senescence associated-β-galactosidase assay. Staining for SA-β-gal activity was performed at day 12 using Senescence β-Galactosidase Staining Kit (Cell Signaling Technology, # 9860) following manufacturer's protocol. Images were captured by fluorescence microscope Zeiss Axioplan 2 (Carl Zeiss Microimaging Inc., Germany) equipped with Plan Neofluar 20x/0.5 objective, color camera Infinity X and Deltapix software (both Deltapix, Denmark).

SDS-PAGE and western blotting. Cells were harvested into Laemmli SDS sample lysis buffer (50 mM Tris pH 6.8; 100 mM DTT; 2% SDS; 0.1% bromphenol blue; 10% glycerol) supplemented with a cocktail of protease inhibitors Complete Mini, EDTA-free (Roche Diagnostics, # 04693159001) and a cocktail of phosphatase inhibitors PhosSTOP (Roche Diagnostics, # 04906845001), sonicated and centrifuged at 16,000x g for 10 minutes. Protein concentration was estimated by the BCA

method (Pierce Biotechnology Inc., # 23225). 0.01% bromphenol and 100 mM DTT were added to lysates before separation in 15% polyacrylamide gels by SDS-PAGE (20 μg of protein was loaded per lane). Proteins were electrotransferred onto nitrocellulose membrane (LI-COR, 926-31092) using semidry transfer followed by staining with Ponceau S to verify transfer and equal loading. Staining with mouse monoclonal antibody against $p16^{ink4a}$ (Sigma, # P0968, 1:130) and mouse antibody against alpha-tubulin (Sigma, T6199, 1:10,000) was performed overnight. Detection was performed by goat anti-mouse IRDye 800CW antibody (LI-COR, # 926-32210) using Odyssey Imaging System equipped with Odyssey software (LI-COR, Nebraska, USA). Alpha-tubulin was used as a marker to ensure equal loading.

Vectors and viral infections. The following lentiviral vectors were used: expression vector pCDH-CMV-MCS-EF1-Puro (System Biosciences, # CD510B-1) empty or with $H\text{-}Ras^{V12}$ insert, packaging vectors pMD2G (Addgene, # 12259) and psPAX2 (Addgene, # 12260). Lentiviral gene transfer was performed as described in reference 78. The infected population was selected using 2 μg/ml puromycin (Sigma, # P7255) for 72 hours.

Human tissue specimens and immunohistochemistry. The paraffin blocks of archival tissue specimens of normal human colon, urinary bladder, skin and series of colon adenomas (n = 38) and carcinomas (n = 44), and urinary bladder tumors (n = 19, including nine cases of Ta lesions and ten cases of T1 lesions) were described previously in reference 48. Samples of frozen tissues of human adenomas (n = 14) were stored at -80°C. All samples were originally collected at the University hospitals in Aarhus and Copenhagen, under ethical approval received from a local Medical Research Ethics Committee in Denmark. The diagnoses were independently verified by two experienced pathologists according to the established criteria of classification recommended by the World Health Organization. The samples of the majority of the tissues (except the 14 cryopreserved adenoma specimens) were fixed in buffered formalin, embedded in paraffin wax and the tissue sections examined by routine histopathology methods and by immunohistochemistry, as reported previously in reference 48 and 53. For immunohistochemistry, formaldehyde-fixed, de-paraffinized tissue sections were stained overnight with rabbit polyclonal antibody against histone H3 trimethylated at lysine 9 (H3K9Me3, Milipore, # 07-442, 1:1,000) and for one hour with secondary antibody Alexa Fluor® 488 goat anti-rabbit (Invitrogen, #A11034, 1:500). Samples were mounted into Vectashield Mounting Medium with DAPI (Vector Laboratories, # H-1200). Data on expression of SA-β-gal on frozen sections, and γH2AX, HP1γ and $p16^{ink4a}$ on the paraffin sections were available from our previous study using immunoperoxidase-based analysis.[48] The newly obtained immunofluorescence images for DAPI and H3K9Me3 were acquired as described above, and examples of the results are presented in **Figure 5**.

Data analysis and statistics. Percentage of BrdU positive cells was determined by counting cells in 35 random fields (approximately 500 cells) for each coverslip. Percentage of SAHF positive cells (based on DAPI staining) and number of γH2AX foci per cell were counted from at least 200 cells for each coverslip. Data analysis was performed in ImageJ (version 1.43u, Wayne Rasband, National Institutes of Health, USA) as described in reference 77, graphs were generated by Prism 5 (GraphPad Software, Ja Jolla, CA USA). The results shown are averages (with 95% confidence interval, tested by unpaired t-test) of a minimum of three independent experiments.

Acknowledgements

We wish to thank Teresa Frisan for the preparation of the bacterial toxin, and Maxwell Sehested and Torben Ørntoft for sharing with us the tissue samples. This study was supported by the Danish Cancer Society, the Danish National Research Foundation, the Novo Nordisk Foundation (R153-A12997), Grant Agency of the Czech Republic (Projects No. 301/08/0353, 204/04/1418 and P301/10/1525), Institutional Grant (Project No. AV0Z5039906), and the European Commission 7th Framework Programme (Projects Infla-Care and TRIREME).

Note

Supplemental materials can be found at:
www.landesbioscience.com/journals/cc/article/14707

References

1. Campisi J, d'Adda di Fagagna F. Cellular senescence: When bad things happen to good cells. Nat Rev Mol Cell Biol 2007; 8:729-40.
2. Campisi J. Cellular senescence: Putting the paradoxes in perspective. Curr Opin Genet Dev 2010.
3. Dimri GP, Lee X, Basile G, Acosta M, Scott G, Roskelley C, et al. A biomarker that identifies senescent human cells in culture and in aging skin in vivo. Proc Natl Acad Sci USA 1995; 92:9363-7.
4. Narita M, Nunez S, Heard E, Lin AW, Hearn SA, Spector DL, et al. Rb-mediated heterochromatin formation and silencing of E2F target genes during cellular senescence. Cell 2003; 113:703-16.
5. de Stanchina E, Querido E, Narita M, Davuluri RV, Pandolfi PP, Ferbeyre G, et al. PML is a direct p53 target that modulates p53 effector functions. Mol Cell 2004; 13:523-35.
6. Janderova-Rossmeislova L, Novakova Z, Vlasakova J, Philimonenko V, Hozak P, Hodny Z. PML protein association with specific nucleolar structures differs in normal, tumor and senescent human cells. J Struct Biol 2007; 159:56-70.
7. Acosta JC, O'Loghlen A, Banito A, Guijarro MV, Augert A, Raguz S, et al. Chemokine signaling via the CXCR2 receptor reinforces senescence. Cell 2008; 133:1006-18.
8. Coppe JP, Patil CK, Rodier F, Sun Y, Munoz DP, Goldstein J, et al. Senescence-associated secretory phenotypes reveal cell-nonautonomous functions of oncogenic RAS and the p53 tumor suppressor. PLoS Biol 2008; 6:2853-68.
9. Kuilman T, Michaloglou C, Vredeveld LC, Douma S, van Doorn R, Desmet CJ, et al. Oncogene-induced senescence relayed by an interleukin-dependent inflammatory network. Cell 2008; 133:1019-31.
10. Novakova Z, Hubackova S, Kosar M, Janderova-Rossmeislova L, Dobrovolna J, Vasicova P, et al. Cytokine expression and signaling in drug-induced cellular senescence. Oncogene 2010; 29:273-84.
11. Rodier F, Coppe JP, Patil CK, Hoeijmakers WA, Munoz DP, Raza SR, et al. Persistent DNA damage signalling triggers senescence-associated inflammatory cytokine secretion. Nat Cell Biol 2009; 11:973-9.
12. Wajapeyee N, Serra RW, Zhu X, Mahalingam M, Green MR. Oncogenic BRAF induces senescence and apoptosis through pathways mediated by the secreted protein IGFBP7. Cell 2008; 132:363-74.
13. Sedelnikova OA, Horikawa I, Zimonjic DB, Popescu NC, Bonner WM, Barrett JC. Senescing human cells and ageing mice accumulate DNA lesions with unrepairable double-strand breaks. Nat Cell Biol 2004; 6:168-70.
14. d'Adda di Fagagna F, Reaper PM, Clay-Farrace L, Fiegler H, Carr P, Von Zglinicki T, et al. A DNA damage checkpoint response in telomere-initiated senescence. Nature 2003; 426:194-8.
15. von Zglinicki T, Saretzki G, Ladhoff J, d'Adda di Fagagna F, Jackson SP. Human cell senescence as a DNA damage response. Mech Ageing Dev 2005; 126:111-7.

16. Wang C, Jurk D, Maddick M, Nelson G, Martin-Ruiz C, von Zglinicki T. DNA damage response and cellular senescence in tissues of aging mice. Aging Cell 2009; 8:311-23.
17. Martin-Ruiz C, Saretzki G, Petrie J, Ladhoff J, Jeyapalan J, Wei W, et al. Stochastic variation in telomere shortening rate causes heterogeneity of human fibroblast replicative life span. J Biol Chem 2004; 279:17826-33.
18. Passos JF, Saretzki G, von Zglinicki T. DNA damage in telomeres and mitochondria during cellular senescence: Is there a connection? Nucleic Acids Res 2007; 35:7505-13.
19. Sedivy JM. Telomeres limit cancer growth by inducing senescence: Long-sought in vivo evidence obtained. Cancer Cell 2007; 11:389-91.
20. Ramirez RD, Morales CP, Herbert BS, Rohde JM, Passons C, Shay JW, et al. Putative telomere-independent mechanisms of replicative aging reflect inadequate growth conditions. Genes Dev 2001; 15:398-403.
21. von Zglinicki T. Oxidative stress shortens telomeres. Trends Biochem Sci 2002; 27:339-44.
22. Serrano M, Lin AW, McCurrach ME, Beach D, Lowe SW. Oncogenic ras provokes premature cell senescence associated with accumulation of p53 and $p16^{INK4a}$. Cell 1997; 88:593-602.
23. Lawless C, Wang C, Jurk D, Merz A, Zglinicki T, Passos JF. Quantitative assessment of markers for cell senescence. Exp Gerontol 2010; 45:772-8.
24. Chen Z, Trotman LC, Shaffer D, Lin HK, Dotan ZA, Niki M, et al. Crucial role of p53-dependent cellular senescence in suppression of Pten-deficient tumorigenesis. Nature 2005; 436:725-30.
25. Collado M, Gil J, Efeyan A, Guerra C, Schuhmacher AJ, Barradas M, et al. Tumour biology: Senescence in premalignant tumours. Nature 2005; 436:642.
26. Braig M, Lee S, Loddenkemper C, Rudolph C, Peters AHFM, Schlegelberger B, et al. Oncogene-induced senescence as an initial barrier in lymphoma development. Nature 2005; 436:660-5.
27. Blagosklonny MV. Aging-suppressants: Cellular senescence (hyperactivation) and its pharmacologic deceleration. Cell Cycle 2009; 8:1883-7.
28. Jeyapalan JC, Ferreira M, Sedivy JM, Herbig U. Accumulation of senescent cells in mitotic tissue of aging primates. Mech Ageing Dev 2007; 128:36-44.
29. Schmitt CA. Cellular senescence and cancer treatment. Biochimica et Biophysica Acta 2007; 1775:5-20.
30. Martin JA, Buckwalter JA. The role of chondrocyte senescence in the pathogenesis of osteoarthritis and in limiting cartilage repair. J Bone Joint Surg Am 2003; 85:106-10.
31. Chen QM, Bartholomew JC, Campisi J, Acosta M, Reagan JD, Ames BN. Molecular analysis of H_2O_2-induced senescent-like growth arrest in normal human fibroblasts: p53 and Rb control G_1 arrest but not cell replication. Biochem J 1998; 332:43-50.
32. Beausejour CM, Krtolica A, Galimi F, Narita M, Lowe SW, Yaswen P, et al. Reversal of human cellular senescence: roles of the p53 and p16 pathways. EMBO J 2003; 22:4212-22.
33. Jackson SP, Bartek J. The DNA-damage response in human biology and disease. Nature 2009; 461:1071-8.
34. Rogakou EP, Pilch DR, Orr AH, Ivanova VS, Bonner WM. DNA double-stranded breaks induce histone H2AX phosphorylation on serine 139. J Biol Chem 1998; 273:5858-68.
35. Lobrich M, Shibata A, Beucher A, Fisher A, Ensminger M, Goodarzi AA, et al. gammaH2AX foci analysis for monitoring DNA double-strand break repair: strengths, limitations and optimization. Cell Cycle 2010; 9:662-9.
36. Zhang R, Adams PD. Heterochromatin and its relationship to cell senescence and cancer therapy. Cell Cycle 2007; 6:784-9.
37. Zhang R, Chen W, Adams PD. Molecular dissection of formation of senescence-associated heterochromatin foci. Mol Cell Biol 2007; 27:2343-58.
38. Ye X, Zerlanko B, Zhang R, Somaiah N, Lipinski M, Salomoni P, et al. Definition of pRB- and p53-dependent and -independent steps in HIRA/ASF1a-mediated formation of senescence-associated heterochromatin foci. Mol Cell Biol 2007; 27:2452-65.
39. Narita M, Narita M, Krizhanovsky V, Nunez S, Chicas A, Hearn SA, et al. A Novel Role for High-Mobility Group A Proteins in Cellular Senescence and Heterochromatin Formation. Cell 2006; 126:503-14.
40. Zhang R, Poustovoitov MV, Ye X, Santos HA, Chen W, Daganzo SM, et al. Formation of MacroH2A-containing senescence-associated heterochromatin foci and senescence driven by ASF1a and HIRA. Dev Cell 2005; 8:19-30.
41. Adams PD. Remodeling of chromatin structure in senescent cells and its potential impact on tumor suppression and aging. Gene 2007; 397:84-93.
42. Blazkova H, Krejcikova K, Moudry P, Frisan T, Hodny Z, Bartek J. Bacterial Intoxication Evokes Cellular Senescence with Persistent DNA Damage and Cytokine Signaling. J Cell Mol Med 2010; 14:357-67.
43. te Poele RH, Okorokov AL, Jardine L, Cummings J, Joel SP. DNA damage is able to induce senescence in tumor cells in vitro and in vivo. Cancer Res 2002; 62:1876-83.
44. Yogev O, Anzi S, Inoue K, Shaulian E. Induction of transcriptionally active Jun proteins regulates drug-induced senescence. J Biol Chem 2006; 281:34475-83.
45. Chang BD, Broude EV, Dokmanovic M, Zhu H, Ruth A, Xuan Y, et al. A senescence-like phenotype distinguishes tumor cells that undergo terminal proliferation arrest after exposure to anticancer agents. Cancer Res 1999; 59:3761-7.
46. Demidenko ZN, Blagosklonny MV. Growth stimulation leads to cellular senescence when the cell cycle is blocked. Cell Cycle 2008; 7:3355-61.
47. Frisan T, Cortes-Bratti X, Chaves-Olarte E, Stenerlow B, Thelestam M. The *Haemophilus ducreyi* cytolethal distending toxin induces DNA double-strand breaks and promotes ATM-dependent activation of RhoA. Cell Microbiol 2003; 5:695-707.
48. Bartkova J, Rezaei N, Liontos M, Karakaidos P, Kletsas D, Issaeva N, et al. Oncogene-induced senescence is part of the tumorigenesis barrier imposed by DNA damage checkpoints. Nature 2006; 444:633-7.
49. Seo HJ, Park HJ, Choi HS, Hwang SY, Park JS, Seong YS. BMI-1026 treatment can induce SAHF formation by activation of Erk1/2. BMB Rep 2008; 41:523-8.
50. Herbig U, Jobling WA, Chen BPC, Chen DJ, Sedivy JM. Telomere shortening triggers senescence of human cells through a pathway involving ATM, p53 and $p21^{CIP1}$, but not $p16^{INK4a}$. Molecular Cell 2004; 14:501-13.
51. Di Micco R, Fumagalli M, Cicalese A, Piccinin S, Gasparini P, Luise C, et al. Oncogene-induced senescence is a DNA damage response triggered by DNA hyper-replication. Nature 2006; 444:638-42.
52. Sedelnikova OA, Bonner WM. GammaH2AX in cancer cells: a potential biomarker for cancer diagnostics, prediction and recurrence. Cell Cycle 2006; 5:2909-13.
53. Bartkova J, Bakkenist CJ, Rajpert-De Meyts E, Skakkebaek NE, Sehested M, Lukas J, et al. ATM activation in normal human tissues and testicular cancer. Cell Cycle 2005; 4:838-45.
54. Bartkova J, Horejsi Z, Koed K, Kramer A, Tort F, Zieger K, et al. DNA damage response as a candidate anti-cancer barrier in early human tumorigenesis. Nature 2005; 434:864-70.
55. Gorgoulis VG, Vassiliou LV, Karakaidos P, Zacharatos P, Kotsinas A, Liloglou T, et al. Activation of the DNA damage checkpoint and genomic instability in human precancerous lesions. Nature 2005; 434:907-13.
56. Bansal R, Nikiforov MA. Pathways of oncogene-induced senescence in human melanocytic cells. Cell Cycle 2010; 9:2782-8.
57. Schmitt CA, Fridman JS, Yang M, Lee S, Baranov E, Hoffman RM, et al. A senescence program controlled by p53 and $p16^{INK4a}$ contributes to the outcome of cancer therapy. Cell 2002; 109:335-46.
58. Sviderskaya EV, Hill SP, Evans-Whipp TJ, Chin L, Orlow SJ, Easty DJ, et al. p16(Ink4a) in melanocyte senescence and differentiation. J Natl Cancer Inst 2002; 94:446-54.
59. Gray-Schopfer VC, Cheong SC, Chong H, Chow J, Moss T, Abdel-Malek ZA, et al. Cellular senescence in naevi and immortalisation in melanoma: a role for p16? Br J Cancer 2006; 95:496-505.
60. Alani RM, Young AZ, Shifflett CB. Id1 regulation of cellular senescence through transcriptional repression of p16/Ink4a. Proc Natl Acad Sci USA 2001; 98:7812-6.
61. Ressler S, Bartkova J, Niederegger H, Bartek J, Scharffetter-Kochanek K, Jansen-Durr P, et al. $p16^{INK4A}$ is a robust in vivo biomarker of cellular aging in human skin. Aging Cell 2006; 5:379-89.
62. Brenner AJ, Stampfer MR, Aldaz CM. Increased p16 expression with first senescence arrest in human mammary epithelial cells and extended growth capacity with p16 inactivation. Oncogene 1998; 17:199-205.
63. Takahashi A, Ohtani N, Hara E. Irreversibility of cellular senescence: Dual roles of $p16^{INK4a}$/Rb-pathway in cell cycle control. Cell Div 2007; 2:10.
64. Bringold F, Serrano M. Tumor suppressors and oncogenes in cellular senescence. Exp Gerontol 2000; 35:317-29.
65. Kim WY, Sharpless NE. The regulation of INK4/ARF in cancer and aging. Cell 2006; 127:265-75.
66. Mallette FA, Ferbeyre G. The DNA damage signaling pathway connects oncogenic stress to cellular senescence. Cell Cycle 2007; 6:1831-6.
67. Bartek J, Lukas J, Bartkova J. DNA damage response as an anti-cancer barrier: damage threshold and the concept of 'conditional haploinsufficiency'. Cell Cycle 2007; 6:2344-7.
68. Campisi J. Senescent cells, tumor suppression and organismal aging: Good citizens, bad neighbors. Cell 2005; 120:513-22.
69. Collado M, Serrano M. The senescent side of tumor suppression. Cell Cycle 2005; 4:1722-4.
70. Cruickshanks HA, Adams PD. Chromatin: a molecular interface between cancer and aging. Curr Opin Genet Dev 2010; DOI: 10.1016/j.gde.2010.10.007.
71. Bartkova J, Moudry P, Hodny Z, Lukas J, Rajpert-De Meyts E, Bartek J. Heterochromatin marks HP1γ, HP1α and H3K9me3 and DNA damage response activation in human testis development and germ cell tumours. Int J Androl 2010; DOI: 10.1111/j.1365-2605.2010.01096.x.
72. Halazonetis TD, Gorgoulis VG, Bartek J. An oncogene-induced DNA damage model for cancer development. Science 2008; 319:1352-5.
73. Ayoub N, Jeyasekharan AD, Venkitaraman AR. Mobilization and recruitment of HP1: A bimodal response to DNA breakage. Cell Cycle 2009; 8:2945-50.
74. Goodarzi AA, Noon AT, Jeggo PA. The impact of heterochromatin on DSB repair. Biochem Soc Trans 2009; 37:569-76.
75. Guerra L, Teter K, Lilley BN, Stenerlow B, Holmes RK, Ploegh HL, et al. Cellular internalization of cytolethal distending toxin: A new end to a known pathway. Cell Microbiol 2005; 7:921-34.
76. Hubackova S, Novakova Z, Krejcikova K, Kosar M, Dobrovolna J, Duskova P, et al. Regulation of the PML tumor suppressor in drug-induced senescence of human normal and cancer cells by JAK/STAT-mediated signaling. Cell Cycle 2010; 9:3085-99.
77. Mistrik M, Oplustilova L, Lukas J, Bartek J. Low-dose DNA damage and replication stress responses quantified by optimized automated single-cell image analysis. Cell Cycle 2009; 8:2592-9.
78. Tiscornia G, Singer O, Verma IM. Production and purification of lentiviral vectors. Nat Protoc 2006; 1:241-5.

Supplemental Figure S1. Examples of SA-β-gal activity in MRC-5, BJ and HEKn promoted to senescence by various stimuli. Cells were assayed for SA-β-gal activity at day 12 after senescence induction.

Supplemental Figure S2. SAHF are absent in cancer cell lines irrespective of the presence of elevated heterochromatinization markers. UMSCC-2, HN-5, T24, HCT116, and Hacat cells were stained for SAHF (DAPI), H3K9Me3 and HP1γ, as indicated. MRC-5 cells transduced with H-ras^{V12} to senescence (day 12) are shown as a SAHF-positive control.

Supplemental Table S1. MRC-5, BJ and HEKn cells were scored for markers of proliferation (percentage of cells incorporating BrdU) and DNA damage (average number of γH2AX foci per cell) at proliferating (Control) and senescent state (day 12) induced by different stimuli, as indicated.

Supplemental Table S2. Semiquantitative assessment of heterochromatinization markers detected by DAPI, H3K9Me3 and HP1γ staining, respectively, in several human cell lines, as indicated. MRC-5 induced to senescence by H-Ras^{V12} lentiviral transduction are shown as a positive control for SAHF formation. (-) no SAHF formation; (+) low, (++) moderate, or (+++) high expression.

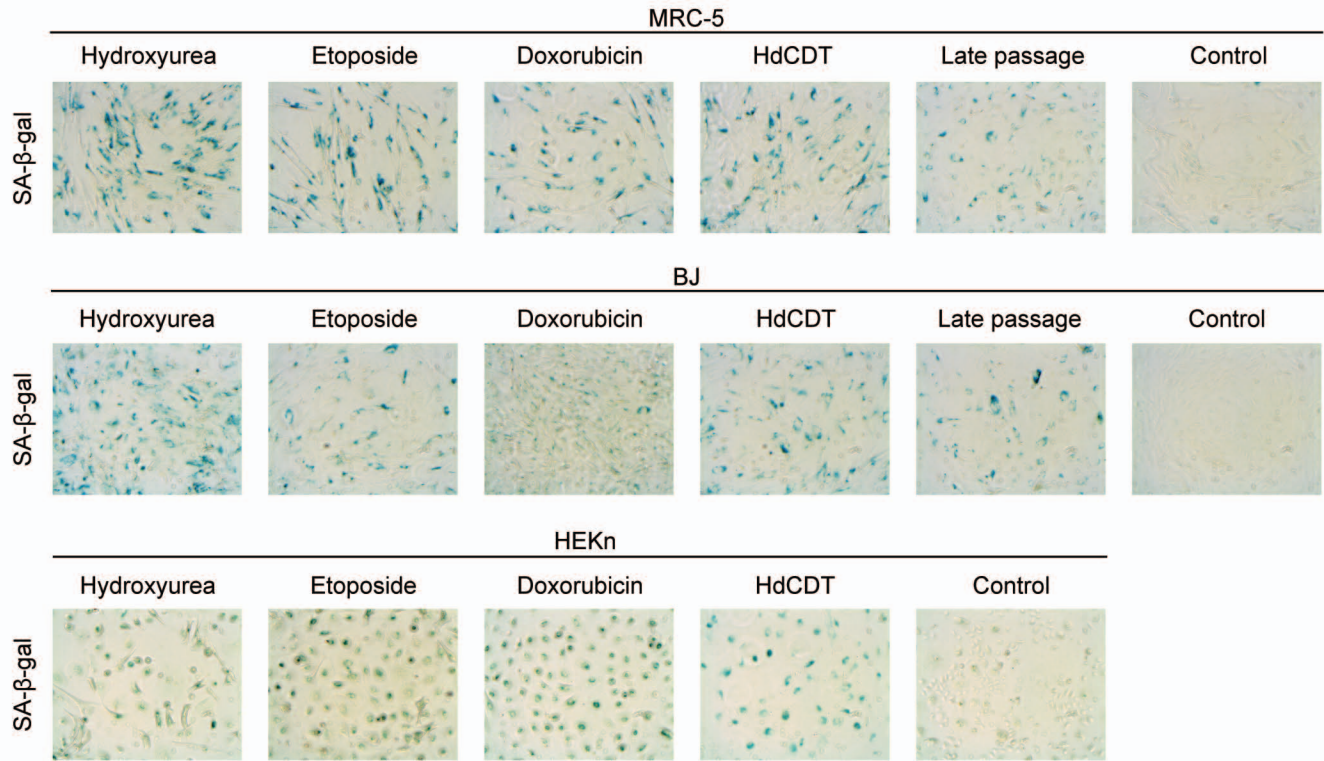
MRC-5
Hydroxyurea
Etoposide
Doxorubicin
HdCDT
Late passage
Control
SA-β-gal
BJ
Hydroxyurea
Etoposide
Doxorubicin
HdCDT
Late passage
Control
SA-β-gal
HEKn
Hydroxyurea
Etoposide
Doxorubicin
HdCDT
Control
SA-β-gal

UMSCC-2 | HN-5 | T24 | HCT116 | Hacat | MRC-5 H-RasV12

DAPI

H3K9Me3

HP1γ

Merge

Supplementary Table 1

Cell type	Insult	% BrdU-positive cells	No. of γH2AX foci/cells
MRC-5	H-RasV12	11	3
	Empty vector	16	1
	Hydroxyurea	4	6
	Control	16	1
	Etoposide	0	8
	DMSO	16	1
	Doxorubicin	0	9
	Control	17	1
	HdCDT	6	2
	Control	18	1
	Late Passage	2	6
	Control	21	2
BJ	H-RasV12	6	4
	Empty vector	31	1
	Hydroxyurea	1	11
	Control	35	2
	Etoposide	0	11
	DMSO	29	1
	Doxorubicin	0	12
	Control	32	2
	HdCDT	9	4
	Control	29	1
	Late Passage	2	3
	Control	24	1
HEKn	H-RasV12	5	2
	Empty vector	20	0
	Hydroxyurea	2	4
	Control	23	1
	Etoposide	0	10
	DMSO	17	1
	Doxorubicin	0	7
	Control	29	1
	HdCDT	0	3
	Control	23	1

MRC-5, BJ and HEKn cells were scored for markers of proliferation (percentage of cells incorporating BrdU) and DNA damage (average number of γH2AX foci per cell) at proliferating (Control) and senescent state (day 12) induced by different stimuli, as indicated.

Supplementary Table 2

	Cell type					
SAHF markers	**UMSCC-2**	**HN-5**	**T24**	**HCT116**	**Hacat**	**MRC-5 H-Ras^{V12}**
DAPI foci	-	-	-	-	-	+++
H3K9Me3	-	+++	++	+	+++	+++
HP1γ	-	+++	+++	-	++	+++

Semiquantitative assessment of heterochromatinization markers detected by DAPI, H3K9Me3 and HP1γ staining, respectively, in several human cell lines, as indicated. MRC-5 induced to senescence by H-Ras^{V12} lentiviral transduction are shown as a positive control for SAHF formation. (-) no SAHF formation; (+) low, (++) moderate, or (+++) high expression.

Editorial

Cytokines shape chemotherapy-induced and 'bystander' senescence

Zdenek Hodny[1], Sona Hubackova[1], Jiri Bartek[1,2]

[1] Department of Genome Integrity, Institute of Molecular Genetics, v.v.i., ASCR, CZ-142 20 Prague 4, Czech Republic

[2] Institute of Cancer Biology and Centre for Genotoxic Stress Research, Danish Cancer Society, DK-2100 Copenhagen, Denmark

E-mail: *jb@cancer.dk; hodny@img.cas.cz*

The permanent proliferation arrest, distended morphology and other phenotypic features characteristic of cellular senescence can be triggered by telomere attrition (replicative senescence) and various stresses such as activated oncogenes or genotoxic treatments (premature senescence). Physiological relevance of cellular senescence is apparent from its emerging roles in aging, in tumor pathogenesis as an inducible barrier to tumor progression, and in response to radiotherapy and chemotherapy [1]. Mechanistically, senescence induction and maintenance involve the major tumor suppressor pathways of pRB and p53, and persistent signaling of the DNA damage response (DDR) machinery [1]. An integral part of DNA damage signaling and senescence is the activation of a complex cytokine network [1,2] including proinflammatory species IL-6 and IL-8 and reorganization/multiplication of a specific nuclear compartment, PML nuclear bodies (PML NBs) [1,3]. Despite the critical roles of promyelocytic leukemia protein (PML), the structural component of PML NBs, in PML NBs assembly, tumor suppression, and stabilization and activation of p53 after various stresses, the molecular basis of PML regulation and its interplay with the senescence-associated secretory cytokine network are not well understood. A new study [4] now sheds light on the involvement of PML NBs in cellular senescence evoked by a spectrum of genotoxic drugs including clinically used chemotherapeutics, and provides important mechanistic insights into regulation of PML expression, causal relationship with cytokine signaling, and surprising lack of dependence on p53.

Relevant findings preceding this study include the recent demonstration of cytokine signaling pathways involved in drug-evoked senescence [5], and the fact that chemotherapy-induced senescence can occur in neighboring cells through so-called 'bystander' effects [6]. The new work by Hubackova and colleagues [4] now shows that exposure of human normal and cancer cells to genotoxic drugs including those used to treat human malignancies such as camptothecin and etoposide, at concentrations evoking senescence and achievable in tissues during chemotherapy, resulted in enhanced formation of PML NBs, elevated PML transcript levels and activated JAK/STAT signaling indicative of cytokine involvement. As both endogenous PML transcript levels and PML promoter-driven luciferase activity were suppressed by chemical inhibition or RNAi-mediated knock-down of JAK1 kinase, the data reveals a key role of JAK1-controlled signaling in PML transcription induced by genotoxic stress. Furthermore, in contrast to oncogene-induced senescence where PML expression is controlled by p53, the experiments of Hubackova et al. with both p53-negative cells and regulatable dominant-negative allele of p53 showed that JAK1-regulated transcription of PML in response to genotoxic drugs is p53-independent [4].

Considered within the context of other data in the field, these new results [4] help us better understand the interplay of PML with cytokine signaling in drug-induced and 'bystander' senescence, phenomena highly relevant for aging, cancer biology and treatment response.

REFERENCES

1. Adams PD. Mol. Cell 2009; 36: 2-14.
2. Rodier F et al. Nat Cell Biol 2009; 11: 973-979.
3. Carbone R et al. Oncogene 2002; 21: 1633-1640.
4. Hubackova S et al. Cell Cycle 2010; 9: in press.
5. Novakova Z et al. Oncogene 2010; 29: 273-284.
6. Di X et al. Cancer Biol Ther 2008; 7: 864-872.

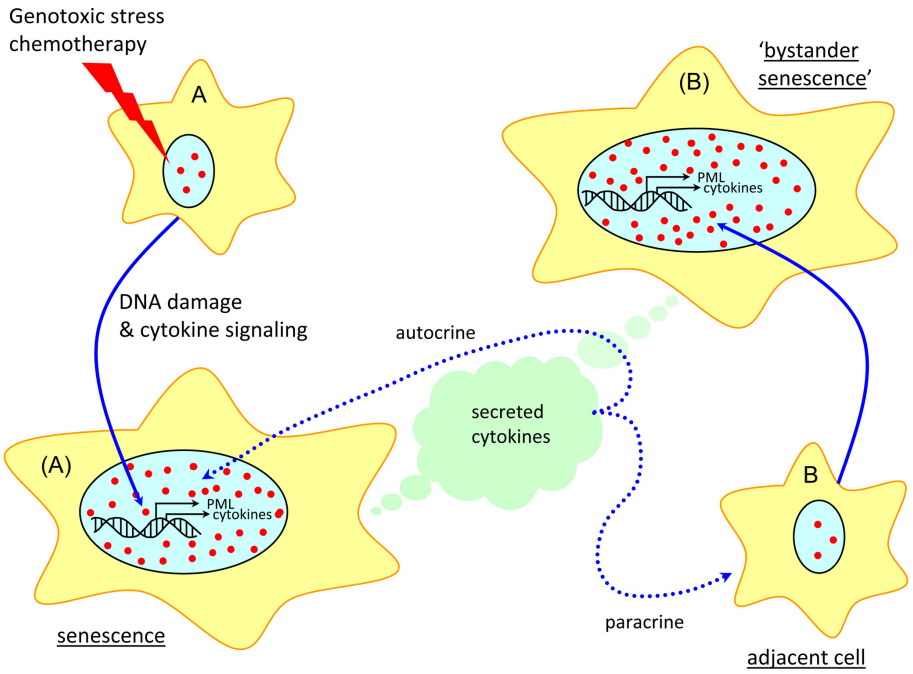

Figure 1. Model of PML and cytokine signaling in drug-induced and 'bystander' senescence. Cytokine secretion and autocrine/paracrine signaling triggered by the DDR machinery upregulate PML expression and formation of PML NBs, collectively leading to cellular senescence, both directly and through 'bystander' effects.